UNIVERSIDAD COMPLUTENSE DE MADRID

FACULTAD DE CIENCIAS BIOLÓGICAS
Departamento de Microbiología III

TESIS DOCTORAL

Expresión heteróloga, caracterización y aplicaciones biotecnológicas de la esterol esterasa-lipasa de *Ophiostoma piceae* y de otras enzimas seleccionadas de genomas fúngicos

MEMORIA PARA OPTAR AL GRADO DE DOCTOR

PRESENTADA POR

María Eugenia Vaquero Morales

Directores

María Jesús Martínez Hernández
Jorge Barriuso Maicas

Madrid, 2016

UNIVERSIDAD COMPLUTENSE DE MADRID

FACULTAD DE BIOLOGÍA

Departamento de Microbiología III

Expresión heteróloga, caracterización y aplicaciones biotecnológicas de la esterol esterasa/lipasa de *Ophiostoma piceae* y de otras enzimas seleccionadas de genomas fúngicos

TESIS DOCTORAL

para optar al grado de doctor presentada por:

María Eugenia Vaquero Morales

Directores:

Dra. María Jesús Martínez Hernández y Dr. Jorge Barriuso Maicas

Centro de Investigaciones Biológicas

Consejo Superior de Investigaciones Científicas

Madrid 2015

UNIVERSIDAD COMPLUTENSE DE MADRID

FACULTY OF BIOLOGY

Department of Microbiology III

Heterologous expression, characterization and biotechnological applications of the sterol esterasa/lipase of *Ophiostoma piceae* and other enzymes selected from fungal genomes

Doctoral Thesis

María Eugenia Vaquero Morales

Directors:

Dra. María Jesús Martínez Hernández and Dr. Jorge Barriuso Maicas

Centro de Investigaciones Biológicas

Spanish National Research Council

CSIC

Consejo Superior de Investigaciones Científicas

Madrid 2015

CSIC
CONSEJO SUPERIOR DE INVESTIGACIONES CIENTÍFICAS

La Dra. **María Jesús Martínez Hernández**, Investigadora Científica del CSIC y el Dr. **Jorge Barriuso Maicas**, Investigador contratado del CSIC certifican que:

Dª **María Eugenia Vaquero Morales**, Licenciada en Biología por la Universidad Complutense de Madrid, ha realizado bajo su dirección la memoria que presenta para optar al grado de doctor con el título: "Expresión heteróloga, caracterización y aplicaciones biotecnológicas de la esterol esterasa/lipasa de *Ophiostoma piceae* y de otras enzimas seleccionadas de genomas fúngicos", en el Departamento de Biología Medioambiental del Centro de Investigaciones Biológicas del CSIC.

Para que así conste y con los efectos oportunos, firman el presente certificado en Madrid a 21 de Septiembre de 2015

Dra. María Jesús Martínez Hernández

Dr. Jorge Barriuso Maicas

A mis padres

A Diana

A Jorge

La ciencia se compone de errores, que a su vez, son los pasos hacia la verdad

Julio Verne

Las experiencias que más te enseñan son las de todos los días

F. Nietzsche

ÍNDICE DE CONTENIDOS

ÍNDICE DE FIGURAS

ÍNDICE DE TABLAS

LISTADO DE ABREVIATURAS/*ABBREVIATIONS*

[θ]	Elipticidad molar (*Molar ellipticity*)
[S]	Concentracion de sustrato (*Substrate concentration*)
ε	Coeficiente de extinción molar (*Molar extinction coefficient*)
2xTY	*Double Tryptone Yeast extrac broth*
3D	Tridimensional (*Three-dimensional*)
ε-CL	ε-caprolactona (ε-*caprolactone*)
aa	Aminoácido (*Amino acid*)

Aaminoácidos (*amino acids*)

Alanina *Alanine*	Ala/A	Leucina *Leucine*	Leu/L
Arginina *Arginine*	Arg/R	Lisina *Lysine*	Lys/K
Asparagina *Asparagine*	Asn/N	Metionina *Methionine*	Met/M
Ácido aspártico *Aspartic acid*	Asp/D	Fenilalanina *Phenylalanine*	Phe/F
Cisteína *Cysteine*	Cys/C	Prolina *Proline*	Pro/P
Glutamina *Glutamine*	Gln/Q	Serina *Serine*	Ser/S
Ácido glutámico *Glutamic acid*	Glu/E	Treonina *Threonine*	Thr/T
Glicina *Glycine*	Gly/G	Triptófano *Tryptophan*	Trp/W
Histidina *Histidine*	His/H	Tirosina *Tyrosine*	Tyr/Y
Isoleucina *Isoleucine*	Ile/I	Valina *Valine*	Val/V

A	Amstrong
a.u	Unidades arbitrarias (*Arbitrarial Units*)
abH	*alpha-beta hydrolase*
ADH1	Alcohol deshidrogenasa (*Alcohol Dehydrogenase*)
AOX1	Alcohol oxidasa (*Alcohol Oxidase*)
Aspni5	Lipasa obtenida del genoma de *Aspergillus niger* (*Lipase from A. niger genome*)
ATCC	*American type culture collection*

Bases nitrogenadas (*nucleobases*)

A	Adenina (*Adenine*)
C	Citosina (*Cytosine*)
G	Guanina (*Guanine*)
T	Timina (*Thymine*)

BSA	Albúmina de suero bovino (*Bovine Serum Albumin*)
BCA	Ácido bicinconínico (*Bicinchoninic Acid*)
BLAST	*Basic Local Alignment Search Tool*
C-terminal	Extremo carboxilo terminal (*C- terminus*)
c(s)	Distribuciones diferenciales del coeficiente de sedimentación (*Sedimentation coefficient distributions*)
CETC	Colección Española de Cultivos Tipo (*Spanish type culture collection*)
CalB	Lipasa B *de Candida antarctica* (*C. antarctica lipase B*)
CHAPS	*3-[(3-cholamidopropyl)dimethylammonio]-1-propanesulfonate*
CRL	Lipasa de *Candida rugosa* (*C. rugosa lipase*)
Da	Dalton
DNA	Ácido desoxirribonucleico (*Desoxiribonucleic Acid*)
dNTPs	Desoxirribonucleótidos (*Desoxiribonucleotides*)

EC	Número de identificacion de la enzima (*Enzyme Commission number*)
EDTA	Acido etilendiaminotetraacético (*Ethylenediaminetetraacetic acid*)
EndoH	Endo-β-N-acetilglucosaminidasa H (*Endo-β-N-acetylglucosaminidase H*)
ESRF	*European Sincrotrón Radiation Facility*
GAL1	Promotor inducible por galactosa (*Galactose-induce promoter*)
GC	Cromatografia de gases (*Gas Chromatography*)
GCL	Lipasa de *Geotrichum candidum(G. candidum lipase*)
GPD1	Gliceraldehido-3-fosfato deshidrogenasa (*Glyceraldehyde 3-Phosphate Dehydrogenase*)
GRAS	*Generally Recognized As Safe*
HPLC	Cromatografía líquida de alta resolución (*High Performance Liquid Chromatography*)
ID	*Identification number*
IPTG	Isopropil-β-D-tio-galactopiranósido (*Isopropyl β-D-1-thiogalactopyranoside*)
JGI	*Joint Genome Institute*
k_{cat}	Constante catalítica (*Turnover frequency*)
k_{cat}/K_m	Eficiencia catalítica (*Catalytic efficiency*)
kDa	1000 Dalton
KEX2	Peptidasa señal (*Signal peptidase*)
K_m	Constante de Michaelis-Menten (*Michaelis-Menten constant*)
LB	*Luria Betani broth*
LED	*Lipase Engineered Database*
Lip1	Lipasa 1 de *C. rugosa* (*C. rugosa lipase* 1)
Lip2	Lipasa 2 de *C. rugosa* (*C. rugosa lipase* 2)
Lip3	Lipasa 3 de *C. rugosa* (*C. rugosa lipase* 3)
m/z	Relación masa-carga (*Mass-to-charge ratio*)
MALDI-TOF	*Matrix-Assisted Laser Desorption/Ionization-Time of Flight*
MALDI-MS	Espectro de masas de MALDI (*MALDI- Mass Spectrometry*)
MALDI MS/MS	Espectro de fragmentación de MALDI (*MALDI with tandem Mass Spectrometry*)
MES	Ácido 2-(N-Morfolino) etanosulfónico / *2-(N-Morpholino)ethanesulfonic acid sodium salt*)
MPVI	*Mating Population* VI
MS	*Mass Spectroscopy*
MWCO	*Molecular Weight Cut Off*
n	Número de unidades *(Number of units)*
NAG	N-acetilglucosamina (*N-acetylglucosamine*)
NCBI-nr	*National Center for Biotechnology Information (non-redundant)*
Necha2	Proteína obtenida del genoma de *Nectria haematoccoca (protein from N. haematoccoca)*
nm	Nanómetros (*nanometers*)
N-terminal	Extremo amino terminal (*N-terminus*)
OD	*Optical Density*
OPE	Esterol esterasa de *Ophiostoma. Piceae* (*sterol esterase from O. piceae*)
OPEc	Estructura de OPE en conformación cerrada (*closed conformation of OPE*)
OPEo	Estructura de OPE en conformación abierta (*open conformation of OPE*)
PCR	*Polymerase Chain Reaction*
PDB	*Protein Data Bank*

PEG	Polietilenglicol (*Polyethyleneglycol*)
PlicB	Lipasa obtenida del genoma de *Plicaturopsis crispa* (*Plicaturopsis crispa lipase*)
*p*NPB	Butirato de *p*-nitrofenilo (*p-nitrophenyl butyrate*)
*p*NPL	Laurato de *p*-nitrofenilo (*p-nitrophenyl laurate*)
*p*NPP	Palmitato de *p*-nitrofenilo (*p-nitrophenyl palmitate*)
psi	Libra por pulgada cuadrada (*Pound per square inch*)
PVDF	Fluoruro de polivinilideno (*Polyvilidene fluoride*)
rmsd	Desviación de la media cuadrática (*root-mean-squares-desviation*)
ROP	*Ring Opening Polimerization*
rpm	Revoluciones por minuto (*Revolutions per minute*)
S	Svedberg
Sarkosyl	*Sodium lauroyl sarcosinate*
SDS-PAGE	*Dodecyl Sulfate Polyacrilamyde-Gel-Electrophoresis*
SEC	Cromatografía de exclusión molecular (*Size Exclusion Chromatography*)
sn	Posición numerada del carbono en la molécula de glicerol (*Stereospecific Numbering*)
STE13	Peptidasa señal (*Signal peptidase*)
T	Temperatura (*Temperature*)
T50	T a la que la enzima retiene el 50% de su actividad inicial tras un tiempo de incubación (T *at which the enzyme loses 50% of its activity*)
Trire2	Enzima obtenida del genoma de *Trichoderma reesei (enzyme from T. reesei)*
Tris-HCl	2-amino-2-hidroximetilpropano-1,3-diol hidrocloruro (*2-Amino-2-hydroxymethyl-propane-1,3-diol hydrochloride*)
U	Unidad de actividad enzimática (*Unit of enzyme activity*)
Uml2	Lipasa 2 de *Ustilago maydis* (*U. maydis lipase 2*)
UV	Ultravioleta (*Ultraviolet*)
UV-Vis	Ultravioleta-visible (*Ultraviolet-visible*)
w/v	Relación peso/volumen (*Ratio weight/volume*)
v/v	Relación volumen/volumen (*Ratio volume/volume*)
X-Gal	*5-Bromo-4-chloro-3-indolyl β-D-galactopyranoside*
YEPS	*Yeast Extract Peptone Sorbitol broth*
YPD	*Yeast Extract Dextrose peptone broth*

Resumen/Summary

RESUMEN

El ascomiceto *Ophiostoma piceae* secreta una esterol esterasa/lipasa (OPE) que presenta una amplia especificidad de sustrato. La proteína fue expresada en la levadura *Pichia pastoris* y los estudios preliminares pusieron de manifiesto su amplio potencial biotecnológico en reacciones de hidrólisis y síntesis. Por ello, a lo largo del presente trabajo se ha tratado de profundizar en el conocimiento de esta enzima y de encontrar enzimas similares, proponiéndose como objetivos:

i. Explorar distintos sistemas de expresión heteróloga en busca del más adecuado para la producción de OPE.
ii. Cristalizar la proteína para conocer su estructura molecular y los mecanismos implicados en la catálisis.
iii. Seleccionar en genomas fúngicos nuevas enzimas similares a OPE, para expresarlas y caracterizarlas.
iv. Evaluar el potencial de las nuevas enzimas en distintas aplicaciones biotecnológicas.

Búsqueda de nuevos sistemas de expresión heteróloga de OPE.

Al utilizar distintas cepas de *Escherichia coli* como hospedador, la esterol esterasa expresada formó cuerpos de inclusión y únicamente se pudo solubilizar en presencia del detergente Sarkosyl, excepto la forma que contenía ciertos aminoácidos extra en el extremo N-terminal, que rindió una fracción de proteína soluble pero inactiva. La enzima producida en el hospedador procariota y solubilizada con Sarkosyl presentó un plegamiento diferente a los de la OPE nativa y la recombinante expresada en *P. pastoris*, lo que puede justificar su falta de actividad. En contraposición, la expresión de OPE en la levadura *Saccharomyces cerevisiae,* que además ostenta la condición de organismo GRAS, permitió obtener enzima soluble y activa con todas las construcciones empleadas. Esta proteína recombinante mostraba un masa molecular, porcentaje de glicosilación y estructura secundaria similar a los de *P. pastoris*. Sin embargo, la cantidad de enzima producida en *S. cerevisiae* y su solubilidad eran menores, y los parámetros cinéticos demostraban su menor eficiencia. A la vista de los resultados, se deduce que

la ausencia de modificaciones post-traduccionales en *E. coli* podría afectar al plegamiento proteico siendo crucial para la obtención de una enzima activa. Aunque los niveles de expresión de OPE en *S. cerevisiae* fueron bajos, queda abierto el camino hacia la mejora de su producción y/o propiedades catalíticas en esta levadura mediante técnicas de evolución dirigida, así como hacia su empleo en procesos relacionados con la alimentación.

Resolución de la estructura tridimensional de OPE: homologías y diferencias con otras lipasas de la familia *C. rugosa-like.*

La resolución de la estructura molecular de OPE en sus conformaciones abierta y cerrada aportó gran cantidad de información interesante. La forma cerrada presenta una tapadera anfifílica que limita el acceso al centro activo. El desplazamiento de este elemento 30 Å desde su posición original permite la entrada de los sustratos al centro activo. Estos se alojan en un bolsillo de sustrato en forma de túnel de 30 Å de longitud con alto contenido en aminoácidos hidrofóbicos, que termina en una zona próxima a la superficie, pudiendo servir como vía de salida de los productos de reacción. El diseño de un mutante que bloqueaba el túnel produjo una reducción drástica de la hidrólisis de sustratos con cadena larga de ácido graso (16 átomos de carbono) pero no de los de cadena corta (4 átomos de carbono) y media (12 átomos de carbono). La forma abierta de OPE se organiza como un homodímero, dejando una amplia cavidad entre ambos monómeros. Mediante ultracentrifugación analítica se constató la transición desde el monómero al dímero en presencia de un sustrato y un inhibidor. La resolución de la estructura tridimensional de OPE en ambas conformaciones ha permitido deducir su estado funcional de dímero y facilitará la realización de futuros estudios estructura-función para conocer mejor sus mecanismos catalíticos y el papel de su túnel interno.

Propiedades de las nuevas esterol esterasas/lipasas seleccionadas de genomas fúngicos. Aplicaciones biotecnológicas.

La expresión de tres enzimas de la familia de lipasas *C. rugosa-like* obtenidas mediante minería *in silico* de genomas fúngicos y pertenecientes a los genomas de *Nectria haematococca*, *Trichoderma reesei* y *Aspergillus niger*, y

su comparación con OPE, permitió extrapolar rasgos comunes a nivel de tamaño, estabilidad y presencia de formas multiméricas en solución. Sin embargo, su caracterización cinética reveló que la lipasa de *A. niger* no presentaba la capacidad para hidrolizar ésteres de colesterol, ni para sintetizar ésteres de sitoestanol, demostrando que esta enzima no era una esterol esterasa. Sin embargo, en la síntesis de policaprolactona se obtuvieron resultados similares con la enzima comercial de *C. rugosa*, OPE y la de *A. niger*. Comparando con las restantes enzimas ensayadas, OPE mostró la mayor eficiencia en la hidrólisis de ésteres de colesterol y en la síntesis de oleato de sitoestanilo por transesterificación, con altos grados de acilación a tiempos muy cortos. La expresión y caracterización de nuevas lipasas de la familia *C. rugosa-like* realizada en este trabajo ha permitido dilucidar semejanzas y diferencias entre ellas, comprobando que la versatilidad en la hidrólisis de triglicéridos y ésteres de esterol no es una característica común de todos los miembros de esta familia. La comparación de las enzimas recién caracterizadas, OPE y el crudo comercial de *C. rugosa* en diversas aplicaciones biotecnológicas señala a OPE como la enzima más prometedora.

Finalmente, se describe la búsqueda en genomas fúngicos de nuevas lipasas similares a la lipasa B de *C. antarctica* (CalB), una de las más empleadas a nivel industrial. Debido a su versatilidad, gran parte de las lipasas que muestran alta homología con CalB se encuentran bajo patente. En este trabajo se identificó la secuencia de la lipasa del basidiomiceto *Plicaturopsis crispa* (PlicB) que mostró un 44% de similitud de secuencia con CalB. PlicB se expresó con éxito en *P. pastoris* y se caracterizó, presentándose como un monómero de masa molecular ~37 kDa, características similares a CalB. Aunque la capacidad de PlicB para hidrolizar ésteres de *p*-nitrofenol era menor que la de CalB, la nueva enzima mostró mayor actividad frente a un análogo de triglicérido. A la vista de los resultados, la minería de genomas se muestra como una alternativa interesante a los métodos de cribado tradicionales.

SUMMARY

The ascomycete *Ophiostoma piceae* secretes a sterol esterase/lipase (OPE) characterized for its wide substrate specificity. This protein was successfully expressed in the yeast *Pichia pastoris*, and preliminary studies showed its broad biotechnological potential in hydrolysis and synthesis reactions. Therefore, across this work we tried to deepen the knowledge on this enzyme and find similar enzymes, being the main objectives:

i. To explore different heterologous expression systems in search of the most suitable for the production of OPE.
ii. To crystallize the protein to get insight into both its structure and the molecular mechanisms involved in catalysis.
iii. To select from fungal genomes new enzymes similar to OPE, to be expressed and characterized.
iv. To evaluate the potential of these new enzymes in various biotechnological applications.

Search for new heterologous expression systems for OPE.

By using different strains of *Escherichia coli* as hosts, the sterol esterase expressed formed inclusion bodies and was solubilized only in the presence of the detergent Sarkosyl, except the form containing certain extra amino acids at the N-terminal terminus that yielded a protein fraction soluble but inactive. The enzyme produced in the prokaryotic host and solubilized with Sarkosyl presented different folding to the native and recombinant OPE expressed in *P. pastoris*, which may explain its lack of activity. In contrast, expression of OPE in the yeast *Saccharomyces cerevisiae*, which also holds the status of GRAS organism, yielded soluble and active enzyme with all constructs and strains. This recombinant protein showed similar molecular weight, glycosylation and secondary structure to that expressed in *P. pastoris*. However, the amount of enzyme produced in *S. cerevisiae* and its solubility were lower, and the kinetic parameters demonstrated its reduced efficiency. In view of the results, it follows that several post-translational modifications, may affect enzymes' folding and be crucial to obtain an active protein. Up to now, the expression levels of OPE in *S. cerevisiae* have been low, but the

current findings open the way towards improving its production and/or catalytic properties in this yeast by directed evolution techniques, as well as to its use in food-related processes.

Resolution of the three dimensional structure of OPE: homologies and differences with other lipases *C. rugosa*-like family.

The resolution of the molecular structure of OPE in both its open and closed conformations gave very interesting information. The closed form has an amphiphilic lid that limits the access to the active site. The displacement of this element 30 Å from its original position allows the entry of substrates to the active site. These are housed in a tunnel-shaped substrate's pocket of 30 Å-length, high in hydrophobic amino acids, ending in an area close to the surface that could serve as a way out of the reaction products. The design of a mutant with a blocked tunnel caused a drastic hydrolysis reduction of long chain fatty acids substrates (16 C atoms), but not of those with short (4 C atoms) or medium acyl chains (12 C atoms). The open form of OPE is organized as a homodimer, leaving a large cavity between the two monomers. Analytical ultracentrifugation experiments showed that the transition from monomer to dimer occurred in the presence of a substrate or inhibitor. The resolution of the three-dimensional structure of OPE in both conformations allowed to deduce its functional dimeric state and will facilitate conducting future structure-function studies to better understand its catalytic mechanisms and the role of the inner tunnel.

Properties of novel sterol esterases/lipases selected from fungal genomes. Biotechnological applications.

Three enzymes of the *C. rugosa*-like lipases' family, belonging to *Nectria haematococca, Trichoderma reesei* and *Aspergillus niger,* were selected after *in silico* search in fungal genomes, expressed and compared to OPE. Common features to all of them, concerning their size, stability and multimeric forms in solution, were extrapolated. However, their kinetic characterization revealed that the *A. niger* lipase was unable of hydrolyzing cholesterol esters or synthesizing sitostanol esters, showing that this enzyme was not an sterol esterase. However, similar results were obtained in the synthesis of

polycaprolactone using either the commercial enzyme of *C. rugosa*, OPE and *A. niger*. Compared to the other enzymes tested, OPE showed the highest efficiency in cholesterol ester hydrolysis and in synthesis sitostanyl oleate by transesterification, producing high acylation degrees in very short times. The expression and characterization of these novel lipases belonging to the *C. rugosa*-like family carried out in this work allowed to find out some of their similarities and differences, and indicated that the versatility in the hydrolysis of triglycerides and sterol esters is not a common feature of all members of this family. Comparing the results for the newly characterized enzymes, OPE, and commercial crude of *C. rugosa* in several biotechnological applications, OPE appeared as the most promising enzyme.

Finally, the search in fungal genomes of novel enzymes similar to the *C. antarctica* lipase B (CalB), one of the most used lipases at industrial level, is described. Because of their versatility, most of the proteins showing high homology with CalB are under patent. In this work, the sequence of a lipase from the basidiomycete *Plicaturopsis crispa* (PlicB), that showed a 44% sequence similarity with CalB, was identified. PlicB successfully expressed in P. pastoris and characterized, appearing as a monomer of molecular mass around ~ 37 kDa, similarly to CalB. Although PlicB hydrolyzed p-nitrophenol esters less efficiently than CalB, the novel enzyme showed greater activity against a triglyceride analog. In view of the results, genome mining appears as an interesting alternative to traditional screening methods.

ESTRUCTURA DE LA TESIS

La presente memoria, para obtener el Título de Doctor, se estructura en cuatro capítulos, que se corresponden con cuatro artículos científicos publicados en revista indexadas en el SCI (*Science Citation Index*). El contenido de los trabajos publicados se ha mantenido íntegramente y el material suplementario, en el caso de que lo hubiera, ha sido incluido al final de cada capítulo. Se ha pedido el permiso correspondiente a cada revista para su inclusión en esta memoria. Todos los capítulos han sido formateados para que este trabajo mantenga una estructura homogénea y todos ellos contienen su propia introducción, materiales y métodos, resultados, discusión y bibliografía. Además se incluye una introducción y una discusión general que relaciona todos ellos y que incluye su propia bibliografía.

Lista de publicaciones

A continuación se muestran las publicaciones que forman parte de la presente Tesis Doctoral:

Capítulo 1. Vaquero ME, Barriuso J, Medrano FJ, Prieto A, Martínez MJ (2015a) Heterologous expression of a fungal sterol esterase/lipase in different hosts: Effect on solubility, glycosylation and production. J Biosci Bioeng doi:10.1016/j.jbiosc.2015.04.005

Capítulo 2 Gutiérrez-Fernández J*, Vaquero ME*, Prieto A, Barriuso J, Martínez MJ, Hermoso JA (2014) Crystal structures of *Ophiostoma piceae* sterol esterase: structural insights into activation mechanism and product release. J Struct Biol 187:215-222

Capítulo 3 Vaquero ME, Prieto A, Barriuso J, Martínez MJ (2015) Expression and properties of three novel fungal lipases/sterol esterases predicted in silico: comparison with other enzymes of the *Candida rugosa*-like family. Appl Microbiol Biotechnol doi: 10.1007/s00253-015-6890-9

Capítulo 4 Vaquero ME, de Eugenio LI, Martínez MJ, Barriuso J (2015) A novel CalB-type lipase discovered by fungal genomes mining. PLoS ONE doi:10.1371/journal.pone.0124882

*Contribución equitativa al trabajo

1 Introducción general

1.1 ASPECTOS GENERALES DE LAS CARBOXILESTER HIDROLASAS

Las carboxil ester hidrolasas son un grupo heterogéneo de enzimas capaces que catalizar la ruptura de los enlaces éster. A este grupo pertenecen las lipasas (EC 3.1.1.3) y las esterol esterasas (EC 3.1.1.13).

Tradicionalmente, la diferencia entre ellas se ha basado principalmente en la naturaleza de los sustratos sobre los que actúan: i) las lipasas son capaces de hidrolizar triglicéridos, sustratos insolubles en agua generalmente esterificados con ácidos grasos de cadena larga (≥10 átomos de carbono) y ii) las esterol esterasas actúan sobre esteroles esterificados con ácidos grasos de longitud de cadena variable, compuestos hidrofóbicos y voluminosos. A continuación se comentan en detalle las características de las lipasas, enzimas sobre las que existe más información, a pesar de que las esterol esterasas presentan características similares como se corroborará a lo largo de esta tesis.

1.2 LAS LIPASAS

1.2.1 Reacciones que catalizan

Las lipasas catalizan la hidrólisis de los enlaces éster de diversos sustratos en solución acuosa. Sin embargo, en condiciones termodinámicamente favorables, como baja actividad de agua y/o presencia de solventes orgánicos, son capaces de llevar a cabo reacciones de síntesis como la esterificación y la transesterificación (**Fig. 1.1**).

La esterificación directa es el proceso opuesto a la hidrólisis, en el que un ácido graso se une a un alcohol formando un éster y liberando una molécula de agua. El equilibrio entre ambas reacciones depende del contenido en agua de la reacción (Rahman et al. 2006). Asimismo, estas enzimas pueden llevar a cabo reacciones de transesterificación y estas reciben distintos nombres, dependiendo del aceptor/donador de grupos acilo: si el aceptor es un ácido, la reacción recibe el nombre de acidólisis mientras que en la alcoholisis es el grupo alcohol el que actúa como aceptor. Por otra parte, las lipasas llevan a cabo reacciones de interesterificación, un tipo de reacción multisustrato donde existe una transferencia del grupo acilo entre ésteres de

distinta naturaleza, siendo necesarias una hidrólisis y esterificación secuenciales (Divakar 2013; Marangoni 2002) .

Por la gran variedad de reacciones que catalizan, estas enzimas son uno de los tipos de catalizadores más comercializados y se utilizan en diferentes sectores industriales como se detallará más adelante (ver tabla **Tabla 1.1**).

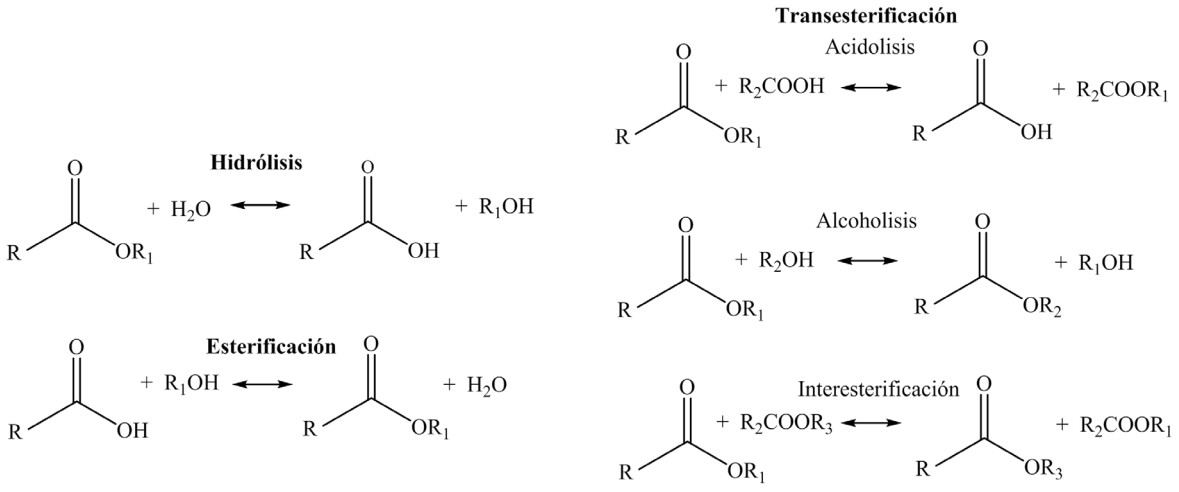

Fig. 1.1 Reacciones catalizadas por lipasas. Izquierda, hidrólisis y esterificación; derecha, reacciones de transesterificación: acidólisis, alcoholisis e interesterificación.

1.2.2 Elementos estructurales

Las lipasas pertenecen a la superfamilia α/β hidrolasa, uno de los grupos más amplios de enzimas que agrupa proteínas con diversas funcionalidades pero que comparten un plegamiento común (Holmquist 2000; Ollis et al. 1992) Entre los miembros de esta familia se incluyen también las esterol esterasas (Calero-Rueda et al. 2009) y otras enzimas como las tioesterasas, proteasas, dehalogenasas, y epoxi hidrolasas (Nardini y Dijkstra 1999). El plegamiento "canónico" de estas proteínas se caracteriza por poseer una lámina beta central formada por ocho hebras, rodeada por dos capas de alfa hélices anfifílicas (**Fig. 1.2A**). Además presentan una tríada catalítica formada por un residuo nucleófilo (generalmente una serina tras la hebra β5), un residuo ácido (glutámico/aspártico, tras la hebra β7) y una histidina posicionada tras la última hebra (β8) (Nardini y Dijkstra 1999).

Otro aspecto estructural destacable de estas enzimas es el llamado agujero oxianiónico, formado por varios residuos que estabilizan el estado de transición tetraédrico durante la catálisis. Los aminoácidos que rodean a los residuos catalíticos y los que constituyen este agujero difieren en las distintas lipasas, surgiendo así una clasificación de estas enzimas en familias y superfamilias en base a la homología de dichos residuos (Pleiss et al. 2000).

En el caso de las lipasas, la mayoría presenta un elemento helicoidal de naturaleza anfifílica, denominado "tapadera", que bloquea el acceso al sitio catalítico de la enzima en ausencia de sustrato o de interfase lípido-agua, constituyendo el estado inactivo o conformación cerrada de la enzima (**Fig. 1.2C**). En presencia de sustrato la tapadera se desplaza permitiendo la entrada de éste al bolsillo de sustrato, dando lugar a la conformación abierta o estado activado (Holmquist 2000) **(Fig. 1.2D)**. Este cambio conformacional se conoce como fenómeno de "activación interfacial" (Cajal et al. 2000; Verger 1997).

La estructura nativa de las lipasas es un sistema dinámico de interconversión entre la conformación cerrada y la abierta. En ausencia de interfase lípido-agua, solo una pequeña proporción de moléculas se encuentran en estado activado, debido al ambiente desfavorable que implica la exposición de un sitio catalítico tan hidrofóbico. La tapa, al interaccionar con el sustrato, juega un papel importante en su reconocimiento y en los cambios conformacionales posteriores que permiten su entrada al centro activo (Secundo et al. 2006). Sin embargo, no se ha descrito activación interfacial en todas las lipasas que presentan tapadera, probablemente debido a que factores como la fuerza iónica, la presencia de detergentes o agentes emulsificantes y/o la agitación pueden interferir en su identificación (Domínguez de María et al. 2006; Pernas et al. 2009; Verger 1997).

Por otro lado, existen familias de lipasas, como en la que agrupa la lipasa B de *Candida antarctica* (CalB, sinónimo *Pseudozyma antarctica*), que carecen de tapadera propiamente dicha, aunque presentan un sitio activo semi-cubierto por una hélice alfa (Uppenberg et al. 1994) (**Fig. 1.2B**).

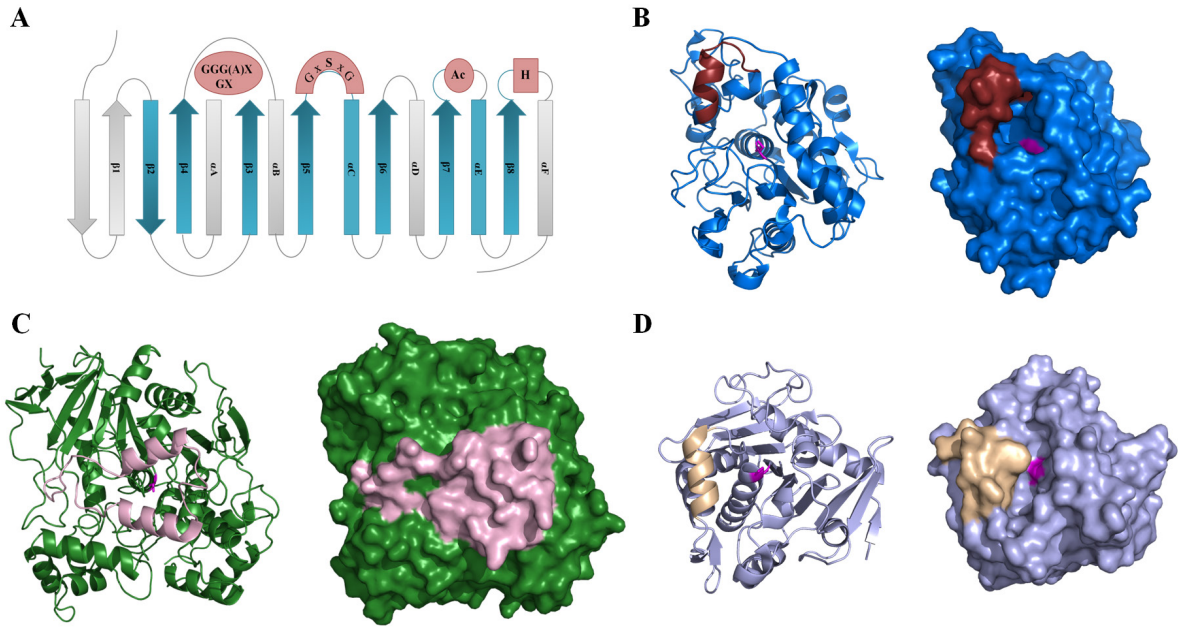

Fig. 1.2 A) Estructura "canónica" del plegamiento de α/β hidrolasa. Adaptado de (Kourist et al. 2010). Las flechas representan las hebras beta y los rectángulos las hélices α. En el interior de las formas color salmón y de izquierda a derecha se muestran: los residuos del agujero del oxianión, del codo nucleófilo, el residuo ácido y la histidina catalítica, respectivamente. Estructuras cristalográficas de: **B)** la lipasa B de *C. antarctica* (PDB:1TCA), **C)** la lipasa 2 de *Geotrichum candidum* (PDB:1THG), y **D)** la lipasa de *Rhizomucor miehei* (PDB:4TGL), representadas utilizando PyMOL v0.99. A la izquierda, representación de la estructura secundaria: las hélices α se simbolizan como espirales y las hebras β como flechas, mientras que a la derecha se representa la superficie. Las hélices α en distinto color indican el elemento móvil y el residuo catalítico aparece en magenta.

En relación con la variabilidad y especificidad de sustrato, el sitio de unión al sustrato es un elemento fundamental. El centro activo se encuentra en un bolsillo en la parte superior de la lámina β central. Los residuos que conforman este bolsillo son mayoritariamente hidrofóbicos, para una mejor interacción con el sustrato. Se distinguen varios tipos de bolsillos en base a su forma, tamaño y profundidad (Pleiss et al. 1998): i) tipo hendidura, como el de las lipasas de *R. miehei* (sinónimo *Mucor miehei*) o *Thermomyces lanuginosus* (antes conocido como *Humicola lanuginosa*) (**Fig. 1.2D**), ii) tipo embudo, como el de la lipasa B de *C. antarctica*, *Burkholderia sp*., *Burkholderia cepacia* (sinónimo *Pseudomonas cepacia*) la lipasa pancreática humana **(Fig. 1.2B)**, y iii) tipo túnel, como en las lipasas secretadas por *Candida rugosa* (antes conocida como *Candida cylindracea*) y *G. candidum*.

1.2.3 Mecanismo catalítico

La presencia de los residuos que componen la tríada catalítica hace posible la catálisis enzimática, que tiene lugar en dos etapas: una fase de acilación y otra de desacilación (**Fig. 1.3**). En la primera, el sustrato se acopla dentro del bolsillo catalítico y su carbono carbonilo sufre un ataque nucleofílico por parte del oxígeno del –OH de la serina catalítica, formándose el primer intermediario tetraédrico. La nucleofilia de la serina es posible gracias a la existencia de los otros residuos de la tríada catalítica. Primero, la histidina debe aceptar un protón del grupo hidroxilo de la serina, y esto ocurre gracias a la presencia del residuo ácido, que orienta el anillo imidazol de la histidina y neutraliza parcialmente la carga formada. El intermediario tetraédrico formado lleva una carga negativa en el oxígeno del grupo carbonilo (el oxianión), y los residuos del agujero oxianiónico (generalmente glicinas y/o alaninas) se encargan de estabilizar esta distribución de cargas y reducir el estado de energía del intermediario, formando para ello al menos dos puentes de hidrógeno. La rotura del enlace éster se produce como consecuencia de la donación de un protón por parte de la histidina al componente alcohol del sustrato. Esto conlleva la liberación del alcohol, mientras que el componente ácido del sustrato esterifica a la serina nucleofílica, formándose un intermediario acil-enzima o intermediario covalente. La etapa de desacilación tiene lugar cuando una molécula de agua (en hidrólisis), o de alcohol, ácido o éster (en alcoholisis, acidólisis o interesterificación, respectivamente) ataca el complejo acil-enzima. La histidina catalítica acepta un protón del agua, y el ion hidroxilo resultante ataca el carbono carbonílico del grupo acido, que se une a la serina formando el segundo intermediario tetraédrico, el cual se estabiliza de la misma forma que el anterior. Finalmente, mediante una transferencia de protones desde la histidina a la serina, se libera el componente acilo, regenerando la enzima (Casas-Godoy et al. 2012; Jaeger et al. 1999).

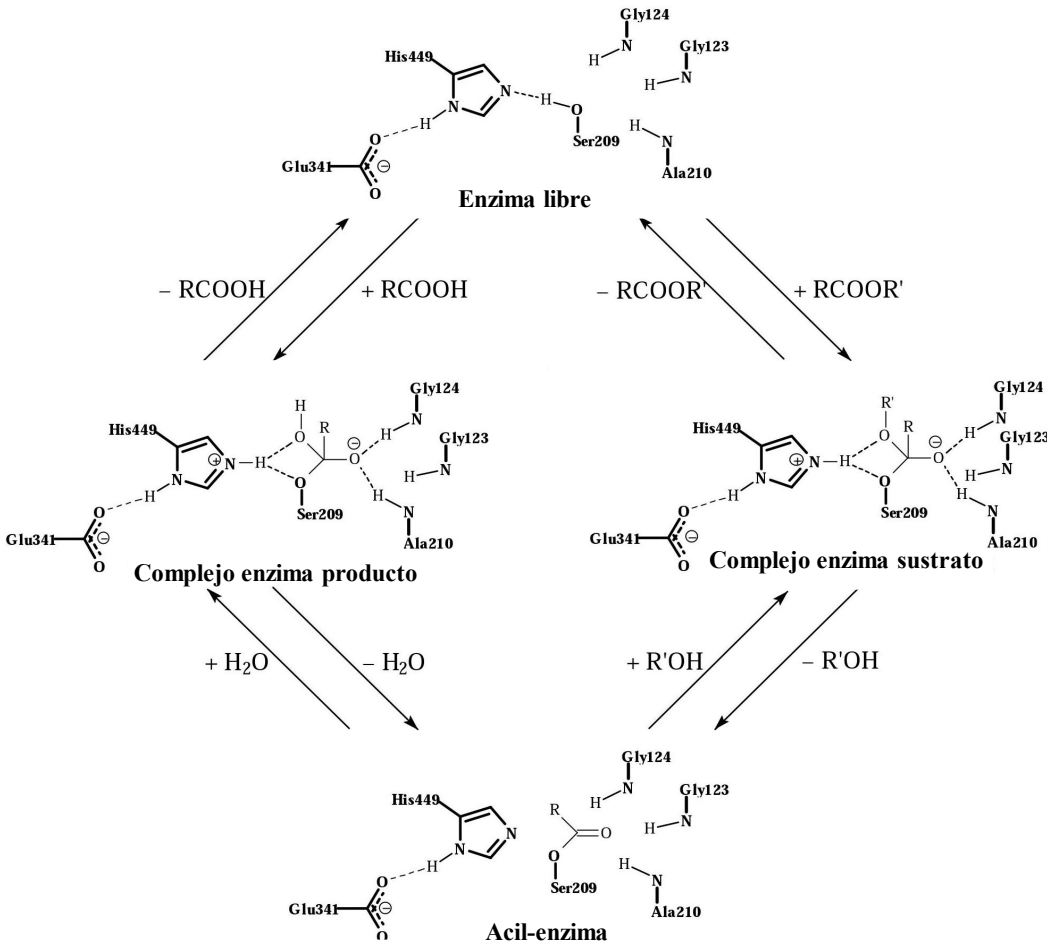

Fig. 1.3 Mecanismo catalítico de la lipasa de *C. rugosa* Adaptado de Monecke et al. (1998).

1.2.4 Fuentes de obtención, rol eco-fisiológico y aplicaciones

Las lipasas se encuentran ampliamente distribuidas en la naturaleza, siendo producidas por plantas, animales y microorganismos, relacionándose su papel fisiológico con la hidrólisis de los triglicéridos y su metabolismo. En eucariotas superiores, estas enzimas están involucradas en diversas etapas del metabolismo de lípidos incluyendo la digestión de las grasas, su absorción, reconstitución y metabolismo de lipoproteínas (Mukherjee 2003). En plantas, están presentes principalmente en semillas de oleaginosas y cereales, contribuyendo como factor defensivo o en el proceso de germinación (Jirage et al. 1999; Rivera et al. 2012). Las lipasas microbianas (de bacterias, levaduras y hongos filamentosos) tienen un alto interés industrial debido a su abundancia, facilidad de producción y versatilidad (Schmid y Verger 1998). La presencia en el medio de triglicéridos y ácidos grasos, que pueden utilizar como fuentes de carbono, induce la producción de estas enzimas. Así

encontramos levaduras lipolíticas en una gran variedad de hábitats, como suelos contaminados con aceites, residuos de aceites vegetales o productos lácteos, o en alimentos deteriorados (Ciafardini et al. 2006; D'Annibale et al. 2006). Por otra parte, existen algunos trabajos que describen el rol de las lipasas como factor de virulencia en hongos (Gaillardin 2010; Reis et al. 2005).

Las lipasas microbianas son las enzimas más usadas en química orgánica en reacciones de síntesis (Reetz 2002) y el tercer grupo de proteínas más comercializado, tras las proteasas y carbohidrolasas (Nguyen et al. 2015). Estas enzimas, dependiendo de su origen, pueden presentar propiedades de gran interés, como por ejemplo estabilidad frente a temperatura y pH y/o presencia de solventes orgánicos, alta especificidad, regioselectividad y enantioselectividad (Bornscheuer 2002; Jaeger et al. 1999). Por esta razón, son consideradas como unos catalizadores muy robustos. Existen muchas lipasas bacterianas caracterizadas, destacando las de los géneros *Pseudomonas, Burkholderia, Bacillus* y *Staphylococcus* (Jaeger y Eggert 2002). Sin embargo, la mayor parte de las lipasas comercializadas son producidas por levaduras, como *C. rugosa* o *C. antarctica*, o por hongos filamentosos, como *Aspergillus niger*, *G. candidum*, *T. lanuginosus*, *R. miehei* y diferentes especies de *Rhizopus* (Singh y Mukhopadhyay 2012).

El mercado de las lipasas mueve millones de dólares y comprende gran variedad de aplicaciones industriales (**Tabla 1.1**), en sectores como el alimentario, cosmético, farmacéutico, papelero, biocombustibles, o en la formulación de detergentes (Hasan et al. 2006; Jaeger y Eggert 2002; Jaeger y Reetz 1998).

Tabla 1.1 Aplicaciones biotecnológicas de las lipasas microbianas

Fuente	Nombre Comercial	Proveedor	Ejemplos aplicaciones	Referencia
Bacterias				
Alcaligenes sp	Lipase PLC-G, QLC-G	Meito Sangio Co.	Degradación bioplásticos	(Hoshino y Isono 2002)
B. cepacia	Lipase SL, PS	Meito Sangio Co., S-A[a]	Industria alimentaria/ Biodiesel	(Noureddini et al. 2005)/ (Korman et al. 2013)
Cromobacterium viscosum	Lipase CV	Asahi-Kasei	Detergentes-productos limpieza	(Minoguchi y Muneyuki 1989)
Pseudomonas fluorescens	Lipase AK	Meito Sangio Co., S-A	Industria alimentaria	(Rajmohan et al. 2002)
Pseudomonas stutzeri	Lipase TL	Meito Sangio Co.	Síntesis orgánica	(van Pelt et al. 2011)
Pseudomonas alcalígenes	Lipomax	Genecor-Dupont	Detergentes-productos limpieza	(Jaeger y Reetz 1998)
Pseudomonas mendocina	Lumafast	Genecor-Dupont	Detergentes-productos limpieza	(Gray et al. 1995)
Hongos y levaduras				
A. niger	Lipase A "Amano"	Amano, S-A	Resolución muestras racémicas	(Carvalho et al. 2006)
Aspergillus oryzae	Resinase A	Novozymes	Industria papelera	(Matsukura et al. 1990)
C. antarctica	Novozym 435, Lipozyme CALB	Novozymes	Biodiesel/ Síntesis de poliésteres	(Yan et al. 2012)/ (Kumar y Gross 2000)
C. antarctica	CAL-A, Novocor AD	S-A, Novozymes	Síntesis orgánica	(Pihko et al. 2004)
C. rugosa	Lipase AY "Amano" 30	Amano, S-A	Industria papelera/Nutracéuticos	(Irie 1990) /(Weber et al. 2001)
G. candidum	Chirazyme L-8,	Boehringer Mannheim,	Sector alimentario (antioxidantes)	(Buisman et al. 1998)
R. miehei	Lipozyme IM	Novozymes	Cosmética/ Nutracéuticos	(Maugard et al. 2002) (Villeneuve et al. 2005)
Rhyzopus oryzae	Palatase, Lipomod 627P	Novozymes/Biocatalysts	Biodiesel	(Yu et al. 2013)
Penicillium camembertii	Lipase G "Amano" 50	S-A	Sector alimentario (saborizantes)	(Arnold et al. 1975)
Penicillium roquefortii	Lipomod 338P-L338P	Biocatalysts	Síntesis orgánica	(van der Deen et al. 1996)
T. lanuginosus	Lipozyme TL, Lipolase	Novozymes	Resolución mezclas racémicas/ Tratamiento aguas residuales	(Faigl et al. 2007)/ (Rigo et al. 2008)

S-A, Sigma-Aldrich

1.2.5 La familia de lipasas *C. rugosa-like*

1.2.5.1 Características principales

La levadura *C. rugosa* secreta una gran variedad de lipasas íntimamente relacionadas en su secuencia de aminoácidos, estructura y propiedades catalíticas (Domínguez de María et al. 2006). Aunque la mayoría de ellas tiene actividad tanto frente a triglicéridos como a ésteres de esteroles, inicialmente fueron comercializadas por Sigma-Aldrich, Amano y Roche como lipasas o colesterol esterasas, en función de su actividad predominante. De las 7 isoenzimas descritas, las mejor caracterizadas, CRL1, CRL2, CRL3, CRL4 y CRL5, poseen una alta homología de secuencia (77-88%) pero difieren en su punto isoeléctrico, sitios de N-glicosilación y contenido en aminoácidos hidrofóbicos (Ferrer et al. 2001). Todo ello contribuye a su diferente afinidad sobre triglicéridos y ésteres de esteroles (Mancheño et al. 2003). Esta amplia especificidad de sustrato mostrada por las enzimas de *C. rugosa*, no es una característica general de todas las lipasas ni de todas las incluidas en esta familia, como se discutirá en este trabajo.

Atendiendo a la base de datos de lipasas de la Universidad de Stuttgart (*Lipase Engineered Database,* LED), existen 336 secuencias proteicas incluidas en la familia *C. rugosa-like* (abH03.01) (Fischer y Pleiss 2003). La mayoría de ellas corresponden a proteínas hipotéticas, derivadas de la secuenciación masiva de genomas de hongos ascomicetos y basidiomicetos, y solo algunas de ellas han sido caracterizadas. La información existente acerca de la afiliación filogenética y la evolución de estas enzimas es muy escasa y su clasificación se basa en la homología de secuencias y en la presencia de motivos conservados. Además de las isoenzimas de *C. rugosa*, se han caracterizado otras proteínas de esta familia (**Tabla 1.2**), como las isoenzimas GCL1 y GCL2 del hongo *G. candidum* (Bertolini et al. 1995; Sidebotton et al. 1991), la lipasa secretada por el hongo de la podredumbre gris *Botrytis cinerea* (Commenil et al. 1995; Commenil et al. 1999) y la lipasa del hongo de podredumbre blanca *Pleurotus sapidus* (Krugener et al. 2009; Zorn et al. 2005). En estas enzimas, caracterizadas como lipasas, solo se ha descrito actividad esterol esterasa en las isoenzimas CRL1-CRL5 de *C. rugosa* y se ha reportado actividad xantofil esterasa en la lipasas de *P. sapidus* y *C. rugosa*

(Zorn et al. 2003). Sin embargo, en esta familia se incluyen enzimas clasificadas como esterol esterasas, secretadas por los ascomicetos *Melanocarpus albomyces* (Kontkanen et al. 2006b) y *Ophiostoma piceae* (OPE) (Calero-Rueda et al. 2002b; Calero-Rueda et al. 2009), que tienen también actividad sobre triglicéridos y ésteres de esteroles y, por su relevancia en el presente trabajo, se tratarán en un apartado específico.

Al analizar el árbol filogenético de estas enzimas, se observa que todos los hongos de la familia *C. rugosa-like* comparten un hábitat asociado a material vegetal. Su papel en la naturaleza podría estar relacionado con su capacidad para degradar la cutícula, formada por una mezcla de ácidos grasos de cadena larga, aldehídos, alcanos, alcoholes primaros y secundarios, cetonas y ésteres de ceras. De acuerdo con esta teoría, al degradar algunos de estos componentes, los polisacáridos quedarían más accesibles y pueden ser utilizados como fuente de carbono, facilitando además la colonización de otras especies patógenas (Juniper y Jeffree 1983).

Tabla 1.2 Lipasas/esterol esterasas caracterizadas de la familia *C. rugosa-like*.

Organismo	Hábitat	% id*	% similitud	aa[c]	Referencia
C. rugosa	Suelo	79-88[a]	88-89[b]	534	(Lotti et al. 1994)
G. candidum	Cosmopolita	41%	57%	544	(Bertolini et al. 1995)
O. piceae	Madera	44%	62%	537	(Calero-Rueda et al. 2009)
M. albomyces	Suelo	43%	58%	558	(Kontkanen et al. 2006b)
B. cinerea	Patógeno vid	46%	61%	558	(Commenil et al. 1999)
P. sapidus	Madera	42%	61%	528	(Krugener et al. 2009)

***** Identidad de secuencia frente a *C. rugosa*
[a] Identidad entre las isoenzimas (CRL1-4)
[b] Similitud entre isoenzimas
[c] Número de aminoácidos en la proteína madura

Las lipasas de esta familia tienen masas moleculares cercanas a 60 kDa, un contenido en N-glicanos entre 3-8%, puntos isoeléctricos entre 4-5,8 e hidrolizan triglicéridos y ésteres de *p*-nitrofenol con diferente longitud de cadena de ácido graso. Además, muchos de sus miembros presentan formas oligoméricas en condiciones nativas.

1.2.5.2 Aspectos estructurales

Las enzimas cristalizadas de esta familia, las CRL1, CRL2 y CRL3 de *C. rugosa*, (Ghosh et al. 1995; Grochulski et al. 1993; Grochulski et al. 1994; Mancheño et al. 2003) y la GCL2 de *G. candidum* (Schrag et al. 1991; Schrag y Cygler 1993), presentan un plegamiento formado por 11 hebras beta y 16 alfa hélices, dos o tres puentes disulfuro, varios puentes salinos encargados de estabilizar los extremos N- y C-terminales y una tapadera anfifílica que bloquea la entrada al centro activo, cuyo movimiento se ve facilitado por un puente disulfuro que actúa a modo de bisagra (**Fig. 1.4**) .

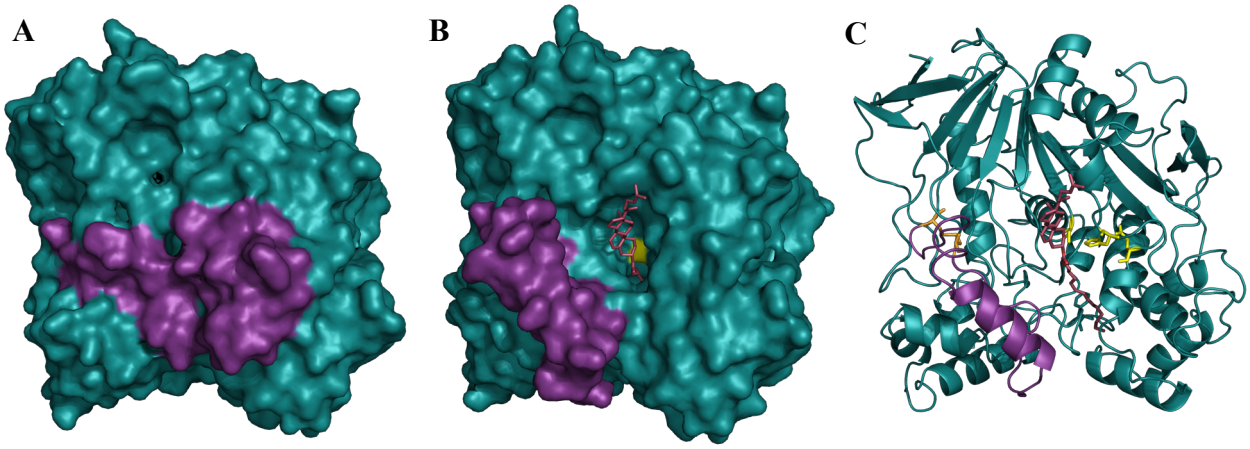

Fig. 1.4 Representación de la estructura tridimensional de la lipasa 1 *C. rugosa* (CRL1). **A)** Conformación cerrada (PDB:1TRH) en modo superficie, con la zona de la tapadera en morado. **B)** Conformación abierta (PDB:1CRL): la tapadera deja accesible el centro activo, en el que se encuentran la serina catalítica (en amarillo) y el sustrato (linoleato de colesterilo). **C)** Plegamiento α/β hidrolasa con el sustrato dentro del bolsillo catalítico y los residuos que intervienen en la catálisis en amarillo. Un puente disulfuro (en naranja) estabiliza la tapadera. Figuras representadas utilizando PyMOL v0.99.

1.2.5.3 Mecanismo de activación y región de la tapa

La resolución de varias estructuras cristalográficas en su conformación abierta y cerrada ha permitido entender los cambios conformacionales asociados al proceso de activación interfacial en las lipasas de *C. rugosa* (**Fig. 1.4**) (Ghosh et al. 1995; Grochulski et al. 1993, 1994). La transición hacia la forma abierta incrementa considerablemente la superficie hidrofóbica de las proteínas ya que la parte hidrofílica de la tapadera se encuentra de cara al solvente en la conformación cerrada, mientras que la hidrofóbica permanece

hacia el interior. La región de la tapa es una de las zonas menos conservadas entre los miembros de esta familia y esto podría estar relacionado con la mayor o menor especificidad de estas enzimas frente a triglicéridos o ésteres de esteroles. En este sentido, destacar que a pesar de la alta homología de secuencia encontrada entre las isoenzimas de *C. rugosa*, la presencia de un mayor porcentaje de aminoácidos hidrofóbicos en las tapaderas de CRL2 y CRL3 se ha relacionado con su mayor capacidad de hidrolizar ésteres de colesterol (Mancheño et al. 2003).

1.2.5.4 Residuos catalíticos y bolsillo de sustrato

La maquinaria catalítica en la familia *C. rugosa-like* está formada por tres residuos catalíticos: serina, ácido glutámico e histidina y se encuentra muy conservada (**Fig. 1.5A**). La sustitución del glutámico por aspártico en la lipasa de *G. candidum* reduce su actividad específica diez veces sobre la cepa salvaje (Vernet et al. 1993). La serina nucleófila se localiza en un bucle muy cerrado, denominado "codo nucleófilo", dentro del motivo conservado Gly-Glu-Ser-Ala-Gly (Barriuso et al. 2013; Pleiss et al. 2000). En CRL1, la depresión que rodea a la serina catalítica tiene un carácter muy hidrofóbico, más que ninguna otra zona expuesta al solvente (Grochulski et al. 1993). El intermediario tetraédrico originado durante la catálisis es estabilizado a través de puentes de hidrógeno entre grupos amida de la cadena principal de dos aminoácidos (generalmente glicinas y/o alanina) y el oxígeno del grupo carbonilo del sustrato. Estos residuos estabilizadores crean el agujero oxianiónico. Uno de los aminoácidos que la forman se sitúa contiguo a la serina catalítica y el otro se engloba dentro del motivo altamente conservado Gly-Gly-Gly-Phe, encontrado en esta familia (Grochulski et al. 1993; Monecke et al. 1998)

La zona de unión al sustrato en las enzimas de la familia *C. rugosa-like* se caracteriza por la presencia de un extenso bolsillo hidrofóbico con un estrecho túnel en el cual se estabiliza la cadena alifática del sustrato (**Fig. 1.5B-D**) (Ghosh et al. 1995; Mancheño et al. 2003; Pletnev et al. 2003). Al comienzo del túnel hay una región rica en aminoácidos aromáticos, con marcadas diferencias en las isoenzimas de *C. rugosa*, y más adelante se encuentra una segunda región muy conservada, rica en aminoácidos alifáticos.

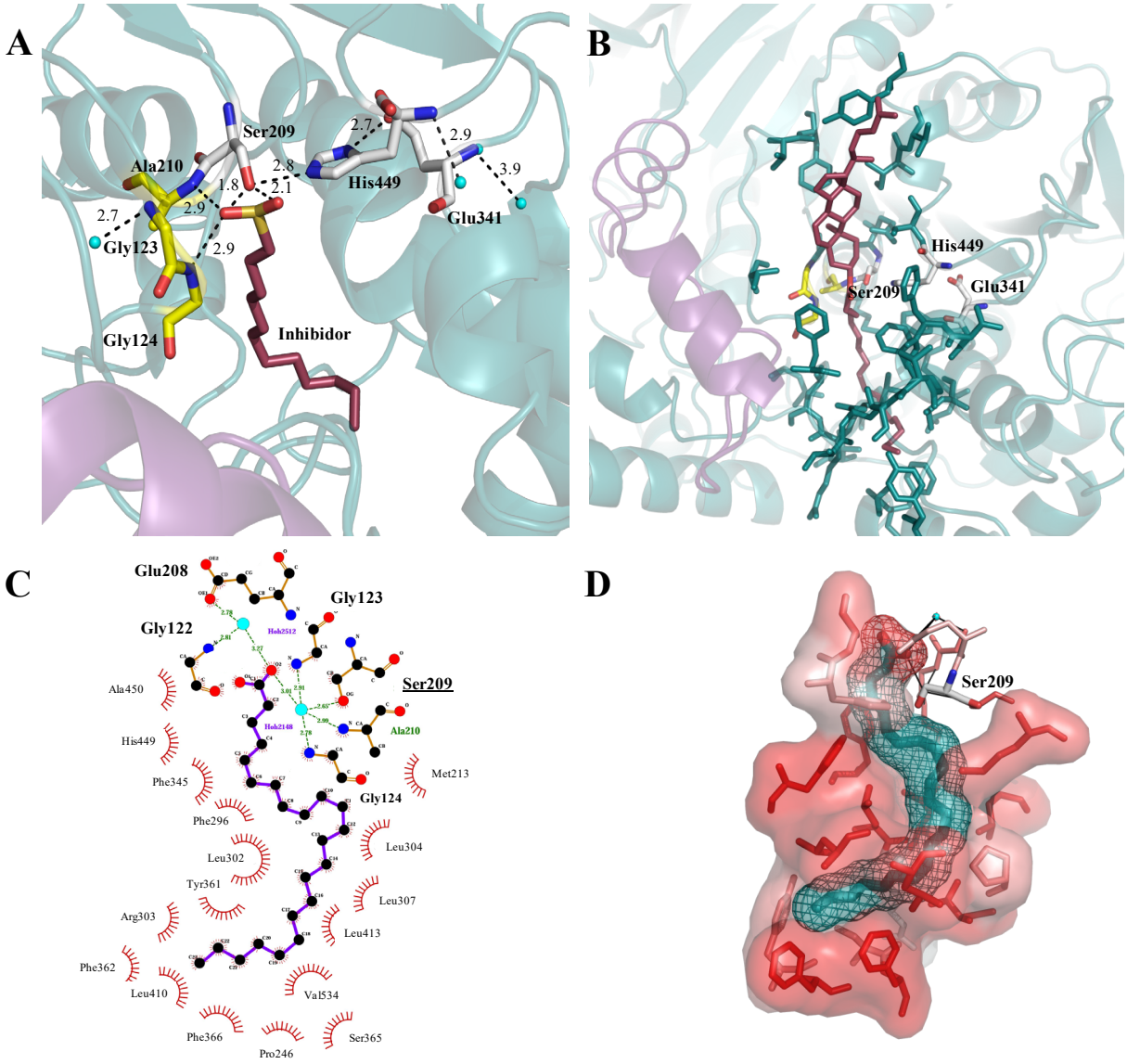

Fig. 1.5 A) Representación de los residuos del centro activo de CRL1 (PDB:1LPN) y las interacciones que estabilizan su conformación (distancia medida en Å). Los residuos de la proteína se ilustran con un modelo de varillas coloreadas, según su composición atómica (gris, carbono; amarillo, azufre; azul, nitrógeno; rojo, oxígeno). Las moléculas de agua aparecen como esferas en azul, los residuos catalíticos en blanco, los residuos del agujero oxianiónico en amarillo y la presencia de un inhibidor (cloruro de 1-dodecanosulfonilo) en granate. **B)** Representación del bolsillo del sustrato de CRL1 (PDB: 1CRL). El sustrato, linoleato de colesterilo, aparece en granate. Los residuos catalíticos y del agujero oxianiónico mantienen el mismo código de colores que en A. **C)** Representación esquemática de CRL3 (PDB: 1LLF) y las interacciones hidrofóbicas (arcos y líneas discontinuas en rojo) con el sustrato (ácido tricosanoico, C23:0). En línea discontinua verde se muestran los puentes de hidrógeno y como esferas azules las moléculas de agua. **D)** Composición del bolsillo de sustrato y el túnel interno de CRL3. El ácido tricosanoico (verde) se encuentra estabilizado por aminoácidos hidrofóbicos. El color rojo intenso

indica la máxima hidrofobicidad. Las figuras se han diseñado utilizando PyMOL v0.99 y LIGPLOT^{+} v.1.4.5

La presencia de este bolsillo de sustrato en forma de túnel es una característica única descrita para las enzimas de esta familia y permite acomodar ácidos grasos de cadena larga en su interior (18-23 carbonos) (Cygler y Schrag 1999; Domínguez de María et al. 2006; Pletnev et al. 2003).

1.2.5.5 Parches hidrofóbicos y estado conformacional

En las isoenzimas de *C. rugosa* existen áreas donde se concentra un mayor número de aminoácidos hidrofóbicos, formando lo que se conoce como "parches hidrofóbicos". Estas regiones se localizan cercanas a la zona de la tapadera y el bolsillo catalítico (**Fig. 1.6A**), pudiendo intervenir en procesos tan cruciales como la estabilización del movimiento de la tapa o la interacción con el sustrato (Grochulski et al. 1993; Mancheño et al. 2003). Por otro lado, la naturaleza hidrofóbica de estas proteínas explica su tendencia a la asociación formando dímeros, tetrámeros, hexámeros o agregados mayores. Además distintos factores, como la alta concentración de enzima y la elevada salinidad en el medio de reacción, favorecen la agregación (Pernas et al. 2001). En general, estas formas multimoleculares exhiben menor actividad específica, posiblemente por el bloqueo de los centros activos por las propias moléculas. Este es el caso de la lipasa 2 de *C. rugosa* expresada en *P. pastoris*, donde solo el monómero mostró actividad (Ferrer et al. 2009) y el de la esterol esterasa de *M. albomyces,* que incrementó su actividad en presencia de detergentes, al favorecerse la forma monomérica (Kontkanen et al. 2006b). Sin embargo, en el caso de la lipasa 3 de *C. rugosa* se ha comprobado su asociación en forma de dímeros activos, estabilizados por puentes de hidrógeno e interacciones de tipo hidrofóbico (**Fig. 1.6**) (Pletnev et al. 2003)

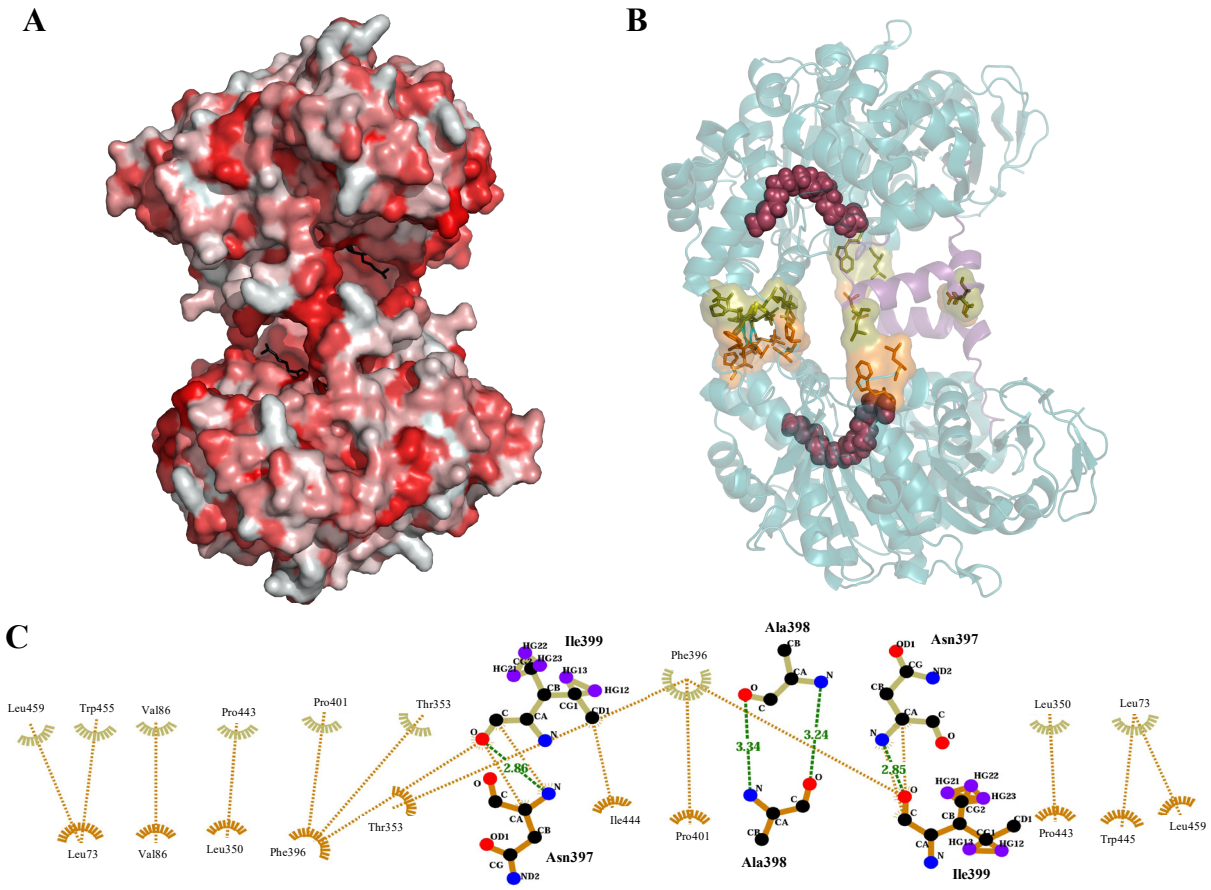

Fig. 1.6 A). Representación de la superficie de CRL3 (PDB:1CLE), en la que se observan las zonas más hidrofóbicas en color rojo más intenso y el sustrato en negro. **B)** Representación tridimensional de las interacciones entre los monómeros de esta proteína. Los aminoácidos implicados en la interacción entre las dos moléculas de CRL3 se representan en naranja y verde oliva. Las figuras 1.6 A y B fueron elaboradas con PyMOL v0.99. **C)** Representación esquemática de las interacciones entre monómeros obtenida utilizando el programa LIGPLOT^{+} v.1.4.5

1.3 ESTEROL ESTERASAS

Como se mencionó al comienzo de la introducción, estas enzimas hidrolizan ésteres de esteroles y juegan un papel importante en la absorción y metabolismo de los compuestos lipídicos en organismos vivos. Las colesterol esterasas humanas y de mamíferos son las mejor caracterizadas por su importancia fisiológica (Chen et al. 1998; Rudd y Brockman 1984), detectándose este tipo de actividades en el páncreas, la aorta, el hígado y la leche materna (Sugihara et al. 2002).

En el caso de microorganismos, se han caracterizado esterol esterasas en bacterias y hongos. En bacterias, se han descrito en *B. cepacia* (Takeda et al. 2006)*, Pseudomonas aeruginosa* (Sugihara et al. 2002) y *P. fluorescens* (Uwajima and Terada 1975) aunque esta última no presenta actividad sobre triglicéridos, a diferencia de lo reseñado para la de *P. aeruginosa*. En el caso de los hongos, se ha referido la presencia de estas enzimas en *S. cerevisiae* (Taketani et al. 1980), *Fusarium oxysporum* (Okawa y Yamaguchi 1977), *Trichoderma sp.* (Maeda et al. 2008) *M. albomyces* (Kontkanen et al. 2006b) y *O. piceae* (Calero-Rueda et al. 2002b), siendo las de estos dos últimos organismos las mejor caracterizadas y en las que se ha comprobado su actividad tanto sobre ésteres de esteroles como sobre triglicéridos.

1.3.1 La esterol esterasa de *O. piceae*

El ascomiceto *O. piceae* es un hongo dimórfico, saprófito de plantas que al crecer sobre maderas produce un efecto conocido como el azulado de la madera (*sap staining*), que ocasiona graves pérdidas económicas en la industria maderera. Este teñido se debe al contenido en melanina de las hifas, pigmento que desempeñaría un papel protector para la supervivencia del hongo en ambientes difíciles y que está relacionado con procesos de desarrollo celular, diferenciación y patogénesis (Haridas et al. 2013).

1.3.1.1 Purificación y caracterización de la enzima

El estudio de esta enzima surgió como resultado de la búsqueda de enzimas fúngicas para evitar la formación de depósitos indeseables durante la fabricación de pasta de papel, responsables de numerosos problemas en el

sector papelero (Gutiérrez et al. 2001). Estos depósitos, conocidos con el nombre de "*pitch",* formados por compuestos presentes en la fracción lipofílica de los extraíbles de la madera, principalmente triglicéridos y esteroles, surgieron tras la introducción de métodos de blanqueo más respetuosos con el medio ambiente (Allen 2000). Para controlar el *pitch* ya existía una lipasa comercializada con el nombre de Cartapip® producida por *Ophiostoma piliferum,* con alta eficacia sobre los triglicéridos pero no sobre los ésteres de esteroles, estos últimos más abundantes en frondosas (Chen et al. 1994).

Inicialmente se realizó una búsqueda de hongos productores de enzimas implicadas en la degradación de ésteres de esteroles. Entre los 28 hongos estudiados, pertenecientes a ascomicetos, basidiomicetos y deuteromicetos, *O. piceae* fue el único que mostró actividad sobre oleato de colesterilo (Calero-Rueda 2001). Tras la purificación y caracterización bioquímica de la enzima secretada por *O. piceae*, se comprobó su actividad sobre ésteres de *p*-nitrofenol, triglicéridos y ésteres de colesterol, clasificándose como una esterol esterasa con amplia especificidad de sustrato (Calero-Rueda et al. 2002b).

1.3.1.2 Aplicaciones biotecnológicas

El potencial de esta enzima se patentó tras comprobar que, tanto en extraíbles como en pastas de diferentes maderas, su aplicación reducía los niveles de los compuestos responsables de la formación de *pitch:* los ésteres de esteroles en *Eucalytus globulus,* los triglicéridos en *Pinus sylvestris*, y la mezcla de ambos compuestos en *Picea abies* (**Fig. 1.7**) (Calero-Rueda et al. 2002a).

Por otro lado, también se ha descrito el potencial de la esterol esterasa de O. piceae en la producción de papel reciclado, ya que esta enzima hidroliza eficazmente el polivinilacetato, principal componente de los denominados "stickies", depósitos indeseados que se producen durante la producción de este tipo de papel, en este caso debido a los aditivos e impurezas de la materia prima (Miranda et al. 2008). La hidrólisis de polivinilacetato por la enzima de O. piceae da lugar a polivinil alcohol, un compuesto más soluble que podría eliminarse con mayor facilidad (Barba Cedillo et al. 2013b).

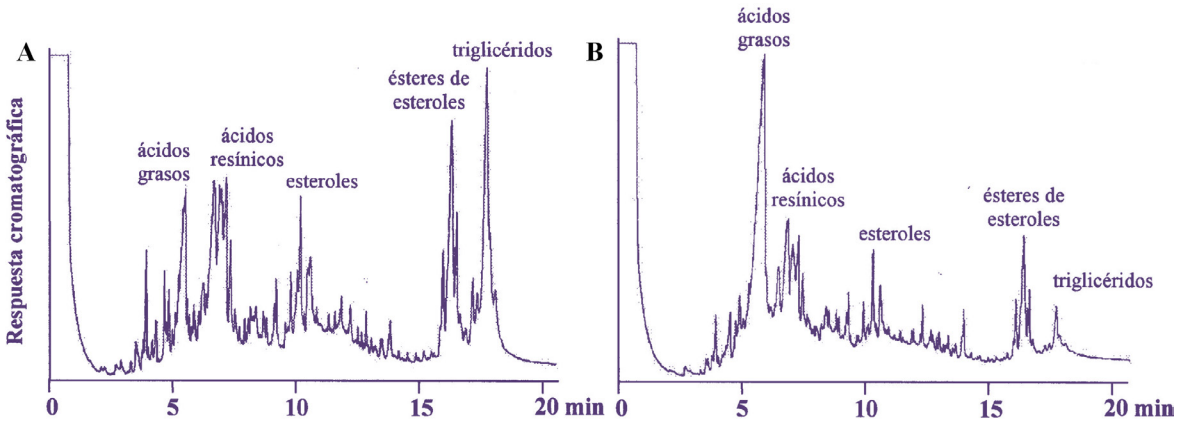

Fig. 1.7 Análisis cromatográfico de los compuestos lipofílicos presentes en los extraíbles de la madera de *Picea abies* **A)** Control. **B)** Tras tratar con la esterol esterasa de *O. piceae* (Calero-Rueda et al. 2002a).

La comparación de la esterol esterasa de *O. piceae* con otras lipasas y colesterol esterasas comercializadas, incluidas las enzimas de *C. rugosa*, puso de manifiesto el interés biotecnológico de esta enzima ya que, en presencia de Genapol X-100 (detergente necesario para obtener una suspensión homogénea de sustratos insolubles), fue la única que hidrolizaba eficazmente tanto los triglicéridos y ésteres de esteroles (Calero-Rueda et al. 2009).

A nivel de síntesis, la esterol esterasa de *O. piceae* se ha utilizado para esterificar mezclas de fitoesteroles con ácidos grasos, ya que estos ésteres se emplean como compuestos nutracéuticos para la reducción de colesterol en sangre (Chen et al. 2008). Esta reacción se realizó utilizando como catalizadores la enzima de *O. piceae* y el preparado comercial de *C. rugosa*, encontrando mayor esterificación con la enzima de *O. piceae* ($\geq$ 75% frente a 60% de esterificación) y recogiendo estos datos en una patente (Barba Cedillo et al. 2013a). Finalmente, comentar que también se han comparado estas enzimas en la producción de biodiesel, utilizando trioleína y metanol como aceptor de grupos acilo, encontrando que la enzima de *O. piceae* fue mucho más estable en presencia de metanol (80% de actividad tras 96 h de reacción) que la de *C. rugosa*, que se inactivó rápidamente (Gómez et al. 2014).

1.3.1.3 Clonación y expresión

La secuenciación del gen que codifica la esterol esterasa de *O. piceae* reveló una identidad de secuencia de ~40% con las lipasas de *C. rugosa* y *G. candidum*. Su modelado, en base a la estructura de las lipasas 1 y 3 de *C. rugosa*, reveló que el sitio de unión a sustrato era similar al de estas enzimas aunque mostraba algunos cambios en la zona de la tapadera y mayor número de aminoácidos aromáticos en la zona del túnel, hechos que podrían estar implicados en su mejor eficacia catalítica (Calero-Rueda et al. 2009).

Esta enzima se ha expresado con éxito en la levadura *P. pastoris* obteniéndose una proteína mucho más eficaz (~ x10) que la nativa en la hidrólisis de triglicéridos y ésteres de esteroles al ser más soluble. La explicación de este fenómeno reside en que la proteína recombinante presenta entre 4-8 aminoácidos extra en su extremo amino terminal debido a la estrategia de clonación utilizada, que deja dos sitios de restricción adicionales, y al incorrecto procesamiento del péptido señal (factor α) por la peptidasa STE13 del huésped (Barba Cedillo et al. 2012).

1.4 EXPRESIÓN HETERÓLOGA DE LAS LIPASAS/ESTEROL ESTERASAS

El uso de cualquier enzima con fines biotecnológicos requiere su producción en un sistema que permita obtener grandes cantidades del biocatalizador a bajo coste. Existen multitud de sistemas de expresión disponibles, cada uno con sus características particulares, pero es necesario tener en cuenta que la elección del hospedador condiciona la expresión de la proteína y/o su posterior aplicación (Schmidt 2004).

1.4.1 Hospedadores procariotas

Los organismos procariotas suelen ser la primera elección para la expresión recombinante de proteínas porque son fácilmente manipulables, bien conocidos y tienen tiempos de generación cortos (Schmidt 2004). La bacteria Gram negativa *Escherichia coli* es el hospedador más utilizado, ya que se dispone de gran cantidad de información genética y fisiológica y se conocen protocolos y herramientas moleculares necesarios para su manipulación.

Como contrapartida, hay factores que limitan el uso de esta bacteria para expresar proteínas eucariotas, como las diferencias en el uso de codones o su incapacidad de llevar a cabo modificaciones post-traduccionales, como la glicosilación o la fosforilación de proteínas, o de formar puentes disulfuro, a veces necesarios para la funcionalidad de las proteínas. Otro inconveniente es que los altos niveles de proteína recombinante en la célula pueden causar la formación de agregados proteicos, conocidos como cuerpos de inclusión (Carrio y Villaverde 2002). Aunque dentro de estos agregados la proteína de interés se encuentra protegida de la degradación proteolítica, es necesaria una laboriosa tarea de solubilización y replegado para obtenerla en su forma activa, y el proceso no es viable a escala industrial. No obstante, *E. coli* ha sido empleada con éxito para la expresión de lipasas bacterianas, como las de *B. cepacia* y *Bacillus thermocatenulatus* (Rúa et al. 1998; Schmidt-Dannert 1999). También se han expresado en esta bacteria lipasas eucariotas, como la lipasa 4 de *C. rugosa*, pero encontrando que solo un 10% de CRL4 se obtenía en forma soluble fuera de cuerpos de inclusión (Tang et al. 2000), y las lipasas de *A. niger* y *Rhizopus delemar* que se encontraban en cuerpos de inclusión y requerían ser replegadas *in vitro* (Joerger et al. 1993; Shu et al. 2007).

Esta bacteria está demostrando su validez para la expresión de diferentes peroxidasas fúngicas en cuerpos de inclusión ya que, tras optimizar los protocolos de replegado *in vitro*, se produce proteína suficiente para llevar a cabo experimentos de diseño racional destinados a la mejora de las propiedades catalíticas de estas enzimas (Morales et al. 2012; Pérez-Boada et al. 2002). Además, recientemente se ha logrado expresar en forma soluble alguna de estas proteínas (Fernández-Fueyo et al. 2015).

1.4.2 Hospedadores eucariotas

Los hospedadores eucariotas ofrecen multitud de posibilidades siendo las levaduras y hongos filamentosos los más empleados a escala industrial (Valero 2012). Las levaduras brindan numerosas ventajas por ser organismos unicelulares capaces de llevar a cabo modificaciones post-traduccionales, de fácil manejo y alta tasa de crecimiento.

S. cerevisiae fue el primer eucariota utilizado para la expresión heteróloga de proteínas terapéuticas (Böer et al. 2007), siendo la vacuna de la hepatitis B la primera vacuna recombinante que se comercializó (Valenzuela et al. 1982). El conocimiento de su genética y fisiología, así como su estatus GRAS (*Generally Recognized As Safe*), favorecen su aplicación en la industria alimentaria. En 2009, prácticamente todos los productos derivados de levaduras en el mercado de la alimentación fueron producidos en *S. cerevisiae* (Mattanovich et al. 2012).

Además, esta levadura se ha desarrollado como plataforma de evolución dirigida por su alta eficiencia de transformación, estabilidad de los vectores episomales disponibles, alta fidelidad de replicación (barajado *in vivo* del ADN o *DNA shuffling*) y elevada frecuencia de recombinación homóloga, que facilita la diversidad genética (González-Pérez et al. 2014). En este sentido, destacar que se está utilizando con éxito para la obtención de nuevas variantes de lacasas y oxidasas fúngicas (Alcalde 2015; Pardo y Camarero 2015). Sin embargo, el empleo de *S. cerevisiae* como hospedador heterólogo se encuentra limitado por distintos factores, como su fuerte metabolismo fermentativo, el bajo rendimiento de la producción de enzimas recombinantes, la hiperglicosilación y la baja capacidad de secreción de las proteínas sintetizadas (Cereghino y Cregg 1999). Entre las lipasas expresadas en esta levadura destacan las de *G. candidum* (Bertolini et al. 1995) y la CRL1 de *C. rugosa* (Brocca et al. 1998).

Por otro lado, la levadura metilotrófica *Pichia pastoris*, reclasificada al género *Komagataella* por Yamada y col. (1995), comenzó a utilizarse a principios de los 70 para la producción de biomasa microbiana (Gellissen et al. 2005). En los últimos años se ha incrementado su uso como hospedador heterólogo, ya que: i) no requiere medios complejos para alcanzar densidades celulares elevadas, ii) posee una alta capacidad de secreción, iii) la posterior recuperación y purificación de la proteína recombinante se ve facilitada por la baja cantidad de proteínas nativas que secreta al medio extracelular y, iv) en el caso de las lipasas, *P. pastoris* carece de esta actividad (Cregg et al. 2000; Krainer et al. 2012). Además, esta levadura presenta la ventaja de que las proteínas secretadas están menos glicosiladas que las producidas por *S.*

cerevisiae (Stratton et al. 1998). La capacidad de *P. pastoris* para utilizar metanol como única fuente de carbono es un aspecto crucial de su metabolismo. Esta levadura tiene dos alcohol oxidasas denominadas AOX1 y AOX2, siendo la AOX1 la de mayor actividad y su promotor, inducible por metanol, se utiliza generalmente para expresar otras proteínas debido a su estrecha regulación (Cereghino y Cregg 2000). Sin embargo, el uso de metanol supone una importante desventaja en el proceso de escalado, y por ello se han propuesto promotores alternativos, como el promotor constitutivo de la gliceraldehído 3-fosfato deshidrogenasa (GAP) que permite obtener niveles de enzima similares. Entre las lipasas extracelulares recombinantes producidas con éxito en esta levadura se encuentran las de las bacterias *P. fluorescens*, *T. lanuginosus* y *Bacillus cereus*, las diferentes isoenzimas de las levaduras *C. rugosa*, *C. antarctica* y *G. candidum,* las de varias especies de los hongos filamentosos *Rhizopus* y *Rhizomucor* y las lipasas pancreáticas humana y porcina (Valero 2012). También se han expresado en *P. pastoris* las esterol esterasas de *O. piceae* (Barba Cedillo et al. 2012) y *M. albomyces* (Kontkanen et al. 2006a).

1.5 BÚSQUEDA DE NUEVAS ENZIMAS Y MEJORA DE SUS PROPIEDADES

Como se ha mencionado anteriormente, el extenso campo de aplicación de las lipasas y esterol esterasas las hace muy atractivas desde el punto de vista biotecnológico. La búsqueda de nuevas enzimas con propiedades más robustas y versátiles continúa siendo de gran interés y por esto, actualmente, se siguen realizando cribados de muestras ambientales para encontrar nuevas enzimas. Sin embargo, aunque los microorganismos constituyen la mayor reserva de diversidad genética del planeta, las especies cultivables representan menos del 1%. Por esta razón se han buscado métodos alternativos, que consisten en realizar cribados funcionales en librerías metagenómicas o en los genomas de microorganismos depositados en bases de datos (Adrio and Demain 2014). Esto ha permitido explorar ambientes extremos, como la tundra ártica, las chimeneas volcánicas o los ecosistemas marinos, y obtener nuevas enzimas, entre ellas lipasas, con interesantes características de

termoestabilidad o enantioselectividad (Fernández-Álvaro et al. 2010; Jeon et al. 2009) .

1.5.1 Búsqueda de nuevas enzimas en genomas y metagenomas

En los últimos años, gracias a las plataformas de secuenciación masiva de ADN, tanto la genómica como la metagenómica han experimentado un gran impulso (Kaul and Asano 2012). Ello, unido al desarrollo de la informática y al gran aumento de la capacidad de computación, ha hecho posible el almacenamiento de una inmensa cantidad de secuencias en bases de datos. Muchas de ellas se encuentran en servidores públicos de almacenamiento de secuencias, como NCBI, Genbank, o Uniprot, o de proteínas, como *Protein Data Bank* (PDB), aunque también existen bases específicas de lipasas, como LED. De esta forma, se dispone de la posibilidad de explorar toda la información acumulada en estas bases de datos, a través de lo que se denomina "minería" de genomas y metagenomas (Challis 2008). Esta se basa en la búsqueda de motivos conservados en secuencias con alta homología, los análisis filogenéticos y la construcción de modelos tridimensionales de estas proteínas hipotéticas, con el fin de encontrar nuevas enzimas con características mejoradas y predecir su funcionalidad (Barriuso et al. 2013; Barriuso y Martínez 2015). El desarrollo de multitud de herramientas bioinformáticas ha contribuido en gran medida a estos avances. El portal ExPASy, del *Swiss Institute of Bioinformatics*, recoge muchas de las herramientas más utilizadas en estos estudios (Artimo et al. 2012).

1.5.2 Mejora de biocatalizadores mediante ingeniería de proteínas

La mejora de enzimas conocidas es posible gracias a la ingeniería de proteínas mediante técnicas de diseño racional o evolución dirigida, encaminadas a la optimización de alguna propiedad catalítica de interés o a la creación de nuevas funciones enzimáticas en una proteína.

El diseño racional consiste en la mutación de posiciones concretas de la secuencia de aminoácidos del biocatalizador, seleccionadas en base a modelos o estructuras cristalográficas, que podrían contribuir a la mejora de su actividad catalítica. En este sentido, la lipasa B de *C. antarctica* (CalB), uno de los biocatalizadores más empleados en síntesis orgánica tanto a escala de

laboratorio como comercial, ha sido ampliamente modificada a través del diseño racional para otorgarle nuevas propiedades, como la mejora de su enantioselectividad frente a alcoholes secundarios o de su estabilidad en solventes orgánicos (Magnusson et al. 2005; Park et al. 2012; Rotticci et al. 2001). Sin embargo, el diseño racional de las enzimas no siempre genera los resultados esperados, ya que la relación estructura/función de las proteínas es muy compleja. Es necesario tener en cuenta que las enzimas, al interaccionar con los sustratos y con el entorno, sufren modificaciones que pueden no quedar recogidas en las estructuras cristalográficas obtenidas en unas determinadas condiciones y, por ello, es complicado predecir ciertos aspectos de la función enzimática y/o de las interacciones que determinan parámetros como la estabilidad (Arnold y Volkov 1999).

Por otro lado, la evolución molecular dirigida se presenta como una estrategia para la que no se requiere información estructural de las proteínas objeto de mejora. Esta técnica recrea a escala de laboratorio los procesos claves de la evolución natural (mutación, recombinación y selección). Mediante procesos de mutagénesis aleatoria y/o recombinaciones en el material genético que codifica una o varias proteínas, se crea una diversidad genética que posteriormente se expresa y explora bajo las condiciones en las que se quiere mejorar la enzima, tales como su nivel de producción, o su estabilidad a pH, temperatura o solventes, entre otros (Bloom et al. 2004). Sin embargo, para que estos experimentos puedan tener éxito son necesarias tres herramientas fundamentales:

- un sistema de expresión heteróloga adecuado. *E. coli* es uno de los más empleados, aunque presenta limitaciones para la expresión de proteínas eucariotas. En este caso suele utilizarse *S. cerevisiae* (Arnold y Georgiou 2003; Camarero et al. 2012; González-Pérez et al. 2012) y también *P. pastoris* a pesar de su menor eficiencia de transformación (Engström et al. 2010).
- el desarrollo de métodos de generación de diversidad génica (mutagénesis aleatorias, mutagénesis saturada y diversos procesos de recombinación tanto *in vitro* como *in vivo*).

- un método de cribado fiable y reproducible para discriminar entre las variantes obtenidas.

Algunos ejemplos de lipasas mejoradas por evolución dirigida utilizando distintos sistemas de expresión son: i) la obtención de una variante de CalB en *S. cerevisiae* resistente a la inactivación térmica (Korman et al. 2013); ii) la conversión en fosfolipasa de la lipasa de *Staphylococcus aureus* expresada en *E. coli* (van Kampen and Egmond 2000); y iii) el incremento de la enantioselectividad de la lipasa A de *C. antarctica* producida en *P. pastoris* frente a ésteres sustituidos en la posición alfa (Engström et al. 2010).

1.6 BIBLIOGRAFÍA

Adrio JL, Demain AL (2014) Microbial enzymes: tools for biotechnological processes. Biomolecules 4:117-139

Alcalde M (2015) Engineering the ligninolytic enzyme consortium. Trends Biotechnol 33:155-162

Allen LH (2000) Pitch control in paper mills. In: Back EL, Allen LH (eds) Pitch control, wood resin and deresination. TAPPI Press, Atlanta, pp 307-328

Arnold FH, Volkov AA (1999) Directed evolution of biocatalysts. Curr Opin Chem Biol 3:54-59

Arnold FH, Georgiou G (2003) Directed enzyme evolution. Screening and selection methods. Humana Press, Totowa

Arnold RG, Shahani KM, Dwivedi BK (1975) Application of lipolytic enzymes to flavor development in dairy products. J Dairy Sci 58:1127-1143

Artimo P, Jonnalagedda M, Arnold K, Baratin D, Csardi G, de Castro E, Duvaud S, Flegel V, Fortier A, Gasteiger E et al. (2012) ExPASy: SIB bioinformatics resource portal. Nucleic Acids Res 40:597-603

Barba Cedillo V, Plou FJ, Martínez MJ (2012) Recombinant sterol esterase from *Ophiostoma piceae*: an improved biocatalyst expressed in *Pichia pastoris*. Microb Cell Fact 11:73

Barba Cedillo V, Prieto A, Martínez AT, Martínez MJ (2013a) Procedimiento de acilación para la obtención de compuestos de interés alimenticio y/o farmacéutico utilizando esterol esterasas fúngicas. Patent No. ES 2395582 B1

Barba Cedillo V, Prieto A, Martínez MJ (2013b) Potential of *Ophiostoma piceae* sterol esterase for biotechnologically relevant hydrolysis reactions. Bioengineered 4:249-253

Barriuso J, Prieto A, Martínez MJ (2013) Fungal genomes mining to discover novel sterol esterases and lipases as catalysts. BMC Genomics 14:712-719

Barriuso J, Martínez MJ (2015) *In silico* metagenomes mining to discover novel esterases with industrial application by sequential search strategies. J Microbiol Biotechn, 25:723-728

Bertolini MC, Schrag JD, Cygler M, Ziomek E, Thomas DY, Vernet T (1995) Expression and characterization of *Geotrichum candidum* lipase I gene - comparison of specificity profile with lipase II. Eur J Biochem 228:863-869

Bloom JD, Wilke CO, Arnold FH, Adami C (2004) Stability and the evolvability of function in a model protein. Biophys J 86:2758-2764

Böer E, Steinborn G, Kunze G, Gellissen G (2007) Yeast expression platforms. Appl Microbiol Biotechnol 77:513-523

Bornscheuer UT (2002) Microbial carboxyl esterases: classification, properties and application in biocatalysis. FEMS Microbiol Rev 26:73-81

Brocca S, Schmidt-Dannert C, Lotti M, Alberghina L, Schmid RD (1998) Design, total synthesis, and fuctional overexpression of the *Candida rugosa lip*1 gene coding for a major industrial lipase. Protein Sci 7:1415-1422

Buisman G, van Helteren C, Kramer G, Veldsink J, Derksen J, Cuperus F (1998) Enzymatic esterifications of functionalized phenols for the synthesis of lipophilic antioxidants. Biotechnol lett 20:131-136

Cajal Y, Svendsen A, De Bolós J, Patkar SA, Alsina MA (2000) Effect of the lipid interface on the catalytic activity and spectroscopic properties of a fungal lipase. Biochimie 82:1053-1061

Calero-Rueda O (2001) Búsqueda de enzimas fúngicas con actividad esterasa para el control biológico del "pitch". Universidad Complutense, Facultad de Ciencias Biológicas, Tesina.

Calero-Rueda O, Gutiérrez A, del Río JC, Muñoz MC, Plou FJ, Martínez ÁT, Martínez MJ (2002a) Method for the enzymatic control of pitch deposits formed during paper pulp production using an esterase that hydrolyses triglycerides and sterol esters. Patent No. WO 02/075045

Calero-Rueda O, Plou FJ, Ballesteros A, Martínez AT, Martínez MJ (2002b) Production, isolation and characterization of a sterol esterase from *Ophiostoma piceae*. BBA Proteins Proteomics 1599:28-35

Calero-Rueda O, Barba V, Rodriguez E, Plou F, Martínez AT, Martínez MJ (2009) Study of a sterol esterase secreted by *Ophiostoma piceae*: Sequence, model and biochemical properties. Biochim Biophys Acta 1794:1099-1106

Camarero S, Pardo I, Cañas AI, Molina P, Record E, Martínez AT, Martínez MJ, Alcalde M (2012) Engineering platforms for directed evolution of laccase from *Pycnoporus cinnabarinus*. Appl Environ Microbiol 78:1370-1384

Carrio MM, Villaverde A (2002) Construction and deconstruction of bacterial inclusion bodies. J Biotechenol 96:3-12

Carvalho PO, Contesini FJ, Bizaco R, Calafatti SA, Macedo GA (2006) Optimization of enantioselective resolution of racemic ibuprofen by native lipase from *Aspergillus niger*. J Ind Microbiol Biotechnol 33:713-718

Casas-Godoy L, Duquesne S, Bordes F, Sandoval G, Marty A (2012) Lipases: an overview. In: Sandoval G (ed) Lipases and Phospholipases. Humana Press-Springer, New York, pp 3-30

Cereghino GPL, Cregg JM (1999) Applications of yeast in biotechnology: protein production and genetic analysis. Curr Opin Biotech 10:422-427

Cereghino JL, Cregg JM (2000) Heterologous protein expression in the methylotrophic yeast *Pichia pastoris*. FEMS Microbiol Rev 24:45-66

Challis GL (2008) Genome mining for novel natural product discovery. J Med Chem 51:2618-2628

Chen JCH, Miercke LJW, Krucinski J, Starr JR, Saenz G, Wang X, Spilburg CA, Lange LG, Ellsworth JL, Stroud RM (1998) Structure of bovine pancreatic cholesterol esterase at 1.6 Å: novel structural features involved in lipase activation. Biochemistry 37:5107-5117

Chen T, Wang Z, Gao Y, Breuil C, Hatton JV (1994) Wood extractives and pitch problems: Analysis and partial removal by biological treatment. Appita 47:463-466

Chen ZY, Jiao R, Ma KY (2008) Cholesterol-lowering nutraceuticals and functional foods. J Agr Food Chem 56:8761-8773

Ciafardini G, Zullo BA, Tride A (2006) Lipase production by yeasts from extra virgin olive oil. Food Microbiol 23:60-67

Commenil P, Belingheri L, Sancholle M, Dehorter B (1995) Purification and properties of an extracellular lipase from the fungus *Botrytis cinerea*. Lipids 30:351-356

Commenil P, Belingheri L, Bauw G, Dehorter B (1999) Molecular characterization of a lipase induced in *Botrytis cinerea* by components of grape berry cuticle. Physiol Mol Plant P 55:37-43

Cregg JM, Cereghino JL, Shi JY, Higgins DR (2000) Recombinant protein expression in *Pichia pastoris*. Mol Biotechnol 16:23-52

Cygler M, Schrag J (1999) Structure and conformational flexibility of *Candida rugosa* lipase. Biochim Biophys Acta 1441:205-214

D'Annibale A, Sermanni GG, Federici F, Petruccioli M (2006) Olive-mill wastewaters: a promising substrate for microbial lipase production. Biores Technol 97:1828-1833

Divakar S (2013) Lipases enzymatic transformation. Springer, New Delhi, pp 23-38

Domínguez de María P, Sánchez-Montero JM, Sinisterra JV, Alcántara AR (2006) Understanding *Candida rugosa* lipases: an overview. Biotechnol Adv 24:180-196

Engström J, Nyhlén J, Sandström AG, Bäckvall JE (2010) Directed evolution of an enantioselective lipase with broad substrate scope for hydrolysis of α-substituted esters. J Am Chem Soc 132:7038-7042

Faigl F, Thurner A, Farkas F, Battancs M, Poppe L (2007) Synthesis and enantioselective rearrangement of (Z)-4-triphenylmethoxy-2,3-epoxybutan-1-ol enantiomers. Chirality 19:197-202

Fernández-Álvaro E, Kourist R, Winter J, Bottcher D, Liebeton K, Naumer C, Eck J, Leggewie C, Jaeger KE, Streit W et al. (2010) Enantioselective kinetic resolution of phenylalkyl carboxylic acids using metagenome-derived esterases. Microb Biotechnol 3:59-64

Fernández-Fueyo E, Linde D, Almendral D, López-Lucendo MF, Ruiz-Dueñas FJ, Martínez AT (2015) Description of the first fungal dye-decolorizing peroxidase oxidizing manganese (II). Appl Microbiol Biotechnol. doi: 10.1007/s00253-015-6665-3

Ferrer P, Montesinos JL, Valero F, Sola C (2001) Production of native and recombinant lipases by *Candida rugosa* - A review. Appl Biochem Biotech 95:221-255

Ferrer P, Alarcón M, Ramón R, Benaiges MD, Valero F (2009) Recombinant *Candida rugosa* LIP2 expression in *Pichia pastoris* under the control of the AOX1 promoter. Biochem Eng J 46:271-277

Fischer M, Pleiss J (2003) The Lipase Engineering Database: a navigation and analysis tool for protein families. Nucleic Acids Res 31:319-321

Gaillardin C (2010) Lipases as pathogenicity factors of fungi. In: Timmis K (ed) Handbook of hydrocarbon and lipid microbiology. Springer Berlin Heidelberg, pp 3259-3268

Gellissen G, Kunze G, Gaillardin C, Cregg JM, Berardi E, Veenhuis M, van der Klei I (2005) New yeast expression platforms based on methylotrophic *Hansenula polymorpha* and *Pichia pastoris* and on dimorphic *Arxula adeninivorans* and *Yarrowia lipolytica* - A comparison. FEMS Yeast Res 5:1079-1096

Ghosh D, Wawrzak Z, Pletnev VZ, Li N, Kaiser R, Pangborn W, Jörnvall H, Erman M, Duax WL (1995) Structure of uncomplexed and linoleate-bound *Candida cylindracea* cholesterol esterase. Structure 3:279-288

Gómez BJ, Prieto A, Barba Cedillo V, Martín J, Martínez MJ (2014) Interesterificación de trioleína para la producción de biodiesel, catalizada por la esterol esterasa de *Ophiostoma piceae*. IV Congreso de Microbiología Industrial y Biotecnología (SEM) 14-16 Nov Salamanca. Póster

González-Pérez D, García-Ruiz E, Alcalde M (2012) *Saccharomyces cerevisiae* in directed evolution. An efficient tool to improve enzymes. Bioengineered 3:172-177

González-Pérez D, García-Ruiz E, Ruiz-Duenas FJ, Martínez AT, Alcalde M (2014) Structural determinants of oxidative stabilization in an evolved versatile peroxidase. ACS Catalysis 4:3891-3901

Gray GL, Power SD, Poulose AJ (1995) Lipase from *Pseudomonas mendocina* having cutinase activity. Patent No. US5389536 A

Grochulski P, Li YG, Schrag JD, Bouthillier F, Smith P, Harrison D, Rubin B, Cygler M (1993) Insights into interfacial activation from an open structure of *Candida rugosa* lipase. J Biol Chem 268:12843-12847

Grochulski P, Li Y, Schrag JD, Cygler M (1994) Two conformational states of *Candida rugosa* lipase. Protein Sci 3:82-91

Gutiérrez A, del Río JC, Martínez MJ, Martínez AT (2001) The biotechnological control of pitch in paper pulp manufacturing. Trends Biotechnol 19:340-348

Haridas S, Wang Y, Lim L, Alamouti SM, Jackman S, Docking R, Robertson G, Birol I, Bohlmann J, Breuil C (2013) The genome and transcriptome of the pine saprophyte *Ophiostoma piceae*, and a comparison with the bark beetle-associated pine pathogen *Grosmannia clavigera*. BMC Genomics 14:373

Hasan F, Shah AA, Hameed A (2006) Industrial applications of microbial lipases. Enzyme Microb Technol 39:235-251

Holmquist M (2000) Alpha/beta-hydrolase fold enzymes: structures, functions and mechanisms. Curr Protein Pept Sc 1:209-235

Hoshino A, Isono Y (2002) Degradation of aliphatic polyester films by commercially available lipases with special reference to rapid and complete degradation of poly(L-lactide) film by lipase PL derived from *Alcaligenes* sp. Biodegradation 13:141-147

Irie Y (1990) Enzymatic pitch control in papermaking system. Abs 1990 Papermakers Confer, 23-25 April, Atlanta

Jaeger KE, Reetz MT (1998) Microbial lipases form versatile tools for biotechnology. Trends Biotechnol 16:396-403

Jaeger KE, Dijkstra BW, Reetz MT (1999) Bacterial biocatalysts: molecular biology, three-dimensional structures, and biotechnological applications of lipases. Annu Rev Microbiol 53:315-351

Jaeger KE, Eggert T (2002) Lipases for biotechnology. Curr Opin Biotechnol 13:390-397

Jeon JH, Kim JT, Kim YJ, Kim HK, Lee HS, Kang SG, Kim SJ, Lee JH (2009) Cloning and characterization of a new cold-active lipase from a deep-sea sediment metagenome. Appl Microbiol Biotechnol 81:865-874

Jirage D, Tootle TL, Reuber TL, Frost LN, Feys BJ, Parker JE, Ausubel FM, Glazebrook J (1999) *Arabidopsis thaliana* PAD4 encodes a lipase-like gene that is important for salicylic acid signaling. Proc Natl Acad Sci U S A 96:13583-13588

Joerger RD, Haas, M.J. (1993) Overexpression of a *Rhizopus delemar* lipase gene in *Escherichia coli*. Lipids 28:81-88

Juniper BE, Jeffree CE (1983) Plant surfaces. Eduard Arnold, Baltimore

Kaul P, Asano Y (2012) Strategies for discovery and improvement of enzyme function: state of the art and opportunities. Microb Biotechnol 5:18-33

Kontkanen H, Reinikainen T, Saloheimo M (2006a) Cloning and expression of a *Melanocarpus albomyces* steryl esterase gene in *Pichia pastoris* and *Trichoderma reesei*. Biotechnol Bioeng 94:407-41

Kontkanen H, Tenkanen M, Reinikainen T (2006b) Purification and characterisation of a novel steryl esterase from *Melanocarpus albomyces*. Enzyme Microb Technol 39:265-273

Korman TP, Sahachartsiri B, Charbonneau DM, Huang GL, Beauregard M, Bowie JU (2013) Dieselzymes: development of a stable and methanol tolerant lipase for biodiesel production by directed evolution. Biotechnol Biofuels 6:70

Kourist R, Jochens H, Bartsch S, Kuipers R, Padhi SK, Gall M, Bottcher D, Joosten HJ, Bornscheuer UT (2010) The alpha/beta-hydrolase fold 3DM database (ABHDB) as a tool for protein engineering. Chembiochem 11:1635-1643

Krainer FW, Dietzsch C, Hajek T, Herwig C, Spadiut O, Glieder A (2012) Recombinant protein expression in *Pichia pastoris* strains with an engineered methanol utilization pathway. Microb Cell Fact 11:22

Krugener S, Zelenaa K, Zorn H, Nimtz M, Bergera RG (2009) Heterologous expression of an extra-cellular lipase from the basidiomycete *Pleurotus sapidus*. J Mol Catal B-Enzym 57:16-21

Kumar A, Gross RA (2000) *Candida antartica* lipase B catalyzed polycaprolactone synthesis: effects of organic media and temperature. Biomacromolecules 1:133-138

Lotti M, Tramontano A, Longhi S, Fusetti F, Brocca S, Pizzi E, Alberghina L (1994) Variability within the *Candida rugosa* lipases family. Protein Eng 7:531-535

Maeda A, Mizuno T, Bunya M, Sugihara S, Nakayama D, Tsunasawa S, Hirota Y, Sugihara A (2008) Characterization of novel cholesterol esterase from *Trichoderma* sp AS59 with high ability to synthesize steryl esters. J Biosci Bioeng 105:341-349

Magnusson AO, Rotticci-Mulder JC, Santagostino A, Hult K (2005) Creating space for large secondary alcohols by rational redesign of *Candida antarctica* lipase B. Chembiochem 6:1051-1056

Mancheño JM, Pernas MA, Martínez MJ, Ochoa B, Rúa ML, Hermoso.J.A. (2003) Structural insights into the lipase/esterase behavior in the *Candida rugosa* lipases family: crystal structure of the lipase 2 isoenzyme at 1.97 Å resolution. J Mol Biol 332:1059-1069

Marangoni AG (2002) Lipases: estructures, function and properties. In: Kuo TM, Gardner HW (eds) Lipid biotechnology. Marcel Dekker, New York, pp 402-434

Matsukura M, Fujita Y, Sakaguchi H (1990) On the use of Resinase^{TM} A for pitch control. Novo Publication A-6122:1-7

Mattanovich D, Branduardi P, Dato L, Gasser B, Sauer M, Porro D (2012) Recombinant protein production in yeasts. In: Lorence A (ed) Recombinant gene expression: reviews and protocols. Humana Press-Springer, Totowa, pp 329-358

Maugard T, Rejasse B, Legoy MD (2002) Synthesis of water-soluble retinol derivatives by enzymatic method. Biotechnol Progr 18:424-428

Minoguchi M, Muneyuki T (1989) Immobilization of lipase on polyacrylamide and its use in detergents. Patent No. 1285188

Miranda R, Balea A, de la Blanca ES, Carrillo I, Blanco A (2008) Identification of recalcitrant stickies and their sources in newsprint production. Ind Eng Chem Res 47:6239-6250

Monecke P, Friedemann R, Naumann S, Csuk R (1998) Molecular modelling studies on the catalytic mechanism of *Candida rugosa* lipase. J Mol Model 4:395-404

Morales M, Mate MJ, Romero A, Martínez MJ, Martínez AT, Ruiz-Dueñas FJ (2012) Two oxidation sites for low redox-potential substrates: a directed mutagenesis, kinetic and crystallographic study on *Pleurotus eryngii* versatile peroxidase. J Biol Chem 287:41053-41067

Mukherjee M (2003) Human digestive and metabolic lipases - a brief review. J Mol Catal B-Enzym 22:369-376

Nardini M, Dijkstra BW (1999) α/β hydrolase fold enzymes: the family keeps growing. Curr Opin Struc Biol 9:732-737

Nguyen Q, Bujna E, Styevkó G, Rezessy-Szabó J, Hoschke A (2015) Fungal biomolecules for the food industry. In: Gupta VK, Mach RL, Sreenivasaprasad S (eds) Fungal biomolecules: sources, applications and recent developments. Wiley and sons, Oxford, pp 11-38

Noureddini H, Gao X, Philkana RS (2005) Immobilized *Pseudomonas cepacia* lipase for biodiesel fuel production from soybean oil. Biores Technol 96:769-777

Okawa Y, Yamaguchi T (1977) Studies on sterol-ester hydrolase from *Fusarium oxysporum*. I. Partial purification and properties. J Biochem 81:1209-1215

Ollis DL, Cheah E, Cygler M, Dijkstra B, Frolow F, Franken SM, Harel M, Remington SJ, Silman I, Schrag J et al. (1992) The α/β hydrolase fold. Protein Eng 5:197-211

Pardo I, Camarero S (2015) Laccase engineering by rational and evolutionary design. Cell Mol Life Sci 72:897-910

Park HJ, Joo JC, Park K, Yoo YJ (2012) Stabilization of *Candida antarctica* lipase B in hydrophilic organic solvent by rational design of hydrogen bond. Biotechnol Bioproc E 17:722-728

Pérez-Boada M, Doyle WA, Ruiz-Dueñas FJ, Martínez MJ, Martínez AT, Smith AT (2002) Expression of *Pleurotus eryngii* versatile peroxidase in *Escherichia coli* and optimisation of *in vitro* folding. Enzyme Microb Technol 30:518-524

Pernas MA, López C, Rúa ML, Hermoso J (2001) Influence of the conformational flexibility on the kinetics and dimerisation process of two *Candida rugosa* lipase isoenzymes. FEBS Letters 501:87-91

Pernas MA, Pastrana L, Fucinos P, Rua ML (2009) Regulation of the interfacial activation within the *Candida rugosa* lipase family. J Phys Org Chem 22:508-514

Pihko AJ, Lundell K, Kanerva L, Koskinen AMP (2004) Enantioselective synthesis of a hindered furyl substituted allyl alcohol intermediate: a case study in asymmetric synthesis. Tetrahedron-Asymmetr 15:1637-1643

Pleiss J, Fischer M, Schimd RD (1998) Anatomy of lipase binding sites: the scissile fatty acid binding site. Chem Phys Lipids 93:67-80

Pleiss J, Fischer M, Peiker M, Thiele C, Schmid RD (2000) Lipase engineering database: understanding and exploiting sequence-structure-function relationships. J Mol Catal B-Enzym 10:491-508

Pletnev V, Addlagatta A, Wawrzak Z, Duax W (2003) Three-dimensional structure of homodimeric cholesterol esterase-ligand complex at 1.4 Å resolution. Acta Crystallogr D Biol Crystallogr 59 :50-56

Rahman RNZA, Salleh A, Basri M (2006) Lipases: Introduction. In: Rahman RNZRA, Salleh AB, Basri M (eds) New Lipases and Proteases. Nova Science, New York, pp 1-14

Rajmohan S, Dodd CER, Waites WM (2002) Enzymes from isolates of *Pseudomonas fluorescens* involved in food spoilage. J Appl Microbiol 93:205-213

Reetz MT (2002) Lipases as practical biocatalysts. Curr Opin Chem Biol 6:145-150

Reis H, Pfiffi S, Hahn M (2005) Molecular and functional characterization of a secreted lipase from *Botrytis cinerea*. Mol Plant Pathol 6:257-267

Rigo E, Rigoni RE, Lodea P, de Oliveira D, Freire DMG, Di Luccio M (2008) Application of different lipases as pretreatment in anaerobic treatment of wastewater. Environ Eng Sci 25:1243-1248

Rivera I, Mateos-Diaz JC, Sandoval G (2012) Plant lipases: partial purification of *Carica papaya* lipase. In: Sandoval G (ed) Lipases and Phospholipases. Humana Press-Springer, New York, pp 115-122

Rotticci D, Rotticci-Mulder JC, Denman S, Norin T, Hult K (2001) Improved enantioselectivity of a lipase by rational protein engineering. Chembiochem 2:766-770

Rúa ML, Atomi H, Schmidt-Dannert C, Schmid RD (1998) High-level expression of the thermoalkalophilic lipase from *Bacillus thermocatenulatus* in *Escherichia coli*. Appl Microbiol Biotechnol 49:405-410

Rudd EA, Brockman HL (1984) Pancreatic carboxyl ester lipase (cholesterol esterase). In: Borgström B, Brockman HL (eds) Lipases. Elsevier Science Publishers, Amsterdam, pp 185-204

Schmid RD, Verger R (1998) Lipases: Interfacial enzymes with atractive applications. Angew Chem 37:1609-1633

Schmidt FR (2004) Recombinant expression systems in the pharmaceutical industry. Appl Microbiol Biotechnol 65:363-372

Schmidt-Dannert C (1999) Recombinant microbial lipases for biotechnological applications. Bioorgan Med Chem 7:2123-2130

Schrag JD, Li Y, Wu S, Cygler M (1991) Ser-His-Glu triad forms the catalytic site of the lipase from *Geotrichum candidum*. Nature 351:761-764

Schrag JD, Cygler M (1993) 1.8 Å Refined structure of the lipase from *Geotrichum candidum*. J Mol Biol 230:575-591

Secundo F, Carrea G, Tarabiono C, Gatti-Lafranconi P, Brocca S, Lotti M, Jaeger KE, Puls M, Eggert T (2006) The lid is a structural and functional determinant of lipase activity and selectivity. J Mol Catal B-Enzym 39:166-170

Shu Z-Y, Yan Y-J, Yang J-K (2007) *Aspergillus niger* lipase: gene cloning, over-expression in *Escherichia coli* and in vitro refolding. Biotechnol lett 29:1875-1879

Sidebotton M, Charton E, Dunn PPJ, Mycock G, Davies C, Sutton JL, Macrae AR, Slabas AR (1991) *Geotrichum candidum* produces several lipases with markedly different sustrate specifities. Eur J Biochem 202:485-491

Singh AK, Mukhopadhyay M (2012) Overview of fungal lipase: a review. Appl Biochem Biotechnol 166:486-520

Stratton J, Chiruvolu V, Meagher M (1998) High cell-density fermentation. *Pichia* Protocols 103:107-120

Sugihara A, Shimada Y, Nomura A, Terai T, Imayasu M, Nagai Y, Nagao T, Watanabe Y, Tominaga Y (2002) Purification and characterization of a novel cholesterol esterase from *Pseudomonas aeruginosa*, with its application to cleaning lipid-stained contact lenses. Biosci Biotech Bioch 66:2347-2355

Takeda Y, Aono R, Doukyu N (2006) Purification, characterization, and molecular cloning of organic-solvent-tolerant cholesterol esterase from cyclohexane-tolerant *Burkholderia cepacia* strain ST-200. Extremophiles 10:269-277

Taketani S, Nishino T, Katsuki H (1980) Purification and properties of sterol-ester hydrolase from *Saccharomyces cerevisiae*. J Biochem 89:1667-1673

Tang SJ, Sun KH, Sun GH, hang TY, Lee GC (2000) Recombinant Expression of the *Candida rugosa lip4* Lipase in *Escherichia coli*. Protein Expr Purif 20:308-313

Uppenberg J, Hansen MT, Patkar S, Jones TA (1994) The sequence, crystal structure determination and refinement of two crystal forms of lipase B from *Candida antarctica*. Structure 2:293-308

Uwajima T, Terada O (1975) Purification and properties of an extracellular cholesterol ester hydrolaseof *Pseudomonas fluorescens*. Agric Biol Chem 39:1511-1512

Valenzuela P, Medina A, Rutter WJ (1982) Synthesis and assembly of hepatitis-B virus surface-antigen particles in yeast. Nature 298:347-350

Valero F (2012) Heterologous expression systems for lipases: a review. In: Sandoval G (ed) Lipases and Phospholipases. Humana Press-Springer, New York, pp 161-178

van der Deen H, Cuiper AD, Hof RP, vanOeveren A, Feringa BL, Kellogg RM (1996) Lipase-catalyzed second-order asymmetric transformations as resolution and synthesis strategies for chiral 5-(acyloxy)-2(5H)-furanone and pyrrolinone synthons. J Am Chem Soc 118:3801-3803

van Kampen MD, Egmond MR (2000) Directed evolution: from a staphylococcal lipase to a phospholipase. Eur J Lipid Sci Tech 102:717-726

van Pelt S, Teeuwen R, Janssen M, Sheldon R, Dunn P, Howard R, Kumar R, Martinez I, Wong J (2011) *Pseudomonas stutzeri* lipase: a useful biocatalyst for aminolysis reactions. Green Chem 13:1791-1798

Verger R (1997) Interfacial activation of lipases: fact and artifacts. Trends Biotechnol 15:32-38

Vernet T, Ziomek E, Recktenwald A, Schrag JD, Demontigny C, Tessier DC, Thomas DY, Cygler M (1993) Cloning and expression of *Geotrichum candidum* lipase II gene in yeast: probing of the enzyme active site by site-directed mutagenesis. J Biol Chem 268:26212-26219

Villeneuve P, Turon F, Caro Y, Escoffier R, Baréa B, Barouh B, Lago R, Piombo G, Pina M (2005) Lipase-catalyzed synthesis of canola phytosterols oleate esters as cholesterol lowering agents. Enzyme Microb Technol 37:150-155

Weber N, Weitkamp P, Mukherjee KD (2001) Fatty acid steryl, stanyl, and steroid esters by esterification and transesterification in vacuo using *Candida rugosa* lipase as catalyst. J Agric Food Chem 49:67-71

Yamada Y, Matsuda I, Maeda K, Mikata K (1995) The phylogenetic relationships of methanol-assimilating yeasts based on the partial sequences of 18S and 26S ribosomal-RNAs: the proposal of *Komagataella* gen. nov. (*Saccharomycetaceae*). Biosci Biotech Bioch 59:439-444

Yan J, Li A, Xu Y, Ngo TPN, Phua S, Li Z (2012) Efficient production of biodiesel from waste grease: one-pot esterification and transesterification with tandem lipases. Biores Technol 123:332-337

Yu XW, Sha C, Guo YL, Xiao R, Xu Y (2013) High-level expression and characterization of a chimeric lipase from *Rhizopus oryzae* for biodiesel production. Biotechnol Biofuels 6:29

Zorn H, Breithaupt DE, Takenberg M, Schwack W, Berger RG (2003) Enzymatic hydrolysis of carotenoid esters of marigold flowers (*Tagetes erecta* L.) and red paprika (*Capsicum annuum* L.) by commercial lipases and *Pleurotus sapidus* extracellular lipase. Enzyme Microb Technol 32:623-628

Zorn H, Bouws H, Takenberg M, Nimtz M, Getzlaff R, Breithaupt DE, Berger RG (2005) An extracellular carboxylesterase from the basidiomycete *Pleurotus sapidus* hydrolyses xanthophyll esters. Biol Chem 386:435-440

2 Objetivos

Como se comentó en el apartado anterior, la esterol esterasa/lipasa secretada por *O. piceae* (OPE) es una enzima muy interesante desde el punto de vista biotecnológico, por lo que el presente trabajo se centró en profundizar en su conocimiento y en el estudio de enzimas relacionadas. Los objetivos planteados en la presente Tesis Doctoral se exponen a continuación:

1. Explorar distintos sistemas de expresión heteróloga en busca del más apropiado para la expresión funcional de OPE.

2. Cristalizar y resolver la estructura tridimensional de OPE con el fin de llevar a cabo estudios estructura-función y conocer los mecanismos moleculares implicados en la catálisis enzimática.

3. Expresar, caracterizar y comparar nuevas enzimas seleccionadas de genomas fúngicos, similares a OPE.

4. Evaluar el potencial de las enzimas caracterizadas en el presente trabajo en distintas aplicaciones biotecnológicas.

3 Publicaciones/*Articles*

3.1 CHAPTER 1

Heterologous expression of a fungal sterol esterase/lipase in different hosts: Effect on solubility, glycosylation and production

María Eugenia Vaquero, Jorge Barriuso, Francisco Javier Medrano, Alicia Prieto, María Jesús Martínez

Journal of Bioscience and Bioengineering (2015)
doi:10.1016/j.jbiosc.2015.04.005

3.1.1 SUMMARY

Ophiostoma piceae secretes a versatile sterol-esterase (OPE) that shows high efficiency in both hydrolysis and synthesis of triglycerides and sterol esters. This enzyme produces aggregates in aqueous solutions, but the recombinant protein, expressed in *Komagataella* (synonym *Pichia*) *pastoris*, showed higher catalytic efficiency because of its higher solubility. This fact owes to a modification in the N-terminal sequence of the protein expressed in *Pichia pastoris*, which incorporated 4-8 additional amino acids, affecting its aggregation behavior. In this study we present a newly engineered *P. pastoris* strain with improved protein production. We also produced the recombinant protein in the yeast *Saccharomyces cerevisiae* and in the prokaryotic host *Escherichia coli*, corroborating that the presence of these N-terminal extra amino acids affected the protein's solubility. The OPE produced in the new *P. pastoris* strain presented the same physicochemical properties than the old one. An inactive form of the enzyme was produced by the bacterium, but the recombinant esterase from both yeasts was active even after its enzymatic deglycosylation, suggesting that the presence of N-linked carbohydrates in the mature protein is not essential for enzyme activity. Although the yield in *S. cerevisiae* was lower than that obtained in *P. pastoris*, this work demonstrates the importance of the choice of the heterologous host for successful production of soluble and active recombinant protein. In addition, *S. cerevisiae* constitutes a good engineering platform for improving the properties of this biocatalyst.

3.1.2 INTRODUCTION

Carboxylic ester hydrolases (EC 3.1.1) are a heterogeneous group of enzymes catalyzing the cleavage of ester bonds, including carboxylesterases (EC 3.1.1.1), triacylglycerol lipases (EC 3.1.1.3) and sterol esterases (EC 3.1.1.13). Triacylglycerol lipases, also known as lipases, have acylglycerols as their natural substrates. In aqueous media, these enzymes catalyze the hydrolysis of triglycerides to free fatty acids, diglycerides and monoglycerides but they are also able to carry out synthesis reactions in the presence of organic solvents (Bornscheuer et al. 2002). Similarly, sterol esterases hydrolyze fatty acid esters of sterols (Calero-Rueda et al. 2009) and carry out the opposite reaction in organic media (Barba Cedillo et al. 2013). They are widespread in nature, being the human cholesterol esterase one of the best studied among this group of enzymes (Brown et al. 2010; Ikeda et al. 2002; Loomes and Senior 1997). However, those from microorganisms have gained special interest due to their broad substrate specificity and their possible use for biotechnological purposes since they can be produced in bulk at low cost.

Both kinds of enzymes, lipases and sterol esterases, belong to the α/β-hydrolase superfamily, where residues responsible for its catalytic activity are highly conserved and form the so-called catalytic triad Ser-Asp/Glu-His (Dijkstra et al. 1972; Nardini and Dijkstra 1999), with the serine as the nucleophile residue participating directly in catalysis. For this reason, they are also known as serine hydrolases. They display a wide range of molecular mass, usually from 20 to 80 kDa, although enzymes with lower masses have been reported (Du et al. 2010) and, in general, their active site is characterized for having a hydrophobic cavity covered by an amphipathic loop named “flap”. Being considerably hydrophobic, these proteins tend to aggregate in dimeric, tetrameric, and even hexameric or more aggregated forms, displaying pseudo-quaternary structures (Pernas et al. 2001; Rúa et al. 1997; Xiang et al. 2007).

Some lipases show broad substrate specificity, including triglycerides and water insoluble sterol esters. This is the case of the *Candida rugosa* (synonym *Candida cylindracea*) lipase family (abH03.01) that comprises a

variety of closely related enzymes from which at least three of them (Lip1, Lip2 and Lip3), display activity on both triglycerides and cholesterol esters, although differing in their substrate specificity (Mancheño et al. 2003). Among sterol esterases, this promiscuity has been reported for the one secreted by the ascomycete *Ophiostoma piceae* (OPE), which shows more than 40% sequence identity with *C. rugosa* lipases and similar substrate-binding sites, as suggested by its structural model (Calero-Rueda et al. 2009). These properties have also been reported for the *Melanocarpus albomyces* sterol esterase (Kontkanen et al. 2006).

The versatile use of these enzymes in hydrolysis or synthesis reactions made them interesting alternative biocatalysts in different industrial sectors. Concerning its hydrolytic ability, the use of OPE for pitch biocontrol during hardwood or softwood pulp production (Calero-Rueda et al. 2002) or to decrease the problems caused by stickies during recycled paper manufacture (Barba Cedillo et al. 2013) have been reported. But OPE can also catalyze the synthesis of phytosterol or phytostanol esters, nutraceuticals currently added to dairy products because of the hypocholesterolemic effect they exert (Barba Cedillo et al. 2013). However, the use of any enzyme for biotechnological purposes requires its production in the adequate system for obtaining high amounts of the biocatalyst at low cost. In this sense, the use of the recombinant DNA technology for the improvement of enzyme production by using different heterologous expression hosts is mandatory. Prokaryotic hosts have proven useful for expression of eukaryotic proteins despite the absence of glycosylation routes (Ruiz-Dueñas et al. 2006) but the advantage of eukaryotic systems is their ability to carry out post-translational modifications (Rosenfeld 1999), which can be essential to express functional recombinant proteins. In addition, for specific applications such as food industry, the production of recombinant proteins in prokaryotic or eukaryotic hosts "Generally Recognized as Safe" (GRAS) is compulsory.

We have previously reported that *Komagataella* (synonym *Pichia*) *pastoris* is the optimal biofactory for the heterologous production of OPE (Barba Cedillo et al. 2012). The aim of this work was to test and compare the yields and activity of the OPE produced in several recombinant hosts. Here

we present the results for OPE cloning and expression in the prokaryotic model organism *Escherichia coli*, that synthesizes non-glycosylated protein, as well as in two eukaryotic hosts: an overproducer strain of *P. pastoris* and the GRAS yeast S*accharomyces cerevisiae*. The production and properties of the recombinant proteins are discussed, keeping in mind the initial goal of finding the best heterologous expression system for OPE, what would be the starting point for the exploitation of this enzyme in biocatalysis applications.

3.1.3 MATERIALS AND METHODS

3.1.3.1 Strains, plasmids, culture media and materials

All heterologous host strains and plasmids used in the present study are summarized in **Table 3.1.1**. *E. coli* DH5α and the plasmid pGEM-T Easy (Promega, Madison, WI, USA) were used for the general cloning procedures. The plasmids pET29a(+), pET28a(+) (Novagen, Merck KGaA, Darmstadt, Germany), pTYB12, pTYB1 (New England Biolabs, Hertfordshire, UK), pGEX-6P-2 (GE Healthcare, Uppsala, Sweden) and pFj1, provided by Dr. F. J. Medrano (CIB-CSIC, Spain), were used for expression in *E. coli*. The *E. coli* strains used for OPE expression were obtained from different providers: C43(DE3) from Lucigen, Middleton, WI, USA; BL21(DE3), BL21(DE3)pLysS, Rosetta(DE3)pLysS and Tuner(DE3) from Novagen Merck, KGaA, Darmstadt, Germany; BL21(DE3)pT-GroE was kindly donated by Dr. F. J. Medrano; K12 (dam^-/dcm^-) and SHuffle T7 express were from New England Biolabs, Hertfordshire, UK.

Three replicative shuttle vectors were used for expression in *S. cerevisiae*: pJRoC30, p426ADH and p426GPD (Camarero et al. 2012; Mumberg et al. 1995). The yeast strains are summarized in **Table 3.1.1** and were obtained from different sources: BJ5465 and Lalvin T73-4a were kindly donated by Dr. S. Camarero (CIB-CSIC, Spain) and Prof. A. Querol (IATA-CSIC, Spain), respectively, and BY4741 was from GE Healthcare, Uppsala, Sweden. Finally, the recombinant *P. pastoris* KM71 strain previously obtained in our laboratory (Barba Cedillo et al. 2012), carrying the construct pPIC9OPE, was re-transformed with the integrative expression vector pPIC9OPE.

E. coli was grown in two different media: LB (10 g/L tryptone, 5 g/L yeast extract, 5 g/L NaCl) and 2x Tryptone-Yeast Extract (2x TY) (16 g/L tryptone, 10 g/L yeast extract, 5 g/L NaCl).

Yeast Extract-Peptone-Dextrose (YPD) plates containing 10 g/L yeast extract, 20 g/L peptone, 20 g/L glucose and 20 g/L agar were used for general growing of the yeast strains. Minimal selection medium for *S. cerevisiae* contained 6.7 g/L Yeast Nitrogen Base without amino acids (Becton, Dickinson and Company, Sparks, MD, USA), 1.92 g/L Yeast Synthetic Drop-out Medium Supplement without uracil (Sigma-Aldrich, Steinheim, Germany), 20 g/L raffinose, 25 mg/L chloramphenicol and 20 g/L agar in the case of minimal selection plates. Expression medium for *S. cerevisiae* contained Bacto Peptone 20 g/L, yeast extract 10 g/L, 100 mM KH_2PO_4 pH 6.0 buffer, 20 g/L galactose or 20 g/L glucose in the case of inducible or constitutive promoters, respectively, and 25 mg/L chloramphenicol. Minimal selection plates for *P. pastoris* contained 6.7 g/L Yeast Nitrogen Base without amino acids, 1.92 g/L Yeast Synthetic Drop-out Medium Supplement without histidine (Sigma-Aldrich, Steinheim, Germany), 20 g/L glucose and 20 g/L agar. Expression medium for *P. pastoris* contained 20 g/L Bacto Peptone, 10 g/L yeast extract, 10 g/L sorbitol, 100 mM KH_2PO_4 pH 6.0 buffer and 0.5 % (w/v) methanol.

Restriction enzymes were from New England Biolabs (Hertfordshire, UK) while the primers were obtained from SigmaeAldrich. Taq DNA polymerase was purchased from Invitrogen (Carlsbad, CA, USA). T4 DNA ligase was provided by Promega and the purification kits from Qiagen (Valencia, CA, USA). CHAPS was purchased from Thermo Scientific (Rockford, IL, USA) and Triton X-100 and Sarkosyl (Sodium lauroyl sarcosinate) were obtained from Sigma Aldrich.

3.1.3.2 Cloning procedures

Cloning and transformation procedures were performed according to established techniques (Sambrook and Russell 2001) and suppliers' manuals.

For cloning in *E. coli,* the gene of sterol esterase from *O. piceae* (*ope*) was amplified from the expression vector pPIC9OPE (Barba Cedillo et al.

2012), using the reverse primer OPER and the forward primers OPEF1 or OPE4F1, to add 4 extra hydrophobic amino acids to the N-terminus (**Table 3.1.2**). The amplifications were carried out in a Mastercycler Pro S (Eppendorf, Hamburg, Germany). The PCR products were purified and ligated into the pGEM T-Easy vector, digested with the restriction enzymes *Nde*I and *Xho*I and subcloned into the expression vectors, pET29a(+), pET28a(+), pTYB12 and pFj1, with the same restriction sites. To create a recombinant GST-OPE protein in the N-terminus we used OPEF2 or OPE4F2, to add the 4 extra hydrophobic amino acids, and OPER as reverse primer (**Table 3.1.2**).The PCR fragments were ligated into the pGEM T-Easy vector and subcloned in the expression vector pGEX-6P-2, using *Bam*HI and *Xho*I as restriction sites. To produce the OPE with the Intein protein in the C-terminus, *ope* was amplified with the forward primers OPEF1 or OPEF2 and the reverse primer without stop codon OPE2R. The PCR product was cloned in pGEM T-Easy and then subcloned into the expression vector pTYB1.

Previous reports described an improved solubility of the recombinant protein expressed in *P. pastoris* (Barba Cedillo et al. 2012) and the reason for this behavior was attributed to the presence of 4, 6 or 8 extra amino acids in its N-terminus due to the cloning strategy. Then, these 4, 6 or 8 extra amino acids were added in this construct. For gene amplification, the forward primers OPE6F1 or OPE8F1 were used with the reverse primers OPER or OPE2R when a 6x histidine tag was added to the C-terminus of the recombinant protein (**Table 3.1.2**). The PCR product was purified and ligated into the pGEM T-easy and, after digestion with *Nde*I and *Xho*I, subcloned into the expression plasmid pET29a(+). All recombinant plasmids were verified by sequencing before use.

Table 3.1.2 Constructs and strains used in this study.

Strain	Strain features	Vector	Vector features Promoter/Inducer	Extra N-t amino acids	Fusion tag and location	Expression
E. coli						
BL21(DE3)	Deficient in both *lon* and *ompT* proteases	pET29a (+)	T7*lac* / IPTG	--/4/6/8	---	+/+/+/+
		pET29a (+)	T7*lac*/ IPTG	6	nHis C-t	+
		pET28a (+)	T7*lac*/ IPTG	--/4	nHis N-t	+/+
		pTYB12	T7*lac*/ IPTG	--/4	Intein N-t	+/+
		pFJ1	PhoA / Constitutive	--/4	---	–/–
BL21(DE3)pLysS	High-stringency, reduces basal expression level	pTYB1	T7*lac*/ IPTG	--/4	Intein C-t	–/–
		pGEX-6P-2	Ptac/ IPTG	--	GST N-t	+
		pET29a (+)	T7*lac*/ IPTG	4	---	+
BL21(DE3)pT-GroE	Contains chaperone GroESL, enhances protein folding	pGEX-6P-2	Ptac / IPTG	--/4	GST N-t	+/+
Rosetta(DE3)pLysS	Provides rare codons tRNAs	pET29a (+)	T7*lac*/ IPTG	--/4	---	–/+
Tuner(DE3)	Allows control of expression levels	pET29a (+)	T7lac/ IPTG	--	---	+
C43(DE3)	Enhances expression of toxic proteins	pET29a (+)	T7*lac*/ IPTG	--/4	---	–/–
K12	No DNA methylation	pGEX-6P-2	Ptac/ IPTG	--	GST N-t	–
		pFJ1	PhoA/ Constitutive	--/4	---	–/–
SHuffle T7 express	Allows disulfide bond formation in the cytoplasm	pET28a (+)	T7*lac*/ IPTG	--	nHis N-t	+
		pET29a (+)	T7*lac*/ IPTG	6	---	+
S. cerevisiae						
BJ5465	Protease-deficient strain	pJRoC30	*GAL1*/Galactose	4-8	---	+
		P426GPD	*GPD1*/ Constitutive	4-8	---	+
		P426ADH	*ADH1*/ Constitutive	4-8	---	+
BY4741	Presents four detectable marker genes	pJRoC30	*GAL1*/Galactose	4-8	---	+
		P426GPD	*GPD1*/ Constitutive	4-8	---	+
Lalvin T73-4a	Wine-growing yeast	pJRoC30	*GAL1*/Galactose	4-8	---	+
		P426GPD	*GPD1*/Constitutive	4-8	---	+
P. pastoris						
KM71 (pPIC9OPE)	Strain previously transformed	pPIC9	*AOX1*/Methanol	4-8	---	+

Abbreviations. n-His: Histidine tag; N-t: N-terminus; C-t: C-terminus; +: positive expression; –: no expression.

The cloning strategy to produce the recombinant OPE in *S. cerevisiae* consisted on amplifying the α-factor pre-pro-leader sequence and the OPE gene from pPIC9OPE, using the pair of primers SCF1 and SCR1 (**Table 3.1.2**). The purified PCR product was ligated into pGEM T-Easy plasmid, digested with *Bam*HI and *Xma*I and subcloned into the episomal vectors p426ADH and p426GPD. The construct for recombinant expression in the plasmid pJRoC30 was developed according to a similar strategy using the primers SCF1 and SCR2, and subcloning in pJRoC30 using *Bam*HI and *Not*I like restriction sites.

Table 3.1.1 Primers used in this study

Primers	Sequence (5'→3') Restriction sites	
E. coli		
OPEF1	CATATGACAACCGTGAATGTAAACTACC	*Nde*I
OPE4F1	CATATGGAGCTCTACGTAACAACCGTGAATGTAAACTACC	*Nde*I
OPEF2	GGATCCACAACCGTGAATGTAAACTACC	*Bam*HI
OPE4F2	GGATCCGAGCTCTACGTAACAACCGTGAATGTAAACTACC	*Bam*HI
OPE8F1	CATATGGGATCCGAAGCGGAAGCGTATGTGGAATTTACAACCGTGAATGTAAACTACC	*Nde*I
OPE6F2	CATATGGGATCCGAAGCGTATGTGGAATTTACAACCGTGAATGTAAACTACC	*Nde*I
OPER	CTCGAGGATGCGGAAGATGCCAATGTTG	*Xho*I
OPE2R	CTCGAGTTAGATGCGGAAGATGCCAATG	*Xho*I
S. cerevisiae		
SCF1	CGGGGATCCATGAGATTTCCTTCAATTTT	*Bam*HI
SCF2	CCCGGGTTAGATGCGGAAGATGCCAATGTTG	*Xma*I
SCF3	TAAGCGGCCGCTTAGATGCGGAAGATGCCAATG	*Not*I

3.1.3.3 Protein expression and analytical procedures

The constructs were introduced into their corresponding host. In the case of *E. coli* different electrocompetent strains (**Table 3.1.1**) were transformed using a MicroPulser electroporator (Bio-Rad, Hércules, CA, USA) following the manufacturer´s protocol. For the expression screening, several clones were grown overnight in 4 mL of 2x TY medium with the corresponding antibiotic

at 37 °C and 250 rpm. To induce the expression, 0.5 mM of IPTG was added to the culture. Protein expression was checked by SDS-PAGE using 10% polyacrylamide gels, staining with Coomassie R-250.To evaluate the solubility of the protein, positive clones were grown at 37 ºC in 50 mL of 2x TY medium, with the corresponding amount of antibiotic, until optical density at 600 nm reached 0.6. Then, the culture was induced with 0.5 mM IPTG and kept overnight at different temperatures (16 °C, 30 °C and 37 °C). The cells were harvested by centrifugation (6,000 x g, 20 min, 4 °C) and resuspended in 5 mL lysis buffer (10 mM Tris-HCl, pH 8, with 150 mM NaCl). Cell pellets were sonicated (Misonix S4000; Qsonica, Newtown, CT, USA), separated from the supernatant fraction and checked for protein solubility using SDS-PAGE gels (as described above). To increase the solubility, three different detergents were assayed: the zwitterionic surfactant CHAPS (20-80 mM), the non-ionic detergent Triton X-100 (1%), and the alkyl anionic surfactant Sarkosyl (7.5-30 mM).

In the case of *S. cerevisiae*, three different episomal vectors (p426ADH, p426GPD and pJRoC30) were introduced into the strains BJ5465, BY4741 and Lalvin T73 following the *S. cerevisiae* transformation kit instructions (Sigma-Aldrich, Steinheim, Germany). Single colonies of the transformed *S. cerevisiae* clones were picked from minimal selection plates, used to inoculate 3 mL of minimal medium and incubated for 48 h at 30 °C and 220 rpm. An aliquot of the cells was used to inoculate a final volume of 20 mL in 100 mL flasks, adjusting the OD_{600} to 0.25, and then incubating for two complete cell divisions (6–8 h). Thereafter, the cells were diluted to OD_{600} = 0.1 in a final volume of 20 mL of expression medium in 100 mL flasks (Pardo et al. 2012). The strain of *P. pastoris* containing the construct pPIC9OPE (Barba Cedillo et al. 2012) was retransformed with the construct PIC9OPE, following the manufacturer's instructions (Invitrogen, Carlsbad, CA, USA), to obtain improved expression levels. Semi-quantitative PCR with four serial dilutions of genomic DNA was carried out to check the number of copies of the *ope* gene in the new strain. Single colonies of the new *P. pastoris* strain were picked from minimal selection plates, used to inoculate 5 mL of YEPS medium without 0.5 % (w/v) methanol and incubated overnight at 28 °C and 250 rpm. An aliquot of the cells was used to inoculate a final

volume of 20 mL of expression medium in 100 mL flasks. Methanol (0.5 %) was added daily for maintaining the induction and counteracting evaporation.

Enzyme activity was routinely measured by monitoring *p*-nitrophenol release from 1.5mM *p*-nitrophenyl-butyrate (*p*NPB) (Sigma-Aldrich, Steinheim, Germany) (Calero-Rueda et al. 2002) in 20mM Tris-HCl pH 7 buffer at 25 ºC in a Shimadzu UV-1800. One unit of activity (1U) is defined as the amount of enzyme releasing 1 μmol of substrate per minute under the defined conditions.

Kinetic studies by using *p*NPB as substrate were assayed in the presence of 1% (v/v) Genapol X-100 (Sigma-Aldrich, Steinheim, Germany) (Gutierrez-Fernández et al. 2014). Experimental data were fitted to hyperbolic Michaelis-Menten curves and statistically analyzed with the Sigma Plot 11.0 software.

Protein concentration was determined by the BCA bioassay (Thermo Scientific, Rockford, IL, USA), using bovine serum albumin as standard. For N-deglycosylation, the purified OPE was dialyzed against sodium citrate buffer, pH 5.5, and then incubated with Endo H at 37 ºC for 24 h, following the manufacturer's instructions. Both the glycosylated and the deglycosylated proteins (around 5 μg each) were analyzed by SDS-PAGE and N-linked-carbohydrate content was estimated based on visual analysis of the stained gel, from the difference between the molecular mass of the sterol esterase before and after deglycosylation with Endoglycosidase H (Endo H; Roche, Mannheim, Germany) (Calero-Rueda et al. 2009).

3.1.3.4 Protein production and purification

A His-tagged version of OPE was expressed in strain *E. coli* BL21(DE3) in order to purify the protein via His-tag affinity purification. 500 mL of the 2x TY medium in 2 L flasks were inoculated and grown at 37 °C, until optical density at 600 nm reached 0.6. Then, the culture was induced with 0.5 mM IPTG and kept at 16 °C and 250 rpm overnight. The cell cultures were harvested by centrifugation (6,000 x g, 20 min, 4 °C), resuspended in 10 mL of lysis buffer with 20 mM Sarkosyl and sonicated. Bacterial lysates were

pelleted at 50,000 x g for 1 h at 4 °C in a 60Ti rotor**.** The supernatant was loaded onto a His-Trap HP 5 mL column (GE Healthcare, Uppsala, Sweden) equilibrated with binding buffer (10 mM Tris-HCl, pH 8.0, with 5 mM imidazole, 500 mM NaCl and 18 mM CHAPS). The target proteins were eluted with 50 mL elution buffer (10 mM Tris-HCl, pH 8.0, with 150 mM imidazole, 500 mM NaCl and 18 mM CHAPS). The purified enzyme was dialyzed against 10 mM Tris-HCl, pH 8, with 18 mM CHAPS to reduce the salt and imidazole content.

The sterol esterase expressed in *S. cerevisiae* BJ5465 strain with pJRoC30OPE*,* was produced in 1 L flasks with 200 mL of expression medium at 22 °C and 220 rpm, and inoculated as described above. The sterol esterase overexpressed in the new strain of *P. pastori*s was produced in 1 L flasks with 100 mL of expression medium at 28 °C and 250 rpm. When maximum activity was reached (generally after 72-96 h in both cases), the cells were harvested by centrifugation (6,000 x g, 4 °C) and the supernatants concentrated in 10,000 MWCO Amicon-Ultra Centrifugal filters (Merck Millipore, Darmstadt, Germany). The esterase purification was carried out in a single hydrophobic chromatography step (Octyl-Sepharose cartridge, GE Healthcare, Uppsala, Sweden) as previously reported (Barba Cedillo et al. 2012). The purified enzyme was dialyzed against 25 mM Tris-HCl, pH 7, to remove the detergent. The fractions containing the purified protein from the different hosts were further concentrated by ultrafiltration (30 kDa cut-off, Merck Millipore, Darmstadt, Germany).

To evaluate the relevance of N-linked glycosylation in OPE, the doubly-transformed *P. pastoris* strain was grown for 6 days in 250 mL flasks with 25 mL expression medium at 28 °C and 250 rpm in the presence of 20 μg/mL of tunicamycin (Sigma-Aldrich Steinheim, Germany). Culture samples (1 mL) were withdrawn periodically and centrifuged (6,000 x g). Esterase activity was evaluated in the supernatant as described above. Yeast biomass was determined gravimetrically after drying yeast pellets until constant weight in an aeration oven at 65 ºC.

3.1.3.5 N-terminal sequencing and analytical ultracentrifugation

The N-terminal sequence of the recombinant protein was obtained by automated Edman degradation of 10 μg of purified sample as previously described (Barba Cedillo et al. 2012).

A sedimentation velocity assay was used to check the aggregation behavior of recombinant proteins. Solutions of the purified protein (0.5 mg/mL) in 20 mM Tris-HCl, pH 7.0, were used for this experiment. Measurements were performed as previously reported (Gutierrez-Fernández et al. 2014). Differential sedimentation coefficient distributions c(s) were calculated by least-squares boundary modeling of sedimentation velocity data using the continuous distribution c(s) Lamm equation model as implemented by SEDFIT (version 14.1.). Experimental *s* values were corrected to standard conditions using the program SEDNTERP.

3.1.3.6 Circular dichroism spectroscopy

Measurements were carried out using a JASCO J-720 spectropolarimeter. Far-UV spectra were recorded in a 0.1 cm path length quartz cell at a protein concentration of 0.1 mg/ mL in 20 mM sodium phosphate buffer, pH 7.0. The spectra from five scans were averaged and corrected for the baseline contribution of the buffer. The observed ellipticities were converted into mean residue ellipticities (θ) based on a mean molecular mass per residue of 110 Da.

3.1.4 RESULTS

3.1.4.1 Expression in *E. coli*

The expression of OPE using *E. coli* as heterologous host (**Table 3.1.1**) was only achieved using vectors carrying inducible promoters such as pGEX-6P-2 or pET family vectors, although the protein produced was not soluble. Many strategies were attempted (**Table 3.1.1**) trying to improve protein solubility: i) fusing the target protein to tags such as 6x-His, GST or Intein; ii) using E. coli strains such as C43, designed for the expression of toxic proteins, Tuner, that allow modulating the induction level, or SHuffle T7, engineered to favor disulfide bond formation in the cytoplasm; iii) improving host cell codon usage by expressing the protein in *E. coli* strain Rosetta; or iv) enhance protein folding using as host the pT-GroE strain. Furthermore, different growth conditions were assayed, using several temperatures to optimize the expression and solubility of the recombinant proteins. However, in all cases, the protein expressed formed big aggregates commonly referred to as inclusion bodies. With the aim of solubilizing the OPE produced in *E. coli*, three different surfactants were tested on the inclusion bodies produced from pET28a(+) 6x-His in the BL21(DE3) strain. Only Sarkosyl above the critical micelle concentration (CMC=14.6 mM) was effective in solubilizing OPE, as observed by SDS-PAGE (**Fig. 3.1.1**). Protein aggregates obtained from overnight cultures was dissolved using Sarkosyl and purified in a single step in a prepacked cartridge for His-tagged recombinant proteins, after replacing Sarkosyl by CHAPS, a detergent easily removable by dialysis (Hjelmeland et al. 1983). Fifteen milligrams of pure enzyme, with a molecular mass around 60 kDa, corresponding to the mass determined using the amino acid composition, were obtained from 1 L of 2x TY medium **(Fig. 3.1.2)**. The circular dichroism spectrum of the purified protein in the far-UV region differed significantly from those registered for the native OPE as well as for the recombinant OPE expressed in the eukaryotic systems (**Fig. 3.1.3**). The purified enzyme revealed to be inactive after checking its performance in *p*NPB hydrolysis.

A second approach to avoid the formation of inclusion bodies, producing soluble OPE from the prokaryotic host, consisted on adding to the sequence of the native protein 4, 6 or 8 extra amino acids in the N-terminus of the protein, emulating the N-terminal region of the very soluble OPE populations expressed in *P. pastoris* (Barba Cedillo et al. 2012). A soluble form of the recombinant protein from *E. coli* was exclusively produced when 6 or 8 extra amino acids were added to the N-terminus (**Fig. 3.1.1**), but none of the proteins were active against the substrate assayed.

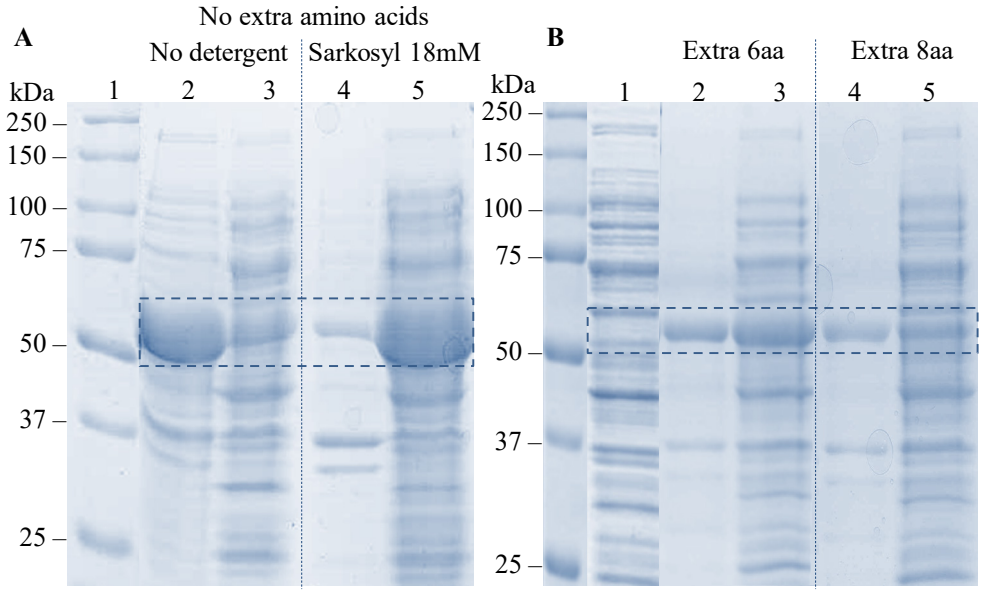

Fig. 3.1.1 SDS-PAGE of the crude extract of *E. coli* BL21(DE3) cultures containing the *ope* gene. The dashed boxes indicate OPE expression. **A)** OPE overexpressed without N-terminal extra amino acids. Lane 1, molecular mass markers. Lanes 2-3, pellet and supernatant, respectively, of the culture induced with IPTG without addition of surfactant. Lanes 4-5, pellet and supernatant, respectively, of the culture induced with IPTG and solubilized with 18 mM of Sarkosyl. **B)** OPE overexpressed with 6 or 8 extra N-terminal amino acids. Lane 1, molecular mass markers. Lane 2, supernatant from an uninduced culture. Lanes 3-4, pellet and supernatant, respectively, of the culture expressing OPE with 6 extra N-terminal amino acids. Lanes 5-6, pellet and supernatant, respectively, the culture expressing OPE with 8 extra N-terminal amino acids.

3.1.4.2 Expression in *S. cerevisiae* and *P. pastoris*

Screening OPE production in the yeast *S. cerevisiae* (**Fig. 3.1.4**) demonstrated the expression of soluble and active protein in all constructs and strains assayed (**Table 3.1.1**). The greatest activity (0.9 U/mL) was achieved in the protease deficient strain BJ5465, with the galactose-inducible promoter *GAL1*, after 3 days of incubation at 22 ºC in 100 mL Erlenmeyer flasks. The clone of the retransformed *P. pastoris* strain giving maximal production yielded 42 U/mL after 4 days of incubation at 28 ºC, 2.4-fold higher than the previous clone (Barba Cedillo et al. 2012). Semi-quantitative PCR suggested that the new clone carried two copies of the OPE construct (data not shown).

The recombinant proteins were purified to homogeneity. As expected, the OPE expressed in the new strain of *P. pastoris* was similar in molecular mass, N-carbohydrate content and comparable activity levels on *p*NPB to the protein previously produced in the same host (Barba Cedillo et al. 2012). Nevertheless, the calculated specific activity differed since protein concentration was now determined by the BCA bioassay, as recommended for very hydrophobic proteins, due to the fact that these proteins are underestimated by the Bradford method (Larsen et al. 2008).

Expression in *S. cerevisiae* yielded 4.1 mg/L of purified OPE, whereas in the new strain of *P. pastoris* 66 mg/L were obtained. Based on visual analysis of the stained gel, both proteins showed a similar molecular mass (around 75 kDa), with around 28% N-linked sugars (**Fig. 3.1.2**). In addition, both had a molecular mass of around 60 kDa after deglycosylation with EndoH, which coincides with the value expected from the amino acid sequence of OPE. The specific activities of the OPE synthesized by *S. cerevisiae,* before and after deglycosylation, were 34 U/mg and 25 U/mg, while for the OPE produced in *P. pastoris*, they were 120 U/mg and 98 U/mg respectively, indicating that most of the activity is retained in the secreted protein in spite of lacking the sugar moiety. The addition of tunicamycin, an inhibitor of N-linked glycosylation, to *P. pastoris* cultures, drastically reduced the OPE production, obtaining 0.4 U per mg of yeast biomass against the 3 U per mg of yeast biomass obtained in untreated cultures after 6 days of incubation.

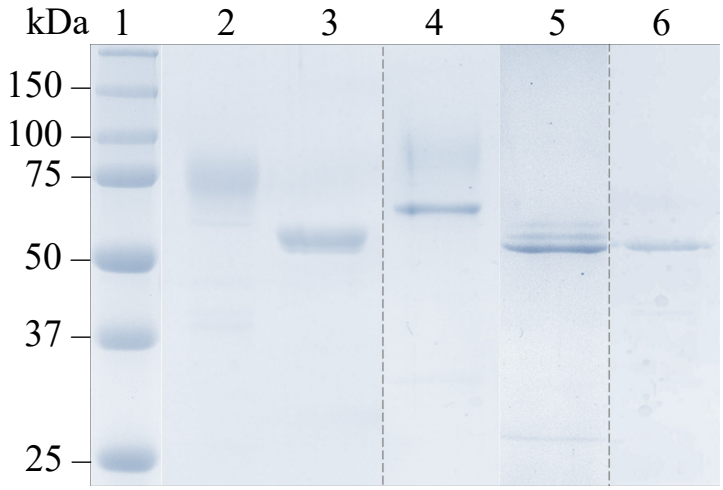

Fig. 3.1.2 SDS-PAGE of purified OPE expressed in different heterologous hosts. Lane 1, molecular mass markers. Lane 2, OPE expressed in *P. pastoris*. Lane 3, OPE expressed in *P. pastoris* and deglycosylated with Endo-H. Lane 4, OPE produced in *S. cerevisiae*. Lane 5, OPE produced in *S. cerevisiae* and deglycosylated with Endo-H. Lane 6, OPE produced in *E. coli*.

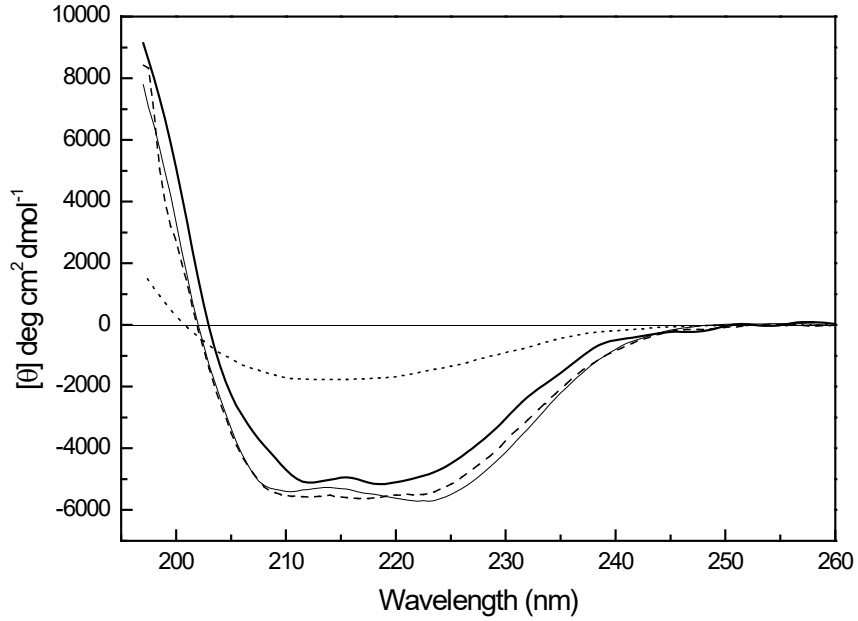

Fig. 3.1.3 Circular dichroism spectra (far UV spectrum) of purified OPE expressed in different heterologous hosts. Bold line, native protein secreted from the fungus *O. piceae*. Thin line, OPE expressed in *P. pastoris*. Dashed line, OPE expressed in *S. cerevisiae*. Dotted line, OPE expressed in *E. coli*.

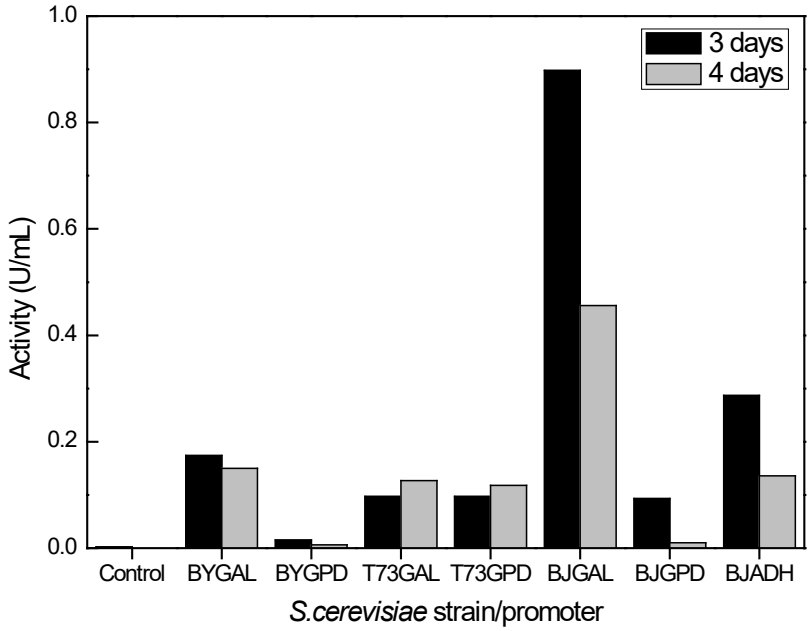

Fig. 3.1.4 Comparison of the esterase activity from different crude extracts from *S. cerevisiae*. The hydrolytic activity was checked against 1.5 mM of pNPB as the substrate. The OPE gene was expressed using the following constructs: the yeast strains Lalvin T73, BJ5465 and BY4741 carrying either the p426 plasmid with the constitutive promoters GPD or ADH, or the pJRoC30 vector with the inducible promoter *GAL1*.

The K_m value against *p*NPB was 0.28 mM for the OPE from S. *cerevisiae* and similar values were found for the protein produced in *P. pastoris* (**Table 3.1.3**). However, the turnover frequency and catalytic efficiency (k_{cat}/K_m) against this substrate were about 3-fold lower in the OPE expressed in *S. cerevisiae* **(Table 3.1.3**).

Table 3.1.2 Comparative heterologous expression levels and apparent kinetics parameters of recombinant protein against *p*NPB.

Host	Production (mg/L)	K_m (mM)	k_{cat} (s^{-1})	k_{cat}/K_m (s^{-1} mM^{-1})
S. cerevisiae	4.1	0.28 ± 0.05	50.0 ± 2.9	175.5 ± 27.6
P. pastoris	66.0	0.26± 0.08	146.9 ± 12.1	567.5± 142.6

In this work, the N-terminal sequence of the recombinant OPE expressed in the two eukaryotic hosts contained the same 4 to 8 extra amino acids described in a previous paper for the protein produced in *P. pastoris* (Barba Cedillo et al. 2012). These additional residues derive from a wrong processing of the EAEA repetition by signal peptidase STE13 and from the cloning procedure that leaves a residual sequence YVEF from the *SnaB*I and *EcoR*I restriction sites. Due to the presence of different protein populations in the sample, we are not able to discriminate if the main population contains 4, 6 or 8 extra amino acids, the ratio between the different populations, or the particular behavior of each one of them in terms of solubility.

The circular dichroism spectrum of the OPE expressed in *S. cerevisiae* revealed a secondary structure similar to those from the native protein and the recombinant form secreted by *P. pastori*s (**Fig. 3.1.3**). However, the measure of the sedimentation velocity of the former by analytical ultracentrifugation (**Fig. 3.1.5**) showed an intermediate aggregation state between those displayed for the native OPE and the recombinant protein expressed in *P. pastoris*.

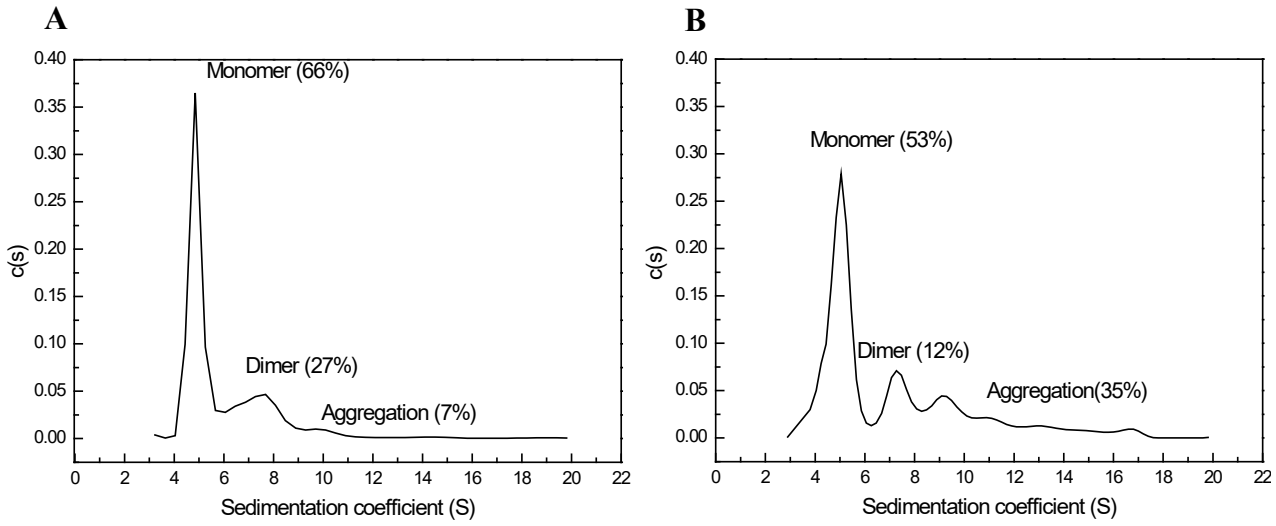

Fig. 3.1.5 Sedimentation velocities obtained by analytical centrifugation of the recombinant OPE expressed in: **A)** *P. pastoris* and **B)** *S. cerevisiae*. The percentages of the different species are represented in brackets. Conditions are described in the experimental section

Whereas the native protein from *O. piceae* showed a tendency to form big aggregates in aqueous solution (Barba Cedillo et al. 2012), the recombinant form expressed in *P. pastoris* was a combination of monomeric (66%) and dimeric (27%) forms with a small amount of big aggregates (7%), while OPE from *S. cerevisiae* appeared as a mixture of monomers (53 %), dimers (12%), and big aggregates (35%).

3.1.5 DISCUSSION

The *O. piceae* sterol esterase has been expressed in two new hosts, the bacterium *E. coli* and the GRAS yeast *S. cerevisiae*, and its production has been improved in the yeast *P. pastoris*. The characteristics of the recombinant proteins have been analyzed and compared with those from the native protein.

Regardless of the *E. coli* strain assayed, the production of recombinant OPE in this bacterial host rendered an insoluble and inactive protein stored inside inclusion bodies. The insolubility of the foreign proteins expressed in this microorganism, is an ordinary problem found when a eukaryotic protein is expressed in a prokaryotic host. Inclusion bodies are formed by deposition of unfolded or partially misfolded protein species that interact through hydrophobic patches, unusually exposed to the solvent (Gasser et al. 2008). Highly hydrophobic proteins, as OPE is, are more prone to accumulation in inclusion bodies (Singh and Panda 2005). This phenomenon can be minimized through the control of parameters such as temperature, the use of fusion tags, the co-expression of plasmid-encoded chaperones (Sorensen and Mortensen 2005) or by using surfactants to solubilize inclusion bodies (Zou et al. 2009). In this particular case, and after assaying several of the aforementioned strategies, recombinant soluble OPE was obtained by addition of Sarkosyl, an alkyl anionic detergent, to *E. coli* cultures. Nevertheless, the soluble protein showed no activity on the substrate assayed. *In vitro* folding is usually required to obtain active recombinant proteins from inclusion bodies, although it has been reported the expression in *E. coli* of Lip4 from *C. rugosa* fused with thioredoxin gene, yielded 10 % of the total recombinant protein in its soluble form (Tang et al. 2000).

On the other hand, previous results from OPE expression in *P. pastoris* (Barba Cedillo et al. 2012), described the increased solubility of the recombinant protein. This interesting feature was related to the presence of 4 to 8 extra amino acids in its N-terminus, although the reasons underlying the observed effect of the extra sequence were not explained. The recently elucidated crystal structures of that protein, in its closed and open conformations, shed light on this point suggesting that the presence of the extra N-terminal residues disrupts a hydrophobic patch in the protein surface, preventing its aggregation (Gutierrez-Fernández et al. 2014). Then, in a last trial to obtain a soluble and active form of OPE in *E. coli*, we tested the effect of adding these extra amino acids at the N-terminal region of the protein. Only the incorporation of 6 or 8 extra amino acids rendered partially soluble protein in *E. coli*, corroborating that they avoid aggregation, albeit the protein was inactive.

N-linked glycosylation is one of the most common posttranslational modifications of proteins. Since *E. coli* cannot perform this complex posttranslational modification, the synthesis of a non-glycosylated recombinant protein could cause the failure to produce an active form of OPE. However, it has been demonstrated that both the native and the recombinant OPE from yeasts maintain their activity levels after enzymatic deglycosylation (Barba Cedillo et al. 2012) indicating that the presence of the glycan moiety is not necessary to preserve the enzymatic activity of the glycoprotein once folded and secreted. Then, the lack of activity of the recombinant protein synthesized by *E. coli* could be more related to its misfolding, taking into account the relevant role played by sugars in the first steps of protein folding inside the endoplasmic reticulum (Helenius 1994; Wei et al. 2013). The far-UV CD spectrum data of OPE from *E. coli* (**Fig. 3.1.3**) support this theory since they suggest an incorrect protein folding in this heterologous expression system. This hypothesis was tested by adding tunicamycin, a drug that prevents the first committed step of N-linked glycosylation of proteins in the endoplasmic reticulum, to *P. pastoris* cultures. The drastic reduction of the amount of OPE per biomass unit secreted in this yeast as a consequence of this treatment upholds the essential role of the

initial glycosylation steps for the correct folding and secretion of the active protein (Helenius and Aebi 2001; Hurt et al. 2012).

The recombinant protein expressed in *S. cerevisiae* was soluble and active, showing similar molecular mass, glycosylation degree and circular dichroism spectrum than OPE from *P. pastoris*. Regarding the solubility of the protein expressed in *S. cerevisiae*, it was more soluble than the native one (Barba Cedillo et al. 2012), but less than that produced in *P. pastoris*, as can be inferred from analytical ultracentrifugation experiments (**Fig. 3.1.5**). The expression levels achieved in *S. cerevisiae* were considerably lower than those obtained in *P. pastoris* in the conditions assayed. Among the strains tested, the best *S. cerevisiae* producer was the protease-deficient strain carrying the inducible promoter. Although being replicative, the plasmid used in this construct showed to have high stability after several evolution cycles in experiments of directed evolution of fungal laccases (Camarero et al. 2012).

Despite the similarity of the OPE expressed in the two eukaryotic hosts, the efficiency of the enzyme produced in *S. cerevisiae* was three times lower than that of the protein expressed in the doubly-transformed *P. pastoris* strain (**Table 3.1.3**). Although both proteins contain the extra N-terminal amino acids, their differences in yield, aggregation behavior and kinetic constants may be explained from having a different ratio of species with 4, 6 or 8 N-terminal residues. In *S. cerevisiae*, the protein is produced at 22 ºC and there is a low protein secretion level. Under these conditions, the peptidase STE13 is likely to process the EAEA repetition more efficiently than it does in *P. pastoris* cultures, where the environment is less favorable in terms of temperature and protein amount. Then, the population of proteins with 4 extra amino acids would be higher in the former situation, but this fact would impact negatively in OPE solubility, as can be deduced from the lack of solubility observed for the recombinant OPE form with only 4 extra amino acids in its N-terminus produced in *E. coli*.

Although we are aware of the low yields of the OPE produced in *S. cerevisiae*, it is interesting to remark that the success in achieving the functional expression of OPE in this yeast, used as platform of directed evolution (Camarero et al. 2012), opens new strategies to produce more

robust tailor-made enzymes. Further experiments would be required to optimize OPE expression in this host.

In summary, here we analyzed the expression, in prokaryotic and eukaryotic hosts, of the sterol esterase from O. piceae, an enzyme with potential biotechnological interest. The results suggest that the first steps of N-glycosylation during OPE synthesis may condition its final folding and are crucial to secrete an active protein. The choice of the heterologous host and growth conditions seem also to be very important to obtain soluble forms (monomeric or dimeric) of OPE, enhancing its catalytic efficiency and preventing its aggregation.

Acknowledgments

This work was supported by the Spanish projects BIO2012-3637, PRI-PIBAR-2011-1402, S-2009AMB-1480, BFU2011-24615 and CSD2009-00088. M.E Vaquero thanks a FPU fellowship from the MINECO and J. Barriuso thanks the financial support from the JAE-DOC CSIC Program.

3.1.6 REFERENCES

Barba Cedillo V, Plou FJ, Martínez MJ (2012) Recombinant sterol esterase from *Ophiostoma piceae*: an improved biocatalyst expressed in *Pichia pastoris*. Microb Cell Fact 11:73

Barba Cedillo V, Prieto A, Martínez AT, Martínez MJ (2013a) Procedimiento de acilación para la obtención de compuestos de interés alimenticio y/o farmacéutico utilizando esterol esterasas fúngicas. Patent No. ES 2395582 B1

Barba Cedillo V, Prieto A, Martínez MJ (2013b) Potential of *Ophiostoma piceae* sterol esterase for biotechnologically relevant hydrolysis reactions. Bioengineered 4:249-253

Bornscheuer UT, Bessler C, Srinivas R, Krishna SH (2002) Optimizing lipases and related enzymes for efficient application. Trends Biotechnol 20:433-437

Brown AW, Hang J, Dussault PH, Carr TP (2010) Plant sterol and stanol substrate specificity of pancreatic cholesterol esterase. J Nutr Biochem 21:736-740

Calero-Rueda O, Gutiérrez A, del Río JC, Muñoz C, Plou FJ, Martínez AT, Martínez MJ (2002a) Method for the enzymatic control of pitch deposits formed during paper

pulp production using an esterase that hydrolyses triglycerides and sterol esters. Patent No. WO 02/075045 A1

Calero-Rueda O, Plou FJ, Ballesteros A, Martínez AT, Martínez MJ (2002b) Production, isolation and characterization of a sterol esterase from *Ophiostoma piceae*. Biochim Biophys Acta 1599:28-35

Calero-Rueda O, Barba V, Rodriguez E, Plou F, Martínez AT, Martínez MJ (2009) Study of a sterol esterase secreted by *Ophiostoma piceae*: Sequence, model and biochemical properties. Biochim Biophys Acta 1794:1099-1106

Camarero S, Pardo I, Canas AI, Molina P, Record E, Martinez AT, Martinez MJ, Alcalde M (2012) Engineering platforms for directed evolution of laccase from *Pycnoporus cinnabarinus*. Appl Environ Microbiol 78:1370-1384

Dijkstra FI, Scheffers WA, Wiken TO (1972) Submerged growth of the cultivated mushroom *Agaricus bisporus*. Antonie Leeuwenhoek 38:329-340

Du L, Huo Y, Ge F, YU J, Li W, Cheng G, Yong B, Zeng L, Huang M (2010) Purification and characterization of novel extracellular cholesterol esterase from *Acinetobacter* sp. J Basic Microbiol 50:S30-S36

Gasser B, Saloheimo M, Rinas U, Dragosits M, Rodríguez-Carmona E, Baumann K, Giuliani M, Parrilli E, Branduardi P, Lang C, et al. (2008) Protein folding and conformational stress in microbial cells producing recombinant proteins: a host comparative overview. Microb Cell Fact 7:11

Gutierrez-Fernández J, Vaquero ME, Prieto A, Barriuso J, Martínez MJ, Hermoso JA (2014) Crystal structures of *Ophiostoma piceae* sterol esterase: structural insights into activation mechanism and product release. J Struct Biol 187:215-222

Helenius A (1994) How N-linked oligosaccharides affect glycoprotein folding in the endoplasmic-reticulum. Mol Biol Cell 5:253-265

Helenius A, Aebi M (2001) Intracellular functions of N-linked glycans. Science 291:2364-2369

Hjelmeland LM, Nebert DW, Osborne J (1983) Sulfobetaine derivatives of bile acids: Nondenaturing surfactants for membrane biochemistry. Anal Biochem 130:72-82

Hurt JK, Fitzpatrick BJ, Norris-Drouin J, Zylka MJ (2012) Secretion and N-linked glycosylation are required for prostatic acid phosphatase catalytic and antinociceptive activity. PLoS One 7:e32741

Ikeda I, Matsuoka R, Hamada T, Mitsui K, Imabayashi S, Uchino A, Sato M, Kuwano E, Itamura T, Yamada K, et al. (2002) Cholesterol esterase accelerates intestinal cholesterol absorption. Biochim Biophys Acta 1571:34-44

Kontkanen H, Reinikainen T, Saloheimo M (2006) Cloning and expression of a *Melanocarpus albomyces* steryl esterase gene in *Pichia pastoris* and *Trichoderma reesei*. Biotechnol Bioeng 94:407-415

Larsen MW, Bornscheuer UT, Hult K (2008) Expression of *Candida antarctica* lipase B in *Pichia pastoris* and various *Escherichia coli* systems. Protein Expr Purif 62:90-97

Loomes KM, Senior HEJ (1997) Bile salt activation of human cholesterol esterase does not require protein dimerisation. FEBS Lett 405:369-372

Mancheño JM, Pernas MA, Martínez MJ, Ochoa B, Rúa ML, Hermoso JA (2003) Structural insights into the lipase/esterase behavior in the *Candida rugosa* lipases family: crystal structure of the lipase 2 isoenzyme at 1.97 Å resolution. J Mol Biol 332:1059-1069

Mumberg D, Muller R, Funk M (1995) Yeast vectors for the controlled expression of heterologous proteins in different genetic backgrounds. Gene 156:119-122

Nardini M, Dijkstra BW (1999) α/β hydrolase fold enzymes: the family keeps growing. Curr Opin Struct Biol 9:732-737

Pardo I, Vicente AI, Alcalde M, Camarero S (2012) Development of chimeric laccases by directed evolution. Biotechnol Bioeng 109:2978-2986

Pernas MA, López C, Rúa ML, Hermoso J (2001) Influence of the conformational flexibility on the kinetics and dimerisation process of two *Candida rugosa* lipase isoenzymes. FEBS Lett 501:87-91

Rosenfeld SA (1999) Use of *Pichia pastoris* for expression of recombinant proteins Methods Enzymol 306:154-169

Rúa ML, Schmidt-Dannert C, Wahl S, Sprauer A, Schmid RD (1997) Thermoalkalophilic lipase of *Bacillus thermocatenulatus*. Large-scale production, purification and properties: aggregation behaviour and its effect on activity. J Biotechnol 56:89-102

Ruiz-Dueñas FJ, Ferreira P, Martínez MJ, Martínez AT (2006) In vitro activation, purification, and characterization of *Escherichia coli* expressed aryl-alcohol oxidase, a unique H_2O_2-producing enzyme. Protein Expr Purif 45:191-199

Sambrook J, Russell DW (2001) Molecular cloning: a laboratory manual 3rd edition. Cold Spring Harbor Laboratory Press, New York, USA

Singh SM, Panda AK (2005) Solubilization and refolding of bacterial inclusion body proteins. J Biosci Bioeng 99:303-310

Sorensen HP, Mortensen KK (2005) Soluble expression of recombinant proteins in the cytoplasm of *Escherichia coli*. Microb Cell Fact 4:1

Tang SJ, Sun KH, Sun GH, Chang TY, Lee GC (2000) Recombinant expression of the *Candida rugosa* lipase in *Escherichia coli*. Protein Expr Purif 20:308-313

Wei W, Chen L, Zou G, Wang QF, Yan X, Zhang J, Wang CS, Zhou ZH (2013) N-glycosylation affects the proper folding, enzymatic characteristics and production of a fungal beta-glucosidase. Biotechnol Bioeng 110:3075-3084

Xiang H, Masuo S, Hoshino T, Takaya N (2007) Novel family of cholesterol esterases produced by actinomycetes bacteria. Biochim Biophys Acta 1774:112-120

Zou Jp, Xu J, Liu L, Li S, Wu C, Du G (2009) Solubilization and purification of *Escherichia coli* expressed GST-fusion human vascular endothelial growth factors with N-Lauroylsarcosine. Afr J Biotechnol 8:5132-513

3.2 CHAPTER 2

Crystal structures of *Ophiostoma piceae* sterol esterase: Structural insights into activation mechanism and product release

Javier Gutiérrez-Fernández[1], María Eugenia Vaquero[1], Alicia Prieto, Jorge Barriuso, María Jesús Martínez, Juan A. Hermoso

[1] Equally contributed to this work

Published in Journal of Structural Biology (2014) 187:215-222

3.2.1 SUMMARY

Sterol esterases are able to efficiently hydrolyze both sterol esters and triglycerides and to carry out synthesis reactions in the presence of organic solvents. Their high versatility makes them excellent candidates for biotechnological purposes. Sterol esterase from fungus *Ophiostoma piceae* (OPE) belongs to the family abH03.01 of the *Candida rugosa* lipase-like proteins. Crystal structures of OPE were solved in this study for the closed and open conformations. Enzyme activation involves a large displacement of the conserved lid, structural rearrangements of loop α16-α17, and formation of a dimer with a large opening. Three PEG molecules are placed in the active site, mimicking chains of the triglyceride substrate, demonstrating the position of the oxyanion hole and the three pockets that accommodate the *sn*-1, *sn*-2 and *sn*-3 fatty acids chains. One of them is an internal tunnel, connecting the active center with the outer surface of the enzyme 30 Å far from the catalytic Ser220. Based on our structural and biochemical results we propose a mechanism by which a great variety of different substrates can be hydrolyzed in OPE paving the way for the construction of new variants to improve the catalytic properties of these enzymes and their biotechnological applications.

3.2.2 INTRODUCTION

Triacylglycerol lipases (EC 3.1.1.3) are enzymes ubiquitous in nature, from microbes to plants and animals, catalyzing the hydrolysis of triglycerides to diglycerides, monoglycerides, free fatty acids and glycerol. In addition, these enzymes can catalyze esterification and transesterification reactions in the presence of organic solvents (Houde et al. 2004). Their interest is related to their application in a wide range of industrial processes: food, detergents, cosmetics, pharmaceutical, textile and paper industry (Reetz 2002; Singh and Mukhopadhyay 2012).

On the other hand, sterol esterases (EC 3.1.1.13) are defined as enzymes that hydrolyze sterol esters releasing free sterols and fatty acids. These enzymes were described in mammal tissues and in some fungi and bacteria (Ghosh et al. 1995; Rahim and Sih 1969). Initially they were proposed to be used to detect cholesterol in blood (Allain et al. 1974) but their importance increased during the last decade since, in addition to their ability to hydrolyze sterol esters, they are able to hydrolyze triglycerides efficiently (Calero-Rueda et al. 2002; Kontkanen et al. 2006; Maeda et al. 2008) and carry out synthesis reactions in the presence of organic solvents (Barba et al. 2011; Morinaga et al. 2011). Due to their high versatility, these enzymes proved to have high biotechnological interest for pitch reduction during paper pulp manufacture (Calero-Rueda et al. 2002) and they can also catalyze the synthesis of phytosterol esters used as food additives (Barba et al. 2011; Morinaga et al. 2011).

Both lipases and sterol esterases are α/β-hydrolases showing a substrate-binding site formed by an extensive hydrophobic pocket (Grochulski et al. 1993) (Mancheño et al. 2003). A traditional criterion accepted to define an enzyme as a lipase deals with the huge increase of their activity in the lipid-water interface, owing to a phenomenon known as interfacial activation (Verger 1997), a process that can be also triggered by micelles (Hermoso et al. 1996; Hermoso et al. 1997). This property is linked usually to the existence of a structural lid in these enzymes, allowing the access of the lipidic substrate to the catalytic site (Holmquist 2000). Nevertheless, the existence of a lid seems not to be the single determinant for

interfacial activation (Mancheño et al. 2003). In the case of sterol esterases, no much information is available since most of them have not been characterized.

The yeast *Candida rugosa* secretes a variety of closely related enzymes, referred as lipases or sterol esterases. In light of biochemical and structural studies, the best-characterized enzymes from this yeast (Lip1, Lip2 and lip3) exhibit a high sequence identity among them (77-88%), but they differ in their substrate specificity on triglycerides and cholesterol esters. These differences in the affinity towards these compounds are explained by small changes in the hydrophobicity of the substrate-binding site and the lid region (Mancheño et al. 2003).

Sterol esterase from *Ophiostoma piceae* (OPE) (UniProt Id Q2TFW1) belongs to the family abH03.01 of the *C. rugosa* lipase like proteins (The Lipase Engineering Database http://www.led.uni-stuttgart.de/) for which 326 members have been sequenced and the three-dimensional structures of lipases from *C. rugosa* (Grochulski et al. 1993), the lipase from *Geotrichum candidum* (Bourne et al. 2004; Schrag and Cygler 1993) and the esterase from *Aspergillus niger* (Bourne et al. 2004) are the only members up to now reported.

Recently, we described a computational model of three-dimensional structure for OPE based on *C. rugosa* Lip1 and lip3 structures (Barriuso et al. 2013; Calero-Rueda et al. 2009). OPE is more efficient than *C. rugosa* lip3 against sterol esters (Barba et al. 2011). Our model indicated that differences in the tunnel region of these enzymes could be related with their catalytic efficiency differences (Calero-Rueda et al. 2009).

Therefore, the development of structural studies is essential to understand the catalytic properties of these enzymes. The use of native *O. piceae* enzyme did not produce crystals suitable for X-ray diffraction (Calero-Rueda et al. 2002). In this work we present the three-dimensional structure of this enzyme, in its open and closed conformations, by using the deglycosylated form of the recombinant protein expressed in *Pichia pastoris*, more soluble than the native one (Barba Cedillo et al. 2012). The activation

mechanism and substrate stabilization is here described. This represents a hotspot in this field, opening the way for the rational design of new improved variants for industrial applications and allowing fine tuning enzyme activity.

3.2.3 MATERIALS AND METHODS

3.2.3.1 OPE expression, purification and characterization

The enzyme was over-expressed in *P. pastoris* and purified in a single hydrophobic chromatography step (Octyl- Sepharose cartridge, GE Healthcare), as previously reported (Barba Cedillo et al. 2012), although in this case the protein was eluted after addition of 18 mM CHAPS in 25 mM Tris-HCl pH 7.0. The purified enzyme was dialyzed against 25 mM Tris-HCl pH 7 to reduce the detergent concentration below 0.5 μM and stored at -20 ºC until used.

Purified OPE was subjected to Size Exclusion Chromatography (SEC) using a Superose 12 GL 10/300 (GE Healthcare) with 20mM Tris-HCl pH 7 plus 0.15M NaCl at 0.3 mL min-1 to separate the multimolecular forms of the purified protein. Dextran blue (2000 kDa), Ferritin (460 kDa), Aldolase (170 kDa), BSA (73 kDa), Ovalbumin (48.2 kDa) and Chymotrypsinogen A (19.5 kDa), (calibration kits, Amersham Pharmacia), were used as standards to calibrate the column. Before deglycosylation with Endoglycosidase H (Roche), OPE was dialyzed against sodium citrate buffer pH 5.5 and then incubated at 37 ºC for 24 h, following the manufacturer's instructions. Deglycosylation was checked by SDS-PAGE, staining the protein bands with Coomassie R-250 or with silver reagent. The deglycosylated enzyme was dialyzed against 25 mM Tris-HCl pH 7.0 for crystallization assays.

Enzyme activity against esters of *p*-nitrophenol was measured by monitoring the hydrolysis of *p*NPB, *p*NPL and *p*NPP. A 20 mM stock solution of the substrates was prepared in HPLC grade acetone. The assay mixture contained 2 mM substrate in 20 mM Tris-HCl pH 7.0 buffer and 1% (v/v) Genapol X-100. The reactions were monitored at 410 nm at room temperature in a Shimadzu UV-1800, in the case of *p*NPP and *p*NPL with magnetic stirring. One unit of activity (1 U) is defined as the amount of

enzyme releasing 1 μmol of *p*-nitrophenol (ε_{410}=15,200 $M^{-1}cm^{-1}$) per minute under the defined conditions.

Protein concentration was determined by BCA bioassay (Thermo) using bovine serum albumin as standard.

Analytical ultracentrifugation was used to check the aggregation behavior of recombinant proteins and the possible transition state between of both closed and open protein forms (monomer and dimer, respectively). Measurements were performed in a XL-I analytical ultracentrifuge (Beckman-Coulter Inc.) equipped with UV-VIS and interference detection optics. Samples, in 25 mM Tris-HCl, pH 7.0, were centrifuged at 48,000 rpm and 20 ºC using an An50Ti eight hole rotor and double-sector Epon-charcoal centerpieces. Differential sedimentation coefficient distributions c(s) were calculated by least-squares boundary modeling of the experimental data using the program SEDFIT (version 12.44) (Schuck 2000). The experiments were carried out, by using both the purified protein after hydrophobic chromatography (0.5 mg/mL), consisting in a mixture of aggregates states (principally monomer and dimer), and the monomer isolated after SEC (0.2 mg/mL). These proteins were analyzed in presence or absence of 5 mM dodecane sulfonyl chloride (Sigma-Aldrich), as enzyme inhibitor, and 5 mM of cholesteryl oleate, as enzyme substrate (after 30 min of incubation at room temperature). The enzyme inhibitor was prepared in isooctane, remaining in the samples at 0.5%, and the substrate was dissolved in 0.02% Genapol X-100 and 150 mM NaCl (final concentration).

3.2.3.2 Construction of an OPE mutant

The mutant I544W was constructed by site-directed mutagenesis. The mutation was introduced by polymerase chain reaction (PCR), using the expression plasmid pPIC9OPE as template (Barba Cedillo et al. 2012). Both a direct and a reverse primer were designed complementary to opposite strands of the same DNA region. The following primers were used (with indication of the changed triplets in bold): OPE I544W (Fw: 5′-CAACAAC**TGG**GGCATCTTCC -3’ and Rv: 5′-GGAAGATGCC**CCA**GTTGTTG -3’). PCRs (50 μL final volume) were

carried out in a Mastercycler Pro S (Eppendorf) using 100 ng of template DNA, each dNTP at 250 μM, 125 ng of direct and reverse primers, 5 units of expand long template enzyme mix (Roche), and the manufacturer's buffer number 3. Reaction conditions were as follows: (i) 95 °C for 1 min; (ii) 18 cycles at 95 °C for 50 s, 55 °C for 50 s, and 68 °C for 10 min; and (iii) a final cycle at 68 °C for 10 min. After amplification, the PCR products were treated with DpnI restriction enzyme (Roche) to digest the parental strand. The mutated gene was completely sequenced using an ABI 3730 DNA analyzer (Applied Biosystems) to ensure that only the desired mutation was introduced.

3.2.3.3 Crystallization and data collection

Initial crystallization trials were performed by the sitting drop vapor-diffusion method at 18 ºC. A wide range of crystallization conditions were assayed by high-throughput techniques, using a NanoDrop robot with Innovadyne SD-2 microplates (Innovadyne Technologies Inc., California, USA). The mixture contained 250 nL of protein solution and 250 nL of precipitant solution, equilibrated against 65 μL of well solution. Successful crystallization conditions were optimized by a hanging-drop vapor-diffusion method, mixing 1 μL of protein solution and 1 μL of precipitant solution, equilibrating against 500 μL of reservoir solution. Native OPE was assayed at 10 mg mL^{-1} in 25 mM Tris-HCl pH 7.0 (Sigma-Aldrich). Two different habits were found in different conditions. Optimized habit I crystals grew in 0.2 M sodium nitrate (Sigma-Aldrich), 0.1 M bis-tris propane pH 7.5 (Sigma-Aldrich) and 20% (w/v) PEG 3350 (Sigma-Aldrich), while habit II crystals grew in 10% (v/v) 1,4-dioxane (Sigma-Aldrich), 0.1 M MES pH 6.5 and 1.6 M ammonium sulphate (Sigma-Aldrich). Native datasets of both habits were collected, using synchrotron radiation, at beamline ID29 in the ESRF (Grenoble, France) and cryoprotected with 20% glycerol (Sigma-Aldrich). Both datasets were processed with XDS (Kabsch 2010) and scaled with SCALA (Evans 2006), from CCP4 suite (Winn et al. 2011). Habit I crystals diffracted up to 2.0 Å resolution and belonged to the tetragonal $I4_1$ space group ($a = b = 164.12$ Å, $c = 93.99$ Å; $\alpha = \beta = \gamma = 90^{o}$). A dimer was found in the asymmetric unit, with a Matthews' coefficient of 2.67 $Å^3\ Da^{-1}$ and a solvent content of 54.03%. Habit

II crystals diffracted up to 2.6 Å resolution and belonged to the hexagonal $P6_322$ space group ($a = b = 119.27$ Å, $c = 206.77$ Å; $\alpha = \beta = 90^o$, $\gamma = 120^o$). One single monomer was found in the asymmetric unit, with a Matthews' coefficient of 3.44 $Å^3\ Da^{-1}$ and a solvent content of 64.24%.

3.2.3.4 Structure determination and refinement

Structure associated to habit I was solved by molecular replacement with Phaser (McCoy et al. 2007), using *C. rugosa* Lip1, PDB code 1LPN, sequence identity = 42.8%; (Grochulski et al. 1994), as initial model. The resulting structure was used as initial model to solve, by molecular replacement, the structure associated to the habit II. The refinement and manual model building of both structures was carried out with Phenix (Adams et al. 2010) and Coot (Emsley et al. 2010), respectively. Figures involving structural elements of these proteins have been created in PyMOL (Schrödinger 2010) and some surface representations have been designed with Hollow (Ho and Gruswitz 2008).

The refinement converged to final values of R_{work} = 0.17 and R_{free} = 0.21 for habit I structure, and of R_{work} = 0.17 and R_{free} = 0.22 for habit II structure. The final model of habit I crystals presents 538 amino acids for one monomer and 537 amino acids for the other, showing both an open conformation. In addition, two N-Acetylglucosamine molecules have been modeled at the glycosilation sites of chain A. In chain B, only one site could be modeled with one additional NAG molecule. Two phospholipid molecules were clearly identified at the interphase between both chains in the active conformation. As they were not present in the crystallization conditions, we think that these molecules come from the purification stage. Since the real nature of these phospholipids was not determined, we have built a ligand in which the number of carbon atoms corresponds to the length of the electronic density at 0.8σ. Finally, some polyethilenglycol (PEG) molecules have been found and modeled. Surrounding chain A, we have modeled one molecule of pentaethilene glycol, three molecules of triethilene glycol and one molecule of di(hidroxiethil)ether. In chain B we have modeled four molecules of di(hidroxiethil)ether and one molecule of triethilene glycol. Habit II crystals contained the closed conformation of the enzyme which presents 538 amino

acids. Contrary to open conformation, no ligands were found in habit II structure. Structural determination parameters and refinement statistics are summarized in **Table 3.2.1**.

Crystallization of OPE I544W mutant was assayed at 9.5 mg mL^{-1} in 25 mM Tris-HCl pH 7.0 (Sigma-Aldrich) and crystals were obtained in 0.2 M sodium nitrate (Sigma-Aldrich), 0.1 M bis-tris propane pH 7.5 (Sigma-Aldrich) and 20% (w/v) PEG 3350 (Sigma-Aldrich), showing a shape similar to habit I. Diffraction datasets for the OPE I544W mutant were collected using synchrotron radiation, at beamline I03 in Diamond Light Source (Oxfordshire, UK). Datasets were processed with XDS (Kabsch 2010) and scaled with SCALA (Evans 2006), from CCP4 suite (Winn et al. 2011). OPE I544W mutant crystals diffracted up to 2.4 Å resolution and belonged to the tetragonal $I4_1$ space group ($a = b = 164.86$ Å, $c = 94.14$ Å; $\alpha = \beta = \gamma = 90^{o}$). A dimer was found in the asymmetric unit, with a Matthews' coefficient of 2.68 $Å^3\,Da^{-1}$ and a solvent content of 54.08%.

The structure of OPE I544W mutant was solved by molecular replacement with Phaser (McCoy et al. 2007), using the previously solved open conformation from OPE as a model. The refinement and manual model building of OPE I544W mutant was carried out with Phenix (Adams et al. 2010) and Coot (Emsley et al. 2010), respectively. The refinement converged to final values of $R_{work} = 0.20$ and $R_{free} = 0.25$. The OPE I544W mutant shows the open conformation and also contains two phospholipids located in the interphase between both chains. Two NAG molecules have been modeled at the glycosilation sites of chain A and one more in chain B. Regarding the PEG chains observed in OPE, only one molecule of triethilen glycol has been modeled inside the tunnel of chain A. Chain B of OPE I544W showed higher B factors than in the open conformation of wild type OPE. Structural determination parameters and refinement statistics are summarized in **Table 3.2.1**.

3.2.3.5 Accession numbers

Coordinates and structure factors have been deposited in the Protein Data Bank with accession numbers 4BE9 and 4BE4 for the OPE open and closed conformations respectively and 4UPD for the OPE-I544W mutant.

3.2.4 RESULTS AND DISCUSSION

3.2.4.1 Overall structure

Two different three-dimensional structures are presented in this report, namely, the structure of OPE in its closed conformation (OPE^c) (**Fig. 3.2.1A**) obtained from habit II crystals and the open conformation of the enzyme (OPE^o) (**Fig. 3.2.1B**) from habit I crystals. Crystal structure of OPE^c follows the protein scaffold of lipases from *C. rugosa* based on an α/β hydrolase fold (Ollis et al. 1992) with a major 11-stranded mixed β-sheet, a small and nearly perpendicular N-terminal 3-stranded β-sheet and 16 helices (**Fig. 3.2.1A**). The major β-sheet, which forms the core of the lipase, exhibits a pronounced twist, being the first (β_0) and last (β_{10}) strands almost perpendicular to each other. In agreement with this, lipase 2 of *C. rugosa* (PDB code 1GZ7, Mancheño et al. 2003) is the closest structural homologue of OPE^c (sequence identity = 42.5%, rmsd = 0.81 Å for 538 Cα atoms, **Fig. 3.2.S1**). OPE^c presents a 37 amino acids lid covering the active site. The lid consists of one α-helix (residues 83-88) and two 3_{10}-helices (residues 90-94 and 96-98) flanked by two loops that end in a disulfide hinge (from Cys72 to Cys108, **Fig. 3.2.1C**). OPE lid differs from that reported for *C. rugosa* and *G. candidum.* While the lid in *C. rugosa* Lip1 and Lip2 contains one α-helix of 10 residues and one 3_{10}-helix of 3 residues, the lid in *G. candidum* is formed by three α-helices containing 12, 4 and 10 residues respectively.

A hydrophobic patch, formed by Ile407, Phe408, Phe458, Pro459 and Phe460, is located close to the lid (**Fig. 3.2.1C**). This Phe-Pro-Phe pattern appears only in OPE and not in the closest homologues. Both phenylalanines closely interact with some residues of the lid (Leu88 and Leu92).

The main structural difference between closed and open structures is the displacement of the lid up to about 30 Å away from its original position (**Fig. 3.2.1C** and **Fig. 3.2.S2**). This movement involves a rearrangement of its secondary structure that upon activation presents two α-helices (residues 84-93 and 96-101). A similar rearrangement is observed for the lipases/esterases from *C. rugosa*, but OPE presents the largest lid displacement among related enzymes (~30 Å in the longest separation) (**Fig. 3.2.S3**). Analysis of both OPE forms (habit I and II) indicates that the lid regions in the closed conformation is not involved in crystal contacts, while the lid in the open conformation is involved in oligomeric arrangement. In agreement with that, observed B-factors are higher for the lid in the closed conformation that in the open **Fig. 3.2.S4**).

Table 3.2.1 Data collection and refinement statistics.

	OPE^{c}	OPE^{o}	OPE-I544W
Data collection			
Space group	$P6_322$	$I4_1$	$I4_1$
Cell dimensions			
a, *b*, *c* (Å)	119.27, 119.27, 206.77	164.12, 164.12, 93.99	164.9, 164.9, 94.14
α, β, γ (º)	90, 90, 120	90, 90, 90	90, 90, 90
T (K)	100	100	100
Wavelength (Å)	0.97908	0.97908	1.00000
Resolution (Å)	46.2 (2.7 – 2.6)	43.6 (2.1 – 2.0)	58.3 (2.5 – 2.4)
No. unique reflections	26901	84190	49299
R_{pim} (%)[a]	8.9 (49.2)	4.5 (32.8)	5.0 (43.3)
‹*I*/σ(*I*)›	6.9 (1.9)	11.7 (2.5)	12.5 (1.9)
Completeness (%)	98.5 (98.2)	100 (100)	99.7 (97.6)
Redundancy	3.4 (3.4)	7.0 (7.1)	6.8 (6.8)
Refinement			
Resolution (Å)	46.22 – 2.6	43.56 – 2.0	58.3 – 2.4
R_{work}/R_{free} [b]	0.17/0.22	0.17/0.21	0.20/0.25
R.m.s. deviations			
Bond length (Å)	0.007	0.008	0.010
Bond angles (º)	1.078	1.051	1.480
PDB code	4BE4	4BE9	4UPD

* Values in parentheses correspond to the highest resolution shell.

[a] $R_{pim} = \Sigma_{hkl}[1/(N-1)]\ 1/2\ \Sigma_i\ |\ I_i(hkl) - [I(hkl)]\ |\ /\ \Sigma_{hkl}\Sigma_i I_i(hkl)$, where $\Sigma_i I_i(hkl)$is the *i*-th measurement of reflection hkl, [I(hkl)] is the weighted mean of all measurements and N is the redundancy for the hkl reflection.

[b] $R_{work}/R_{free} = \Sigma_{hkl}|\ F_o - F_c\ |\ /\ \Sigma_{hkl}\ |\ F_o\ |$, where F_c is the calculated and F_o is the observed structure factor amplitude of reflection hkl for the working / free (5%) set , respectively.

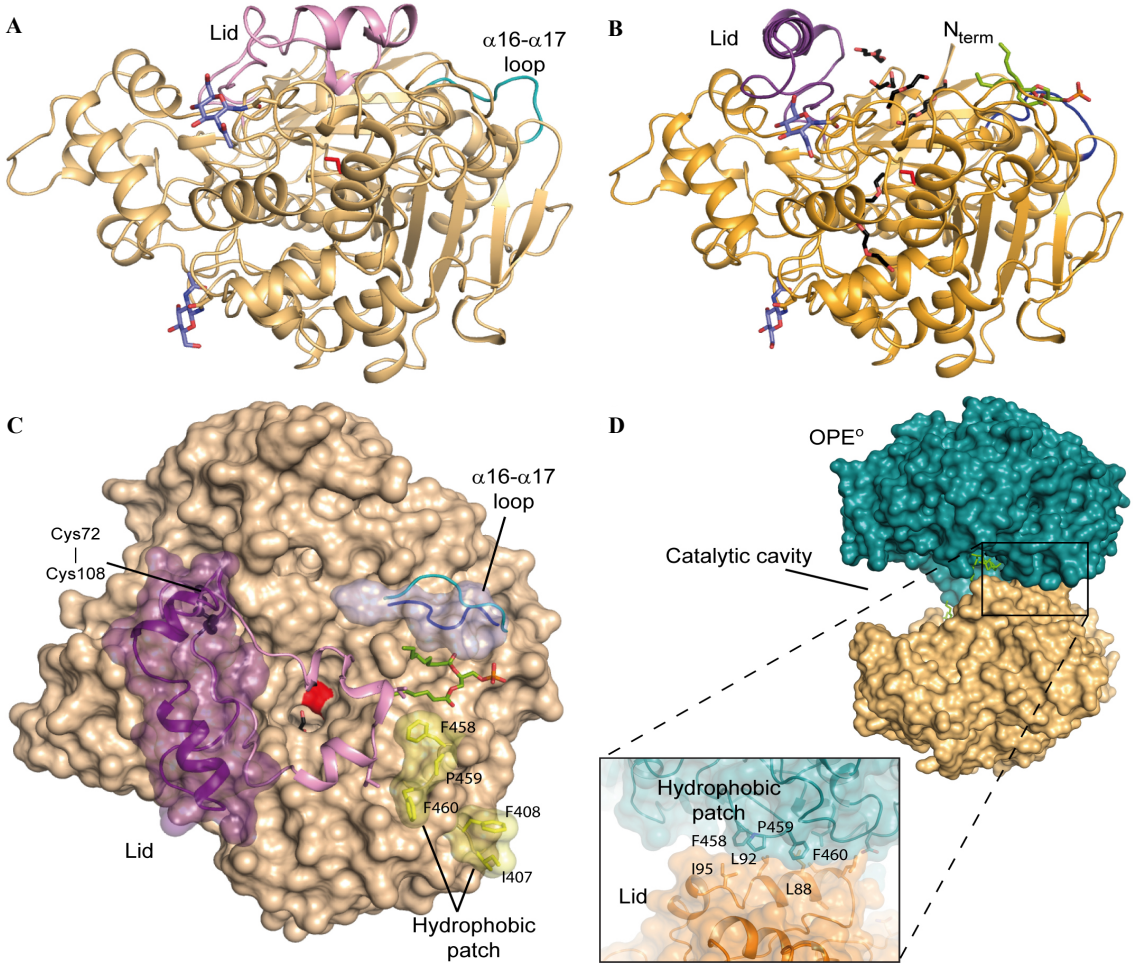

Fig. 3.2.1 Overall structure of the closed and open conformations of OPE. **A)** View of the closed OPE structure with the α/β hydrolase core colored in yellow and the lid colored in magenta. Glycan molecules attached to the glycosylation sites are represented as blue sticks. Catalytic Ser220 is shown in blue sticks. The α16–α17 loop is labeled. **B)** View of the open OPE structure with the α/β hydrolase core colored in yellow and the lid colored in magenta. Glycan molecules attached to the glycosylation sites are represented as blue sticks. Catalytic Ser220 is shown in blue sticks. PEG chains are shown as black sticks and the phospholipid as green sticks. **C)** Detailed view of the changes between closed and open states in OPE at the entry channel. Large displacements are observed for Val476 (9 Å) and for Leu477 (4 Å) between the closed (blue) and open (magenta) states. **D)** Dimeric form of OPE in its open conformation, showing the catalytic cavity and the non-bonded contacts between the open lid of one chain and the hydrophobic patch of the other.

3.2.4.2 Oligomeric arrangement in OPE

A dimeric arrangement was observed for the open conformation OPE^o as also reported for crystal structures of the open forms of Lip1 (Grochulski et al. 1993) and Lip3 (Ghosh et al. 1995). However, in contrast with that observed for Lip1 and Lip3 which monomers tightly associate forming dimers, OPE^o presents a dimer associated by regions in which aliphatic residues from the lid of one chain (Leu84, Leu85, Leu88, Leu92 and Ile95) interact with the hydrophobic patch of the opposite chain (**Fig. 3.2.1D**) with few contacts between OPE^o monomers and presenting a large cavity opened to the solvent (about 23 Å x 38 Å). Ultracentrifugation experiments carried out with native *O. piceae* enzyme showed protein multi-aggregates in aqueous solution while, in the same conditions, monomeric and dimeric forms were observed in the protein expressed in *P. pastoris* (Barba Cedillo et al. 2012).

Analytical ultracentrifugation studies (**Table 3.2.2**) showed a change in the percentages of monomer and dimer in the presence of inhibitor or substrate enzyme. In both cases, the purified OPE or monomeric-rich fraction, the predominant form was the monomer. In the presence of both, enzyme inhibitor or substrate, a significant amount of the monomer was converted into the dimer, suggesting the transition from the closed to the open enzyme form in the presence of both, inhibitor or substrate. The phenomenon of transition between the two conformations has been previously described in *C. rugosa* lipases, where exposure of the monomeric form of the enzyme to triolein dramatically accelerated its transition to the open form (Turner et al. 2001).

3.2.4.3 Activation mechanism in OPE

Besides opening of the lid, activation in OPE involves changes in the conformation of the loop α16–α17 (residues Tyr474-Tyr480), that stabilizes a phospholipid molecule located at the interface between both monomers of the dimer into a groove (11 Å wide, 8 Å deep and 15 Å long) connecting the outer part of the enzyme to the active site (**Fig. 3.2.1C** and **Fig. 3.2.2**).

Table 3.2.2 Percentage of monomer and dimer forms of the esterase, obtained after analytical ultracentrifugation, in protein samples in absence or presence of dodecane sulfonyl chloride, as enzyme inhibitor, and cholesteryl oleate, as enzyme substrate. OPE corresponds to the *O. piceae* esterase expressed in *P. pastoris* after hydrophobic interaction columns. The monomeric fraction was obtained in an additional step by using SEC to separate the different aggregate forms present in the purified protein.

	% Monomer	% Dimer
OPE	63.1	19.6
OPE + inhibitor	33.4	40.1
OPE + substrate	19.1	71.5
Monomer fraction	69.9	30.1
Monomer fraction+ inhibitor	18.6	75.9
Monomer fraction + substrate	16.8	83.2

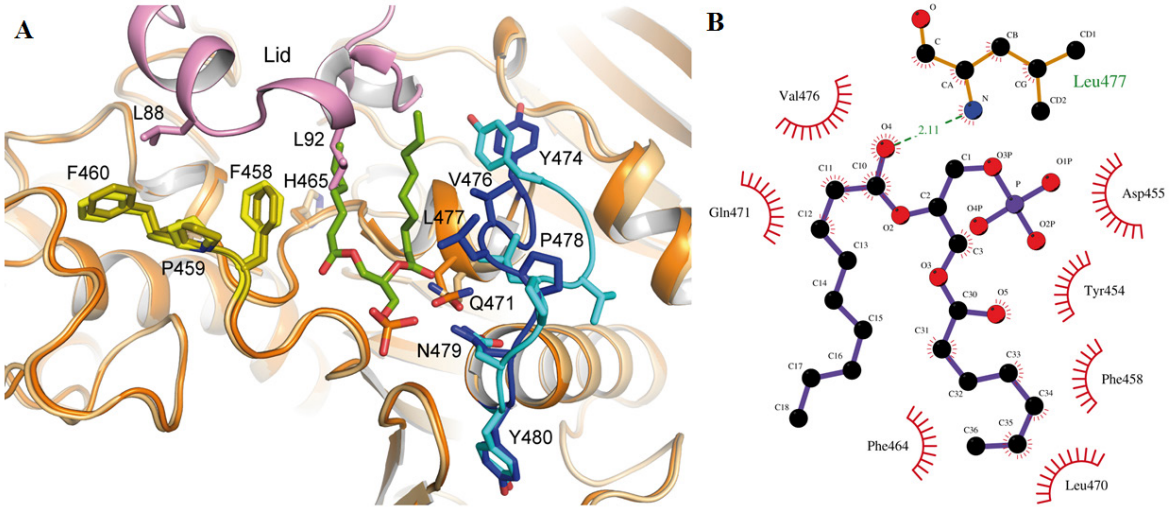

Fig. 3.2.2 Phospholipid site and recognition in active OPE. A) The phospholipid (green sticks) is located in a groove formed by the α16–α17 loop (in blue) and the hydrophobic patch (in yellow). Residues involved in substrate stabilization are labeled. Lid from the closed conformation is colored in pink. **B)** Schematic representation of the interactions between the phospholipid and the active OPE.

This phospholipid was not included in the crystallization conditions and very likely was incorporated during the purification process (see Section **3.2.3**). A twist in Pro478 residue causes the displacement of the entire loop, with displacements of 9 Å in Val476 and 4 Å in Leu477 with regard to OPE^c, increasing the interactions with the lipid found in this groove (**Fig. 3.2.1C**). H-bond interactions affecting residues at the extremes of the loop (Asn479, Tyr480 and Tyr474 in **Fig. 3.2.S3**) serve as anchoring point for the α16–α17 loop. Structural analysis also provides indications about what could trigger lid movement. In OPE^c, Leu92 is lying on the entry channel and interacting with Phe458 and Phe464 from the hydrophobic patch. Upon activation, the position of Leu92 is now occupied by one of the aliphatic chains of the phospholipid (**Fig. 3.2.2**).

Amino acid composition of loop α16–α17 is not conserved among the abH03.01 family members and structural conformation of OPE loop α16–α17, in both closed and open states, is also unique (**Fig. 3.2.S3**).

3.2.4.4 The active site cleft and substrate binding

The catalytic machinery of OPE is formed by the triad Ser220, Glu352 and His465. As observed in other members of the fungal family, and unlike other lipases, the acidic residue of the triad is a Glu residue and not an Asp residue. The catalytic region is well conserved between OPE and the other fungal lipases/esterases. The catalytic triad remains unchanged in the open and close conformation of the enzyme. By comparison with homologous enzymes, the backbone NH groups of two Gly residues (Gly134-Gly135) build the oxyanion hole that stabilizes the oxyanion produced in the tetrahedral intermediate generated during the hydrolysis. A water molecule is located close to the oxyanion hole. The oxyanion is the intermediate formed in the transient state of the hydrolysis reaction. Different molecules of PEG from the crystallization condition (see Section **3.2.3**) were identified occupying the hydrophobic active site cleft, very likely mimicking the position of substrate (**Fig. 3.2.3A**).

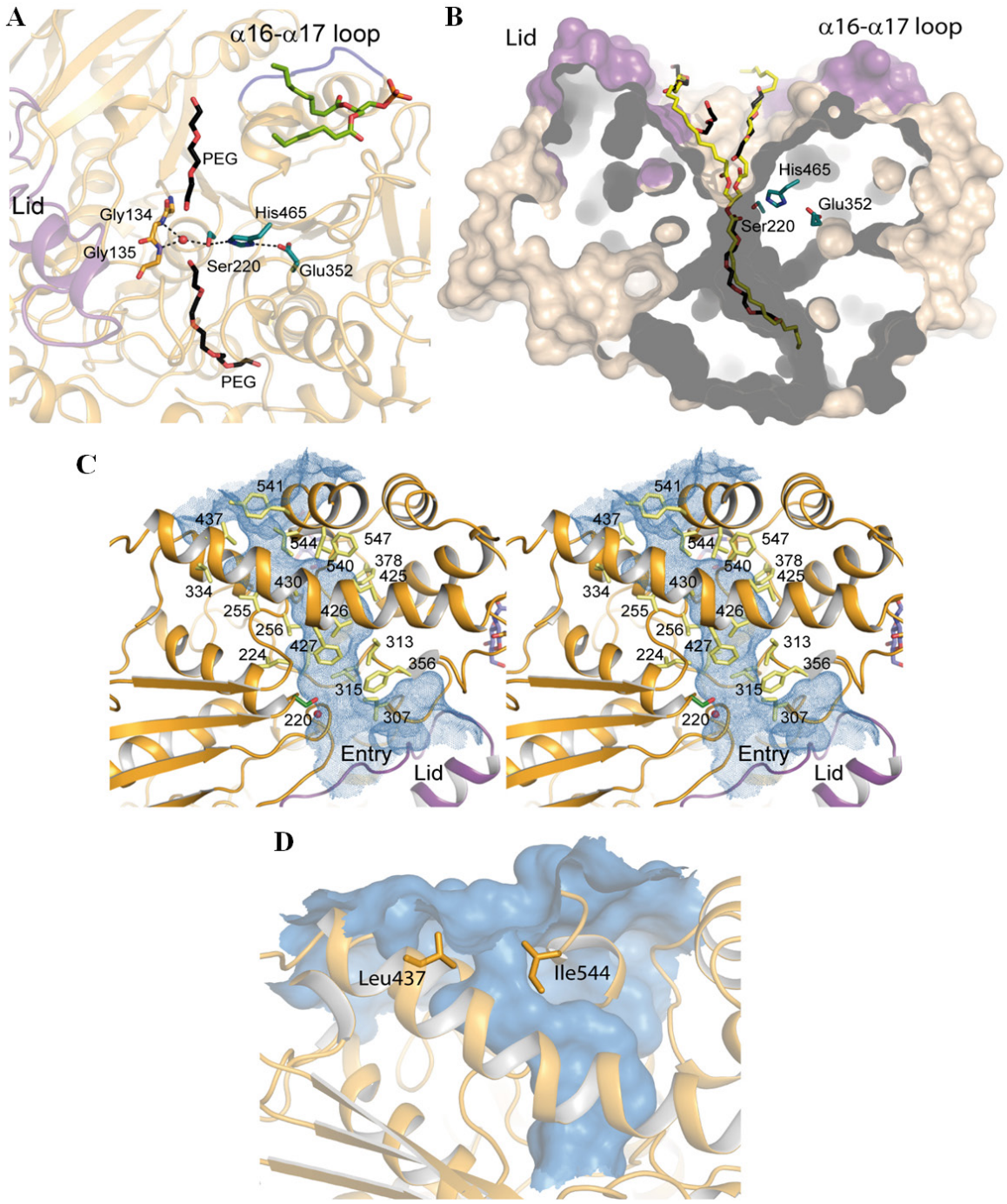

Fig. 3.2.3 The active site and internal tunnel in OPE. A) OPE Structural rearrangements upon activation. Molecular surface of OPE (brown) with the catalytic Ser residue highlighted in red. Changes from the closed (inactive state) to open (active state) structures are represented; lid and α16–α17 loop in the closed state are colored in blue; same regions in the open state in purple. Upon activation, structural rearrangements imply a 30 Å displacement of the lid to unmask the catalytic site. The hydrophobic patch is shown in yellow sticks and the phospholipid (green sticks) can be seen in between this region and the α16–α17 loop. Close to the catalytic serine there is an internal tunnel that contains a PEG chain (black sticks). **B)** Surface representation of the substrate binding site of OPE.

The catalytic triad (Ser220, Glu352, His465) is represented as green sticks. PEG moieties are represented as black sticks. The structure of the triglyceride in a fork conformation (yellow sticks) is superimposed. **C)** Stereo view of the surface of the OPE tunnel (colored in blue) leading from the catalytic site to the exit. Residues lining the tunnel are represented as yellow sticks and labeled. Catalytic serine is shown in green sticks. **D)** Narrowing of the OPE internal tunnel is produced by Leu437 and Ile544 (orange sticks).

The phospholipid molecule attached to the groove leading to the OPE active site was found in both chains of OPE^{o} and presented an excellent electron density (**Fig. 3.2.2** and **Fig. 3.2.S5**) This is the first time in this family of lipases/esterases, that a potential substrate (phospholipid), is localized in a channel leading to the active site. This groove is built by the α16–α17 loop and the previously described hydrophobic patch. The phospholipid is ensconced by hydrophobic interactions with residues from the α16–α17 loop (Val476 and Leu477) and with Phe458 from the hydrophobic patch. The glycerol moiety of the phospholipid is stabilized by polar interactions with Asp455, Gln471 and Asn479 from the α16–α17 loop (**Fig. 3.2.2**). The observed groove in OPE^{o} does not exist in the structure of other homologous enzymes for which a Trp or Phe residue fills the cavity in *C. rugosa* and *G. candidum* lipases respectively (**Fig. 3.2.S3**).

3.2.4.5 The internal tunnel

OPE^{o} esterase presents a substrate binding-site formed by an extensive hydrophobic pocket (residues Tyr76, Tyr143, Tyr144, Leu355, Phe458, Leu461, Phe464, Ile469, Leu470 and Tyr474) with a narrow internal tunnel in which aliphatic chains can be stabilized. Different elongated electron densities were observed in both chains (A and B) of the OPE^{o} active site that were modeled as PEG molecules from the crystallization condition (**Fig. 3.2.3B**). Interestingly some of these chains superimpose with the structure of a triglyceride in a fork conformation with the central aliphatic chain entering into the internal tunnel (**Fig. 3.2.3B**). The PEG molecule stabilized in the tunnel presents a well-defined electron density for a chain of 16 atoms (**Fig. 3.2.S6**). Noteworthy, this 30Å-long internal tunnel connects the active site cleft to the outside at the opposite side (**Fig. 3.2.3C** and **Fig. 3.2.S7**). Internal tunnel is formed by aromatic and aliphatic residues that confer a high

hydrophobic environment all along it (**Fig. 3.2.3C**). There is a narrowing produced between Leu437 and Ile544 residues (**Fig. 3.2.3D**), the average width in the tunnel being 9 Å and 5.5 Å in the narrowing.

Comparison with the structures of the other abH03.01 members shows that *C. rugosa* lipases, Lip1, PDB code 1CRL (Grochulski et al. 1993), Lip2 PDB code 1GZ7 (Mancheño et al. 2003); Lip3 PDB code 1CLE (Ghosh et al. 1995), present a similar tunnel but oriented towards a different region of the protein surface (**Fig. 3.2.S7B**). Lipase from *G. candidum* displays also a tunnel, similarly oriented than *C. rugosa* lipases, but with different narrowing along the tunnel (**Fig. 3.2.S7C**). The esterase from *A. niger* completely lacks the tunnel (**Fig. 3.2.S7D**). In this sense, it is worth to note how proteins sharing a similar overall structure (**Fig. 3.2.S3**) can display strong differences concerning its internal tunnel. As revealed by structural analysis, small changes in amino acid composition and/or rotamers can result in a completely different structural arrangement of the tunnel, e.g. while the first half of the tunnel follows the same path in *O. piceae*, in *C. rugosa* and *G. candidum* lipases, a substitution of a serine by Tyr377 in OPE blocks the path redirecting it about 150º apart (**Fig. 3.2.S7**).

In an attempt to ascertain the potential role of the tunnel in the product release of the reaction, we constructed a site-directed mutant, replacing Ile544 by a Trp residue (OPE-I544W). The goal with this mutant was to block the substrate exit by inserting a bulky hydrophobic residue. The OPE-I544W mutant was purified and its structure solved at 2.4Å resolution (**Table 3.2.1**). Both native and mutated proteins showed no differences in their secondary structure (rmsd of 0.147 Å for 518 Cα atoms). As expected, substitution of Ile544 residue by bulky Trp residue completely blocks the potential exit of the internal tunnel (**Fig. 3.2.4**).

Different activity studies were carried out comparing wild type *versus* mutated enzyme (**Fig. 3.2.4B**). Our results (**Table 3.2.3**) show that while enzyme activity against *p*NPB and *p*NPL was similar in the mutated and wild type enzymes, the activity was completely lost with *p*NPP (~0.2% of the wt enzyme). These results suggest that the length of the substrate affects the activity of the mutated protein at the end of the tunnel; while short-medium

substrates (4 and 12 C atoms) remain mostly unaffected, hydrolytic activity with substrates having more than 16 C atoms is severely reduced *versus* that of wt.

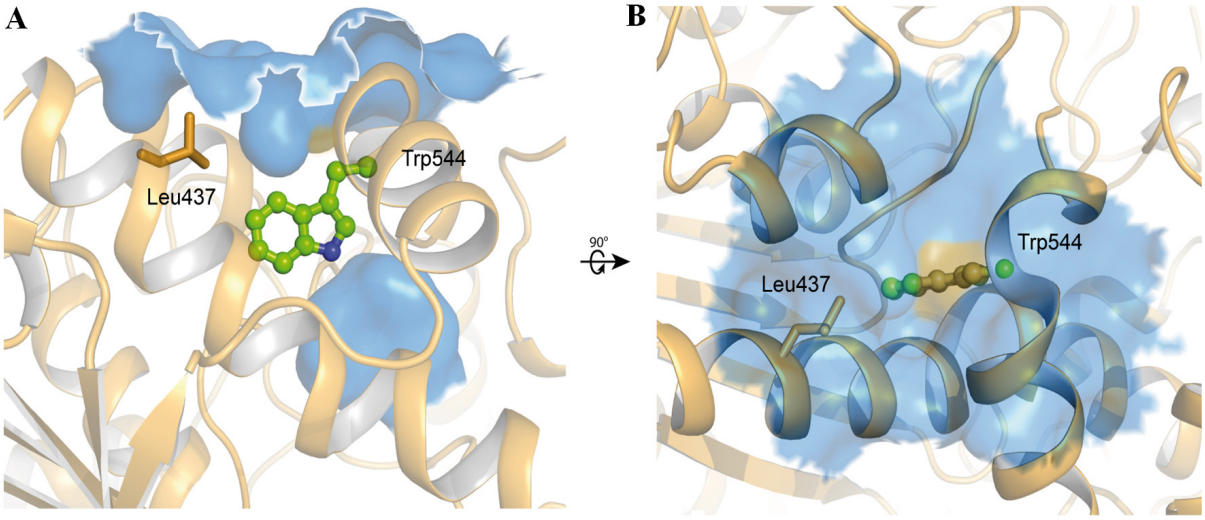

Fig. 3.2.4 Blocking tunnel exit by site directed mutagenesis. View of the molecular surface in the OPE I544W mutant. The mutation blocks the potential exit of the tunnel (surface for the mutated position is colored in orange on the right panel).

Table 3.2.3 Specific activity of the recombinant protein expressed in *P. pastoris*, as well as on the mutant I544W constructed by site-directed mutagenesis, on 2mM *p*NPB, *p*NPL and *p*NPP, in presence of 1% genapol.

		Specific activity (U mg^{-1})	
Substrate	Fatty acids	OPE native	I544W
*p*NPB	C4:0	103.17± 2.54	113.44 ± 3.52
*p*NPL	C12:0	162.72 ± 6.82	203.65± 12.93
*p*NPP	C16:0	65.78 ±5.30	0.13 ± 0.013

On the other hand, amino acid composition in the internal tunnel of *C. rugosa* lipases has been associated to differences in substrate specificity between Lip1 and Lip3 (Ghosh et al. 1995). Structural comparison among the three *C. rugosa* isoenzymes (Lip1, Lip2 and Lip3) has been reported to show two distinctive regions according to their amino acid composition: an aromatic-rich region at the beginning of the tunnel and an aliphatic-rich region at the bottom (Mancheño et al. 2003; Mancheño et al. 2003). Whereas this second region remained essentially identical in the three isoenzymes and thus the interactions with the alkyl chains of the substrates would be very similar, the phenylalanine content of the first region differs in the three proteins (Mancheño et al. 2003), a fact that was associated with the substrate recognition properties of the isoenzymes, namely, to their lipase/esterase character. The differences of *C. rugosa* lipases activity on cholesterol esters (Lip2>Lip3>Lip1) have been related to the higher Phe content in the hydrophobic region of the tunnel (Lip1>Lip3>Lip2) (Mancheño et al. 2003). In the case of OPE, the Phe content in this region is similar to Lip2. It could explain its ability to hydrolyze sterol esters. However, its high efficiency, when compared to the commercial *C. rugosa* cholesterol esterase to hydrolyze triglycerides with long chain fatty acids or different cholesterol esters (Calero-Rueda et al. 2009), could be related to its specific internal tunnel and its unique dimeric structure. The presence of large opening in the active dimer could allow the entrance of different substrates that can be stabilized in the 30Å-long internal tunnel.

3.2.4.6 Proposed model of substrate entry and product release in OPE

Crystal structures of OPE provide clues about the fate of the substrate to be hydrolyzed by the enzyme. The closed conformation of OPE is a monomer with the large lid masking the active site. Activation involves both, opening of the lid and the rearrangement of α16–α17 loop and the formation of a dimeric structure. As proven by our experiments, isolation of the monomeric form results in an increase of the dimer upon activation of the enzyme. Once the lid is open, the hydrophobic surface behind it is exposed, allowing the substrate to move to the catalytic cleft where the catalytic Ser220 residue is located. The hydrocarbon chain of the substrate is inserted into the tunnel up

to the point at which the ester bond reaches the Ser220. After reaction, the acidic moiety of the ester (a fatty acid) could remain in the tunnel, while the sterol moiety is released. The fatty acid inside the tunnel has to be released in order to recover the active state of the enzyme.

Our mutagenesis experiments indicate that a single modification blocking the exit of the tunnel 30 Å far from active site (by replacing Ile544 by bulky Trp residue) did not affect significantly the OPE activity on substrates with short-medium chain fatty acids. While an appealing hypothesis is that substrates could be released by the exit of the tunnel, our crystallographic and biochemical experiments indicate that the exit of the tunnel is not required for efficient hydrolysis in OPE against these substrates. The observed lost of activity of the OPE I544W mutant with *p*NPP could be explained by the presence of bulky Trp residue at the end of the tunnel that decreases its effective length avoiding the right positioning of long substrates to be cleaved at catalytic site. This has been observed in the cholesterol esterase Lip3 from *C. rugosa* where the cholesteryl linoleate ligand was found with the aliphatic chain entering into the internal tunnel orienting the cholesteryl moiety to be cleaved by catalytic Ser residue (**Fig. 3.2.S8**). Therefore the length and amino acid composition of the internal tunnel seems to be crucial to understand the catalytic versatility of OPE. The other essential parameter is the dimeric nature of the active form. Contrary to the previously observed dimer in the cholesterol esterase Lip3 from *C. rugosa*, that presented a tight homodimer with small cavities entering into the active sites (**Fig. 3.2.S9**), the dimer in the OPE^{o} shows a pacman-like structure with a very large opening (23 Å x 38 Å) (**Fig. 3.2.S9**) that could allow both the entrance of large substrates and also quick release of the reaction products. Further experiments will be needed to corroborate this hypothesis and study the role of the internal tunnel in this protein for its action on long-chain fatty acids substrates.

3.2.5 CONCLUSIONS

Here we describe, for the first time, the structural rearrangements required for the activation and degradation mechanism of the OPE cholesterol esterase from abH03.01 family of fungal lipases/esterases. Structural analysis revealed

different pockets that, upon activation, are responsible of dimerization and stabilization of the acyl chains of the substrate. Based on our structural and biochemical results, we propose a mechanism by which a great variety of different substrates can be hydrolyzed and released in OPE. These results reveal a new scenario in which not only the activation of the enzyme but also the release of its hydrolysis products could be handled paving the way for the construction of new variants to improve the catalytic properties of these enzymes and their biotechnological applications.

Acknowledgements

This work was supported by Grants BFU2011-25326 and BIO2012-3637 from Spanish Ministry of Economy and Competitiveness and by S2010/BMD-2457 and S-2009AMB-1480 Grants from Autonomous Community of Madrid**.** M.E. Vaquero thanks the Spanish Ministry of Economy for a FPU fellowship. Authors thank the help of the Analytical Ultracentrifugation CIB facility for ultracentrifugation experiments.

3.2.6 REFERENCES

Adams PD, Afonine PV, Bunkoczi G, Chen VB, Davis IW, Echols N, Headd JJ, Hung LW, Kapral GJ, Grosse-Kunstleve RW et al. (2010) PHENIX: a comprehensive Python-based system for macromolecular structure solution. Acta Crystallogr D Biol Crystallogr 66:213-221

Allain CC, Poon LS, Chan CSG, Richmond W, Fu PC (1974) Enzymatic determination of total serum-cholesterol. Clin Chem 20:470-475

Barba Cedillo V, Plou FJ, Martinez MJ (2012) Recombinant sterol esterase from *Ophiostoma piceae*: an improved biocatalyst expressed in *Pichia pastoris*. Microb Cell Fact 11:73

Barba V, Prieto A, Martínez AT, Martínez MJ (2011) Procedimiento para la obtención de compuestos de interés alimenticio y/o farmacéutico mediante reacciones de acilación de fitoesteroles libres con ácidos grasos catalizadas por una esterol esterasa procedente de hongos del género *Ophiostoma*. Patent No. P201131098

Barriuso J, Prieto A, Martínez MJ (2013) Fungal genomes mining to discover novel sterol esterases and lipases as catalysts. BMC Genomics 14:712-719

Bourne Y, Hasper AA, Chahinian H, Juin M, de Graaff LH, Marchot P (2004) *Aspergillus niger* protein EstA defines a new class of fungal esterases within the alpha/beta hydrolase fold superfamily of proteins. Structure 12:677-687

Calero-Rueda O, Gutiérrez A, del Río JC, Muñoz C, Plou FJ, Martínez AT, Martínez MJ (2002a) Method for the enzymatic control of pitch deposits formed during paper pulp production using an esterase that hydrolyses triglycerides and sterol esters. Patent No. WO 02/075045 A1

Calero-Rueda O, Plou FJ, Ballesteros A, Martínez AT, Martínez MJ (2002b) Production, isolation and characterization of a sterol esterase from *Ophiostoma piceae*. Biochim Biophys Acta 1599:28-35

Calero-Rueda O, Barba V, Rodriguez E, Plou F, Martínez AT, Martínez MJ (2009) Study of a sterol esterase secreted by *Ophiostoma piceae:* Sequence, model and biochemical properties. Biochim Biophys Acta 1794:1099-1106

Emsley P, Lohkamp B, Scott W, Cowtan K (2010) Features and development of Coot. Acta Crystallogr D Biol Crystallogr 66:486-501

Evans P (2006) Scaling and assessment of data quality. Acta Crystallogr D Biol Crystallogr 62:72-82

Ghosh D, Wawrzak Z, Pletnev VZ, Li N, Kaiser R, Pangborn W, Jörnvall H, Erman M, Duax WL (1995) Structure of uncomplexed and linoleate-bound *Candida cylindracea* cholesterol esterase. Structure 3:279-288

Grochulski P, Li YG, Schrag JD, Bouthillier F, Smith P, Harrison D, Rubin B, Cygler M (1993) Insights into interfacial activation from an open structure of *Candida rugosa* lipase. J Biol Chem 268:12843-12847

Grochulski P, Li Y, Schrag JD, Cygler M (1994) Two conformational states of *Candida rugosa* lipase. Protein Sci 3:82-91

Hermoso J, Pignol D, Kerfelec B, Crenon I, Chapus C, FontecillaCamps JC (1996) Lipase activation by nonionic detergents - The crystal structure of the porcine lipase-colipase-tetraethylene glycol monooctyl ether complex. J Biol Chem 271:18007-18016

Hermoso J, Pignol D, Penel S, Roth M, Chapus C, FontecillaCamps JC (1997) Neutron crystallographic evidence of lipase-colipase complex activation by a micelle. EMBO J 16:5531-5536

Ho BK, Gruswitz F (2008) HOLLOW: Generating accurate representations of channel and interior surfaces in molecular structures. BMC Struct Biol 8:49

Holmquist M (2000) Alpha/beta-hydrolase fold enzymes: structures, functions and mechanisms. Curr Protein Pept Sci 1:209-235

Houde A, Kademi A, Leblanc D (2004) Lipases and their industrial applications - An overview. App Biochem Biotech 118:155-170

Kabsch W (2010) Xds. Acta Crystallogr D Biol Crystallogr 66:125-132

Kontkanen H, Tenkanen M, Reinikainen T (2006) Purification and characterisation of a novel steryl esterase from *Melanocarpus albomyce*s. Enzyme Microb Technol 39:265-273

Maeda A, Mizuno T, Bunya M, Sugihara S, Nakayama D, Tsunasawa S, Hirota Y, Sugihara A (2008) Characterization of novel cholesterol esterase from *Trichoderma* sp AS59 with high ability to synthesize steryl esters. J Biosci Bioeng 105:341-349

Mancheño JM, Pernas MA, Martínez MJ, Ochoa B, Rua ML, Hermoso JA (2003) Structural insights into the lipase/esterase behavior in the *Candida rugosa* lipases family: crystal structure of the lipase 2 isoenzyme at 1.97A resolution. J Mol Biol 332:1059-1069

McCoy AJ, Grosse-Kunstleve RW, Adams PD, Winn MD, Storoni LC, Read RJ (2007) Phaser crystallographic software. J Appl Crystallogr 40:658-674

Morinaga N, Maeda A, Mizuno T, Bunya M, Sugihara S, Sugihara A (2011) Synthesis of fatty acid sterol esters using cholesterol esterase from *Trichoderma* sp AS59. Enzyme Microb Technol 48:498-504

Ollis DL, Cheah E, Cygler M, Dijkstra B, Frolow F, Franken SM, Harel M, Remington SJ, Silman I, Schrag J, et al. (1992) The alpha/beta-hydrolase fold. Protein Eng 5:197-211

Rahim MA, Sih CJ (1969) Microbial steroid esterases. Methods Enzymol 15:675-684

Reetz MT (2002) Lipases as practical biocatalysts. Curr Opin Chem Biol 6:145-150

Schrag JD, Cygler M (1993) 1.8-Angstrom Refined structure of the lipase from *Geotrichum candidum*. J Mol Biol 230:575-591

Schrödinger L (2010) The PyMOL molecular graphics system. Version 1.2r2'.

Schuck P (2000) Size-distribution analysis of macromolecules by sedimentation velocity ultracentrifugation and Lamm equation modeling. Biophys J 78:1606-1619

Singh AK, Mukhopadhyay M (2012) Overview of fungal lipase: A review. Appl Biochem Biotechnol 166:486-520

Turner NA, Needs EC, Khan JA, Vulfson EN (2001) Analysis of conformational states of *Candida rugosa* lipase in solution: Implications for mechanism of interfacial activation and separation of open and closed forms. Biotechnol Bioeng 72:108-118

Verger R (1997) Interfacial activation of lipases: fact and artifacts. Trends Biotechnol 15:32-38

Winn MD, Ballard CC, Cowtan KD, Dodson EJ, Emsley P, Evans PR, Keegan RM, Krissinel EB, Leslie AG, McCoy A et al. (2011) Overview of the CCP4 suite and current developments. Acta Crystallogr D Biol Crystallogr 67:235-242

3.2.7 SUPPLEMENTARY MATERIAL

```
O. piceae OPE     1 -----MPKRRDQSIEPRTTVNVNYPEGE-VVGVSVLGIESFRGVPFAQPP   44
                      :......:..|..|:    ..|: :.|::.:..|.|.|:|||:||
C. rugosa Lip2    1 MKLCLLALGAAVAAAPTATL----ANGDTITGLNAIVNEKFLGIPFAEPP   46

O. piceae OPE    45 VGNLRLKPPVRYTENIGTKDTTGIGPSCPQMYLSTGNGELLFQLVGNLI-   93
                    ||.||.||||.|:.::..:..|..||||.||.......:.|.:...:|:
C. rugosa Lip2   47 VGTLRFKPPVPYSASLNGQQFTSYGPSCMQMNPMGSFEDTLPKNARHLVL   96

O. piceae OPE    94 NIPLFQTATLSSEDCLTLNIQRPAGTTSNSSLPVLFWIFGGGFELGTNQY   43
                    ...:||....:.|||||:|:.||.||.:::.|||:.||||||||||.:..
C. rugosa Lip2   97 QSKIFQVVLPNDEDCLTINVIRPPGTRASAGLPVMLWIFGGGFELGGSSL  146

O. piceae OPE   144 YDGIDLLTEGISLGEPFIFVAINYRVGGFGFLGGKEIKADGSSNLGLLDQ  193
                    :.|..::.:.:.:|:|.|.|::||||..:|||.|.:|:.:||.|.||.||
C. rugosa Lip2  147 FPGDQMVAKSVLMGKPVIHVSMNYRVASWGFLAGPDIQNEGSGNAGLHDQ  196

O. piceae OPE   194 RIALEWVADNIASFGGDPSKVTIWGESAGSISVFDQMALYGGNNKYKGKA  243
                    |:|::|||||||.||||||||||:||||||:|.|..:....|:|.|.||.
C. rugosa Lip2  197 RLAMQWVADNIAGFGGDPSKVTIYGESAGSMSTFVHLVWNDGDNTYNGKP  246

O. piceae OPE   244 LFRGGIMNSGSVVPAAPVDGVKAQAIYDHVVSEAGCAGTSDTLACLRTVD  293
                    |||..||.||.:||:.||||.....||:.||:.|||...||.|||||.:.
C. rugosa Lip2  247 LFRAAIMQSGCMVPSDPVDGTYGTEIYNQVVASAGCGSASDKLACLRGLS  296

O. piceae OPE   294 YTKFLTAVNSVPGIVSYSSIALSYLPRPDGVVLIDSPEEIVKNKQYAAVP  343
                    ......|.:..||:::|.|:.|||||||||..:.|....:|::.:||.||
C. rugosa Lip2  297 QDTLYQATSDTPGVLAYPSLRLSYLPRPDGTFITDDMYALVRDGKYAHVP  346

O. piceae OPE   344 MIIGDQEDEGTLFAVLPNNITSTAKIVQYFQDLYFYNATKEQLTAFVNTY  393
                    :|||||.||||||.:...|:|:.|:...||:. .|.:|:..::...:..|
C. rugosa Lip2  347 VIIGDQNDEGTLFGLSSLNVTTDAQARAYFKQ-SFIHASDAEIDTLMAAY  395

O. piceae OPE   394 PTDITAGSPFNTGIFNELYPGFKRLAAILGDMTFTLARRAFLQLCSEVNP  443
                    .:|||.||||:|||||.:.|.|||::|:|||:.||||||.||....
C. rugosa Lip2  396 TSDITQGSPFDTGIFNAITPQFKRISALLGDLAFTLARRYFLNYYQ----  441

O. piceae OPE   444 DVPSWSYLASYDYGFPFLGTFHATDILQVFYGVLPNYASGSI--QKYYIN  491
                    ....:|:|:....|.|.||||||..||:...|.|    .|||:  ...:|.
C. rugosa Lip2  442 GGTKYSFLSKQLSGLPVLGTFHGNDIIWQDYLV----GSGSVIYNNAFIA  487

O. piceae OPE   492 FVTTGDPNKGAAVDIQWPQWSAK----KNILQIYATKAVIVADNFRAKSY  537
                    |....|||| |.:...||.:::.    .|::||.........||||..:|
C. rugosa Lip2  488 FANDLDPNK-AGLWTNWPTYTSSSQSGNNLMQINGLGLYTGKDNFRPDAY  536

O. piceae OPE   538 EYLYNNIGIFRI  549
                    ..|::|...|.:
C. rugosa Lip2  537 SALFSNPPSFFV  548
```

Fig. 3.2.S1 Sequence alignment between OPE and Lip2 from *C. rugosa*.

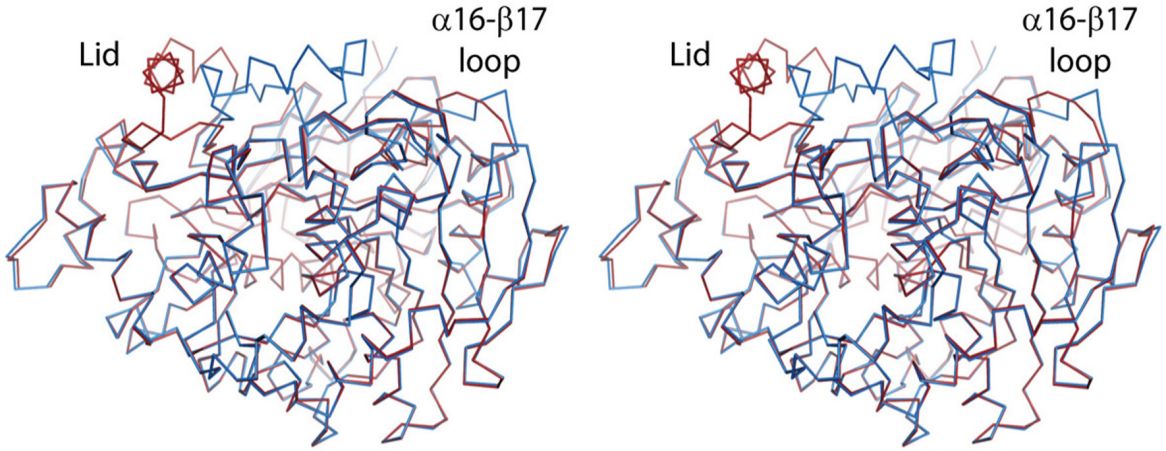

Fig. 3.2.S2 Stereo view of the structural alignment between OPE^{c} (blue) and OPE^{o} (red). The lid and the α16-α17 loop are labeled.

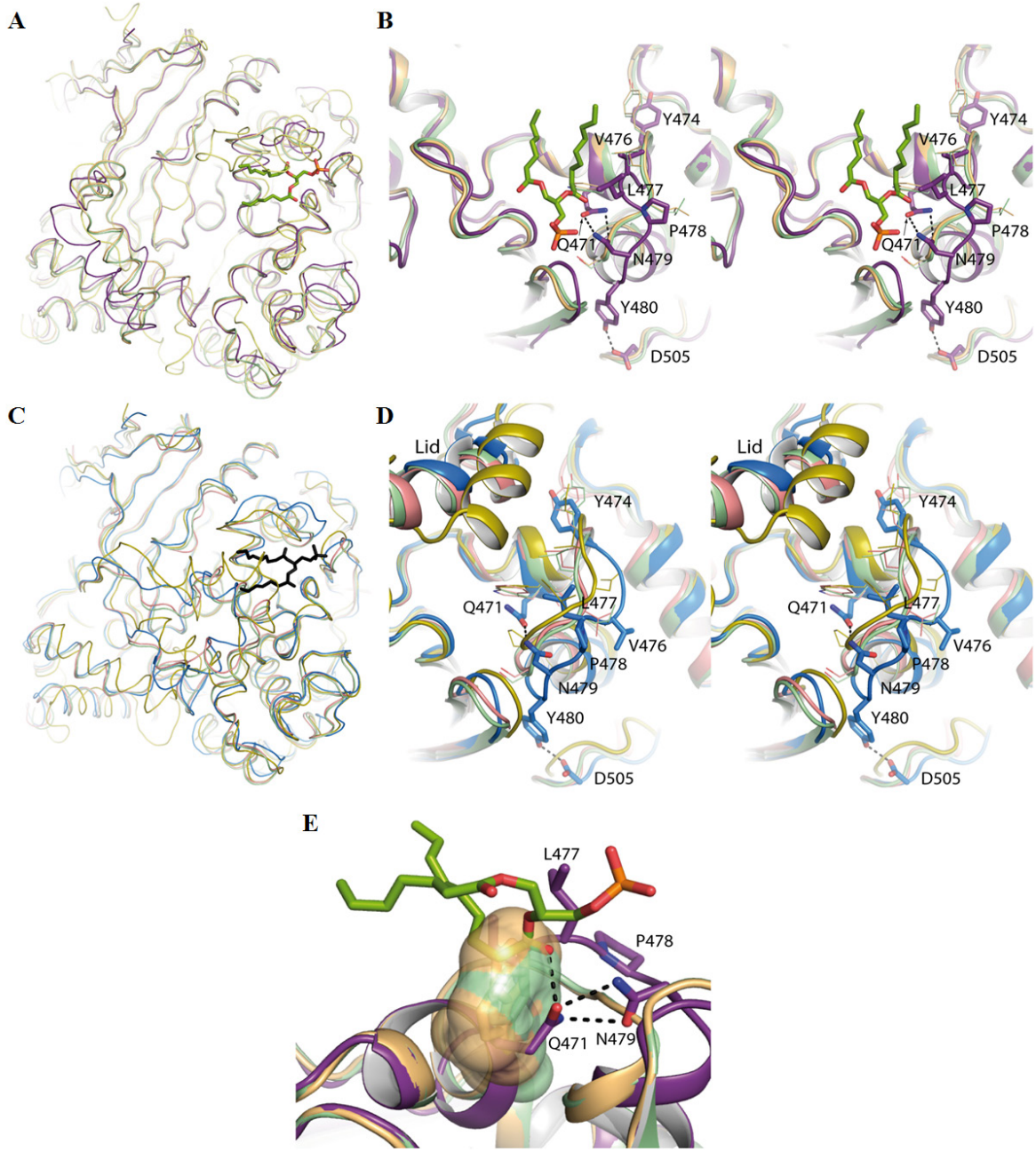

Fig. 3.2.S3 Structural alignment between OPE and lipases from abH03.01 family. **A)** Structural alignment of the open conformations of OPE (purple), *C. rugosa* Lip1 (PDB code 1CRL, (Grochulski et al. 1993); shown in green), *C. rugosa* Lip3 (PDB code 1CLE, (Ghosh et al. 1995); shown in orange) and *A. niger* esterase (PDB code 1UKC, (Bourne et al. 2004); shown in yellow). **B)** Stereo view of the open conformations focused on the α16-α17 loop, showing the main residues involved in substrate intake. For clarity reasons, *A. niger* esterase has been removed because of high deviation in this region. **C)** Structural alignment of the closed conformations of OPE (blue), *C. rugosa* Lip1 (PDB code 1TRH, (Grochulski et al. 1994); shown in green), *C. rugosa* Lip2 (PDB code 1GZ7, (Mancheño et al. 2003); shown in red) and *G. candidum* lipase (PDB code 1THG, (Schrag and Cygler 1993); shown in yellow). The position of the phospholipid found in the open conformation

of OPE has been superimposed (black sticks) to locate the entry channel. **D)** Stereo view of the closed conformations focused on the α16-α17 loop, showing the main residues at the entry channel. **E)** The presence of a phenylalanine in Lip1 and a tryptophan in Lip3 at the same position of Q471 in OPE avoids the entering of the substrate through this channel, blocking the interactions that occur in OPE.

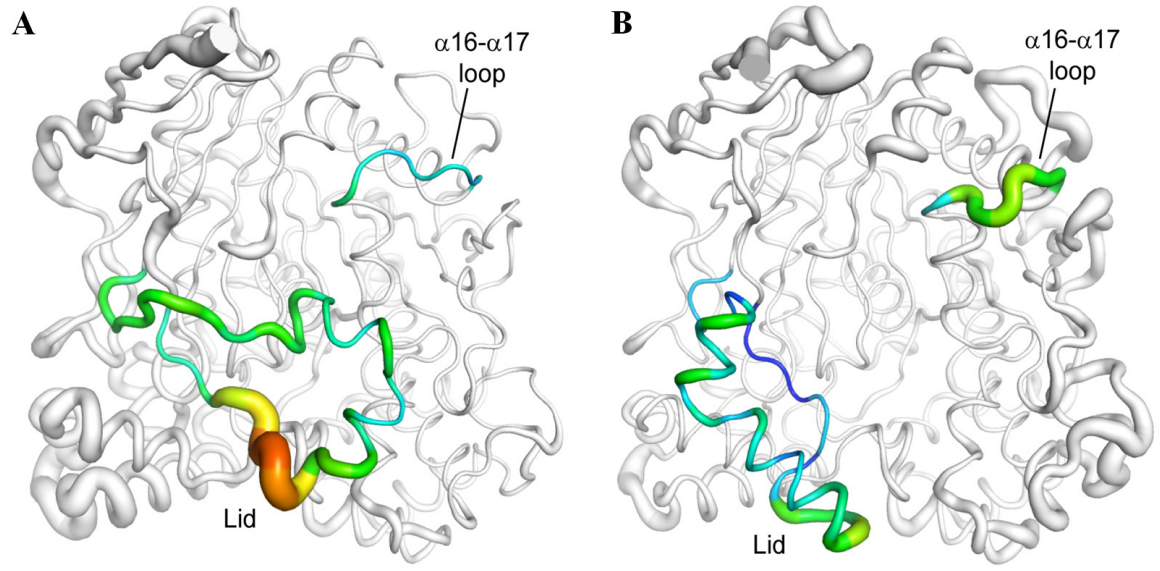

Fig. 3.2.S4 B-factor distribution for lid and α16-α17 loop in the closed and open conformations of OPE. A) B-putty representation of OPE in its closed conformation, being the lid and the α16-α17 loop colored, following a rainbow scheme, from blue (low thermal factors) to red (high thermal factors). **B)** B-putty representation of OPE in its open conformation.

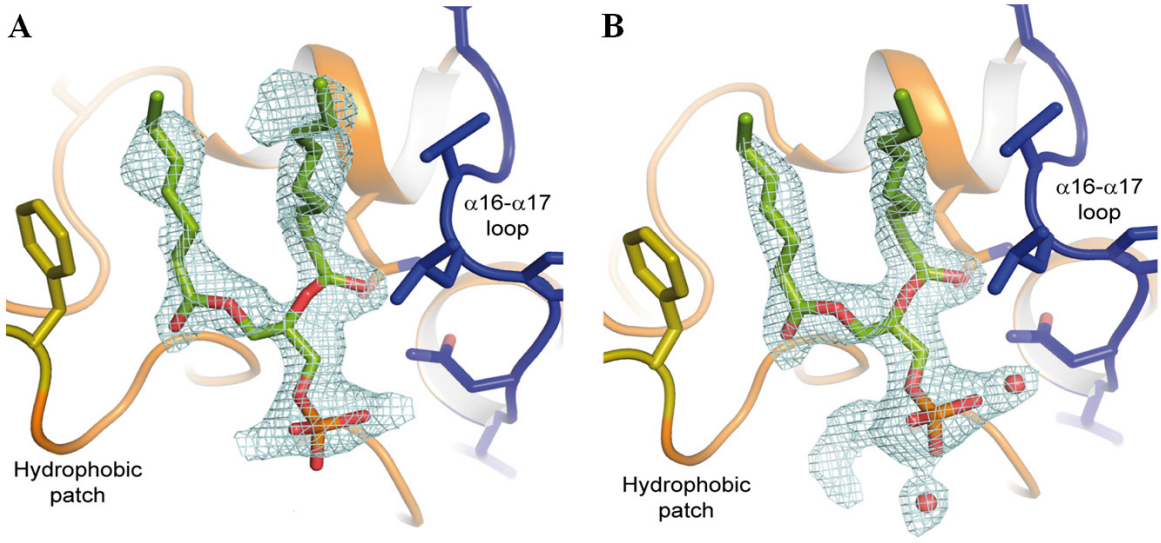

Fig. 3.2.S5 Electron density for the phospholipid molecule located in the entry channel. A) Omit map at the phospholipid region, contoured at 1.0 σ. The phospholipid is represented in green sticks, the hydrophobic patch in yellow and the α16-α17 loop in dark blue. **B)** The 2|Fo|-|Fc| electron density map, contoured at 1.0 σ.

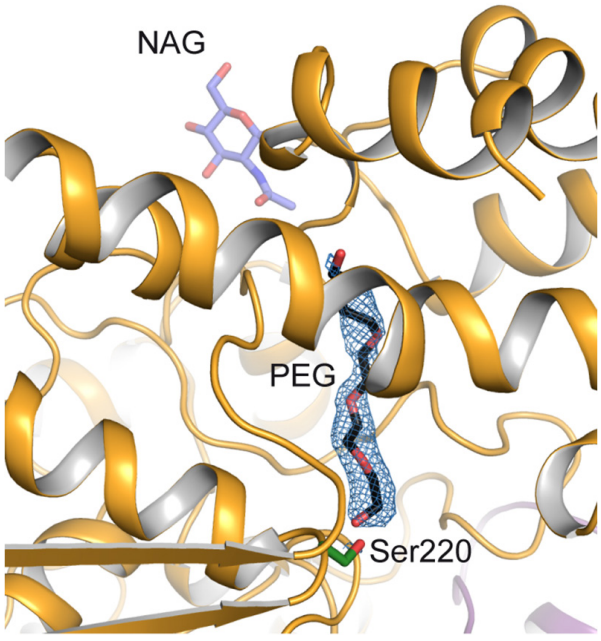

Fig. 3.2.S6 Electron density map for the PEG in the tunnel of active OPE. 2|Fo|-|Fc| electron density map, contoured at 1.0 σ, for the electron density map of the PEG molecule located in the tunnel.

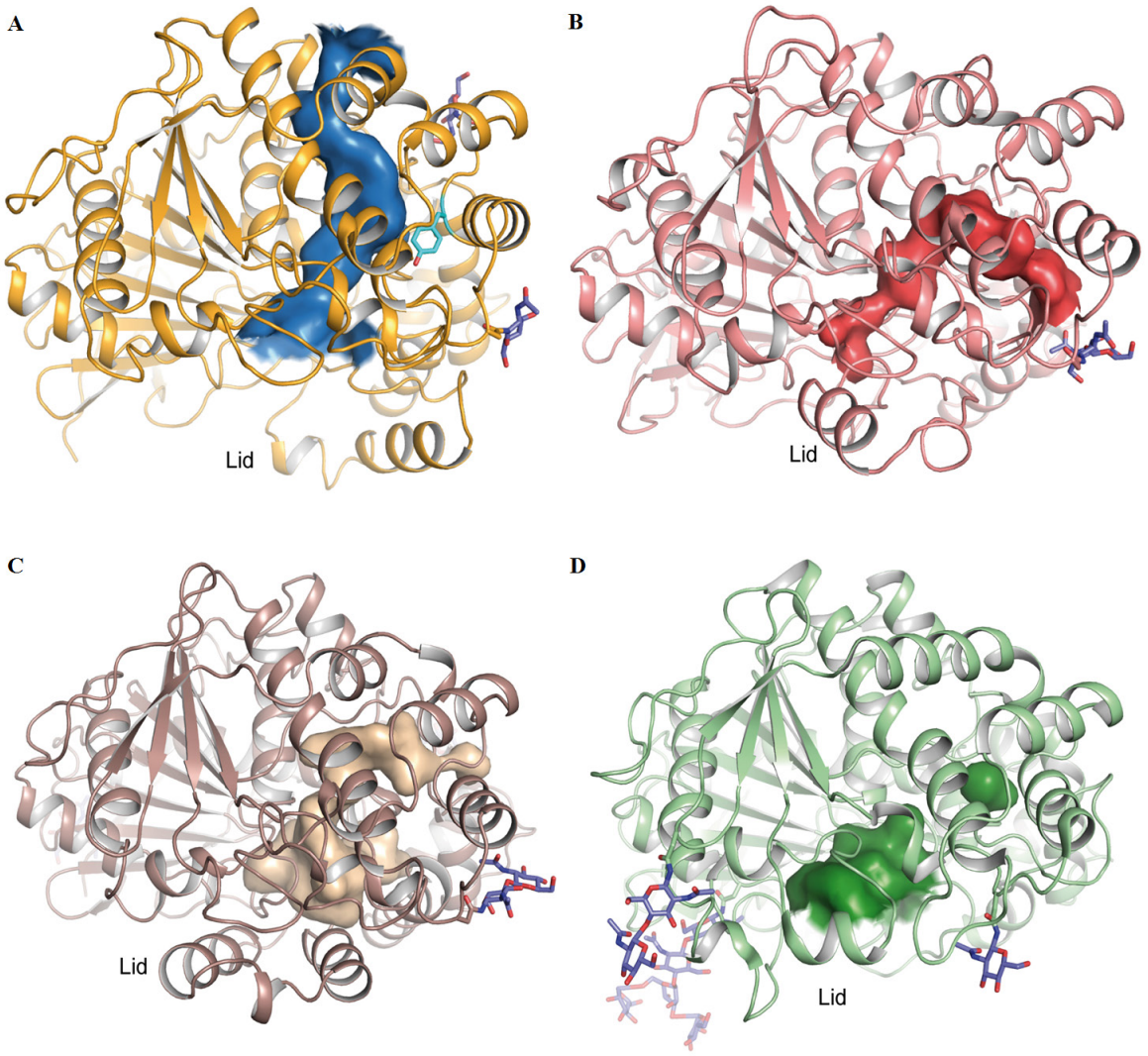

Fig. 3.2.S7 Internal tunnels in lipases/esterases from the abH03.01 family. A) Open conformation of the sterol esterase from *O. piceae* (OPE). Internal tunnel is represented as a solid surface and colored in blue. The exit of the tunnel is located on the top of the protein. Glycosilations are shown in blue sticks. **B)** *C. rugosa* Lip2 (PDB code 1GZ7, (Mancheño et al. 2003)). Internal tunnel is represented as a solid surface and colored in red. The other solved lipases from *C. rugosa* (Lip1 and Lip3) present the same tunnel than Lip2. **C)** *G. candidum* lipase (PDB code 1THG, (Schrag and Cygler 1993). Internal tunnel is represented as a solid surface and colored in brown. **D)** *A. niger* esterase (PDB code 1UKC, (Bourne et al. 2004)), as other typical esterases, does not present a lid and there is no internal tunnel (the corresponding region is represented as a solid surface and colored in green). For comparison purposes all the proteins are oriented the same way.

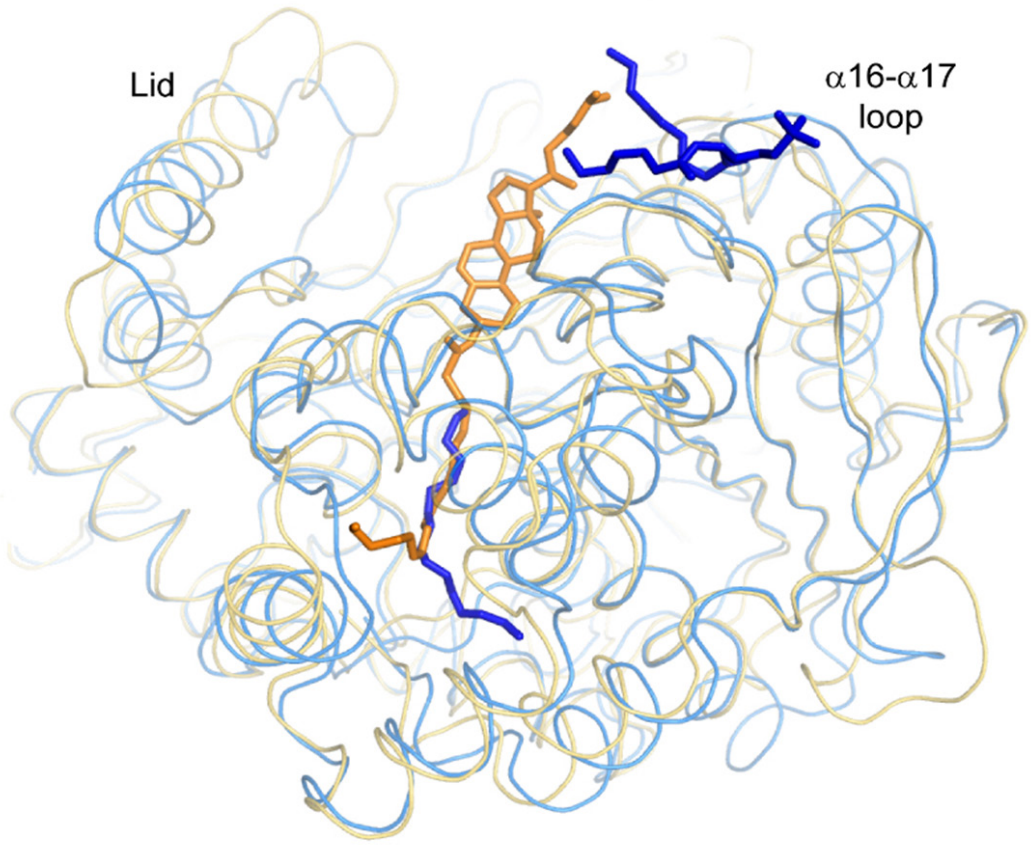

Fig. 3.2.S8 Substrate recognition in OPE (blue ribbons) and *C. rugosa* Lip3 (yellow ribbons). Cholesteryl linoleate (orange sticks) in *C. rugosa* Lip3 (PDB code 1CLE, (Ghosh et al. 1995) presents its aliphatic chain inserted into the internal tunnel as also observed for the PEG molecule (blue sticks) inserted into the internal tunnel of OPE. As observed, the middle end of the tunnel follows an opposite direction in Lip3 and in OPE. The phospholipid attached close to the α16-α17 loop of OPE is also represented as blue sticks.

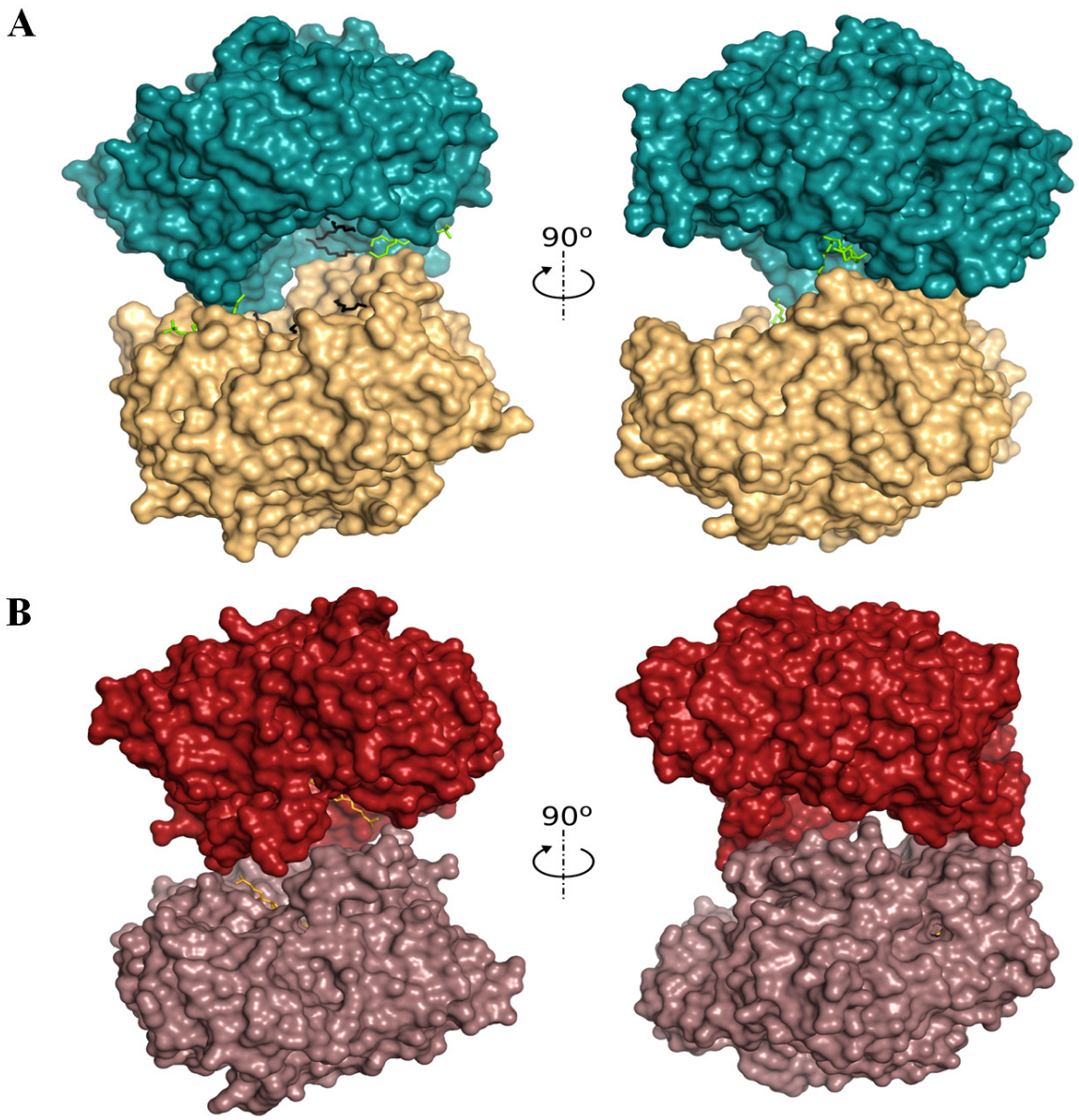

Fig. 3.2.S9 Different dimeric arrangement in the open conformations of OPE and *C. rugosa* Lip3. A) Surface representation of active OPE dimer, showing the phospholipids (green sticks) and the PEG molecules (black sticks) filling the catalytic cavity. **B)** Surface representation of *C. rugosa* Lip3 (PDB code 1CLE, (Ghosh et al. 1995), showing the cholesteryl linoleate in the catalytic cavity (orange sticks)

.

3.3 CHAPTER 3

Expression and properties of three novel fungal lipases/sterol esterases predicted in silico: comparison with other enzymes of the *Candida rugosa*-like family

María Eugenia Vaquero, Alicia Prieto, Jorge Barriuso, María Jesús Martínez,

Published in Applied Microbiology and Biotechnology (2015)
doi 10.1007/s00253-015-6890-9

3.3.1 SUMMARY

Lipases from the *C. rugosa*-like family are enzymes with great biotechnological interest. In a previous work, several enzymes from this family were identified by in silico mining of fungal genomes. Here we describe the cloning, expression, and characterization of putative lipases from the genomes of *Nectria haematococca*, *Trichoderma reesei* and *Aspergillus niger* and compared their catalytic properties with those of OPE, a well characterized sterol esterase/lipase from *Ophiostoma piceae*. All of them hydrolyzed *p*-nitrophenol esters and triglycerides with different efficiency, but their activity against sterol esters was dissimilar, and the enzyme from *A. niger* was unable of hydrolyzing these substrates while OPE showed the best k_{cat} values, which in general leads to an improved catalytic efficiency. Similarly, OPE was the best catalyst in the synthesis of β-sitostanyl oleate, followed by the commercial CRL from *Candida rugosa*, while the *A. niger* enzyme was unable to produce this compound. When the enzymes were evaluated for caprolactone oligomerization, the *A. niger* enzyme gave similar results than CRL, being OPE slightly more efficient. The expression of the putative selected proteins allowed their functional validation, suggesting that the hydrophobicity of the lid region may be an important factor, although the enzymatic efficiency is also influenced by other parameters, as the aggregation state and the size and morphology of the tunnel, where substrate recognition and catalysis takes place.

3.3.2 INTRODUCTION

Lipases (E.C. 3.1.1.3) and sterol esterases (E.C. 3.1.13) are enzymes with great biotechnological interest because of their broad substrate specificity and their ability to carry out hydrolysis in aqueous media and synthesis in the presence of organic solvents (Bornscheuer 2002; Jaeger and Eggert 2002). The distinction between these carboxyl esterases is not clear. Lipases usually are able of releasing long-chain fatty acids from water-insoluble carboxylic esters in hydrolysis reactions, while sterol esterases act on sterol esters. However, there are enzymes showing both lipase and sterol esterase activities (Casas-Godoy et al. 2012). This is the case of the well known *Candida rugosa* lipases (Mancheño et al. 2003) and the sterol esterase from *Ophiostoma piceae* (Calero-Rueda et al. 2002).

Lipases are the third largest group of commercialized enzymes with a wide range of applications in different industrial sectors, such as biofuels, oleochemical, food, detergents, cosmetics, pharmaceutical, textile and paper industry (Bornscheuer et al. 2002; Gupta et al. 2015; Hasan et al. 2006; Jaeger and Eggert 2002). Moreover, most of them are stable in organic solvents, and they have been reported as potential catalysts for ring-opening polymerization (ROP) of lactones and lactides to produce polyesters (Kobayashi et al. 1998; Uyama and Kobayashi 1993; Varma et al. 2005).

Sterol esterases with high affinity on triglycerides and sterols esters, such as those from *O. piceae* (Calero-Rueda et al. 2002) and *Melanocarpus albomyces* (Kontkanen et al. 2006), have been reported for pitch (Calero-Rueda et al. 2002; Kontkanen et al. 2004) or stickies reduction (Barba Cedillo et al. 2013) during paper pulp or recycled paper manufacture, respectively. However, the use of lipases/sterol esterases with high affinity on sterol esters as catalysts of the enzymatic esterification of free sterols and stanols from plant extracts has also been proposed. This reaction is of particular interest since the intake of these esters help to reduce LDL cholesterol (Barba Cedillo et al. 2011; He et al. 2010; Norinobu et al. 2003; Teixeira et al. 2011).

The enzymes from *O. piceae* and *M. albomyces* belong to the so-called *C. rugosa*-like lipase family (Barriuso et al. 2013; Pleiss et al. 2000). *C.*

rugosa secretes a variety of closely related extracellular lipases, well characterized at the structural and biochemical level and with a high sequence identity (77-88%), but displaying different substrate specificity on sterol esters and triglycerides (Mancheño et al. 2003). These changes seem to be due to small variations in the lid region, the substrate binding pocket and the hydrophobic tunnel (Domínguez de María et al. 2006). The monomeric form of enzymes from the *C. rugosa* like-family shows molecular masses ≥ 60 kDa, shares more than 40% sequence identity with *C. rugosa* isoenzymes, and contains the conserved motif "GESAG", which comprises the catalytic serine, that together with a conserved glutamic and histidine residues constitutes the "catalytic triad". This family also contains the "GGGF" conserved sequence involved in the formation of the oxyanion hole (Barriuso et al. 2013).

The sterol esterase secreted by the ascomycete *O. piceae* (OPE) possesses 44% sequence identity with *C. rugosa* isoenzymes (CRL). Its structure was recently determined, in both the closed and open conformations (Gutiérrez-Fernández et al. 2014), revealing that the active form is dimeric and the existence of a possible exit tunnel for products release. These factors could be responsible for its high efficiency hydrolyzing cholesterol esters or triglycerides with long chain fatty acids, when compared to *C. rugosa* enzymes (Calero-Rueda et al. 2009).

There is an increasing interest in the discovery and design of novel enzymes from this family (Gupta et al. 2015), since they have a wide potential for different biotechnological applications. A novel strategy to achieve this goal is the mining of fungal genomes and metagenomes from environmental samples (Barriuso et al. 2013; Barriuso and Martínez 2015). In a previous study, several candidates were identified in silico in fungal genomes, and their catalytic properties predicted taking into account their hydrophobicity and tunnels shape (Barriuso et al. 2013).

One of the aims of this work was to validate the predicted kinetic properties of three putative enzymes selected from *Nectria haematococca*, *Trichoderma reesei* and *Aspergillus niger* genomes. After expressing these proteins in *Pichia* (=*Komagataella*) *pastoris,* we have carried out their purification and characterization, discussing their catalytic properties and

comparing them with those of the enzyme from *O. piceae*. In addition, we evaluated the ability of the three new candidates, OPE, and the commercial enzyme CRL to catalyze enzymatic ring-opening polymerization (ROP) reactions of lactones and to synthesize β-sitostanyl oleate.

3.3.3 MATERIALS AND METHODS

3.3.3.1 Cloning of the lipases/sterol esterases

The genes *necha2, trire2* and *aspni5,* coding for putative proteins in the genomes of *N. haematococca* (jgi|Necha2|30050|), *T. reesei* (jgi|Trire2|78828|) and *A. niger* (jgi|Aspni5|50770|), were amplified from genomic DNA of *Fusarium solani* MPVI, (imperfect form of *N. haematococca* UPM-177No11So*,* from the fungi collection of the Plant Protection Laboratory at the Technical University of Madrid, provided by Dr. Daniel Palmero), *T. reesei* CECT 20918T, and *A. niger* ATCC 20739, respectively. Fungal DNA was extracted with the DNeasy Plant Mini Kit (Qiagen, Valencia, CA, USA) and used as template for amplification. PCR was carried out in 50 µL reactions containing 100 ng of template DNA, 1x PCR buffer, 1.5 mM $MgCl_2$, 0.8 mM dNTPs, 0.5 µM of each primer and 1 U of Taq DNA polymerase (Invitrogen, Carlsbad, CA , USA), using the following primers (restriction sites added are underlined): Aspni5Fw: 5'-TACGTAGAATTCACTCCAGTTCAACGGGATGCAGCT-3'; Aspni5Rv: 5'- GCGGCCGCTCAGATGTGGAACGCCGCGGTATTC-3'; Necha2Fw: 5'- GAATTCGCTCCAGCTGCTGTGCCTGTTC-3'; Necha2Rv: 5'-GCGGCCGCTCAAACCCGCAACACACCAACG-3'; Trire2Fw: 5'-GAATTCGCCCCAACGCCAGAAAAGATTG-3'; Trire2Rv: 5'-GCGGCCGCTCACACCCTCAAGACAGCAGAATTG___-3'. Reaction conditions were as follows: initial denaturation at 94 °C for 5 min; 30 cycles of amplification, each at 94 °C for 45 s; 55 °C for 45 s; 72 °C for 1.5 min; and a final extension step at 72 °C for 5 min. The PCR products harboring *Eco*RI and *Not*I sites were transferred to the cloning vector pGem T- easy (Promega, Madison, WI, USA) and subcloned in the vector pPIC9 (Invitrogen, Carlsbad, CA, USA) for expression in *P. pastoris*. In order to introduce an additional four amino acids sequence that the other proteins carry in the N-terminal region, an extra *Eco*RI site was included after the *Sna*BI site in the gene of

Aspni5 lipase. These additional residues come from the restriction sites employed in the cloning strategy, and have shown to improve protein solubility (Vaquero et al. 2015). According to predictions, these genes were intron-less and therefore further processing was not required. The constructs were subjected to restriction analysis and sequenced to confirm the accuracy of the sequences.

3.3.3.2 Protein expression, production and purification

The constructs were transformed into *P. pastoris* KM71 and GS115 strains, following the manufacturer's protocol (Invitrogen, Carlsbad, CA, USA). Activity screening was performed inoculating single colonies from the transformed *P. pastoris* plates in 100 mL flasks with 20 mL YEPS medium (Vaquero et al. 2015). The flasks were incubated at 28 ºC and 250 rpm and 0.5% methanol (w/v) was added daily for maintaining protein induction. Esterase activity was checked in the supernantants using *p*-nitrophenyl butyrate (*p*NPB), as previously described (Vaquero et al. 2015).

For each enzyme, the clone with the highest activity level was selected for protein production and purification. One-liter flasks with 100 mL of YEPS medium, inoculated with 3.5 mL of fresh cultures grown overnight in YEPS (OD_{600nm} 8-10), were incubated at 28 ºC and 250 rpm. When maximum activity was reached (generally after 4-6 days), the cells were harvested by centrifugation (6,000 x *g* at 4 °C) and the supernatants concentrated in 10,000 Da MWCO Amicon-Ultra Centrifugal filters (Merck-Millipore, Darmstadt, Germany). The recombinant *O. piceae* enzyme was produced as described by (Vaquero et al. 2015). The purification of lipases/sterol esterases was carried out in a single hydrophobic chromatography step as previously reported (Gutiérrez-Fernández et al. 2014).

3.3.3.3 Molecular mass, enzymatic N-deglycosylation, N-terminal sequence and zymogram

The apparent molecular mass of the purified proteins was estimated from SDS-PAGE. Precision Plus Protein™ Dual Color Standards (Bio-Rad, Hércules, CA, USA) were used in 10% polyacrylamide gels, staining with Coomassie R-250. N-linked-carbohydrate content (%) was estimated as the difference between the apparent molecular mass of the protein before and after deglycosylation with Endoglycosidase H (Endo H, Roche, Mannheim, Germany). For N-deglycosylation, the purified protein was dialyzed against sodium citrate buffer, pH 5.5, and then incubated with Endo H at 37 ºC for 24 h, following the manufacturer's instructions. Protein concentration was determined by the BCA bioassay (Thermo Scientific, Rockford, IL, USA) with bovine serum albumin as standard.

N-terminal protein sequence was determined by automated Edman degradation (Procise 494 instrument, Perkin Elmer, Waltham, MA, USA) after the transference of protein bands (~10 μg), separated by SDS-PAGE, to a PVFD membrane (Barba Cedillo et al. 2012).

To detect lipolytic activity a zymogram was carried out. A sample of non-denatured protein, avoiding boiling and β-mercapto-ethanol in the loading buffer, was loaded into a SDS-PAGE. Gels were soaked for 30 min at room temperature in 2.5% (v/v) Triton X-100, washed twice in 50 mM phosphate buffer (pH 7.0) for 20 min at room temperature, and covered by a solution of 100 μM methylumbelliferyl-butyrate (Sigma-Aldrich, Steinheim, Germany) in the same buffer. Activity bands resulting from methylumbelliferyl liberation became visible in a short time (~1 min) under UV trans-illumination (Diaz et al. 1999).

In addition, the presence of possible metalloproteins was checked adding 1 mM EDTA to the fungal cultures 24 h after inoculation. The crude extracts were analyzed by SDS-PAGE after 4 days of incubation.

3.3.3.4 Stability to pH and temperature

To determine the enzymes' stability at different pH values, they were incubated in 10 mM Britton-Robinson buffer from pH 4 to 11 and 0.1% BSA at 4 ºC. Samples were taken at 24, 48 and 72 h to calculate residual activity using *p*NPB as substrate. The initial activity of the enzyme was taken as the 100%.

To determine the enzymes' stability to temperature, the proteins were incubated at their optimum pH in 20 mM Tris-HCl pH 7 buffer at different temperatures (30 to 60 °C) for 24 h, cooled on ice, and re-warmed to room temperature for 5 min prior to determine the residual activity using *p*NPB as substrate. The maximum value of residual activity, regardless of the temperature, was taken as 100%. The temperature producing 50% activity loss in 24 h of incubation (T_{50} value) was also checked.

3.3.3.5 Aggregation behavior

Analytical ultracentrifugation was used to check the aggregation behavior of recombinant proteins by determining their sedimentation coefficient and the possible transition state between the closed and open forms of the protein, monomer and dimer, respectively. Measurements were performed in a XL-I analytical ultracentrifuge (Beckman-Coulter Inc. Brea, CA, USA) equipped with UV–VIS and interference detection optics as previously reported (Gutiérrez-Fernández et al. 2014). The experiments were carried out by using the purified protein after hydrophobic chromatography (0.5 mg/mL). These proteins were analyzed in the absence or presence of a suspension of 5 mM cholesteryl oleate, as enzyme substrate, after 30 min of incubation at room temperature. The substrate was dissolved in 0.02% Genapol X-100 (Sigma-Aldrich) and 150 mM NaCl (final concentration).

3.3.3.6 Kinetic parameters

The apparent kinetic constants of the three novel lipases and OPE were analyzed following the hydrolysis of *p*-nitrophenol (*p*NP) esters, triglycerides and cholesterol esters (Sigma-Aldrich).

The hydrolysis of *p*NPB, *p*-nitrophenyl laurate (*p*NPL) and *p*-nitrophenyl palmitate (*p*NPP) were assayed as previously described (Gutiérrez-Fernández et al. 2014). One unit of activity (1 U) is defined as the amount of enzyme releasing 1 μmol of *p*-nitrophenol (ε_{410} = 15,200 $M^{-1}cm^{-1}$) per minute under the defined conditions.

The hydrolysis of glycerol and cholesterol esters was assayed titrimetrically in a pH-stat model DL50 (Mettler Toledo, Greifensee, Switzerland), using 0.1 N NaOH as titrant at 30 °C and 30% stirring rate. The reactions were carried out in 1 mM Tris-HCl buffer pH 7.0, with 0.15 M NaCl and 5% (v/v) Genapol X-100 in a final volume of 20 mL containing the substrate, which was previously emulsified in the detergent. One unit of activity (1 U) is defined as the amount of enzyme releasing 1 μmol of free fatty acid per minute.

The values for the kinetic parameters and their correspondent errors were calculated using the Sigma Plot 12.5 software (Systat Software Inc., San Jose, CA). Means and standard errors for the apparent affinity constant (K_m) and enzyme turnover (*k*cat) were obtained by non-linear least-squares fitting of the experimental measurements to the Michaelis-Menten model. Fitting of these constants to the normalized equation $v = (k_{cat}/K_m)[S]/(1+[S]/K_m)$ yielded the catalytic efficiency values (k_{cat}/K_m) with their standard errors.

3.3.3.7 Enzymatic ring-opening polymerization of lactones

Crude extracts with the enzymes from the *A. niger*, *N. haematococca*, *T. reesei* and *O. piceae* enzyme produced in *P. pastoris*, as well as the commercial crude from *C. rugosa* (L1754 Sigma-Aldrich), were assayed for the synthesis of polyesters. The reaction mixture contained 0.5 g of ε-caprolactone (ε-CL) (Sigma-Aldrich), 1 mL of isooctane, and 250 U against *p*NPB of freeze dried crude enzyme, in a final volume of 1.5 mL. The polymerization reactions were carried out in an oil bath, at 60 ºC and with magnetic stirring (500 rpm). Reactions were performed in triplicate, and samples were taken at 8, 12, 16 and 21 days. The reaction products were extracted with tetrahydrofuran. The average molecular mass of the oligomers was determined by size exclusion chromatography (SEC) in an Agilent 1200

series system with a TSKgel3000H_{HR} (7.8 x 300 mm) column, and equipped with a refractive index detector. Polystyrene standards (Agilent Technologies, Palo Alto, CA, USA) with a molecular mass distribution of 162-18,340 Da were used for calibration. Tetrahydrofuran was used as mobile phase with a flow of 0.5 mL/min at 30 °C. Moreover, after 21 days of reaction, the molecular mass of the oligomers was also determined by MALDI-TOF. In this case, the polymer was first dried at room temperature and then dissolved in chloroform. MALDI-TOF MS spectra of polycaprolactone were recorded on an Autoflex III Bruker-Daltonics (Bremen, Germany) instrument previously calibrated with peptide and protein standard solutions from the same distributor. For the analyses, 1 µL of the reaction solution was mixed 1:1 (v:v) with 2,5-dihidroxybenzoic acid matrix (10 mg/mL) dissolved in 10% (v:v) ethanol. One microliter of the sample-matrix solution was spotted onto the stainless steel target plate (MTP384, Bruker-Daltonics) and allowed to dry at room temperature. Positive ion mass spectra were recorded in reflectron (m/z range 500-3,500) and linear modes (m/z range 3,500-10,000). FlexControl (version 3.4) was used for data analysis (Bruker-Daltonics). The oligomerization degree can be calculated from the mass of individual peaks detected by this technique taking into account the mass of the caprolactone ring (114 Da) and its open form (132 Da) which incorporated a water molecule. Then, the mass of the oligomers owes to the formula [(n x 114) + 18], where n corresponds to the number of monomeric units. Since caprolactone oligomers were detected as their potassium and sodium adducts the measured mass of the oligomers increased in 39 or 23 Da, respectively.

3.3.3.8 Synthesis of phytostanol esters

The ability of the enzyme crudes to catalyze transesterification reactions was assayed using 10 mM β-sitostanol in 100% methyl oleate. Three units per milliliter on *p*NPB of each esterase were added, and the reaction proceeded at 28 ºC with magnetic stirring (1,200 rpm). All reactions were conducted in duplicate and controls without enzyme were performed in parallel. Fifteen microliters was periodically withdrawn, diluting with 150 µL of isooctane. Fifteen microliters of a 2.5 mM solution of cholesterol in the same organic solvent was immediately added as internal standard (final concentration 0.21

mM) and 1 µL was injected in a 7890A gas chromatograph (Agilent, Palo Alto, CA, USA). Injector and flame ionization detector were set up at 350 °C, and He (20 psi) was used as the carrier gas. Separation was performed using a fused-silica capillary column SPB-1 (5 m x 250 µm x 0.25 µm, Supelco, Bellefonte, PA, USA), maintained at 115 °C for 1 min followed by a two-step temperature program with a 10 °C/min ramp rate to 170 °C, and a second ramp rate of 20 °C/min to reach a final temperature of 350 °C, held for 4 min. The progress of the reactions was deduced from the total amount of residual free β-sitostanol, calculated using the internal standard.

3.3.3.9 Nucleotide sequence accession number

The nucleotide sequence of the Necha2 gene presented in this work has been deposited in GenBank. The accession number assigned was KR914668.

3.3.4 RESULTS

3.3.4.1 Production, purification, molecular mass determination and N-linked sugar content

The sequences of the expressed enzymes were identical to those deposited in the JGI database for the three putative proteins, except for the sequence of *N. haematococca* MPVI that, being a different strain, shared 98% sequence identity with JGI sequence jgi|Necha2|30050 (**Fig. 3.3.S1**). These small differences do not affect the hydrophobic content of the protein.

After *P. pastoris* transformation, several positive clones were screened for esterase activity. The maximum activity detected in culture supernatants of Necha2 and Trire2 clones reached 30.5 U/mL and 15 U/mL, after 4 incubation days, while the best clone from Aspni5 reached around 2.6 U/mL after 6 incubation days. The purification process of the three novel lipases/esterases rendered 36, 22 and 9 mg/L for Necha2, Trire2 and Aspni5, respectively. The molecular mass of these proteins and OPE was estimated by SDS-PAGE (**Fig. 3.3.1A**). As previously described, OPE showed a molecular mass around 75 kDa with 28% N-linked carbohydrates (Barba Cedillo et al. 2012). The molecular mass of Trire2 and Aspni5 were 63 and 67 kDa, respectively. Based on the differences of molecular mass after enzymatic

deglycosylation, we concluded that Trire2 and Aspni5 contained 10% and 18% N-linked carbohydrate, respectively.

In the case of Necha2, the SDS-PAGE showed two bands with different intensity, 65 and 62 kDa, respectively. After Endo H treatment the mass of both bands was smaller, indicating around 6.5% N-linked carbohydrate content (**Fig. 3.3.1A**). The analysis of the N-terminal sequence of the two Necha2 bands revealed that the minor band (~62 kDa) corresponded to a truncated protein form with a loss of 31 amino acids (~3,400 Da smaller). Both bands were active proteins as demonstrated by zymograms (**Fig. 3.3.1B**). The analysis by SDS-PAGE of the Necha2 crude extract expressed in *P. pastoris* in the presence of EDTA resulted in a smaller concentration of the protein band with lower molecular mass (**Fig. 3.3.1B**), although no significant difference was detected in the total esterase/lipase activity in the culture.

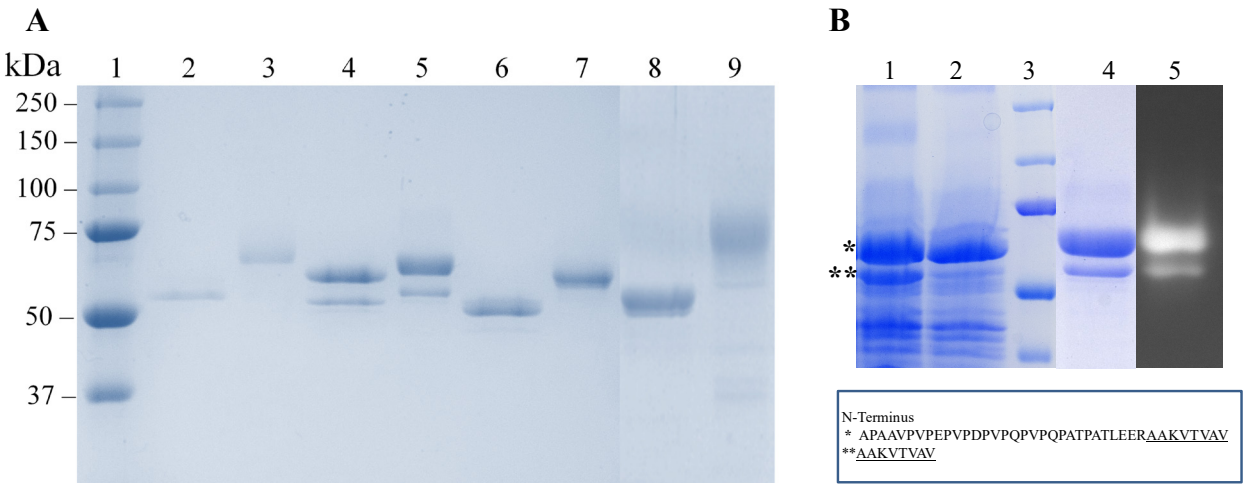

Fig. 3.3.1 Electrophoretic analysis of the recombinant enzymes. **A)** SDS-PAGE of purified recombinant proteins. *Lane* 1, molecular mass markers; *lanes* 2, 4, 6, 8 deglycosylated Aspni5, Necha2, Trire2, and OPE; *lanes* 3, 5, 7 and 9, non-deglycosylated Aspni5, Necha2, Trire2, and OPE. **B)** Effect of EDTA, as metalloprotease inhibitor, on the production of Necha2 crude extracts: *lane* 1, without; and *lane* 2, with EDTA. *Lane* 3, molecular mass markers. *Lane* 4, Necha2 purified recombinant proteins and *lane* 5 zymogram against methylumbelliferyl-butyrate. (*) Not truncated protein and (**) truncated protein.

3.3.4.2 pH and temperature stability

The three novel enzymes and OPE were incubated in a pH range from 4 to 11 (**Fig. 3.3.2A**). All of them were active in the pH range 4-10.The pH profiles of Trire2 and OPE were similar, with maximum activity at pH 7-8 and keeping over 30% residual activity at pH 9 after 72 h. Aspni5 showed highest activity at pH 6, and after 48 h it was nearly inactivated at alkaline pH values. Interestingly, Necha2 was the most stable enzyme at alkaline pH, maintaining 85% activity at pH 9 and 10 after 72 h, and it was the unique preserving around 50% activity at pH 11 at 72 h.

Temperature stability after 24 h was evaluated in the range from 30 to 60 ºC (**Fig. 3.3.2B**), observing similar T_{50} values for all enzymes: 40 ºC, 46 ºC, 42 ºC and 43 ºC for Aspni5, Necha2, Trire2 and OPE, respectively.

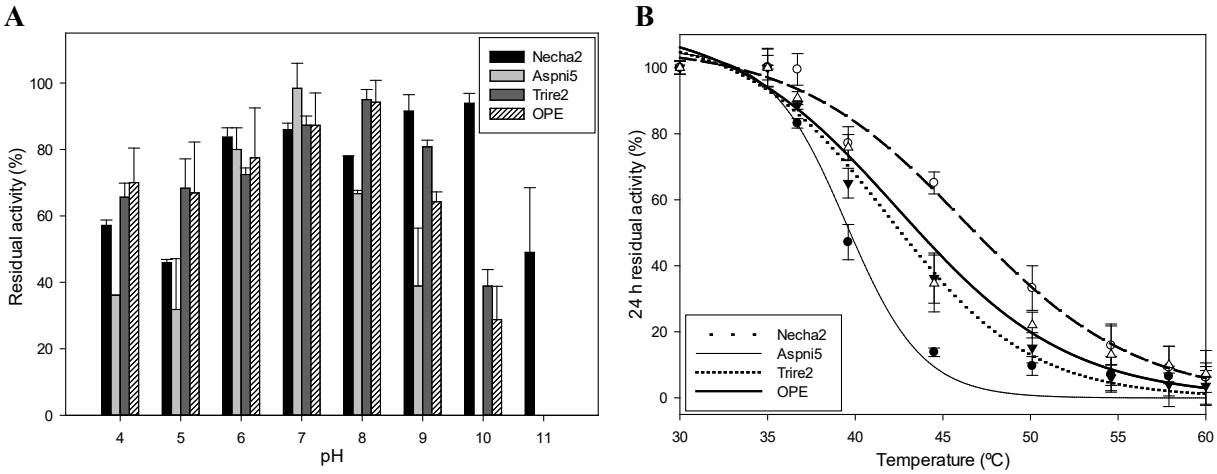

Fig. 3.3.2 Proteins stability. **A)** pH stability of the three novel lipases and OPE after 72 h of incubation at different pHs. **B)** Temperature stability after 24 h of incubation at several temperatures.

3.3.4.3 Aggregation behavior

The improved kinetic parameters of OPE expressed in yeasts are related to a lower aggregation tendency. Hence, we studied the aggregation state of the novel recombinant lipases/sterol esterases by ultracentrifugation analysis (**Fig. 3.3.S2**). The sedimentation coefficient for Aspni5 and OPE corresponded mostly (> 64%) to the monomeric form (~4.9 S). By contrast, Necha2 appeared as dimeric (50%) and multimeric species (40%). Trire2 was

present as a mixture of the monomer (34%) and aggregated forms with higher sedimentation coefficient (54%).

Recently, Gutiérrez-Fernández et al. (2014) have reported the crystal structures of OPE showing that the active state of this protein is dimeric since the monomeric form is strongly reduced (< 10%) in the presence of a substrate as cholesteryl oleate. However, in the case of Aspni5, Necha2 and Trire2 no differences in the monomer/dimer ratio were detected after incubating these proteins with this substrate (data not shown).

3.3.4.4 Kinetic studies

Comparison of the catalytic properties of the three novel lipases with OPE, based on the estimation of the apparent steady-state kinetic constants for *p*NP esters, triglycerides and cholesteryl esters, is shown in **Fig. 3.3.3**.

The apparent K_m values for Aspni5, Necha2 and OPE against *p*NP esters were in general similar (0.11-0.28 mM), although the affinity of OPE towards *p*NPL was smaller (K_m = 1.06 mM). On the other hand, the slightly lower K_m value of Trire2 against *p*NP esters was compensated by a high turnover frequency. As a consequence, the catalytic efficiencies of Trire2, Necha2 and OPE are in the same range.

Concerning triglycerides, all enzymes showed similar affinity against triolein, although OPE presented the highest catalytic efficiency due to its high turnover frequency. More variability was observed in K_m and k_{cat} values calculated for tributyrin, although Necha2 compensated its scarce affinity for this substrate with a high turnover frequency, resulting in a catalytic efficiency similar to that of OPE.

Aspni5 was unable to promote the hydrolysis of cholesterol esters, while the other enzymes had similar K_m against both short and long chain esters, excepting OPE, which displayed less affinity against cholesteryl butyrate. As occurred with the short-chain triglyceride, a high k_{cat} value resulted in a catalytic efficiency comparable to those of Necha2 and Trire2.

			*p*NPB	*p*NPL	*p*NPP	Tributyrin	Triolein	Chol butyrate	Chol oleate
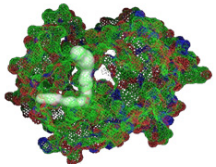	Aspni5	K_m	0.17±0.04	0.15±0.05	0.11±0.02	2.4±1.4	1.3±0.4	-[b]	-
		k_{cat}	36.4±2.3	13.9±1.3	0.80±0.04	69.9±9.7	30.1±2.3	0	0
		k_{cat}/K_m	216.2±40.7	94.4±27.4	7.5±1.2	29.0±13.2	23.7±5.9	0	0
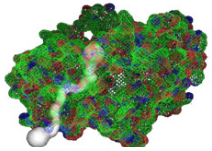	Necha2	K_m	0.28±0.08	0.21±0.05	0.25±0.08	9.9±1.9	2.5±0.1	6.6±2.1	2.7±0.3
		k_{cat}	180.8±16.9	221.1±17.5	123.0±10.9	231.3±12.6	108.5±1.3	10.2±1.2	11.9±0.6
		k_{cat}/K_m	641.9±142.5	1064.5±214.9	496.3±126.7	23.4±3.6	42.9±1.3	1.5±0.3	4.4±0.4
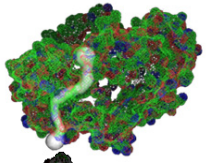	Trire2	K_m	0.92±0.25	0.73±0.19	0.77±0.26	14.3±1.9	2.2±0.5	5.5±2.8	1.7±0.3
		k_{cat}	404.9± 43.7	461.5±57.6	208.02±29.2	839.2±26.7	61.6±4.2	19.6±3.8	5.9±0.4
		k_{cat}/K_m	440.5±80	628.4±98.7	268.1±56.9	58.8±6.5	28.5±5.2	3.5±1.2	3.4±0.4
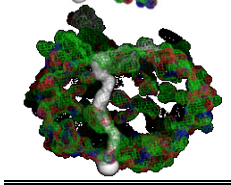	OPE	K_m	0.26±0.08	1.06±0.22	0.24±0.09	6.2±1.3	3.4±0.1	25.6±4.6	2.5±0.5
		k_{cat}	146.9±12.1	600.1±48.7	103.3±10.9	283.7±11.4	456.6±29.3	52.7±5.3	514.3±40.5
		k_{cat}/K_m	567.5±142.6	552.6±73.2	434.4±125.5	45.6±8.5	132.5±17.1	2.1±0.2	208.7±27.3

Fig. 3.3.3 Shape of the tunnels and kinetic parameters of the different enzymes. The 3D model of the putative proteins and their internal tunnel is represented at the left of each protein. (-[b]) Dashes correspond to undetermined K_m values when no activity was detected (k_{cat}=0), Chol.: Cholesteryl.

It should also be noticed that the k_{cat} of OPE for cholesteryl oleate was two orders of magnitude higher than those calculated for Necha2 and Trire2, resulting in a very superior catalytic efficiency.

3.3.4.5 Enzymatic ring-opening polymerization of lactones

To study the lipase-catalyzed ROP of lactones, five different lipases were tested: Aspni5, Necha2, Trire2, OPE and the commercial CRL crude, as a positive control. The SEC profiles (**Fig. 3.3.4A**) showed that Necha2 and Trire2 hardly initiated the polymerization, producing only very small oligomers at the final reaction time. However, the evident displacement of the products' peaks to shorter retention times in reactions catalyzed by Aspni5, CRL and OPE demonstrated that these were capable of promoting oligomerization of caprolactone throughout the reaction (maximum average molecular mass around 1,600 Da). The mass distribution of the oligomers in 21 days reactions was analyzed by MALDI-TOF (**Fig. 3.3.4B**). As expected for a polymer, a polydisperse distribution was observed. The average molecular mass and caprolactone units in reactions catalyzed by OPE, Aspni5 and CRL were around 1,540 Da (n=13), 1,425 Da (n=12) and 1,311 Da (n=11), respectively. In addition, the mass spectrum of OPE showed oligomers up to n=30, although their amount decreased with increasing size. For Aspni5 and CRL the maximum oligomers size detected was n= 23 and 24, respectively.

3.3.4.6 Synthesis of β-sitostanol esters

The same five enzymes were evaluated to test their ability to synthesize β-sitostanyl esters by transesterification in solventless reactions (**Fig. 3.3.5**). Sixty-five and 75% transesterification was achieved in 15 and 30 min, respectively, in reactions catalyzed by OPE while CRL synthesized only around 10% and 15% in the same times. Trire2 and Necha2 showed little transesterification activity during the first 30 min, and produced around 60 and 40% of β-sitostanyl oleate at the final reaction time. From 2 h of incubation onwards, conversion yields with OPE remained around 90%. CRL was gradually increasing its synthetic activity, reaching a conversion over

90% at 48 h. Aspni5 was unable to synthesize this ester under the conditions tested.

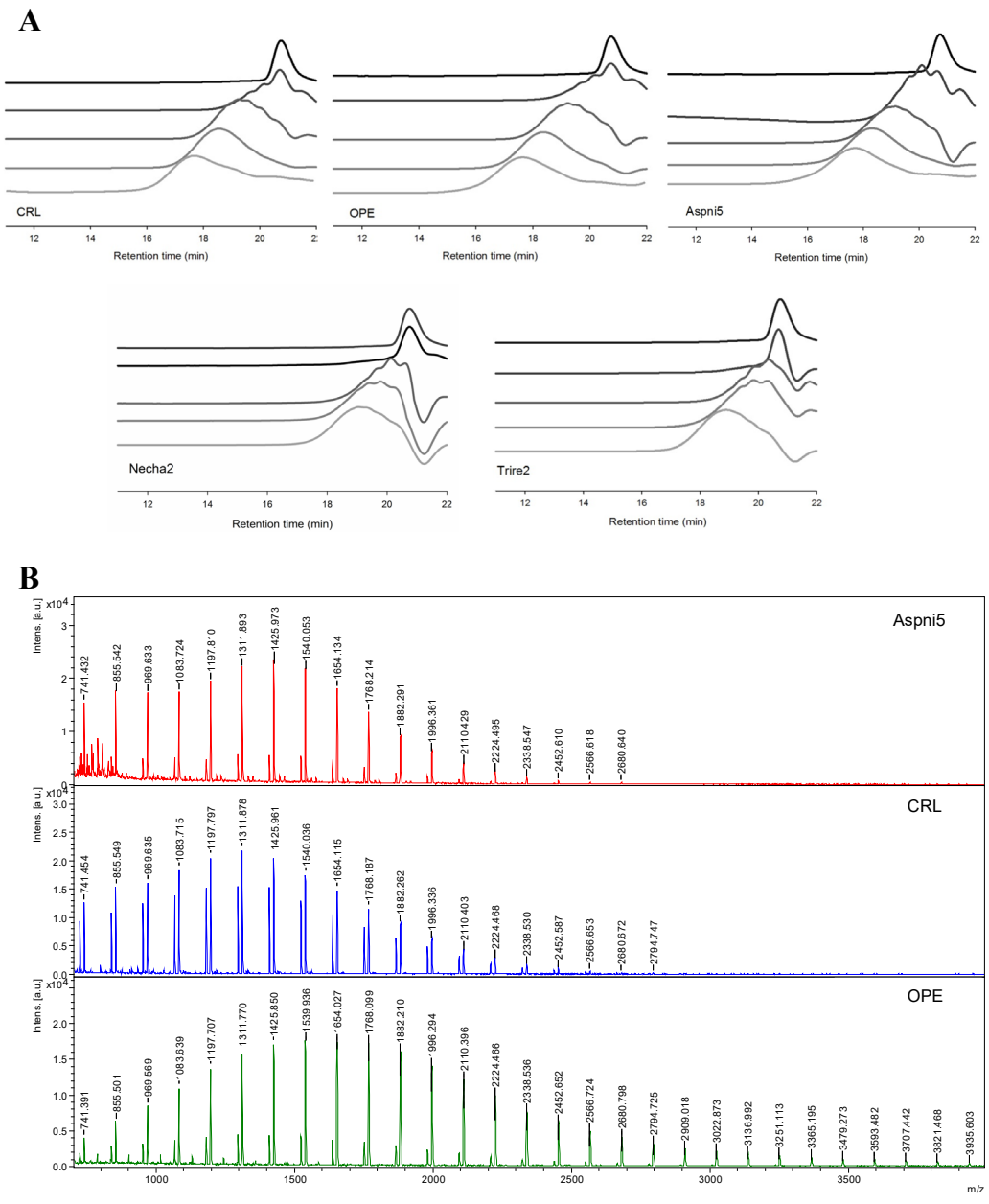

Fig. 3.3.4 Analysis of the caprolactone oligomers synthesized by the three novel lipases, OPE and CRL. **A)** SEC chromatograms of the ROP reactions with the different enzymes at 60 ºC. From top to bottom: 0, 8, 12, 16 and 21 days of incubation. **B)** MALDI-TOF spectra of the ROP reactions at 21 days of incubation. Upper panel, oligomers of caprolactone synthesized by CRL; medium panel, oligomers produced by Aspni5; lower panel, oligomers synthesized by OPE.

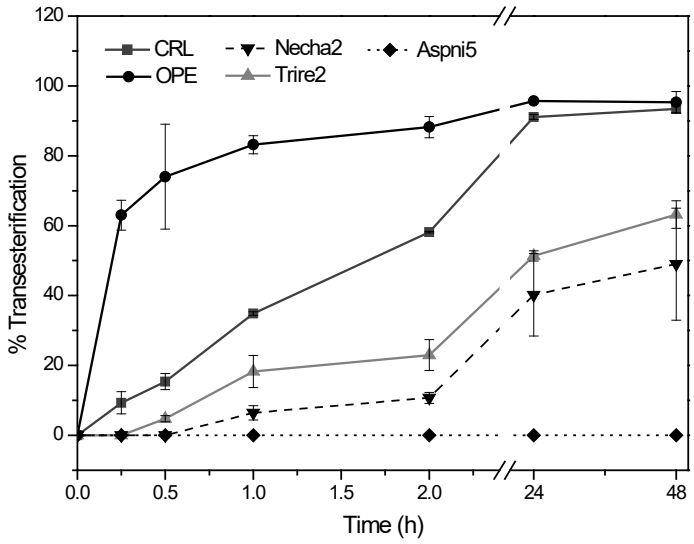

Fig. 3.3.5 Synthesis of β-sitostanyl oleate by the three novel lipases, OPE and CRL. Reaction rates of the lipase-catalyzed transesterification of β-sitostanol with methyl oleate.

3.3.5 DISCUSSION

Three putative lipases/sterol esterases, selected from a previous work (Barriuso et al. 2013), have been expressed in *P. pastoris* and purified, appearing as single bands in SDS-PAGE, except Necha2. In this case, a minor band corresponding to a truncated, but active form of the protein (**Fig. 3.3.1B**), was detected. Upon adding EDTA to the crudes, the intensity of the minor band decreased significantly, suggesting that this truncated Necha2 could be the result of the action of a metalloprotease from the culture supernatants. One of the reported effects of methanol addition for the expression of recombinant proteins in this host is induction of undesirable proteins, like proteases (Sinha et al. 2005), which agrees with the results observed for Necha2.

Regarding their glycosylation degree, Aspni5 and Trire2 were more strongly N-glycosylated than Necha2 (**Fig. 3.3.1A**) as they have two additional putative N-glycosylation sites, according to in silico predictions (Barriuso et al. 2013). The highly-conserved glycosylation site Asn351 of CRL isoenzymes is also present in Necha2, Aspni5 and OPE (Calero-Rueda et al. 2009; Domínguez de María et al. 2006).

Most lipases tend to be stable around pH 6-8 (Saxena et al. 2005), and hence finding catalysts able to work in a broad pH range can be interesting for

different biotechnological applications. The lipases/sterol esterases studied in this work were stable in a wide pH range and it can be highlighted that Necha2 maintained more than 90% activity at pH 9-10 (**Fig. 3.3.2A**). The thermal stability of the purified enzymes was similar to those reported for other fungal lipases that remained active in the range 30-50 ºC for a few hours (Kontkanen et al. 2006; López et al. 2004).

The enzymes from *A. niger* and *T. reesei* were mainly detected as monomers, while that from *N. haematococca* was predominantly dimeric. However, all of them presented different aggregation states in variable amounts. This finding agrees with the dimeric, tetrameric and higher aggregation forms reported by other authors in lipases/sterol esterases, which are very hydrophobic proteins (Hyun et al. 1971; Kontkanen et al. 2006; Pernas et al. 2001). The transition from monomer to dimer in the presence of a substrate has been recently demonstrated for OPE (Gutiérrez-Fernández et al. 2014). However, there is no evidence of such behavior for the novel proteins, suggesting that this is not a general property of enzymes belonging to the *C. rugosa*-like family.

Several reports relate the number of hydrophobic residues in the lid region of CRL isoenzymes with differences in affinity towards triglycerides or sterol esters (Domínguez de María et al. 2006; Mancheño et al. 2003).(Brocca et al. 2003) expressed a chimeric form of CRL1 replacing the lid sequence for that of CRL3, improving its cholesterol esterase activity. In this context, OPE has more hydrophobic residues than CRL isoforms in this region and proved to be more efficient on sterol esters than these and other commercial lipases and sterol esterases (Calero-Rueda et al. 2004; 2009).

The *A. niger* enzyme, which is the most similar to CRL isoenzymes, in terms of lid's hydrophobicity and tunnel shape, was unable of hydrolyzing (**Fig. 3.3.3**) or synthesizing sterol esters (**Fig. 3.3.5**). Its catalytic efficiency towards *p*NP esters and triglycerides was the lowest, although all enzymes had similar affinity. This suggests that Aspni5 recognized these substrates efficiently but the catalysis is not effective due to its low turnover frequency. On the contrary, the other three enzymes hydrolyzed all substrates regardless of the length of acyl chain, although with different efficiency. For *p*NP esters,

a comparable catalytic efficiency was obtained, while using triglycerides and cholesterol esters as substrates, more differences were found and the affinity was higher when the acyl chain was longer, which agrees with data previously reported for other enzymes of the *C. rugosa* like-family (Calero-Rueda et al. 2002; Plou et al. 1997). In any case, the hydrolytic activity of OPE, which showed to have low K_m values and high catalytic efficiency on triolein and cholesteryl oleate, merits special mention. These long chain acylated esters are target compounds, since they are responsible for undesired lipidic deposits during pulp paper manufacture (Gutiérrez et al. 2001; Tenkanen et al. 2002).

The results obtained in this work suggest that even though the hydrophobicity of the lid is an important factor for enzyme performance, other structural characteristics should be considered, as they can affect kinetic parameters. The improved activity of OPE, the most versatile enzyme among the tested in this study, could be attributed to its active form as a functional dimer, its internal tunnel, straight and wider than those from similar proteins and with a possible exit region (Gutiérrez-Fernández et al. 2014). Further studies are required to explain why Necha2 and Trire2, whose hydrophobicity in the lid region and tunnel morphology are similar to OPE, are less effective in the conditions assayed.

The enzymatic synthesis is an attractive alternative to substitute the chemical methods because of the mild conditions required, avoiding the addition of chemicals and the removal of residues that may constitute environmental concerns (Varma et al. 2005). We have evaluated the efficiency of the enzymes from the *C. rugosa*-like family catalyzing ROP of lactones (**Fig. 3.3.4**). OPE, Aspni5 and CRL succeeded in producing caprolactone oligomers, although after long reaction times, as described for CRL (Kobayashi et al. 1998; Uyama and Kobayashi 1993). The results were slightly better for OPE, but the polymerization degrees for this enzyme are still far from those reported for other lipases (Kumar and Gross 2000), since this reaction is greatly affected by the lipase type (Kobayashi et al. 1998; Namekawa et al. 1999).

On the other hand, these enzymes were assayed in the synthesis of β-sitostanol esters. These are more soluble and reduce more effectively LDL

cholesterol than free sterols/stanols and sterol esters (Musa-Veloso et al. 2011). Weber et al. (2001a, b) described almost quantitative yields for transesterification of sitostanol with methyl oleate in vacuo, at 40 ºC using 50 mg of CRL. In our work, reactions were carried out with a low catalyst dosage, under very mild conditions, at 28 ºC and atmospheric pressure. More than 80% conversion after 1 h was found in OPE-catalyzed reactions, but CRL, Trire2 and Necha2 produced less than 35% β-sitostanyl oleate in the same reaction time (**Fig. 3.3.5**). In contrast, Aspni5 was unable to catalyze this transesterification reaction, as occurred in hydrolysis of cholesterol esters, indicating that not all the enzymes from the *C. rugosa*-like family are versatile enzymes with both lipase and sterol esterase activities.

In conclusion, we have expressed and characterized three putative lipase/esterase enzymes, selected from in silico mining of fungal genomes, and compared their properties and activity with those from the versatile OPE. We corroborate that, in general, a wider and straighter internal tunnel favors a higher turnover frequency, as demonstrated from the values calculated for Necha2, Trire2 and OPE. However, the hydrophobicity of the lid region seems not to be the unique factor conditioning the activity against sterol esters. The results of in silico mining are very useful for selecting new putative candidates in extensive screenings of proteins, but expression and characterization of proteins are needed to corroborate their catalytic properties.

Acknowledgments

This work was supported by the Spanish projects BIO2012-36372, RTC-2014-1777-3 and S2013/MAE-2907. M.E. Vaquero gratefully acknowledges an FPU fellowship from MINECO. J. Barriuso thanks the financial support from the JAE-DOC CSIC program. The authors thank the help of the Proteomics (a member of ISCIII ProteoRed) and Analytical Ultracentrifugation CIB facilities, as well as to Dr. M. Hakkarainen for introducing M.E. Vaquero in polymerization reactions and Dr. F.J. Plou for his help in the pH-stat experiments.

Conflict of interest

The authors declare that they have not competing interests.

3.3.6 REFERENCES

Barba Cedillo V, Prieto A, Martínez AT, Martínez MJ (2011) Acylation procedure to obtain food and/or pharmaceutical compounds of interest using fungal sterol esterases. Patent No. ES 2395582 B1.

Barba Cedillo V, Plou FJ, Martínez MJ (2012) Recombinant sterol esterase from *Ophiostoma piceae*: an improved biocatalyst expressed in *Pichia pastoris*. Microb Cell Fact 11:73

Barba Cedillo V, Prieto A, Martínez MJ (2013) Potential of *Ophiostoma piceae* sterol esterase for biotechnologically relevant hydrolysis reactions. Bioengineered 4:249-253

Barriuso J, Prieto A, Martínez MJ (2013) Fungal genomes mining to discover novel sterol esterases and lipases as catalysts. BMC Genomics 14:712-719

Barriuso J, Martínez MJ (2015) *In silico* metagenomes mining to discover novel esterases with industrial application by sequential search strategies. J Microbiol Biotechn, 25:723-728

Bornscheuer U, Bessler C, Srinivas R, Hari KS (2002) Optimizing lipases and related enzymes for efficient application. Trends Biotechnol 20:433-437

Bornscheuer UT (2002) Microbial carboxyl esterases: classification, properties and application in biocatalysis. FEMS Microbiol Rev 26:73-81

Brocca S, Secundo F, Ossola M, Alberghina L, Carrea G, Lotti M (2003) Sequence of the lid affects activity and specificity of *Candida rugosa* lipase isoenzymes. Protein Sci 12:2312-2319

Calero-Rueda O, Gutiérrez A, del Río JC, Muñoz MC, Plou FJ, Martínez ÁT, Martínez MJ (2002a) Method for the enzymatic control of pitch deposits formed during paper pulp production using an esterase that hydrolyses triglycerides and sterol esters. Patent No. WO 02/075045 A1

Calero-Rueda O, Plou FJ, Ballesteros A, Martínez AT, Martínez MJ (2002b) Production, isolation and characterization of a sterol esterase from *Ophiostoma piceae*. Biochim Biophys Acta 1599:28-35

Calero-Rueda O, Gutiérrez A, del Río JC, Prieto A, Plou FJ, Ballesteros A, Martínez AT, Martínez MJ (2004) Hydrolysis of sterol esters by an esterase from *Ophiostoma piceae*: Application for pitch control in pulping of *Eucalyptus globulus* wood. Intern J Biotechnol 6:367-375

Calero-Rueda O, Barba V, Rodríguez E, Plou F, Martínez ÁT, Martínez MJ (2009) Study of a sterol esterase secreted by *Ophiostoma piceae*: Sequence, model and biochemical properties. BBA-Proteins Proteom 1794:1099-1106

Casas-Godoy L, Duquesne S, Bordes F, Sandoval G, Marty A (2012) Lipases: an overview. In: Sandoval G (ed) Lipases and Phospholipases. Humana Press-Springer, New York, pp 3-30

Diaz P, Prim N, Pastor FIJ (1999) Direct fluorescence-based lipase activity assay. Biotechniques 27:696-700

Domínguez de María P, Sánchez-Montero JM, Sinisterra JV, Alcántara AR (2006) Understanding *Candida rugosa* lipases: An overview. Biotechnol Adv 24:180-196

Gupta R, Kumari A, Syal P, Singh Y (2015) Molecular and functional diversity of yeast and fungal lipases: Their role in biotechnology and cellular physiology. Prog Lipid Res 57:40-54

Gutiérrez A, del Río JC, Martínez MJ, Martínez AT (2001) The biotechnological control of pitch in paper pulp manufacturing. Trends Biotechnol 19:340-348

Gutiérrez-Fernández J, Vaquero ME, Prieto A, Barriuso J, Martinez MJ, Hermoso JA (2014) Crystal structures of *Ophiostoma piceae* sterol esterase: Structural insights into activation mechanism and product release. J Struct Biol 187:215-222

Hasan F, Shah AA, Hameed A (2006) Industrial applications of microbial lipases. Enzyme Microb Technol 39:235-251

He WS, Jia CS, Ma YA, Yang YB, Zhang XM, Feng BA, Yue L (2010) Lipase-catalyzed synthesis of phytostanyl esters in non-aqueous media. J Mol Cat B Enzym 67:60-65

Hyun J, Steinberg M, Treadwell CR, Vahouny GV (1971) Cholesterol esterase. A polymeric enzyme. Biochem Biophys Res Commun 44:819-825

Jaeger KE, Eggert T (2002) Lipases for biotechnology. Curr Opin Biotechnol 13:390-397

Kobayashi S, Takeya K, Suda S, Uyama H (1998) Lipase-catalyzed ring-opening polymerization of medium-size lactones to polyesters. Macromol Chem Physic 199:1729-1736

Kontkanen H, Tenkanen M, Fagerström R, Reinikainen T (2004) Characterisation of steryl esterase activities in commercial lipase preparations. J Biotechnol 108:51-59

Kontkanen H, Tenkanen M, Reinikainen T (2006) Purification and characterisation of a novel steryl esterase from *Melanocarpus albomyces*. Enzyme Microb Technol 39:265-273

Kumar A, Gross RA (2000) *Candida antartica* lipase B catalyzed polycaprolactone synthesis: Effects of organic media and temperature. Biomacromolecules 1:133-138

López N, Pernas MA, Pastrana LM, Sánchez A, Valero F, Rúa ML (2004) Reactivity of pure *Candida rugosa* lipase isoenzymes (Lip1, Lip2, and Lip3) in aqueous and organic media. Influence of the isoenzymatic profile on the lipase performance in organic media. Biotechnol Progr 20:65-73

Mancheño JM, Pernas MA, Martínez MJ, Ochoa B, Rúa ML, Hermoso.J.A. (2003) Structural insights into the lipase/esterase behavior in the *Candida rugosa* lipases family: crystal structure of the lipase 2 isoenzyme at 1.97 Å resolution. J Mol Biol 332:1059-1069

Musa-Veloso K, Poon TH, Elliot JA, Chung C (2011) A comparison of the LDL-cholesterol lowering efficacy of plant stanols and plant sterols over a continuous dose range: Results of a meta-analysis of randomized, placebo-controlled trials. Prostag Leukotr Ess 85:9-28

Namekawa S, Suda S, Uyama H, Kobayashi S (1999) Lipase-catalyzed ring-opening polymerization of lactones to polyesters and its mechanistic aspects. Int J Biol Macromol 25:145-151

Norinobu S, Seo N, Sato F, Kaneko S, Mankura M (2003) Process for producing dietary sterol fatty acid esters. Patent No US 6,660,491 B2

Pernas MA, López C, Rúa ML, Hermoso J (2001) Influence of the conformational flexibility on the kinetics and dimerisation process of two *Candida rugosa* lipase isoenzymes. FEBS Lett 501:87-91

Pleiss J, Fischer M, Peiker M, Thiele C, Schmid RD (2000) Lipase engineering database: understanding and exploiting sequence-structure-function relationships. J Mol Catal B-Enzym 10:491-508

Plou FJ, Sogo P, Calvo M-V, Burguillo FJ, Ballesteros A (1997) Kinetic and enantioselective behaviour of isoenzymes A and B from *Candida rugosa* lipase in the hydrolysis of lipids and esters. Biocatal Biotransform 15:75-89

Saxena RK, Agarwal L, Meghwanshi GK (2005) Diversity of fungal and yeast lipases: present and future scenario for the 21th century. In: Satayanarayana T, Johri BN (eds) Microbial diversity: current perspectives and potential applications. I.K: International Publishing House Pvt ltd., New Delhi, pp. 791-814

Sinha J, Plantz BA, Inan M, Meagher MM (2005) Causes of proteolytic degradation of secreted recombinant proteins produced in methylotrophic yeast *Pichia pastoris*: Case study with recombinant ovine interferon-τ. Biotechnol Bioeng 89:102-112

Teixeira ARS, Santos JLC, Crespo JG (2011) Production of steryl esters from vegetable oil deodorizer distillates by enzymatic esterification. Ind Eng Chem Res 50:2865-2875

Tenkanen M, Kontkanen H, Isoniemi R, Spetz P, Holmbom B (2002) Hydrolysis of steryl esters by a lipase (Lip 3) from *Candida rugosa*. Appl Microbiol Biotechnol 60:120-127

Uyama H, Kobayashi S (1993) Enzymatic ring-opening polymerization of lactones catalyzed by lipase. Chem Lett1149-1150

Vaquero ME, Barriuso J, Medrano F, Prieto A, Martinez MJ (2015) Heterologous expression of a fungal sterol esterase/lipase in different hosts: Effect on solubility, glycosylation and production. J Biosci Bioeng doi: 10.1016/j.jbiosc.2015.04.005

Varma IK, Albertsson AC, Rajkhowa R, Srivastava RK (2005) Enzyme catalyzed synthesis of polyesters. Prog Polym Sci 30:949-981

Weber N, Weitkamp P, Mukherjee KD (2001) Fatty acid steryl, stanyl, and steroid esters by esterification and transesterification in vacuo using *Candida rugosa* lipase as catalyst. J Agr Food Chem 49:67-71

Weber N, Weitkamp P, Mukherjee KD (2001) Steryl and stanyl esters of fatty acids by solvent-free esterification and transesterification in vacuo using lipases from *Rhizomucor miehei*, *Candida antarctica*, and *Carica papaya*. J Agr Food Chem 49:5210-5216

3.3.7 SUPPLEMENTARY MATERIAL

```
Necha2JGI APAAVPVPEPVPDPVPQPVPQPATPATLEERAAKVTVAVPSGTVIGSSLGKVESFRGIPF 60
Necha2    APAAVPVPEPVPDPVPQPVPQPATPATLEERAAKVTVAVPSGTVIGSSLGKVESFRGIPF 60
          ************************************************************

Necha2JGI ADPPTGSLRLKPPKKLSKALGNFDASGLIGPSCPQMFISTGAEDVISEFLSNFLSIPFLQ 120
Necha2    ADPPTGSLRLKPPKKLSKPLGSFDASGLIGPSCPQMFISTGAEDVISEFLSNFLSIPFLQ 120
          ***************** **.************************************

Necha2JGI VVTGQEDCLTMTVQRPVGTKAGDKLPVLFWIFGGGFELGSSAMYDGTSLLGTGIDQDQPF 180
Necha2    VVTGQEDCLTMTVQRPVGTKAGDKLPVLFWIFGGGFELGTSAMYDGTSLLXTGIDQDQPF 180
          ************************************:********** *********

Necha2JGI IFVAVNYRVAGFGFMPGAELADEGSTNLGLLDQRMGLEWVADNIAAFGGDPDKVTIWGES 240
Necha2    IFVAVNYRVAGFGFMPGAELADEGSTNLGLLDQRMGLEWVADNIAAFGGDPDKVTIWGES 240
          ************************************************************

Necha2JGI AGAISVLDQMTLFGGDADYKGKPLFRGAIMNSGSVVPAEPVDSPKAQEIFDTVVKNAGCA 300
Necha2    AGAISVLDQMTLFGGDADYKGKPLFRGAIMNSGSVVPAEPVDSPKAQEIFDTVVKNAGCS 300
          ************************************************************:

Necha2JGI SASSSLACLRGLPYDKFLDAANSVPGLLSYNSLALSYLPRPDGHVLPDSPEALIAAGRYH 360
Necha2    SVSSSLACLRALPYDKFLDAANSVPGLLSYNSLALSYLPRPDGHVLPDSPEALIAAGRYH 360
          *.********.************************************************

Necha2JGI AVPMINGNQEDEGTLFALFQPNLTTAAKLVDYLQEFYFSAASKTQLTNLVNSYSSSITAG 420
Necha2    AVPMINGNQEDEGTLFALFQPNLTTTARLVDYLQEFYFAAASKTQLTNLVNSYSSSITAG 420
          *************************:*:**********:********************

Necha2JGI SPFRTGILNEIFPGFKRRAAIFGDLVFTLTRRLFLQTATDTNPDVPAWSYLASYDYGTPI 480
Necha2    SPFRTGILNEIFPGFKRRAAIFGDLVFTLTRRLFLQTATDTNPDVPAWSYLASYDYGTPV 480
          ************************************************************:

Necha2JGI LGTLHGSDLLQVFFGIVPNNAMRSIRTYYYNFLYNLDPNVGVTKYANWPEWKESKKLMWF 540
Necha2    LGTLHGSDLLQVFFGIVPNNAMRSIRTYYYNFLYNLDPNVGVTKYANWPEWKESKKLMWF 540
          ************************************************************

Necha2JGI KSANGNDILNDDFRQNSYNWIASNVGVLRV 570
Necha2    KSANGNDILNDDFRQNSYNWIASNVGVLRV 570
          ******************************
```

Fig. 3.3.S1 Sequence alignment of putative enzymes from *F. solani* (imperfect state of *N. haematococa*). The lipase/esterase sequence from *F. solani* shared 98% sequence homology with JGI sequence jgi|Necha2|30050, resulting in 10 amino acids substitutions. These substitutions are highlighted in blue boxes.

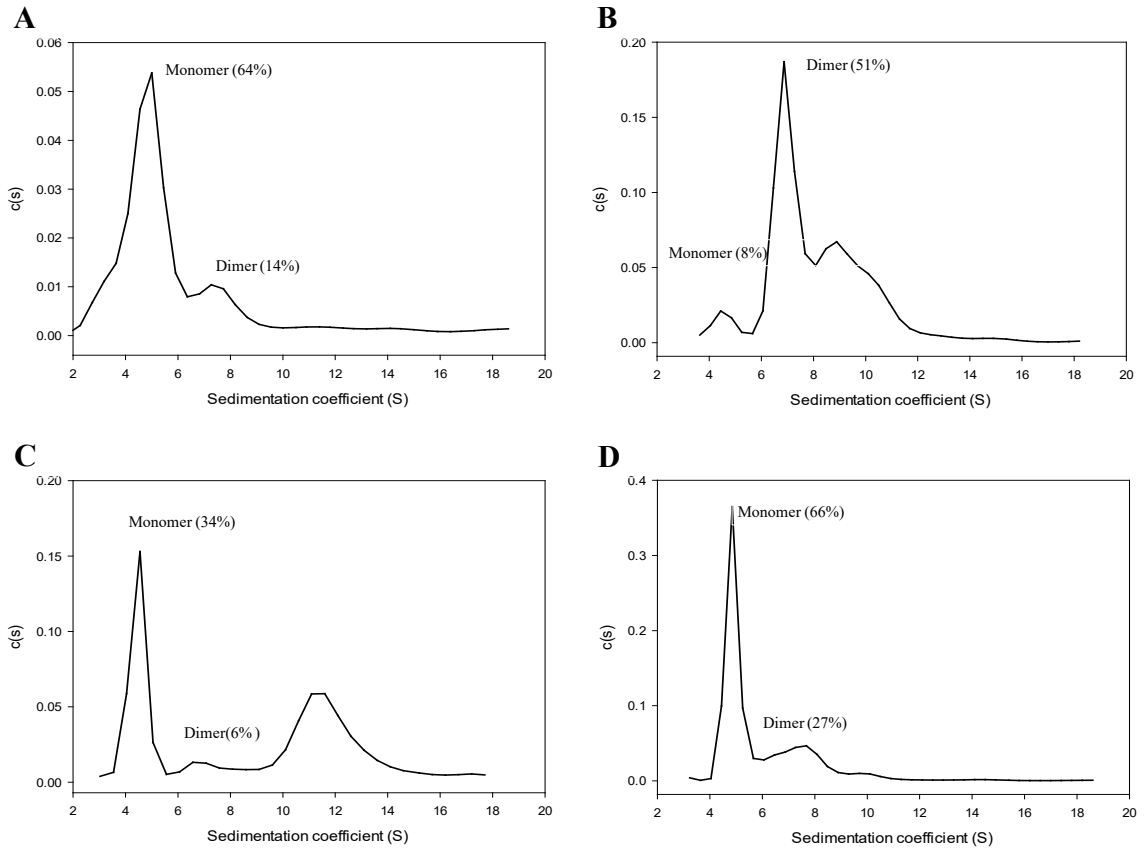

Fig. 3.3.S2 Aggregation behavior of the three novel enzymes and OPE. Sedimentation coefficient obtained by analytical centrifugation of the recombinant proteins. **A)** Aspni5, **B)** Necha2, **C)** Trire2, and **D)** OPE.

3.4 CHAPTER 4

A novel CalB-type lipase discovered by fungal genomes mining

María Eugenia Vaquero, Laura I de Eugenio, María Jesús Martínez, Jorge Barriuso

Published in PLoS ONE (2015) 10(4): e0124882
doi: 10.1371/journal.pone.0124882

3.4.1 SUMMARY

The fungus *Pseudozyma antarctica* produces a lipase (CalB) with broad substrate specificity, stability, high regio- and enantio-selectivity. It is active in non-aqueous organic solvents and at elevated temperatures. Hence, CalB is a robust biocatalyst for chemical conversions on an industrial scale. Here we report the *in silico* mining of public metagenomes and fungal genomes to discover novel lipases with high homology to CalB. The candidates were selected taking into account homology and conserved motifs criteria, as well as, phylogeny and 3D model analyses. The most promising candidate (PlicB) presented interesting structural properties. PlicB was expressed in a heterologous host, purified and partially characterized. Further experiments will allow finding novel catalytic properties with biotechnological interest.

3.4.2 INTRODUCTION

Carboxylester hydrolases (E.C. 3.1.1) are a group of enzymes which includes: esterases (E.C.3.1.1.1) defined by their ability of hydrolyze carboxyl esters from short chain acylglycerol and lipases (triacylglycerol lipase, E.C. 3.1.1.3) enzymes which are capable of releasing long-chain fatty acids from water-insoluble carboxylic esters (Casas-Godoy et al. 2012). Both enzymes are able to catalyze esterification and transesterification reactions in presence of organic solvents. The distinction between lipases and esterases is not clear. Several unsuccessful attempts aimed at differentiating "lipases" from "esterases" by using criteria such as primary sequence comparisons, structural features, and kinetic parameters have been analyzed (Verger 1997). A single feature is not sufficient to differentiate esterases from lipases, and therefore, a new bio-physico-chemical classification of lipolytic enzymes was proposed (Ben Ali et al. 2012).

These closely related enzymes are distributed among animals, plants and microorganism. One of the most important lipases used in biotechnological applications is CalB from the basidiomycete *Pseudozyma antarctica*, formerly known as *Candida antarctica* (Shivaji and Prasad 2009). This yeast belongs to the *Ustilagomycetes* class, which includes the plant pathogen *Ustilago maydis,* where few lipases have been recently characterized (Brundiek et al. 2012; Buerth et al. 2014). CalB shows broad substrate specificity, stability, and high regio- and enantio-selectivity. Moreover, it is active under conditions that are unnatural to most other enzymes like in non-aqueous organic solvents and at elevated temperatures (Uppenberg et al. 1994). Hence, CalB is a robust biocatalyst for chemical conversions on an industrial scale (Idris and Bukhari 2012).

Structurally, CalB belongs to the α/β hydrolase fold family, represented by a conserved core structure composed of seven central β strands, flanked on both sides by ten α-helices (Uppenberg et al. 1994). The fold presents a stable scaffold for the catalytic triad composed by Ser105, His224 and Asp 187, in nearly all lipases the residues around the nucleophile serine are highly conserved presenting the motif GXSXG; exceptions to this pattern are: TWSQG in CalB and AHSMG in lipase from *Saccharomyces cerevisiae*

(Pleiss et al. 2000). CalB presents a potential lid formed by helix α5, however, in contrast with other lipases, does not shows interfacial activation (Martinelle et al. 1995).

Advances in DNA sequencing have allowed studying the genomes of an enormous number of organisms in a short time. As an example, the Joint Genome Institute (JGI) from the US department of energy (DOE) has more than 300 fungal genomes completed and available in its website (http://www.jgi.doe.gov/). Furthermore, the study of DNA directly sequenced from environmental samples it is known as metagenomics. There are many metagenomes sequencing projects deposited in public databases, such as MG-RAST, IMG/M, and CAMERA (Barriuso and Martínez 2015). Bioinformatics approaches to analyze these datasets allow the finding of new enzymes in the available DNA sequences (Barriuso et al. 2013).

In this work, we report the *in silico* mining of public fungal genomes to discover lipases with high homology to CalB. The candidates were selected taking into account homology and conserved motifs criteria, as well as, phylogeny and 3D model analyses. The most promising candidate was expressed in heterologous hosts, purified and its catalytic properties studied.

3.4.3 MATERIALS AND METHODS

3.4.3.1 Screening and selection of candidate

To identify the conserved motifs in the sequences of the *P. antarctica* lipase B family (abH37.01) all sequences available in "The Lipase Engineering Database"(Pleiss et al. 2000) from this family were downloaded (http://www.led.uni-stuttgart.de/), and subjected to analysis using MEME software (http://meme.sdsc.edu/meme/intro.html). The only conserved amino acids sequence detected in all cases was WSQG, comprising the catalytic Ser from CalB (Pleiss et al. 2000; Uppenberg et al. 1994)

To look for the putative lipases containing the conserved motifs WSQG in the fungal genomes and environmental metagenomes, automatically predicted proteins from all 300 fungal genomes at the JGI web-site containing the terms "esterase" (26,089 sequences) or "lipase" (16,855 sequences) were

downloaded using the Advanced Search option. Also, eighty-one nucleotide datasets from different metagenomes, selected from diverse environments to maximize genetic variability, were downloaded from the databases MG-RAST (http://metagenomics.anl.gov/) and IMG/M (http://img.jgi.doe.gov) (7 million assembled contigs, (Barriuso and Martínez 2015)), and translated in the six possible reading frames to aminoacidic sequences. From the total pool of sequences, the ones contained the conserved motifs WSQG were selected using the Bioedit 7.1.3 software (32 hits). Alternatively, as a second screening strategy, protein similarity searches were performed at the JGI and the NCBI-NR databases using BLASTp algorithm (e value 10^{-2}) using CalB lipase as a query (29 hits).

3.4.3.2 Sequence and phylogenetic analysis

Candidate sequences were compared by means of BLASTp against the "The Lipase Engineering Data Project" (LED) databases; those belonging to the CalB-family were subjected to a phylogenetic analysis. Selected candidates were aligned using MUSCLE, and an un-rooted tree was created using Maximum-likelihood methods with a bootstrap of 2,000 (MEGA6 software).

3.4.3.3 Structure modeling

Selected sequences were aligned versus CalB using ClustalW. Putative signal peptides were predicted using SignalP 4.0. N-glycosylation sites and disulphide bonds were predicted using NetNGlyc1.0 server and DiANNA 1.1 web server respectively. The three-dimensional structures of candidates were modeled on the SWISS-MODEL server in the automatic mode. The models were exhaustively analyzed using PyMol 1.1.

3.4.3.4 Cloning procedures and heterologous expression

DNA coding sequences for the mature protein of putative lipase gene from the *Plicaturopsis crispa* genome (JGI protein ID 57710) was codon optimized for its expression in *Escherichia coli* and *Komagataella* (=*Pichia*) *pastoris* and synthesized by ATG:biosynthetics (Merzhausen, Germany). The gene was cloned into the vectors pET28a(+) (Merck, Darmstadt, Germany), using *Nco*I and *Not*I sites, under the transcriptional control of the T7 promoter for its

expression in *E. coli*. The pET28:PlicB construct was transformed into *E. coli* BL21(DE3)pLysS cells. Expression and solubility was checked by SDS-PAGE gels, using lysates from single colonies grown at 37 ºC in LB with kanamycin (50 μg/mL) and chloramphenicol (34 μg/mL) until optical density at 600 nm reached 0.6. Then, the cultures were induced with IPTG (1mM), grown at 37°C or 16°C for 16h, and harvested by centrifugation (6,000 x g, 20 min, 4°C). Cell pellets were resuspended in 5 mL lysis buffer (10 mMTris-HCl, pH 7), sonicated (Misonix S4000; Qsonica, Newtown, CT, USA), separated from the supernatant fraction, and checked for protein solubility using 10% polyacrylamide gels.

For expression in *P. pastoris,* plicB gene was cloned into pPIC9 vector (Invitrogen, Calrsbad, CA, USA) under the transcriptional control of the methanol-inducible AOX1 promoter, using *Eco*RI and *Not*I sites.The pPIC9:PlicB construct was transformed into *P. pastoris* KM71 and GS115 strains as described before (Gutiérrez-Fernández et al. 2014). Activity screening was performed using single colonies from the transformation plates grown in 20 mL YEPS medium in 100 mL flasks with 0.5% w/v of methanol to induce gene expression. The flasks were incubated at 28 ºC and 250 rpm and 0.5% w/v methanol was added daily for maintaining the induction. The esterase activity was checked using the lipase activity assay kit II (Sigma-Aldrich, Steinheim, Germany).

3.4.3.5 PlicB production, purification and characterization

Positive clones from *P. pastoris*, secreting PlicB were selected for protein production and purification. One liter flasks with 100 mL of YEPS medium, inoculated with 3,5 mL of overnight YPD cultures (DO_{600} 8-10), were incubated at 28 ºC and 250 rpm. When maximum activity was reached (4 days), the cells were harvested by centrifugation (6,000 × *g* at 4 °C) and the supernatant concentrated in 10,000 MWCO Amicon-Ultra Centrifugal filters (Merck-Millipore, Darmstadt, Germany). Supernatant was equilibrated with 0.5 M ammonium sulfate in 20 mM Tris-HCl pH 7 buffer and applied to a Octyl-Sepharose cartridge (GE Healthcare Life Sciences, Uppsala, Sweden). Proteins were eluted with a linear decreasing gradient (0.5-0 M) of ammonium sulfate in the same buffer. Fractions containing lipase activity

were concentrated, dialyzed and subjected to size exclusion chromatography in a HiLoad 16/600 Superdex 75 pg (GE Healthcare) column equilibrated and eluted with 20 mM Tris-HCl pH 7 buffer containing 0.15 M NaCl. Dextran blue (2,0 kDa), Aprotinin (6,5 kDa), Ribonuclease A (13,7 kDa), Carbonic anhidrase (29 kDa), Ovoalbumin (44 kDa) and Conalbumin (75 kDa), (Calibration kits; GE Healthcare), were used as standards to calibrate the column in order to evaluate PlicB quaternary structure.

The apparent molecular weight of the purified PlicB was estimated from SDS-PAGE. Precision Plus Protein Dual Color Standards (Bio-Rad, Hércules, CA, USA) were used in running 10% polyacrylamide gels. N-linked-carbohydrate content (%) was estimated as the difference between the apparent molecular mass of the protein before and after deglycosylation with Endoglycosidase H (Roche, Mannheim, Germany). For N-deglycosylation, the purified protein was dialyzed against sodium citrate buffer, pH 5.5, and then incubated with Endo H at 37 ºC for 24 h, following the manufacturer's instructions. Protein concentration was determined by the Bradford (Bio-Rad), bovine serum albumin was used as standard (Buerth et al. 2014).

3.4.3.6 Peptide mass fingerprinting using MALDI-TOF mass spectrometry

The purified protein was analyzed by SDS-PAGE in a 10% polyacrylamide gel and stained with SYPRO Ruby (Bio-Rad). The band was excised and subjected to tryptic in-gel digestion in a DigestPro MS digestor (Intavis, Köln, Germany). MS analyses of the tryptic peptides were performed in an Autoflex III MALDI-TOF/TOF mass spectrometer (Bruker Daltonics, Bremen, Germany) controlled by the flexControl 3.0 software (Bruker Daltonics). Three of the tryptic peptides were chosen to carry out fragmentation and sequencing. MALDI-MS and MS/MS data were combined through the BioTools 3.0 program (Bruker Daltonics) to search against the non-redundant protein database from the NCBI using the MASCOT 2.3 search engine (Matrix Science, London, UK). Scores greater than 75 were considered significant ($p<0.05$).

3.4.3.7 Esterase and lipase activity assays

PlicB activity against triglycerides was tested in tributyrin agarose plates (1% agarose, 1% glyceryl tributyrate previously homogenized in 20 mM Tris-HCl pH 7 buffer). Twenty-five micrograms of purified protein were dropped onto the plates, followed by incubation at 28 °C overnight. Alternately, plates with Tween20/40/80 substrates were used (1% agarose, 0.2% Tween 20/40/80 and 0.6 mM $CaCl_2$). Fifty micrograms of purified protein were dropped onto the plates followed by incubation at 28 °C for 24-48h. Fatty acids released from substrates produced a turbid halo. On the other hand, PlicB lipase activity was quantified spectrophotometrically using the Lipase activity assay kit II (Sigma-Aldrich), and compared with that from commercial non immobilized CalB (lyophilized powder; Sigma-Aldrich).

The hydrolysis of *p*-nitrophenyl butyrate (*p*NPB), *p*-nitrophenyl laurate (*p*NPL) and *p*-nitrophenyl palmitate (*p*NPP) were assayed in presence of 1% (v/v) Genapol X-100 as surfactant, as described previously (Gutiérrez-Fernández et al. 2014), using an Shimadzu UV-1800 spectrophotometer with magnetic stirring (600 rpm) and temperature control at 25 °C. One unit of activity (1U) is defined as the amount of enzyme releasing 1 μmol of *p*-nitrophenol (ε_{410} = 15,200 $M^{-1}cm^{-1}$) per minute under the defined conditions.

3.4.3.8 pH and temperature stability

To determine the enzymes stability at different pHs, the enzyme were incubated in 10 mM Britton-Robinson buffer from pH 4 to 9 at 4 ºC. Samples were taken at 24 h to calculate residual activity using the *p*NPB assay as describe above. The initial activity of the enzyme was taken as 100%. Thermal stability was determined by the temperature at which 50% of activity was lost in 10 min incubation (T_{50} value) the protein was incubated in 20 mM Tris-HCl pH 7 buffer at a range from 30 to 60 °C, cooled on ice, and rewarmed to room temperature for 5 min prior to residual activity determination by Lipase activity assay kit II (Sigma-Aldrich).

3.4.4 RESULTS AND DISCUSSION

3.4.4.1 Genomes and metagenomes screening

After the search of conserved sequence WSQG in 81 environmental metagenomes and putative proteins annotated as lipase and/or esterase in more than 300 fungal genomes, only 21 and 11 candidates contained the motif, respectively. Moreover, analysis and comparison of these sequences in "The Lipase Engineering Database" retrieved no C. *antarctica* lipase B family members (abH37.01). In the case of candidates from metagenomes all belonged to bacteria; as previously reported the abundance of fungal sequences in this data sets it is very low (Barriuso and Martínez 2015).

Alternatively, a second strategy based on sequence homology search against JGI and NCBInr databases using CalB as query rendered 29 sequences. After a deeper analysis of these sequences, 8 belonged to the abH37.01 family and were subjected to a phylogenetic study (**Fig. 3.4.1**).

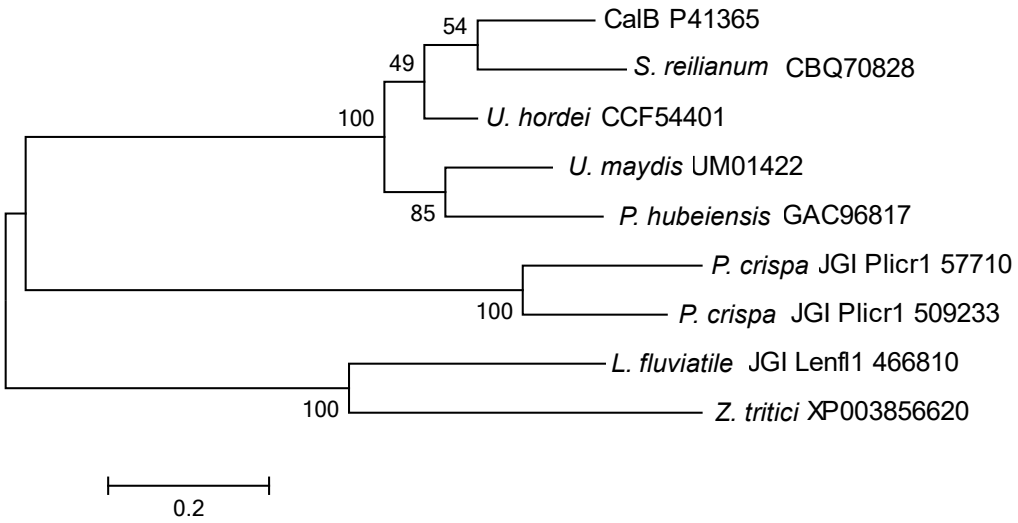

Fig. 3.4.1 Phylogenetic analysis of CalB and eight potential CalB-like lipase candidates. The tree was built using MEGA6 software, boostrap values (2,000 replicates) are shown next to the branches. The name of the specie is followed by the sequence accession number.

Interestingly, candidates from *P. crispa* and *Lentithecium fluviatile* only arise using the second search strategy. This is due to absence of the conserved WSQG motif in *P. crispa* sequences, and to the annotation of *L. fluviatile* sequence as an α/β-hydrolase instead of "lipase" or "esterase" in the database.

In this sense it is worthy to mention the convenience of applying different search strategies to avoid the loss of potential candidates.

Lipase sequences from *Ustilago* and *Sporisorium*, Gramineae parasites closely related and commonly known as smut fungi (Stoll et al. 2003), grouped in the same branch than CalB and lipases from the anamorphic yeast-like fungus *Pseudozyma*, that also belongs to the *Ustilaginales* (Wang et al. 2006). Several of these lipases are protected by international patents due to its biotechnological potential interest (Besenmatter et al. 2013), and lipase B from *U. maydis* (Ulm2) has been recently characterized (Buerth et al. 2014). In a second cluster with a higher phylogenetic distance from CalB, grouped the putative lipases from the *Dothideomycetes*: *Zymoseptoria tritici* (ID XP003856620), a wheat pathogen (Hibbett et al. 2014) and *Lentithecium fluviatile* (JGI/Lenfl1/ID 466810), from fresh water habitats.

Finally, lipases from the Agarical *Plicaturopsis crispa* (JGI/Plicr1/ID 57710 and 509233) grouped in a different branch at an intermediate phylogenetic distance between *Ustilaginales* and *Dothideomycetes*. Putative protein ID 509233 seems to be a truncated form of the putative protein ID 57710 presenting 70 amino acids less, probably due to a wrong automatic genome annotation. *P. crispa* is a white rot basidiomycete, and is the first member of the Amylocorticiales order to be sequenced (Gordon et al. 2014). This fungus is an effective decayer, colonizing predominantly dead branches of deciduous trees (Hibbett et al. 2014).

In this kind of fungi, secreted lipases may play a role for nutrition and/or damage of host cells to help penetrate host tissues. These enzymes may be implicated in the initial degradation of the epicuticular waxes and cuticle, which consist of a mixture of long-chain fatty acids, aldehydes, alkanes, primary and secondary alcohols, ketones and wax esters (Gaillardin 2010).

3.4.4.2 Sequence analysis and structural model

The putative lipase sequence PlicB from basidiomycete *P. crispa* (protein ID 57710) was selected as the most promising candidate, since it was very similar to the characterized enzymes CalB and Ulm2, but still presented some interesting differences. PlicB possess 367 amino acids with a theoretical mass

of 37 kDa and contains a predicted signal sequence of 19 amino acids. Mature PlicB presented 30% sequence identity and 44% similarity against CalB (**Fig. 3.4.2**). Molecular models of the selected candidate were generated using SWISS-MODEL server and the template automatically chosen was CalB structure (PDB: 4K6H). The 3D model from PlicB adjusted with a Qmean value of -5.25 (**Fig. 3.4.S1**).

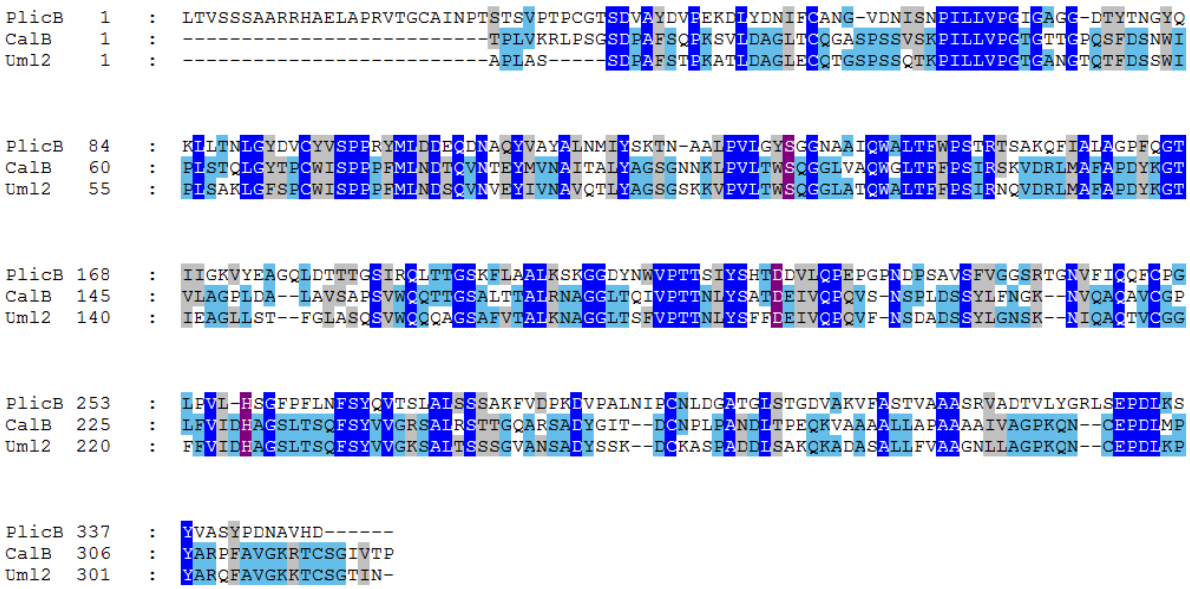

Fig. 3.4.2 Protein sequences alignment of the mature regions of PlicB, CalB and Ulm2. Residues completely conserved at a given position are indicated in white on blue. Putative catalytic residues are highlighted on purple. Potential N-glycosylation sites are marked by a star.

Residues Ser122, Asp218 and His257 are probably responsible for the catalytic activity of the protein as they superpose in the model with the catalytic triad of CalB. It is worth to notice that PlicB was the only candidate found that did not presented the conserved motif WSQG forming the shoulder of the catalytic Ser. Instead of a tryptophan PlicB presented a tyrosine preceding the catalytic serine (**Fig. 3.4.2**), similar to cutinases from *Fusarium solani* and *Aspergillus oryza*e (Pleiss et al. 2000). The tryptophan in CalB seems not to be crucial as it is shown in the mutant W104A, which presents an expanded pocket with increase activity against alcohols (Magnusson et al. 2005).

Analyzing potential disulphide bonds, PlicB possesses two (Cys54-Cys94 and Cys-250-Cys293), one less than CalB and Ulm2 (Buerth et al. 2014). The overall structure of PlicB (**Fig. 3.4.S1**) is a globular α/β-type protein with a central β-sheet composed of seven β-strands flanked by α-helices. CalB has a semi-covered active site consisting of α5 (as the lid) and α10 (as activation element), forming a narrow hydrophobic channel with the catalytic residues inside (Ganjalikhany et al. 2012). In PlicB model α5 is replaced by a loop forming a cleft-like enzymatic cavity.

3.4.4.3 PlicB production, purification and characterization

Taking into account sequence and phylogenetic analysis, as well as the 3D molecular models, protein from *P. crispa* ID 57710 was selected for heterologous expression. The mature sequence of *plicB* gene was expressed in *E. coli* and *P. pastoris*. In the first case, the protein obtained was insoluble, inactive and located inside inclusion bodies (**Fig. 3.4.3**). The deposition of unfolded or partially misfolded protein is a common problem in this host, especially when expressing eukaryotic proteins (Gasser et al. 2008). On the other hand, *P. pastoris* resulted to be an optimum heterologous host for this kind of enzymes, as previously described (Valero 2012). Different *P. pastoris* strains were tested, and the best producer clone was obtained from strain GS115. Purification of PlicB was performed from methanol-induced cultures grown for 96 h: culture supernatant was applied onto hydrophobic and size exclusion chromatography columns, yielded 4mg/L of purified protein of an estimated molecular mass of 48 kDa (**Fig. 3.4.3**), although its theoretical molecular mass was 37 kDa. After enzymatic deglycosylation of the protein by Endoglycosidase H treatment, a unique band of approximately 37 kDa appeared as seen by SDS-PAGE, indicating a 20% of sugars N-liked (**Fig. 3.4.3**), in accordance with the two N-glycosylation sites predicted (Asn60 and Asn264). The molecular weight of PlicB calculated by size exclusion chromatography using a HiLoad 16/600 Superdex 75 pg column was 47.8 kDa, very similar to that obtained under denaturing conditions in SDS-PAGE, which would indicate that PlicB is a monomer in the conditions tested, according to CalB previous results (Qian et al. 2009). PlicB identity was confirmed by mass fingerprinting analysis (data not shown).

Lipase activity of purified enzyme was checked on tributyrin and Tween 20/40/80 plates (**Fig. 3.4.S2**). Tween 20/40/80 are polysorbate detergents containing esters of fatty acids with different chain length: lauric acid, palmitic acid and oleic acid, respectively.

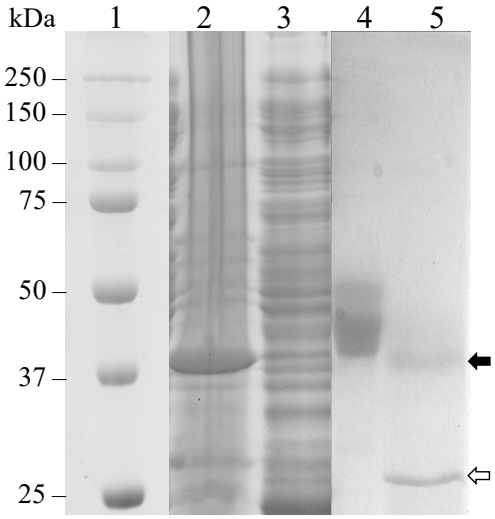

Fig. 3.4.3 SDS-PAGE of PlicB expressed in *E. coli* and *P. pastoris*. Lane 1, molecular mass markers; lane 2-3 pellet and supernatant respectively, of crude extract from PlicB expressed in *E. coli* BL21(DE3)pLysS grown at 37 °C. The dashed box indicates the insoluble expression of PlicB. Lane 4, purified PlicB expressed in *P. pastoris* GS115. Lane 5, purified PlicB expressed in *P.pastoris* after Endoglycosidase H treatment. The migration of deglycosylated PlicB (black arrow) and Endoglycosidase H (open arrow) are indicated.

Although the purified protein was able to hydrolyze all the substrates assayed, PlicB produced a more visible halo in Tween 40 compared to Tween 20 after overnight incubation, while the halo in Tween 80 plates appeared only after 48 h incubation. This ability has already been shown in CalB and Ulm2 (Buerth et al. 2014). PlicB lipase activity was quantified and compared to CalB by using a spectrophotometric approach (Lipase assay kit II, Sigma-Aldrich) (**Table 3.4.1**). By this method, PlicB showed 4-fold higher lipase activity compared to CalB. Esterase activity against *p*-nitrophenyl (*p*NP) esters of different fatty acids length chain (**Table 3.4.1**), revealed that PlicB presented higher activity towards short chain substrates as *p*-NPB (C4), than towards fatty acid esters of 12 and 16 carbons of acyl chain. Although CalB presented 43-fold higher activity than PlicB against *p*NPB and *p*NPL, hydrolysis of long chain *p*NPP by the two lipases was similar. Furthermore, (Buerth et al. 2014) compared the specific activity of Uml2 and CalB against

*p*NP-esters in reactions containing DMSO (5% v/v) and 5mM deoxycholate. CalB resulted around 10 times more active towards *p*NPB and *p*NPL than Uml2, while the activity was similar against *p*NPP.

Table 3.4.1 Specific activity of of PlicB and commercial non-immobilized CalB.

		Specific activity (mU mg^{-1})	
Substrate	Fatty acids	PlicB	CalB
*p*NPB	C4:0	100± 19	4300 ± 500
*p*NPL	C12:0	32 ± 2	209 ± 5
*p*NPP	C16:0	22 ± 4	15 ± 8
Lipase kit	C4:0	1400 ± 106	343 ± 6

Esterase activity was assayed using different acyl long chain *p*NP esters as substrate (1.5mM in presence of 1% Genapol X-100). Lipase activity was assayed using the lipase assay kit II (Sigma-Aldrich).

Inspection of the molecular surfaces of PlicB model and CalB revealed notable structural differences in the substrate binding pocket. CalB showed a funnel-like binding site able to accommodate large substrates (Naik et al. 2010; Pleiss et al. 1998), while PlicB showed a cleft-like enzymatic cavity. Moreover, it has been suggested that α5 helix in CalB possessed flexibility and interacts with the acyl part of a substrate (Skjøt et al. 2009); in the case of PlicB this α5 helix it is not present. Marked differences in lid regions among CalB homologues have previously been described. Substitution of CalB lid with that from related lipases resulted in chimeric proteins with altered catalytic properties and enantioselectivity (Skjøt et al. 2009). These facts could contribute to the different substrate recognition and hydrolytic efficiency of PlicB.

In terms of regioselectivity toward the position of the acyl group of triglycerides, lipases can be classified into *sn*-1,3-regiospecific (*Rhizomucor miehei* lipase), *sn*-2 specific (*C. antarctica* lipase A) and nonspecific lipases (*C. rugosa* lipase). The substrate utilized in the Lipase activity assay kit II (Sigma-Aldrich) is a thioester analog of tributyrin (2,3 dimercapto-1-propanol tributyrate, DMPTB) (Choi et al. 2003). Thus, *sn*1,3-specific lipase can hydrolyze only one of the DMPTB-thioester groups, whereas nonspecific

lipases could hydrolyze two groups (Farias et al. 1997). According to that, the differences in lipase activity with this substrate could be related with the fact that PlicB may be classified as nonspecific lipase while CalB would be an 1,3-specific lipase.

In spite of the substrate specificity differences found, the temperature stability (T_{50}) (**Fig. 3.4.4**) and pH stability of PlicB (42 °C and stable between pH 6 and 9) revealed a thermal and pH stability situated in the same range of CalB (46 °C) and other CalB-like lipases (Xie et al. 2014). Enzymes stable at wide range of pH and temperature are desirable for their biotechnological application (Casas-Godoy et al. 2012)**.**

In summary, genome mining has been proved as useful strategies in order to discover new enzyme with potential improved properties. Putative lipases from the CalB family were screened using two different strategies. Most of the selected candidates corresponded with previously characterized proteins, however, a new putative lipase (PlicB), lacking the conserved motif (WSQG) in the catalytic Ser shoulder, was identified. PlicB was expressed in two different heterologous hosts, purified, and partly characterized.

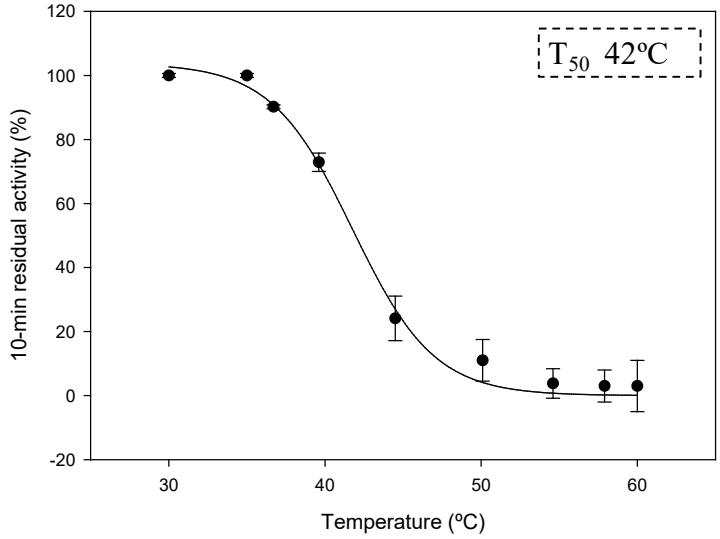

Fig. 3.4.4 Temperature stability. Purified PlicB in 20mM Tris-HCl pH 7 was incubated 10 min at different temperatures (30-60 °C). Temperature stability is presented as T_{50} value (dashed box).

Acknowledgments

This work was supported by the Spanish projects BIO2012-36372, RTC-2014-1777-3 and S2013/MAE-2907. J. Barriuso thanks the financial support from the JAE-DOC CSIC program.

Conflict of interest

The authors have declared thaht no competing interest exist.

Author contributions

Conceived and designed the experiments: JB MJM. Performed the experiments: MEV LIE JB. Analyzed the data: MEV LIE JB. Wrote the paper: MEV JB MJM.

3.4.5 REFERENCES

Barriuso J, Prieto A, Martinez MJ (2013) Fungal genomes mining to discover novel sterol esterases and lipases as catalysts. BMC Genomics 14:712

Barriuso J, Martínez MJ (2015) *In silico* metagenomes mining to discover novel esterases with industrial application by sequential search strategies. J Microbiol Biotechn, 25:723-728

Ben Ali Y, Verger R, Abousalham A (2012) Lipases or esterases: Does it really matter? toward a new Bio-Physico-chemical characterization. In: Sandoval, G (ed) Lipases and Phospholipases. Humana Press-Springer, New York, pp 31-51

Besenmatter W, Svendsen A, Rannes JB, Jäckel C (2013) Lipase variants and polynucleotides encoding same. Patent No. WO2013010783 A1

Brundiek H, Sass S, Evitt A, Kourist R, Bornscheuer UT (2012) The short form of the recombinant CAL-A-type lipase UM03410 from the smut fungus *Ustilago maydis* exhibits an inherent trans-fatty acid selectivity. Appl Microbiol Biotechnol 94:141-150

Buerth C, Kovacic F, Stock J, Terfruchte M, Wilhelm S, Jaeger KE, Feldbrugge M, Schipper K, Ernst JF, Tielker D (2014) Uml2 is a novel CalB-type lipase of *Ustilago maydis* with phospholipase A activity. Appl Microbiol Biotechnol 98:4963-4973

Casas-Godoy L, Duquesne S, Bordes F, Sandoval G, Marty A (2012) Lipases: an overview. In: Sandoval G (ed) Lipases and Phospholipases. Humana Press-Springer, New York, pp 3-30

Choi SJ, Hwang JM, Kim SI (2003) A colorimetric microplate assay method for high throughput analysis of lipase activity. J Biochem Mol Biol 36:417-420

Farias RN, Torres M, Canela R (1997) Spectrophotometric determination of the positional specificity of nonspecific and 1,3-specific lipases. Anal Biochem 252:186-189

Gaillardin C (2010) Lipases as pathogenicity factors of fungi. In Timmis KN (ed) Handbook of hydrocarbons and lipid microbiology. Springer-Verlag Berlin, Heidelberg, pp 3259-3268

Ganjalikhany MR, Ranjbar B, Taghavi AH, Tohidi Moghadam T (2012) Functional motions of *Candida antarctica* lipase B: A survey through open-close conformations. PLoS ONE 7:e40327

Gasser B, Saloheimo M, Rinas U, Dragosits M, Rodríguez-Carmona E, Baumann K, Giuliani M, Parrilli E, Branduardi P, Lang C et al. (2008) Protein folding and conformational stress in microbial cells producing recombinant proteins: a host comparative overview. Microb Cell Fact 7:11

Gordon S, Tseng E, Salamov A, Zhang J, Meng X, Zhao Z, Kang DD, Underwood J, Grigoriev IV, Figueroa M et al. (2014) Widespread polycistronic transcripts in mushroom-forming fungi revealed by single-molecule long-read mRNA sequencing. BioRxiv doi:10.1101/012542

Gutiérrez-Fernández J, Vaquero ME, Prieto A, Barriuso J, Martínez MJ, Hermoso JA (2014) Crystal structures of *Ophiostoma piceae* sterol esterase: Structural insights into activation mechanism and product release. J Struct Biol 187:215-222

Hibbett DS, Bauer R, Binder M, Giachini AJ, Hosaka K, Justo A, Larsson E, Larsson KH, Lawrey JD, Miettinen O et al. (2014) Agaricomycetes. In: McLaughlin DJ, Spatafora JW (eds) The mycota VII Part A systematic and evolution, 2nd edition. Springer-Verlag Berlin, Heidelberg, pp 373-429

Idris A, Bukhari A (2012) Immobilized *Candida antarctica* lipase B: Hydration, stripping off and application in ring opening polyester synthesis. Biotech Adv 30:550-563

Magnusson AO, Rotticci-Mulder JC, Santagostino A, Hult K (2005) Creating space for large secondary alcohols by rational redesign of *Candida antarctica* Lipase B. Chembiochem 6:1051-1056

Martinelle M, Holmquist M, Hult K (1995) On the interfacial activation of *Candida antarctica* lipase A and B as compared with *Humicola lanuginosa* lipase. Biochim Biophys Acta 1258:272-276

Naik S, Basu A, Saikia R, Madan B, Paul P, Chaterjee R, Brask J, Svendsen A (2010) Lipases for use in industrial biocatalysis: Specificity of selected structural groups of lipases. J Mol Cat B Enzym 65:18-23

Pleiss J, Fischer M, Schimd RD (1998) Anatomy of lipase binding sites: the scissile fatty acid binding site. Chem Phys Lipids 93:67-80

Pleiss J, Fischer M, Peiker M, Thiele C, Schmid RD (2000) Lipase engineering database: understanding and exploiting sequence-structure-function relationships. J Mol Catal B-Enzym 10:491-508

Qian Z, Horton JR, Cheng X, Lutz S (2009) Structural redesign of lipase B from *Candida antarctica* by circular permutation and incremental truncation. J Mol Biol 393:191-201

Shivaji S, Prasad GS (2009) Antarctic yeasts: biodiversity and potential applications.In: Satyanarayana T, Kunze G (eds) Yeast biotechnology: diversity and applications. Springer-Verlag Berlin, Heidelberg, pp 3-18

Skjøt M, De Maria L, Chatterjee R, Svendsen A, Patkar SA, Østergaard PR, Brask J (2009) Understanding the plasticity of the a/b hydrolase fold: lid swapping on the *Candida antarctica* lipase B results in chimeras with interesting biocatalytic properties. Chembiochem 10:520-527

Stoll M, Piepenbring M, Begerow D, Oberwinkler F (2003) Molecular phylogeny of *Ustilago* and *Sporisorium* species (Basidiomycota, Ustilaginales) based on internal transcribed spacer (ITS) sequences. Can J Bot 81:976-984

Uppenberg J, Hansen MT, Patkar S, Jones TA (1994) The sequence, crystal structure determination and refinement of two crystal forms of lipase B from *Candida antarctica*. Structure 2:293-308

Valero F (2012) Heterologous expression systems for lipases: a review. In: Sandoval G (ed) Lipases and Phospholipases. Humana Press-Springer, New York, pp 161-178

Verger R (1997) Interfacial activation of lipases: fact and artifacts. Trends Biotechnol 15:32-38

Wang QM, Jia JH, Bai FY (2006) *Pseudozyma hubeiensis* sp nov and *Pseudozyma shanxiensis* sp nov., novel ustilaginomycetous anamorphic yeast species from plant leaves. Int J Syst Evol Microbiol 56:289-293

Xie Y, An J, Yang G, Wu G, Zhang Y, Cui L, Feng Y (2014) Enhanced enzyme kinetic stability by increasing rigidity within the active site. J Biol Chem 289:7994-8006

3.4.6 SUPPLEMENTARY MATERIAL

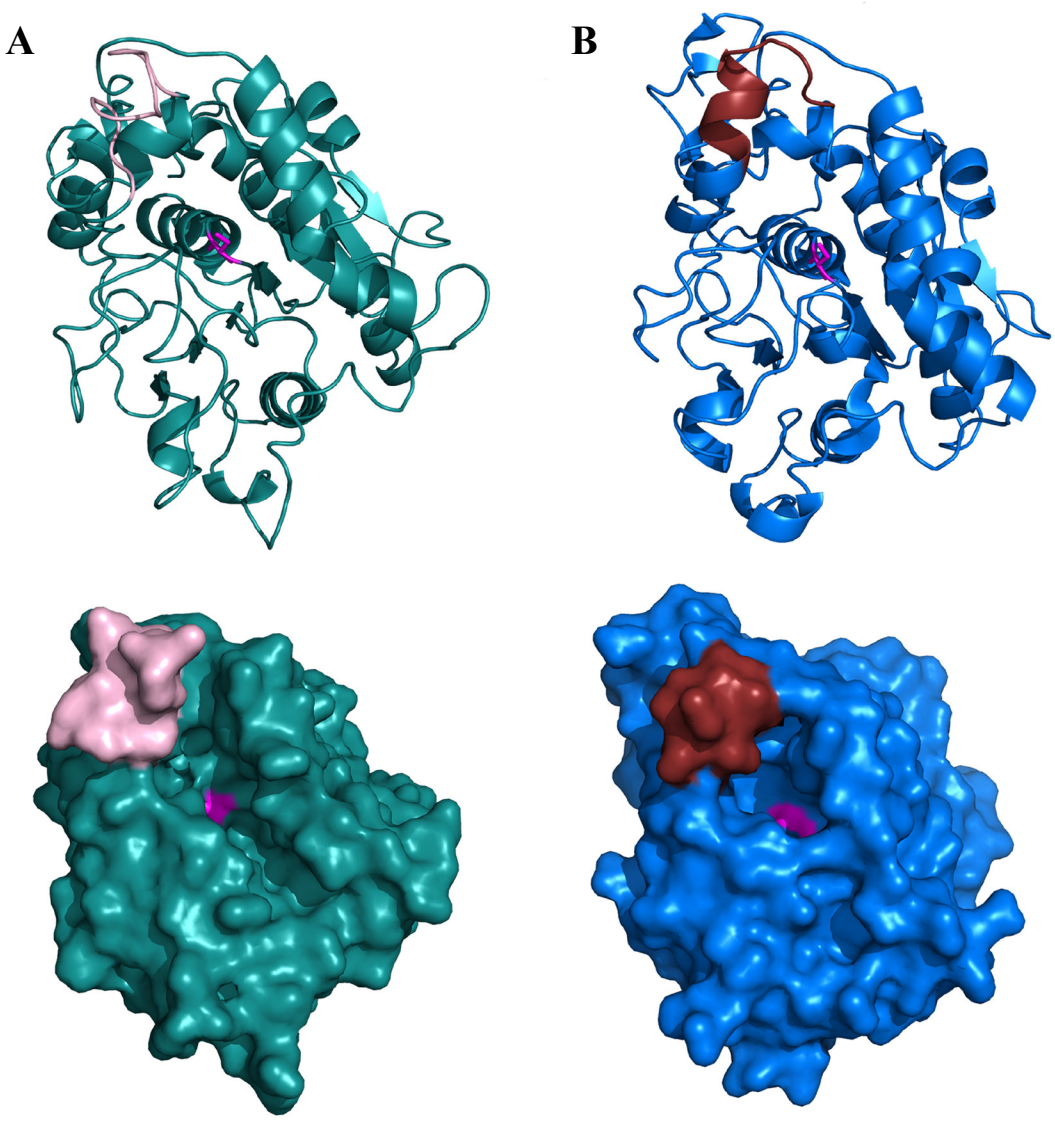

Fig. 3.4.S1 Comparison of PlicB 3D model and the molecular structure of CalB. A) PlicB structural model, ribbon diagram (upper part) and molecular surface (lower part)**. B)** CalB structure (PDB: 1TCA) ribbon diagram (upper part) and molecular surface (lower part). Catalytic serine is represented in magenta. The alpha helix delimiting the enzyme´s lid region in CalB is represented in red, while PlicB model presents a loop (in pink). PlicB posses a cleft-like enzymatic cavity, while CalB posses a funnel-like binding site (lower part).

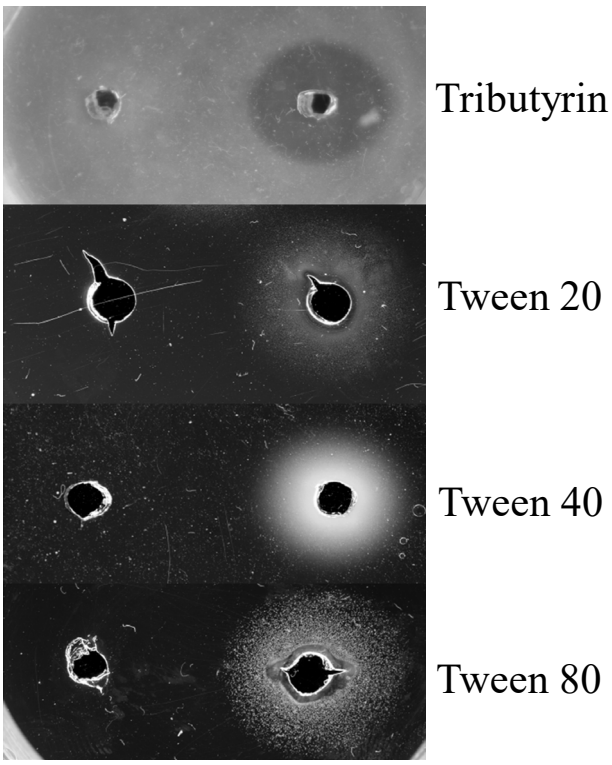

Fig. 3.4.S2 PlicB lipase activity tested in Tributyrin and Tween 20/40/60 plates. Twenty-five micrograms and 50 µg were dropped into Tributyrin and Tween20/40/60 plates respectively and incubated at 28°C for 24 h, in the case of Tween60 the incubation was for 48 hours

4 Discusión general

4.1 BÚSQUEDA DE NUEVOS SISTEMAS DE PRODUCCIÓN DE OPE

Desde que la esterol esterasa secretada por *O. piceae* (OPE) fue caracterizada, se ha demostrado que esta enzima posee propiedades muy interesantes para su potencial aplicación en la industria papelera y en la síntesis de compuestos nutracéuticos, como se recoge en las patentes ya mencionadas de Calero-Rueda y col. (2002a) y Barba Cedillo y col. (2013), respectivamente. Sin embargo, de cara a su posible empleo a escala industrial es necesario disponer de un buen sistema de expresión heterólogo. Por ello, aunque OPE se había expresado eficientemente en *P. pastoris* (Barba Cedillo et al. 2012), se decidió explorar sistemas alternativos.

4.1.1 Expresión en *E. coli*

Los organismos procariotas aparecen como una opción atractiva para la expresión heteróloga de proteínas porque se dispone de multitud de herramientas moleculares que facilitan su manipulación genética (Baneyx 1999) y esta fue la principal razón por la que se comenzó a trabajar con la bacteria Gram negativa *E. coli* como hospedador. Pero además, esta bacteria presentaba una ventaja adicional: carece de rutas de glicosilación y produce proteínas no glicosiladas, lo que podría facilitar la cristalización de OPE, uno de los objetivos de esta Tesis, ya que experimentos previos utilizando la proteína nativa no habían tenido éxito. Por otra parte, *E. coli* aparece como el organismo más utilizado en estudios de cristalización: en 2010, el 88% de las estructuras depositadas en *Protein Data Bank* (PDB) provinieron de proteínas producidas en esta bacteria (Nettleship 2012). Esto podría estar relacionado con la ausencia de formas glicosiladas de las proteínas bacterianas, presentando por ello menos heterogeneidad que las expresadas en hospedadores eucariotas, que muchas veces son glicoproteínas en las que las cadenas glucídicas generan flexibilidad y dificultan la posibilidad de obtener cristales que difracten con buena resolución (Chang et al. 2007).

Como ya hemos comentado, las lipasas presentan generalmente un elevado contenido en aminoácidos hidrofóbicos, lo que explica su tendencia natural a agregar. Como consecuencia, la mayor parte de las veces se encuentran en forma insoluble dentro de cuerpos de inclusión (Singh y Panda 2005), como la lipasa B de *C. antarctica* expresada en *E. coli* (Rotticci-Mulder et al. 2001). Otros ejemplos serían la lipasa de *R. delemar* que rindió proteína activa tras su solubilización y replegado *in vitro* (Joerger et al. 1993). En el caso de la lipasa 4 de *C. rugosa* también se obtuvieron niveles bajos de proteína soluble y activa tras fusionar el gen de CRL4 al de la tiorredoxina de la bacteria, al favorecer la formación de puentes disulfuro (Tang et al. 2000). Sin embargo, Larsen y col. (2008) consiguieron la expresión funcional de CalB en el periplasma de *E. coli* cultivando la bacteria a 16 ºC, aunque con rendimientos lejanos de los que estos mismos autores obtuvieron expresando en *P. pastoris* (5,2 y 44 mg/L, respectivamente).

En este trabajo se probaron numerosas estrategias para producir la forma activa de OPE en *E. coli*. En primer lugar, se intentó limitar la acumulación de la enzima en agregados disminuyendo la temperatura de crecimiento, y se ensayaron distintas cepas de la bacteria entre las que destacan estirpes portadoras de elementos que contribuyen al plegamiento proteico (cepa BL21(DE3)pT-GroE), otras diseñadas para aumentar la expresión de proteínas eucariotas que poseen codones de baja frecuencia en *E. coli* (Rosetta(DE3)pLysS), o cepas que favorecen la formación de puentes disulfuro (SHuffle T7 express). En cualquier caso, solo se logró expresar la proteína en cuerpos de inclusión (**Fig. 3.1.1**).

Para tratar de solubilizar la proteína se utilizaron distintos detergentes: CHAPS, Tritón X-100 y Sarkosyl, pero solo se consiguió proteína parcialmente soluble con este último, un detergente zwitteriónico cuyo empleo para la solubilización de otras proteínas expresadas en cuerpos de inclusión ya había sido descrito previamente (Burgess 1996; Frankel et al. 1991). Por otro lado, se obtuvieron cantidades pequeñas de proteína soluble utilizando la cepa BL21(DE3), siguiendo la estrategia de fusionar en la región N-terminal del gen que codifica para OPE la

secuencia de los 6 u 8 aminoácidos extra que aparecen en la enzima producida en *P. pastoris* y que aumentan la solubilidad de la proteína (Barba Cedillo et al. 2012). Son numerosos los trabajos que describen mejoras en la producción al modificar el extremo amino terminal de las proteínas, tanto de enzimas expresadas en *E. coli* (Gaudry et al. 2012; Hammarstrom et al. 2006; Terpe 2003) como en levaduras (García-Ruiz et al. 2012; Mate et al. 2013; Romanos et al. 1991).

No se detectó actividad esterasa en los lisados de *E. coli* con ninguna de las estrategias utilizadas, pero como en ocasiones la producción de la proteína es tan baja que solo es posible detectar la actividad tras su purificación (De Eugenio 2009), se trató de aislar la enzima a partir de las construcciones donde se había obtenido proteína soluble y de las fracciones solubilizadas con Sarkosyl. Solo se logró purificar una de ellas, concretamente la que llevaba una cola de histidinas fusionada en su extremo N-terminal, y para ello bastó un único paso de cromatografía de afinidad en una columna de níquel, pero la proteína expresada carecía de actividad. Tras analizar el espectro de dicroísmo circular de esta OPE inactiva se observaron importantes diferencias en su plegamiento con respecto a los observados en la proteína nativa y la recombinante en *P. pastoris*, lo que podría explicar esta falta de actividad.

Cuando se trata de producir proteínas de origen eucariota en *E. coli* el resultado es dispar y, en ocasiones, es difícil obtener proteínas funcionales. Como se ha comentado en la introducción, la ausencia de ciertos mecanismos de modificación post-traduccional en esta bacteria, como es el caso de la glicosilación, puede ser esencial para el correcto plegamiento de ciertas proteínas (Helenius 1994; Wei et al. 2013). Esto podría contribuir a explicar la falta de funcionalidad de OPE expresada en la bacteria, ya que la enzima nativa es una glicoproteína y se había expresado sin problemas en *P. pastoris*, que secreta una proteína mucho más glicosilada (8 y 30%, respectivamente).

4.1.2 Expresión en *S. cerevisiae*

La expresión de lipasas fúngicas en levaduras parece una opción más factible y ha dado mejores resultados (Brocca et al. 1998; Chang et al. 2006; Lee et al. 2002; Minning et al. 2001; Rotticci-Mulder et al. 2001; Tang et al. 2001), probablemente porque la producción tiene lugar en un sistema eucariota con una maquinaria de secreción semejante a la de hongos filamentosos.

Se escogió *S. cerevisiae* por ser una levadura GRAS (Albertin et al. 2011), con vistas a la posible utilización de la enzima en el sector alimentario. Como se mencionó en la introducción, se pueden emplear lipasas/esterasas en multitud de aplicaciones gracias a la amplia versatilidad de sustrato de estas enzimas (Hasan et al. 2006). Cabe resaltar que se ha descrito su uso para la mejora de las características organolépticas de alimentos (Macedo et al. 2003), la síntesis de lípidos estructurados ricos en ácidos grasos poliintasurados o la síntesis de ésteres de esteroles y estanoles vegetales que, incorporados en ciertos alimentos, generalmente derivados lácteos o grasas, tendrían un efecto beneficioso para la salud (Barba Cedillo et al. 2013; Ferreira-Dias et al. 2013; Miettinen et al. 1995).

Se consiguió expresar OPE en todas las cepas de *S. cerevisiae* utilizadas en este trabajo (BJ5465, BY4741 y Lalvin T73-4a), obteniendo los mayores niveles de actividad en la cepa deficiente en proteasas (BJ5465). Sin embargo, dichos valores fueron menores que los alcanzados en *P. pastoris*. Este hecho ha sido descrito en otras lipasas de la familia *C. rugosa-like*: la expresión de CRL1 fue entre 12-17 veces menor en *S. cerevisiae* que en *P. pastoris* (Brocca et al. 1998), lo mismo que ocurrió con las lipasas 1 y 2 de *G. candidum*, aunque en este caso se obtuvo un rendimiento 60 veces menor (Holmquist et al. 1997a). El fuerte metabolismo fermentativo de *S. cerevisiae*, junto con la retención de las proteínas en el espacio periplásmico, son factores que contribuyen a la menor capacidad secretora de esta levadura (Mattanovich et al. 2012). En el caso de OPE, se encontró que la proteína presentaba distinto grado de agregación, menor que el de la enzima nativa pero mayor que el de OPE

expresada en *P. pastoris* (**Fig. 3.1.5**). En este último hospedador la enzima producida es muy soluble, predominantemente monomérica y, como se ha comentado anteriormente, esto se debe a la presencia de 4-8 aminoácidos adicionales en su extremo N-terminal, resultado de la estrategia de clonación utilizada y del procesamiento incorrecto del péptido señal (Barba Cedillo et al. 2012). Se ha descrito que este fenómeno tiene lugar cuando los niveles de expresión heteróloga son elevados y la peptidasa STE13 no es capaz de procesar correctamente el fragmento pro-líder del péptido señal (Zsebo et al. 1986). Las condiciones de fermentación empleadas para producir la proteína en *S. cerevisiae*, con menor temperatura y agitación, favorecerían el procesamiento correcto del péptido señal. De este modo, podríamos relacionar la menor expresión de OPE en *S. cerevisiae* con la producción de varias especies moleculares, algunas con el péptido pro-líder completamente procesado, y por tanto menos solubles, y otras procesadas incorrectamente y más solubles por contener los aminoácidos extra.

Los niveles de OPE secretados por *S. cerevisiae* están lejos de ser los deseables y deberían ser mejorados si se quisiera utilizar esta proteína para cualquier aplicación. Sin embargo, la expresión en este hospedador abre las puertas para el diseño de enzimas a la carta, mediante mecanismos de evolución dirigida. Cabe destacar que la cepa con la que se han obtenido los mejores resultados se está empleando desde hace algunos años para mejorar ciertas enzimas fúngicas mediante experimentos de evolución dirigida (Alcalde 2015; Camarero et al. 2012). Este método se ha utilizado previamente para mejorar otras lipasas (Korman et al. 2013; Liebeton et al. 2000) y en el caso de OPE podría servir tanto para optimizar su expresión como para mejorar su estabilidad a la temperatura, pH o solventes orgánicos.

4.2 RESOLUCIÓN DE LA ESTRUCTURA TRIDIMENSIONAL DE OPE: HOMOLOGÍAS Y DIFERENCIAS CON OTRAS LIPASAS DE LA FAMILIA *C. rugosa-LIKE*

Para profundizar en las relaciones estructura-función de una proteína y entender las bases moleculares de su mecanismo de acción, e incluso para tratar de mejorar su actividad, es esencial conocer su estructura molecular.

En el caso de OPE, en un primer abordaje se ensayaron multitud de condiciones de cristalización utilizando la enzima nativa, pero solo se consiguieron agregados no cristalinos de la proteína. Por otra parte, empleando la enzima producida en *P. pastoris* los cristales obtenidos no tenían la calidad suficiente para obtener un patrón de difracción que permitiera la resolución de la estructura. El problema parecía estar relacionado con el alto grado de glicosilación de esta proteína ya que, como hemos comentado anteriormente, la flexibilidad de las cadenas glucídicas puede disminuir la resolución del patrón de difracción de estos cristales.

Con el propósito de obtener enzima desglicosilada en cantidades suficientes para realizar los experimentos de cristalografía iniciamos los estudios de expresión de OPE en *E. coli* aunque, como ya se ha explicado, no se consiguieron los resultados deseados (Vaquero et al. 2015a). Por esta razón, y teniendo en cuenta que estudios previos habían demostrado que la actividad catalítica de la proteína secretada por *P. pastoris* se mantenía tras su desglicosilación enzimática (Barba Cedillo et al. 2012), se optó por desglicosilar altas cantidades de esta enzima con Endo H para continuar con los experimentos. De este modo, se conseguía eliminar los N-glicanos de la OPE recombinante, quedando unido solo un residuo de N-acetilglucosamina a la asparagina de la cadena proteica. Este procedimiento había sido empleado con éxito para la resolución de la estructura molecular de otras glicoproteínas, como el receptor adrenérgico β_2 humano y el complejo formado por el factor intrínseco gástrico y la vitamina B12 (Noguchi and Satow 2006).

La cristalización de OPE se realizó en colaboración con el grupo del Dr. Juan Hermoso (Instituto de Química-Física Rocasolano, CSIC). Tras evaluar 500 condiciones de cristalización se obtuvieron cristales en dos hábitos diferentes, que sugerían la posibilidad de distintos empaquetamientos estructurales de la proteína. Esto se confirmó al analizar los patrones de difracción de los cristales obtenidos en ambas condiciones y tras la resolución de la estructura de la proteína en su configuración abierta y cerrada (Gutiérrez-Fernández et al. 2014). En un caso, la enzima tenía el centro activo accesible al sustrato (conformación abierta) y en otro

permanecía bloqueado por la presencia de una "tapadera" (conformación cerrada). Este fenómeno fue descrito a principios de los 90, con la resolución de la primera estructura de la lipasa del hongo *R. miehei* en ambas conformaciones (Brady et al. 1990; Brzozowski et al. 1991), corroborándose posteriormente en otras lipasas de la familia *C. rugosa-like*. Así, se han resuelto estructuras en forma abierta, gracias a la presencia del sustrato natural y/o inhibidores, en la lipasa 1 de *C. rugosa* (PDB: 1CRL, 1LPP, 1LPN, 1LPO) (Grochulski et al. 1993, 1994a) y la lipasa 3 de esta misma levadura (antes conocida como *C. cylindracea*), que fue clasificada inicialmente como colesterol esterasa (1CLE, 1LLF) (Ghosh et al. 1995; Pletnev et al. 2003). Por otro lado, se han caracterizado las estructuras de la forma inactiva de CRL1 (PDB:1TRH) (Grochulski et al. 1994b), CRL2 (1GZ7) (Mancheño et al. 2003) y la lipasa 2 de *G. candidum* (PDB: 1THG) (Schrag y Cygler 1993).

La estructura de la esterol esterasa de *O. piceae* es muy similar a la de otras enzimas de la familia *C. rugosa-like,* cuyas principales características se describieron en el apartado de introducción. Entre los rasgos estructurales de OPE, destaca la presencia de una tapadera móvil de 37 aminoácidos formada por una hélice de tipo α y dos hélices 3_{10} rodeadas por dos lazos que confluyen en un puente disulfuro. Esto la diferencia de las lipasas de *C. rugosa* (Ghosh et al. 1995; Grochulski et al. 1993, 1994b; Mancheño et al. 2003) y *G. candidum* (Schrag et al. 1991; Schrag y Cygler 1993), que muestran una hélice α y una de tipo 3_{10} y tres hélices α, respectivamente. El desplazamiento de la tapadera de aproximadamente 30 Å en la conformación abierta facilita la exposición del bolsillo de sustrato, exhibiendo una gran cantidad de aminoácidos hidrofóbicos que favorecen la estabilización del sustrato (**Fig. 4.1A**).

La apertura de la tapadera origina un reordenamiento estructural que desencadena la organización dimérica de la enzima. Esta dimerización se produce como resultado de uniones exclusivamente hidrofóbicas entre aminoácidos de la zona de contacto de ambos monómeros y de la región de la tapa (**Fig. 4.1B-C**). En el caso de CRL3 es diferente, ya que el dímero se

estabiliza a través de varios puentes de hidrógeno e interacciones hidrofóbicas (**Fig. 1.6**) (Ghosh et al. 1995; Pletnev et al. 2003).

La dimerización en OPE crea una cavidad altamente hidrofóbica y muy amplia (23 Å x 38 Å), en comparación con la de CRL3 (7,3 Å de radio) (Pletnev et al. 2003). La funcionalidad de las dos formas (monomérica y dimérica) de OPE se estudió tras separarlas en una columna de exclusión molecular, incubando por un lado la forma monomérica con el sustrato (oleato de colesterilo) o un inhibidor (cloruro de 1-dodecanosulfonilo), y por otro lado la mezcla de ambas formas de la enzima con estos mismos compuestos.

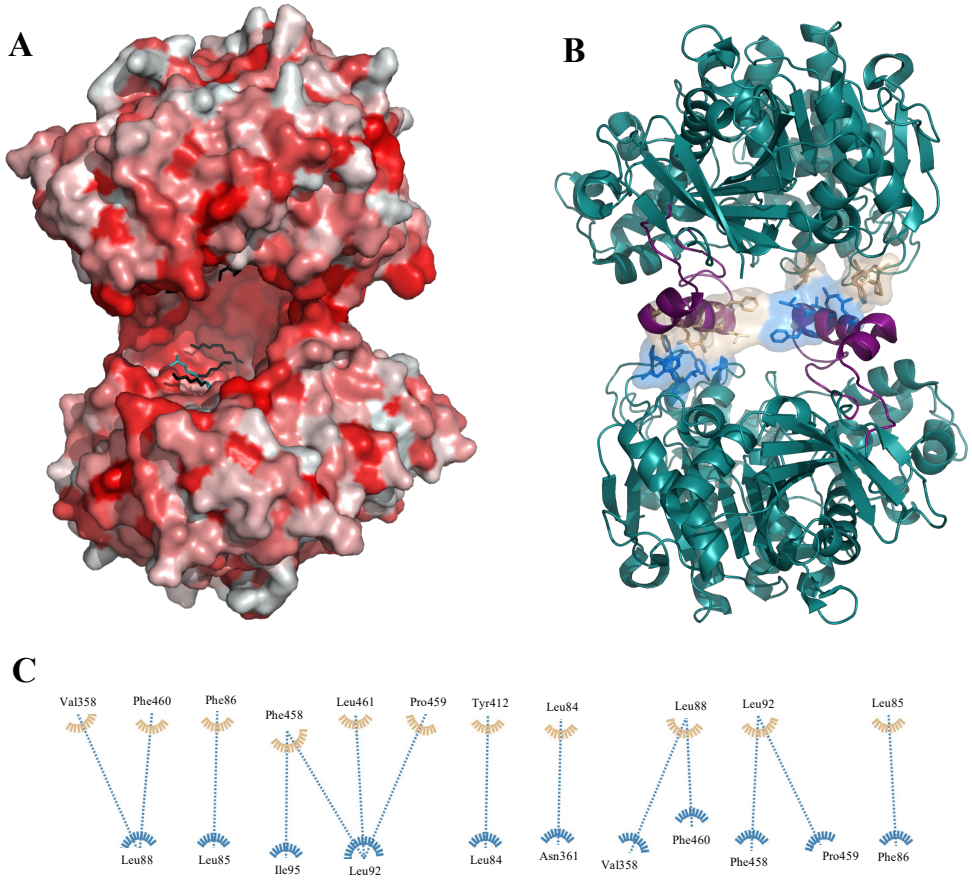

Fig. 4.1 A) Representación de la superficie de OPE (PDB: 4BE9), en la que se representan las zonas más hidrofóbicas en color rojo más intenso y en color negro las moléculas de polietilenglicol en la cavidad que da acceso al centro activo. **B)** Representación tridimensional de las interacciones entre los monómeros de esta proteína. En morado, la región de la tapadera; en azul y marrón claro se representan los aminóacidos que interaccionan entre las dos moléculas. **C)** Representación esquemática de las interacciones entre monómeros obtenida mediante el programa DIMPLOT.

Tras las incubaciones, las mezclas se analizaron mediante ultracentrifugación analítica, encontrando que la proporción de monómero disminuía, incrementándose la del dímero, tanto en el caso de la mezcla de las dos especies como cuando se incubaba solo el mónomero con el sustrato o el inhibidor, siendo en este último caso el incremento mucho mayor. Esto sugiere que la forma funcional de OPE es dimérica y que existe una transición entre monómero y dímero en presencia del sustrato o un análogo de este. Varios trabajos describen la presencia de dímeros de CRL3 en solución (Kaiser et al. 1994; Pernas et al. 2000), y otros autores indican que no presenta activación interfacial (Pernas et al. 2001) y que el polietilenglicol promueve el equilibrio hacia la forma abierta en esta enzima (Otero et al. 2005). OPE parece tener características similares a CRL3, ya que la enzima nativa no mostró activación interfacial (Calero-Rueda et al 2002b y además se localizaron algunas moléculas de polietilenglicol, procedentes de la condición de cristalización, en los alrededores del centro activo en la forma abierta que favorecerían la dimerización (**Fig. 4.1A**).

Como se ha comentado anteriormente, las lipasas son proteínas con alto contenido en aminoácidos hidrofóbicos y poseen regiones donde se acumulan varios de estos residuos, originando parches hidrofóbicos. En el caso de OPE, uno de estos parches interacciona directamente con aminoácidos de la tapa, estabilizando la conformación cerrada, mientras que en la conformación abierta son estos mismos residuos los que interaccionan con la tapa del otro monómero para estabilizar el dímero. El residuo Phe458 parece ser clave en este mecanismo, ya que en la conformación cerrada interacciona con tres aminoácidos de la tapa (Val89, Leu88 y Leu92), mientras que en la conformación abierta lo hace con residuos de la tapa de la otra molécula (Ile95 y Leu92), estabilizando la conformación dimérica.

Es probable que el aumento de solubilidad con respecto a la enzima nativa, observado en las proteínas expresadas en *P. pastoris* (Barba Cedillo et al. 2012) y *S. cerevisiae* (Vaquero et al. 2015b) que contienen los aminoácidos adicionales en el extremo N-terminal, se produzca por la

ruptura de un parche hidrofóbico superficial, cercano a la región N-terminal. De hecho, una de las estrategias descritas para reducir la agregación proteica consiste en incrementar la carga (positiva o negativa) de la superficie. Una variante de la lipasa de *Bacillus subtilis*, obtenida por evolución dirigida, mostró mayor solubilidad que la proteína original debido a la introducción de residuos polares de tipo ácido que reducían considerablemente la superficie de los parches hidrófobicos (Kamal et al. 2011). En el caso de la OPE recombinante, tres de los residuos adicionales del extremo amino terminal son ácidos glutámicos y esto podría contribuir a la reducción del área hidrofóbica circundante.

En cuanto a la maquinaria catalítica, OPE presenta un centro activo muy conservado, formado por los residuos de la tríada catalítica (Ser, Glu e His), y dos glicinas como estabilizadoras del oxianión. Sustratos voluminosos, como los ésteres de colesterol, podrían alojarse en el centro activo, albergando la cadena de ácido graso en el interior del bolsillo, mientras que el colesterol se situaría hacia el exterior.

El bolsillo del sustrato en OPE está formado por un túnel interno de aproximadamente 30 Å de longitud, desde la serina catalítica hasta los residuos Lys335, Tyr541 y Asn542, próximos a la superficie. El túnel está constituido por residuos alifáticos y aromáticos que le confieren un ambiente altamente hidrofóbico. En el caso de *C. rugosa*, Mancheño y col. (2003) definen dos zonas en el sitio de unión al sustrato, la más externa rica en aminoácidos aromáticos, diferente entre las isoenzimas CRL2>CRL3>CRL1, y la segunda, rica en aminoácidos alifáticos, que está muy conservada y se orienta perpendicular a la primera (**Fig. 4.2A**). En el caso de la OPE, la primera región del túnel contiene tres fenilalaninas al igual que CRL2, considerada la isoenzima de *C. rugosa* con mayor actividad sobre ésteres de colesterol (Mancheño et al. 2003). Sin embargo, la segunda región del túnel, que albergaría la cadena de ácido graso, se orienta hacia otra zona de la molécula, a continuación de esta y dando lugar a un túnel de aspecto más recto (**Fig. 4.2A**). Tanto estudios computacionales previos realizados con CRL1, como la estructura de CRL3, sugerían una vía alternativa para la liberación de la cadena acilada

durante la hidrólisis (Foresti y Ferreira 2004; Ghosh et al. 1995), ya que el final del túnel se sitúa en una región próxima a la superficie. Para evaluar el papel del túnel interno en OPE, como posible vía de salida de productos de hidrólisis de cadena larga, se diseñó un mutante que bloqueaba el último tramo del túnel, sustituyendo la isoleucina 544 por un triptófano mediante mutagénesis dirigida (**Fig. 4.2B-C**).

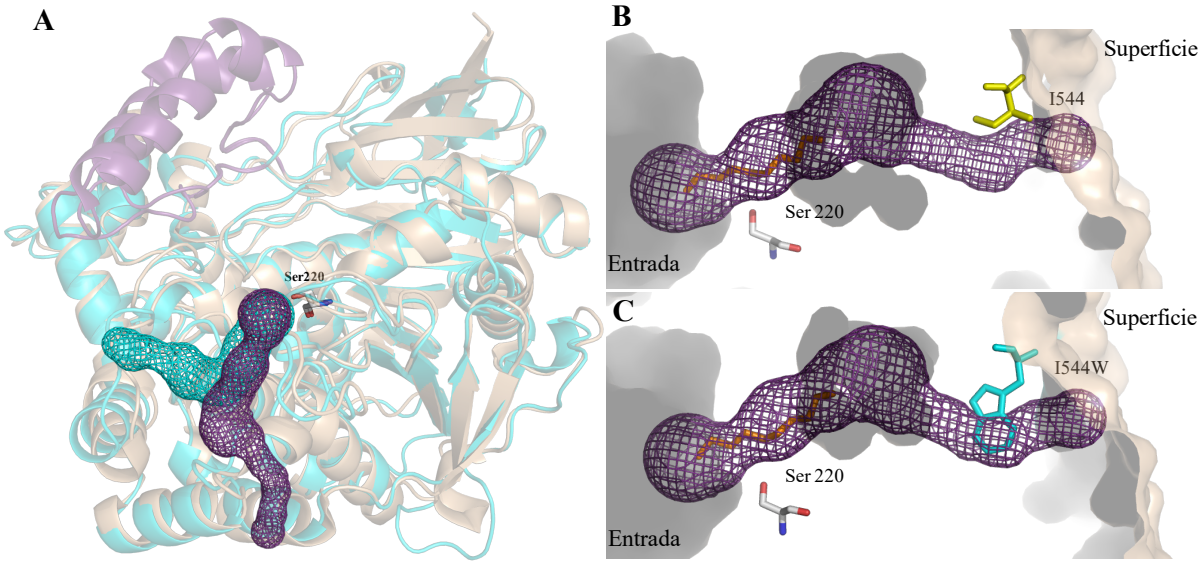

Fig. 4.2 A) Superposición de las estructuras de CRL3 en azul (PDB:1CLE) y OPE (PDB:4BE9) en marrón claro. Ambas tapaderas en color morado. Representación del túnel de CRL3 en azul y del de OPE en morado. **B)** Túnel de OPE sin mutar, con la Ile544 marcada en amarillo. **C)** Mutante de OPE I544W (PDB:4UPD), en el que en azul turquesa se señala el triptófano que bloquea el túnel.

Al analizar la actividad específica de este mutante utilizando distintos ésteres de *p*-nitrofenol, se observó que la catálisis de los ácidos grasos de cadena corta y media no estaba afectada, pero se reducía drásticamente con los de cadena larga (≥ C16:0). Este fenómeno puede deberse a que la presencia al final del túnel de un residuo voluminoso como el triptófano lo bloquearía, limitando el correcto posicionamiento de los sustratos de cadena larga y, por tanto, su hidrólisis. Estudios realizados con CRL1 describen que las mutaciones en distintos puntos del túnel modifican la hidrólisis de sustratos de cadena media y larga, destacando la importancia de su longitud en la catálisis (Schmitt et al. 2002). Sin embargo, aunque se ha observado la reducción de la actividad al bloquear

el túnel en OPE, no se ha podido confirmar la hipótesis del túnel de salida de los productos de reacción con esta estrategia.

A pesar de ello, la resolución de la estructura de OPE en su conformación abierta y cerrada ha aportado el conocimiento necesario para continuar con nuevos estudios estructura-función que contribuyan a explicar porque OPE es más eficaz que otras enzimas de la familia *C. rugosa-like* hidrolizando triglicéridos y ésteres de colesterol (Calero-Rueda et al. 2002b; Calero-Rueda et al. 2009) y para obtener variantes que presenten mejores propiedades físico-químicas y cinéticas.

4.3 BÚSQUEDA DE NUEVAS ENZIMAS EN GENOMAS FÚNGICOS

El desarrollo de las grandes plataformas de secuenciación masiva (Illumina, SOLiD sequencer, Roche GS-FLX 454, Helicos, etc) ha permitido reducir los costes de secuenciación de ADN y analizar un gran número de genomas en poco tiempo (Shendure y Ji 2008). En este sentido el portal MycoCosm, desarrollado por el *Joint Genome Institute* (JGI) (http://jgi.doe.gov/), del departamento de energía de los Estados Unidos, proporciona la integración y el análisis de los datos derivados de proyectos a gran escala, como por ejemplo el proyecto sobre "la secuenciación de mil genomas fúngicos". El objetivo de este proyecto es la obtención de al menos dos genomas de referencia de las más de 500 familias reconocidas de hongos, existiendo actualmente más de 500 genomas secuenciados. El interés de este proyecto está relacionado con la exploración del reino *Fungi* ya que estos organismos pueden aportar soluciones a problemas relacionados con la energía y el medio ambiente por tener un papel esencial en el ciclo del carbono y ser capaces de degradar tanto polímeros naturales como sintéticos (Grigoriev et al. 2014). En este sentido, destacar que existen publicaciones que tratan de explorar estos genomas en busca de enzimas con características interesantes y/o mejoradas, como es el caso de la búsqueda de nuevas peroxidasas ligninolíticas (Fernandez-Fueyo et al. 2014) y de lipasas o hidrolasas en general con potencial biotecnológico (Feldbrügge et al. 2013).

4.3.1 Búsqueda de enzimas de la familia *C. rugosa-like*

El potencial biotecnológico de las lipasas/esterol esterasas ha promovido la búsqueda de enzimas pertenecientes a la familia *C. rugosa-like* en genomas y metagenomas públicos (Barriuso et al. 2013; Barriuso y Martínez 2015). Tras un análisis exhaustivo de los dominios conservados, alineamiento de secuencias, análisis filogenético y posterior estudio del modelo tridimensional, se obtuvieron 6 candidatos potenciales, y se predijeron sus propiedades catalíticas *in silico*, en base al número de aminoácidos hidrofóbicos presentes en la región de la tapadera de cada proteína y, tras modelar estas proteínas, a la forma de su túnel interno, posible vía de salida de productos durante la catálisis.

Posteriormente, tres de estas proteínas hipotéticas (Necha2, Trire2 y Aspni5), pertenecientes a los genomas secuenciados de *N. haematococca* (teleomorfo de *F. solani*), *T. reseii* y *A. niger,* se seleccionaron por su diversa agrupación filogenética, forma del bolsillo del sustrato y contenido en aminoácidos hidrofóbicos en la zona de la tapadera, para continuar su estudio. Las enzimas se expresaron y produjeron satisfactoriamente en *P. pastoris,* corroborando la adecuación de la levadura como hospedador heterólogo de esta familia de lipasas (Vaquero et al. 2015a). La expresión funcional de enzimas de la familia *C. rugosa-like* en este hospedador ya se había descrito con anterioridad. Este es el caso de las distintas isoenzimas de *C. rugosa* (Brocca et al. 1998; Chang et al. 2006; Lee et al. 2002; Lee et al. 2011; Tang et al. 2001), *G. candidum* (Holmquist et al. 1997a) y de OPE (Barba Cedillo et al. 2012). Sin embargo no siempre es así, ya que la producción de la esterol esterasa de *M. albomyces* en *P. pastoris* no dio buenos resultados, detectando en los sobrenadantes una actividad muy inferior a la secretada por el hongo (~8 veces menos) y, dependiendo del transformante, entre 30-85% de actividad intracelular (Kontkanen et al. 2006a). Este hecho, según los autores, podría deberse a la incapacacidad de la levadura para llevar a cabo el correcto plegamiento y/o secreción de la proteína, aunque otros factores, como la alta tendencia a la agregación de esta enzima (es un tetrámero en condiciones nativas), podrían ser responsables de su secreción limitada.

Por otro lado, la purificación y caracterización bioquímica de las tres nuevas lipasas encontradas en genomas fúngicos permitió confirmar algunas propiedades comunes de esta familia. En cuanto al estado de agregación, la presencia en solución de monómeros, dímeros y otras formas de asociación mayores, ratifica lo descrito por otros autores para este tipo de enzimas (Barba Cedillo et al. 2012; Ferrer et al. 2009; Kontkanen et al. 2006b; Pernas et al. 2001; Zorn et al. 2005). Sin embargo, el fenómeno de transición de monómero a dímero de OPE en presencia de sustrato no es una característica general de la familia, ya que únicamente se ha descrito para OPE (Gutiérrez-Fernández et al. 2014) y CRL3 (Turner et al. 2001) y ambas proteínas dimerizan de manera distinta, como se ha comentado en el apartado anterior.

Respecto a la especificidad de sustrato de las enzimas caracterizadas en la familia *C. rugosa-like*, solo en algunas de ellas se había descrito que son capaces de hidrolizar sustratos sintéticos (ésteres de *p*-nitrofenol) y naturales (triglicéridos y ésteres de esterol). Este es el caso de las isoenzimas de *C. rugosa* (CRL1-CRL4) (Lee et al. 2002; López et al. 2004; Mancheño et al. 2003) y las esterol esterasas de *O. piceae* y *M. albomyce*s (Calero-Rueda et al. 2002b; Kontkanen et al. 2006b). En este trabajo se estudiaron las propiedades catalíticas frente a estos sustratos de las nuevas lipasas/esterol esterasas seleccionadas de genomas fúngicos y expresadas en *P. pastoris*. La lipasa de *A. niger* (Aspni5), que por su menor contenido en aminoácidos hidrofóbicos en la región de la tapa es la que más se asemeja a las isoenzimas de *C. rugosa*, fue incapaz de hidrolizar los ésteres de colesterol en las condiciones ensayadas y mostró menor eficiencia frente a los otros sustratos analizados, a pesar de su elevada afinidad por ellos. Esta es la enzima que presentaba el túnel más estrecho y menos recto, sugiriendo que parámetros como la geometría del túnel interno tienen un efecto importante sobre la eficiencia catalítica de estas enzimas. En este sentido tampoco se ha descrito actividad esterol esterasa en el crudo comercial con actividad lipasa de *G. candidum* (Kontkanen et al. 2004). No obstante, Jensen (1974) y Charton y Macrae (1992), sí habían detectado bajos niveles de esta actividad en una de las dos isoenzimas purificadas. Ambas presentan también un túnel similar al de *C. rugosa* y *A. niger*, lo

que indica que la catálisis de este tipo de sustratos no es rasgo común en todos los miembros de la familia *C. rugosa-like*.

Sin embargo, las enzimas de *N. haematoccoca* y *T. reseei* fueron capaces de actuar sobre todos los sustratos ensayados: triglicéridos y ésteres de *p*-nitrofenol y colesterol. Ambas proteínas poseen un porcentaje de aminoácidos hidrofóbicos en la región de la tapa ligeramente superior a los de OPE, Aspni5 y las diferentes isoenzimas de *C. rugosa*, y un túnel interno con forma más parecida al de OPE.

Las enzimas pertenecientes a esta familia parecen mostrar cierta preferencia para hidrolizar sustratos que contienen ácidos grasos de cadena larga y con insaturaciones en la posición cis-9 del ácido graso, como el ácido oleico, tal y como se ha descrito para las isoenzimas 2 y 4 de *C. rugosa*, y la lipasa 1 de *G. candidum*, así como para las esterol esterasas de *M. albomyces* y *O. piceae* (Calero-Rueda et al. 2004; Holmquist et al. 1997b; Kontkanen et al. 2006b; Lee et al. 2002; Lee et al. 2007). Esta preferencia por sustratos de cadena larga se relaciona, por un lado, con la longitud del bolsillo de sustrato en forma de túnel que poseen todas las enzimas de esta familia, que permite acomodarlos más fácilmente (Domínguez de María et al. 2006). Por otro lado, la amplitud y geometría del túnel (en forma de L o recto) así como la posible existencia de una vía alternativa de salida del ácido graso podría contribuir a su eficiencia catalíticas. Cabe destacar que las mayores diferencias de eficiencia catalítica entre las enzimas de *T. reseei*, *N. haematococca* y *O. piceae*, se observaron cuando el sustrato fue un éster de colesterol de cadena larga, sobre el que OPE mostró valores de velocidad máxima muy superiores. El hecho de que el dímero de OPE sea la forma activa de esta proteína, dejando una cavidad amplia entre los dos monómeros, podría favorecer la estabilización y el acceso al centro activo de los sustratos contribuyendo a la catálisis de sustratos voluminosos.

La producción y caracterización de tres nuevas enzimas pertenecientes a la familia *C. rugosa-like* ha permitido extrapolar propiedades comunes de sus miembros, aumentando el conocimiento disponible sobre esta familia. Los estudios derivados de la búsqueda *in*

silico de enzimas en genomas y su posterior análisis (alineamientos, filogenia, búsqueda de sitios de glicosilación, puentes disulfuro, modelado tridimensional, *docking*, etc) mediante herramientas bioinformáticas, resultan muy útiles para acotar la selección de candidatos, requiriéndose su posterior expresión y caracterización para verificar sus propiedades catalíticas.

Por último, es importante señalar que la versatilidad de sustrato en referencia a la hidrólisis de triglicéridos y de ésteres de colesterol no es un rasgo común en los miembros descritos y caracterizados de esta familia. Algunas, como hemos visto, no muestran actividad sobre ésteres de esteroles o esta es muy limitada, mientras que otras enzimas muestran una amplia versatilidad de sustrato. En consecuencia, la inclusión dentro de esta familia no es sinónimo de versatilidad, siendo necesaria una caracterización enzimática más profunda para confirmar dicho rasgo. Por otro lado, apuntar que aunque las bases de datos son extremadamente útiles, la clasificación de enzimas hipotéticas se basa únicamente en su secuencia aminoacídica y no en otras propiedades como la actividad enzimática debido a las dificultades técnicas que esto conlleva, lo que origina que muchas enzimas aparezcan erróneamente clasificadas.

4.3.2 Búsqueda de otras lipasas de interés biotecnológico

Existen lipasas de gran interés biotecnológico que no pertenecen a la familia *C. rugosa-like*. Este es el caso de la lipasa B de *C. antarctica* (CalB), la enzima más empleada en biotecnología y en química orgánica en los últimos años. Entre las distintas aplicaciones en las que se utiliza, destaca la resolución de alcoholes secundarios quirales (Rotticci et al. 2001), la producción de biodiesel (Yan et al. 2012) o la síntesis de poliésteres (Kumar y Gross 2000). Esta enzima posee una estabilidad única, y en su forma inmovilizada resiste altas temperaturas (Lozano et al. 2003), solventes orgánicos con alta polaridad (Magnusson et al. 2005), y es estable en líquidos iónicos (Park et al. 2003) así como en atmósferas supercríticas de dióxido de carbono (Ottosson et al. 2002). Además, presenta unos rasgos estructurales que difieren de los descritos para otras lipasas. La secuencia consenso G-x-S-x-G existente en la mayoría de

lipasas, donde se encuentra la serina catalítica, se sustituye en CalB por la secuencia T-W-S-Q-G (Uppenberg et al. 1994). Tradicionalmente se ha considerado que CalB no tiene tapadera, aunque diversos autores destacan la flexibilidad de la hélice α5, sugiriendo que podría desempeñar la función de este elemento móvil (Ganjalikhany et al. 2012). El bolsillo del sustrato tiene forma de embudo, más limitado espacialmente en comparación con otras lipasas, y esto podría intervenir en su enantioselectividad frente a alcoholes secundarios (Rotticci et al. 1998)

La búsqueda de enzimas con propiedades similares se ha potenciado en los últimos años y varias enzimas relacionadas filogenéticamente con CalB han sido recientemente caracterizadas. Entre ellas se encuentra una lipasa de *Ustilago maydis*, hongo basidiomiceto patógeno del maíz (Buerth et al. 2014), y otras de *Hyphozyma sp.*, *Sporisorium reilianum* y *Pseudozyma tsukubaensis* que han sido patentadas recientemente por Novozymes como posibles alternativas a CalB en diferentes aplicaciones (Besenmatter et al. 2013).

Debido a la potencial aplicabilidad biotecnológica de esta familia de lipasas, en la última fase de esta tesis se realizó la búsqueda de enzimas similares a CalB en los genomas depositados en el JGI. Tras la búsqueda de motivos conservados de CalB, la construcción de un árbol filogenético, el análisis de estas secuencias y su modelado 3D, se obtuvieron varios candidatos. De todos ellos, se seleccionó para su expresión y caracterización la secuencia de *Plicaturopsis crispa* (PlicB) por no estar patentada y presentar la menor distancia filogénetica al clado en el que agrupa CalB.

Este basidiomiceto de podredumbre blanca es el primer miembro del orden amilocorticiales secuenciado (http://jgi.doe.gov/). La única lipasa de otro hongo de podredumbre blanca caracterizada y expresada heterólogamente hasta el momento es la secretada por *P. sapidus* (Krugener et al. 2009; Zorn et al. 2005). Sin embargo, como se ha comentado previamente, esta enzima pertenece a la familia *C. rugosa-like* y posee baja identidad de secuencia con PlicB (< 13%).

Los hongos de podredumbre blanca son capaces de degradar la pared celular de plantas, preferencialmente la lignina, y para ello poseen un complejo sistema enzimático extracelular (Ruiz-Dueñas y Martínez 2009). Han sido numerosos los esfuerzos por caracterizar el sistema ligninolítico de estos hongos, pero aún se conoce poco acerca de su actividad lipolítica (Rajarathnam et al. 1998). En este sentido, el papel fisiológico de PlicB podría estar relacionado con el aprovechamiento de los lípidos y ácidos grasos de la planta, algo comúnmente descrito para este tipo de enzimas (Brockerhoff y Jensen 1974).

La comparación de la secuencia de PlicB con la de enzimas relacionadas, CalB y la lipasa 2 de *U. maydis* (Ulm2), así como el modelo estructural de esta, indican que la tríada catalítica de PlicB está formada por los residuos Ser122, Asp218 e His257 rasgo común en este tipo de lipasas (Buerth et al. 2014; Uppenberg et al. 1994). No obstante, cabe destacar que los aminoácidos del codo nucleófilo de PlicB difieren de los residuos observados en otras enzimas, ya que posee una tirosina en lugar del triptófano que precede a la serina catalítica en CalB y otras proteínas relacionadas filogenéticamente. Esto se ha descrito también para las cutinasas de *F. solani* y *A. oryzae* (Pleiss et al. 2000), capaces de hidrolizar tanto sustratos solubles como insolubles, que muestran un comportamiento cinético intermedio entre lipasas y esterasas (Egmond y van Bemmel 1997; Martinez et al. 1992). La expresión de PlicB requirió de un proceso de optimización de codones. Esto se debe a que los hongos basidiomicetos suelen tener en sus secuencias codificantes un contenido en G+C (50-60%) mayor al de los ascomicetos (40-50%) y, por ello, hacen diferente uso de codones (Storck 1966). Con esta estrategia se consiguió expresar esta proteína en *P. pastoris* y caracterizarla. PlicB mostró propiedades comunes a CalB, como la masa molecular de su secuencia peptídica, de alrededor de 35 kDa, y su configuración monomérica (Larsen et al. 2008; Qian et al. 2009). En relación a la especificidad de sustrato, PlicB, al igual que CalB y Ulm2, hidroliza sustratos esterificados tanto con ácidos grasos de cadena corta como larga. CalB mostró mayor actividad específica para los sustratos de tipo *p*-nitrofenol, mientras que PlicB fue la más activa en la hidrólisis de un tioéster análogo de la tributirina. Este hecho puede deberse

a la distinta regioselectividad de ambas enzimas (Farias et al. 1997). En este sentido, CalB podría tener mayor regioselectividad por la posición sn-1,3 del triglicérido, fenómeno observado previamente en reacciones de síntesis (Watanabe et al. 2009), mientras que PlicB podría hidrolizar cualquier posición y, por tanto, sería una lipasa menos específica.

A la vista de los resultados obtenidos con las lipasas pertenecientes a los genomas de *N. haematococca*, *T. reesei*, *A. niger* y *P. crispa*, podríamos concluir que la minería de genomas aparece como una alternativa robusta a los cribados tradicionales, permitiendo seleccionar y evaluar enzimas con propiedades biotecnológicas de interés.

4.4 APLICACIONES BIOTECNOLÓGICAS

Dada la versatilidad descrita para las lipasas de *C. rugosa* y la enzima secretada por *O. piceae*, se compararon estas enzimas con las nuevas lipasas pertenecientes a la familia *C. rugosa-lik*e producidas y caracterizadas en el presente trabajo, con objeto de evaluar su eficacia en dos procesos de síntesis con potencial aplicación biotecnológica: la polimerización de poliésteres y la síntesis de ésteres de fitoestanoles

4.4.1 Síntesis de oligómeros de caprolactona.

La policaprolactona es un poliéster alifático, biodegradable y biocompatible. Este polímero muestra además buenas propiedades mecánicas y de adhesión. Todo ello hace que sea un polímero muy atractivo para la industria médica y farmacéutica, como material para implantes y vehículo en los sistemas liberadores de fármacos. Su síntesis se produce generalmente por el proceso conocido como polimerización por apertura del anillo (ROP), habitualmente catalizado por compuestos organometálicos derivados de metales pesados (Labet y Thielemans 2009). El empleo de catalizadores enzimáticos para la polimerización, como las lipasas, supondría una alternativa interesante, permitiendo el uso de condiciones de reacción más suaves de temperatura y pH y menos restrictivas a nivel de oxígeno y agua. Además no sería necesario eliminar completamente el catalizador para las aplicaciones en biomedicina o la industria farmacéutica al no ser perjudiciales (Varma et al. 2005).

En la presente Tesis Doctoral se evaluó la eficacia de las nuevas enzimas de la familia *C. rugosa-like* (Necha2, Trire2 y Aspni5) caracterizadas en este trabajo para sintetizar policaprolactona, y se comparó su eficacia con la de OPE y la lipasa comercial de *C. rugosa*. La síntesis se llevó a cabo empleando condiciones suaves de temperatura (60 ºC), en presencia de oxígeno y en ausencia de agua. De entre los catalizadores ensayados, la lipasa comercial de *C. rugosa* (en la que se encuentra mayoritariamente CRL1, aunque también hay CRL3 y, en mucho menor proporción, CRL2), los crudos de OPE y la lipasa de *A. niger* resultaron ser los más eficientes para la oligomerización de caprolactona. Con estas tres enzimas se obtuvieron oligómeros mayoritarios de alrededor de 1400 Da, llegando a alcanzar, en el mejor de los casos, compuestos de 34 unidades en reacciones catalizadas por OPE. Los resultados obtenidos en este trabajo son comparables a los descritos por otros autores (Kobayashi et al. 1998; Uyama y Kobayashi 1993) que llevan a cabo un estudio con distintas lipasas comerciales, indicando la necesidad de largos tiempo de incubación con la enzima de *C. rugosa*. Estos autores sugieren el empleo de enzimas más eficaces para producir policaprolactona, poniendo de manifiesto la importancia de la elección de lipasa para esta u otras aplicaciones.

4.4.2 Síntesis de ésteres de estanoles vegetales como compuestos nutracéuticos

En la actualidad, el aumento en el consumo de grasas saturadas y el sedentarismo provoca que una parte de la población presente niveles elevados de colesterol sérico, propiciando el desarrollo de enfermedades cardiovasculares (Calpe-Berdiel et al. 2009). Por ello, el uso de compuestos que reduzcan los niveles de colesterol ha suscitado gran interés. En este sentido, los esteroles y estanoles vegetales que poseen una estructura similar a la del colesterol, con un anillo de ciclopentanoperhidrofenantreno, han demostrado su capacidad para disminuir el colesterol LDL en sangre ya que se reduce su absorción a nivel intestinal (Miettinen et al. 1995). Para la incorporación de los esteroles y estanoles vegetales a la dieta, incluyéndolos en derivados lácteos o de aceites vegetales, es conveniente esterificarlos con ácidos grasos de cadena larga para así aumentar su solubilidad (Carr y Jesch 2006). Este proceso suele llevarse a cabo

mediante síntesis química pero, como alternativa medioambientalmente limpia, se ha ensayado la esterificación con diferentes lipasas (Weber et al. 2001a,b). Comercialmente existen una amplia gama de productos que incorporan ésteres de fitoesteroles, como por ejemplo Danacol (Danone) y Flora Pro-Activ (Unilever), o ésteres de fitoestanoles, como por ejemplo Benecol (Kaiku). La ingesta diaria de 2-2,5 g de estos alimentos funcionales produce una reducción media de colesterol en torno al 14% (Calpe-Berdiel et al. 2009).

En esta Tesis se ha realizado la esterificación del fitoestanol más abundante (β-sitoestanol o estigmastanol) con ácido oleico mediante un proceso de transesterificación enzimática. Como catalizadores, se ensayaron las nuevas lipasas de la familia *C. rugosa-like* producidas en este trabajo, OPE y el crudo comercial de *C. rugosa*. Todas las enzimas empleadas, excepto la lipasa de *A. niger*, realizaron la transesterificación en mayor o menor grado, corroborando los resultados obtenidos en reacciones de hidrólisis de sustratos similares (**Fig. 3.3.3**). Son destacables los altos rendimientos alcanzados con OPE a tiempos cortos, indicando que es la enzima más prometedora para esta aplicación de entre las ensayadas. La mayor eficiencia de OPE frente a la lipasa comercial de *C. rugosa* ha sido demostrada previamente tanto a nivel de hidrólisis (Calero-Rueda et al. 2009) como en la esterificación directa de fitoesteroles (Barba Cedillo et al. 2013). Eso puede atribuirse a ciertos aspectos estructurales, descritos en la presente Tesis Doctoral, que hacen de OPE una esterol esterasa/lipasa única, como la presencia de un túnel de 30 Å que desemboca en la superficie de la molécula y que podría servir como vía alternativa para la salida de los productos, o la formación de un estado funcional dimérico, con una amplia cavidad que favorecería la catálisis de sustratos de gran tamaño.

4.5 BIBLIOGRAFÍA

Albertin W, Marullo P, Aigle M, Dillmann C, de Vienne D, Bely M, Sicard D (2011) Population size drives industrial *Saccharomyces cerevisiae* alcoholic fermentation and is under genetic control. Appl Environ Microbiol 77:2772-2784

Alcalde M (2015) Engineering the ligninolytic enzyme consortium. Trends Biotechnol 33:155-162

Baneyx F (1999) Recombinant protein expression in *Escherichia coli*. Curr Opin Biotechnol 10:411-421

Barba Cedillo V, Plou FJ, Martínez MJ (2012) Recombinant sterol esterase from *Ophiostoma piceae*: an improved biocatalyst expressed in *Pichia pastoris*. Microb Cell Fact 11:73

Barba Cedillo V, Prieto A, Martínez AT, Martínez MJ (2013) Procedimiento de acilación para la obtención de compuestos de interés alimenticio y/o farmacéutico utilizando esterol esterasas fúngicas. Patent No. ES 2395582 B1

Barriuso J, Prieto A, Martínez MJ (2013) Fungal genomes mining to discover novel sterol esterases and lipases as catalysts. BMC Genomics 14:712-719

Barriuso J, Martínez MJ (2015) *In silico* metagenomes mining to discover novel esterases with industrial application by sequential search strategies. J Microbiol Biotechn, 25:723-728

Besenmatter W, Svendsen A, Rannes JB, Jäckel C (2013) Lipase variants and polynucleotides encoding same. Patent No. WO2013010783 A1

Brady L, Brzozowski AM, Derewenda ZS, Dodson E, Tolley S (1990) A serine protease triad forms the catalytic centre of a triacylglycerol lipase. Nature 343:767-770

Brocca S, Schmidt-Dannert C, Lotti M, Alberghina L, Schmid RD (1998) Design, total synthesis, and fuctional overexpression of the *Candida rugosa lip*1 gene coding for a major industrial lipase. Protein Sci 7:1415-1422

Brockerhoff H, Jensen R (1974) Lipolytic enzymes. Academic Press, New York

Brzozowski AM, Derewenda U, Derewenda ZS, Dodson GG, Lawson DM, Turkenburg JP, Bjorkling F, Hugejensen B, Patkar SA, Thim L (1991) A model for interfacial activation in lipases from the structure of a fungal lipase-inhibitor complex. Nature 351:491-494

Buerth C, Kovacic F, Stock J, Terfruchte M, Wilhelm S, Jaeger KE, Feldbrugge M, Schipper K, Ernst JF, Tielker D (2014) Uml2 is a novel CalB-type lipase of *Ustilago maydis* with phospholipase A activity. Appl Microbiol Biotechnol 98:4963-4973

Burgess RR (1996) Purification of overproduced *Escherichia coli* RNA polymerase sigma factors by solubilizing inclusion bodies and refolding from Sarkosyl. In: Adhya S, Abelson J, Simon M (eds) RNA Polymerase and Associated Factors, Part A. Academic Press, San Diego, pp 145-149

Calero-Rueda O, Gutiérrez A, del Río JC, Muñoz C, Plou FJ, Martínez AT, Martínez MJ (2002a) Method for the enzymatic control of pitch deposits formed during paper pulp production using an esterase that hydrolyses triglycerides and sterol esters. Patent No. WO 02/075045 A1

Calero-Rueda O, Plou FJ, Ballesteros A, Martínez AT, Martínez MJ (2002b) Production, isolation and characterization of a sterol esterase from *Ophiostoma piceae*. Biochim Biophys Acta 1599:28-35

Calero-Rueda O, Gutiérrez A, del Río JC, Prieto A, Plou FJ, Ballesteros A, Martínez AT, Martínez MJ (2004) Hydrolysis of sterol esters by an esterase from *Ophiostoma piceae*: Application for pitch control in pulping of Eucalyptus globulus wood. Intern J Biotechnol 6:367-375

Calero-Rueda O, Barba V, Rodriguez E, Plou F, Martínez AT, Martínez MJ (2009) Study of a sterol esterase secreted by *Ophiostoma piceae*: Sequence, model and biochemical properties. Biochim Biophys Acta 1794:1099-1106

Calpe-Berdiel L, Escolâ-Gil JC, Blanco-Vaca F (2009) New insights into the molecular actions of plant sterols and stanols in cholesterol metabolism. Atherosclerosis 203:18-31

Camarero S, Pardo I, Canas AI, Molina P, Record E, Martínez AT, Martínez MJ, Alcalde M (2012) Engineering platforms for directed evolution of laccase from *Pycnoporus cinnabarinus*. Appl Environ Microbiol 78:1370-1384

Carr TP, Jesch ED (2006) Food components that reduce cholesterol absorption. Adv Food Res 51:165-204

Chang SW, Lee GC, Shaw JF (2006) Efficient production of active recombinant *Candida rugosa* LIP3 lipase in *Pichia pastoris* and biochemical characterization of purified enzyme. J Agric Food Chem 54:5831-5838

Chang VT, Crispin M, Aricescu AR, Harvey DJ, Nettleship JE, Fennelly JA, Yu C, Boles KS, Evans EJ, Stuart DI et al. (2007) Glycoprotein structural genomics: solving the glycosylation problem. Structure 15:267-273

Charton E, Macrae AR (1992) Substrate specificities of lipases A and B from *Geotrichum candidum* CMICC 335426. Biochim Biophys Acta 1123:59-64

De Eugenio LI (2009) Estudio bioquímico, genético y fisiológico de la degradación intracelular de polihidroxialcanoatos en *Pseudomonas putida*: aplicaciones biotecnológicas. Universidad Complutense, Facultad de Biología. Tesis Doctoral

Domínguez de María P, Sánchez-Montero JM, Sinisterra JV, Alcántara AR (2006) Understanding *Candida rugosa* lipases: an overview. Biotechnol Adv 24:180-196

Egmond MR, van Bemmel CJ (1997) Impact of structural information on understanding lipolytic function. In: Rubin B, Dennis EA (eds) Methods in Enzymology. Academic Press, New York, pp 119-119

Farias RN, Torres M, Canela R (1997) Spectrophotometric determination of the positional specificity of nonspecific and 1,3-specific lipases. Anal Biochem 252:186-189

Feldbrügge M, Kellner R, Schipper K (2013) The biotechnological use and potential of plant pathogenic smut fungi. Appl Microbiol Biotechnol 97:3253-3265

Fernandez-Fueyo E, Ruiz-Duenas FJ, Martinez MJ, Romero A, Hammel KE, Medrano FJ, Martinez AT (2014) Ligninolytic peroxidase genes in the oyster mushroom genome: heterologous expression, molecular structure, catalytic and stability properties, and lignin-degrading ability. Biotechnol Biofuels 7:114

Ferreira-Dias S, Sandoval G, Plou F, Valero F (2013) The potential use of lipases in the production of fatty acid derivatives for the food and nutraceutical industries. Electron J Biotechn 16:3

Ferrer P, Alarcón M, Ramón R, Benaiges MD, Valero F (2009) Recombinant *Candida rugosa* LIP2 expression in *Pichia pastoris* under the control of the AOX1 promoter. Biochem Eng J 46:271-277

Foresti ML, Ferreira ML (2004) Computational approach to solvent-free synthesis of ethyl oleate using *Candida rugosa* and *Candida antarctica* B lipases. I. Interfacial activation and substrate (ethanol, oleic acid) adsorption. Biomacromolecules 5:2366-2375

Frankel S, Sohn R, Leinwand L (1991) The use of sarkosyl in generating soluble-protein after bacterial expression. Proc Natl Acad Sci U S A 88:1192-1196

Ganjalikhany MR, Ranjbar B, Taghavi AH, Tohidi Moghadam T (2012) Functional motions of *Candida antarctica* lipase B: a survey through open-close conformations. PLoS ONE 7:e40327

García-Ruiz E, Gonzalez-Perez D, Ruiz-Duenas FJ, Martinez AT, Alcalde M (2012) Directed evolution of a temperature-, peroxide- and alkaline pH-tolerant versatile peroxidase. Biochem J 441:487-498

Gaudry A, Lorber B, Neuenfeldt A, Sauter C, Florentz C, Sissler M (2012) Re-designed N-terminus enhances expression, solubility and crystallizability of mitochondrial protein. Protein Eng Des Sel 25:473-481

Ghosh D, Wawrzak Z, Pletnev VZ, Li N, Kaiser R, Pangborn W, Jörnvall H, Erman M, Duax WL (1995) Structure of uncomplexed and linoleate-bound *Candida cylindracea* cholesterol esterase. Structure 3:279-288

Grigoriev IV, Nikitin R, Haridas S, Kuo A, Ohm R, Otillar R, Riley R, Salamov A, Zhao XL, Korzeniewski Fet al. (2014) MycoCosm portal: gearing up for 1000 fungal genomes. Nucleic Acids Res 42:699-704

Grochulski P, Li YG, Schrag JD, Bouthillier F, Smith P, Harrison D, Rubin B, Cygler M (1993) Insights into interfacial activation from an open structure of *Candida rugosa* lipase. J Biol Chem 268:12843-12847

Grochulski P, Bouthillier F, Kazlauskas RJ, Serreqi AN, Schrag JD, Ziomek E, Cygler M (1994a) Analogs of reaction intermediates identify a unique substrate-binding site in *Candida rugosa* lipase. Biochemistry 33:3494-3500

Grochulski P, Li Y, Schrag JD, Cygler M (1994b) Two conformational states of *Candida rugosa* lipase. Protein Sci 3:82-91

Gutiérrez-Fernández J, Vaquero ME, Prieto A, Barriuso J, Martínez MJ, Hermoso JA (2014) Crystal structures of *Ophiostoma piceae* sterol esterase: structural insights into activation mechanism and product release. J Struct Biol 187:215-222

Hammarstrom M, Woestenenk EA, Hellgren N, Hard T, Berglund H (2006) Effect of N-terminal solubility enhancing fusion proteins on yield of purified target protein. J Struct Funct Genomics 7:1-14

Hasan F, Shah AA, Hameed A (2006) Industrial applications of microbial lipases. Enzyme Microb Technol 39:235-251

Helenius A (1994) How N-linked oligosaccharides affect glycoprotein golding in the endoplasmic reticulum. Mol Biol Cell 5:253-265

Holmquist M, Tessier DC, Cygler M (1997a) High-level production of recombinant *Geotrichum candidum* lipases in yeast *Pichia pastoris*. Protein Expr Purif 11:35-40

Holmquist M, Tessier DC, Cygler M (1997b) Identification of residues essential for differential fatty acyl specificity of *Geotrichum candidum* lipases I and II. Biochemistry 36:15019-15025

Jensen R (1974) Characteristics of the lipase from the mold, *Geotrichum candidum*: a review. Lipids 9:149-157

Joerger RD, Haas, M.J. (1993) Overexpression of a *Rhizopus delemar* lipase gene in *Escherichia coli*. Lipids 28:81-88

Kaiser R, Erman M, Duax WL, Ghosh D, Jörnvall H (1994) Monomeric and dimeric forms of cholesterol esterase from *Candida cylindracea*: primary structure, identity in peptide patterns, and additional microheterogeneity. FEBS Letters 337:123-127

Kamal MZ, Ahmad S, Molugu TR, Vijayalakshmi A, Deshmukh MV, Sankaranarayanan R, Rao NM (2011) *In vitro* evolved non-aggregating and rhermostable lipase: structural and thermodynamic investigation. J Mol Biol 413:726-741

Kobayashi S, Takeya K, Suda S, Uyama H (1998) Lipase-catalyzed ring-opening polymerization of medium-size lactones to polyesters. Macromol Chem Physic 199:1729-1736

Kontkanen H, Tenkanen M, Fagerström R, Reinikainen T (2004) Characterisation of steryl esterase activities in commercial lipase preparations. J Biotechnol 108:51-59

Kontkanen H, Reinikainen T, Saloheimo M (2006a) Cloning and expression of a *Melanocarpus albomyces* steryl esterase gene in *Pichia pastoris* and *Trichoderma reesei*. Biotechnol Bioeng 94:407-415

Kontkanen H, Tenkanen M, Reinikainen T (2006b) Purification and characterisation of a novel steryl esterase from *Melanocarpus albomyces*. Enzyme Microb Technol 39:265-273

Korman TP, Sahachartsiri B, Charbonneau DM, Huang GL, Beauregard M, Bowie JU (2013) Dieselzymes: development of a stable and methanol tolerant lipase for biodiesel production by directed evolution. Biotechnol Biofuels 6:70

Krugener S, Zelenaa K, Zorn H, Nimtz M, Bergera RG (2009) Heterologous expression of an extra-cellular lipase from the basidiomycete *Pleurotus sapidus*. J Mol Catal B-Enzym 57:16-21

Kumar A, Gross RA (2000) *Candida antartica* lipase B catalyzed polycaprolactone synthesis: effects of organic media and temperature. Biomacromolecules 1:133-138

Labet M, Thielemans W (2009) Synthesis of polycaprolactone: a review. Chem Soc Rev 38:3484-3504

Larsen MW, Bornscheuer UT, Hult K (2008) Expression of *Candida antarctica* lipase B in *Pichia pastoris* and various *Escherichia coli* systems. Protein Expr Purif 62:90-97

Lee GC, Lee LC, Sava V, Shaw JF (2002) Multiple mutagenesis of non-universal serine codons of the *Candida rugosa lip*2 gene and biochemical characterization of purified recombinant LIP2 lipase overexpressed in *Pichia pastoris*. Biochem J 366:603-611

Lee LC, Chen YT, Yen CC, Chiang TCY, Tang SJ, Lee GC, Shaw JF (2007) Altering the substrate specificity of *Candida rugosa* LIP4 by engineering the substrate-binding sites. J Agric Food Chem 55:5103-5108

Lee LC, Yen CC, Malmis CC, Chen LF, Chen JC, Lee GC, Shaw JF (2011) Characterization of codon-optimized recombinant *Candida rugosa* lipase 5 (LIP5). J Agric Food Chem 59:10693-10698

Liebeton K, Zonta A, Schimossek K, Nardini M, Lang D, Dijkstra BW, Reetz MT, Jaeger KE (2000) Directed evolution of an enantioselective lipase. Chem Biol 7:709-718

López N, Pernas MA, Pastrana LM, Sánchez A, Valero F, úa ML (2004) Reactivity of pure *Candida rugosa* lipase isoenzymes (Lip1, Lip2, and Lip3) in aqueous and

organic media. Influence of the isoenzymatic profile on the lipase performance in organic media. Biotechnol Progress 20:65-73

Lozano P, De Diego T, Carrie D, Vaultier M, Iborra JL (2003) Lipase catalysis in ionic liquids and supercritical carbon dioxide at 150 degrees C. Biotechnol Prog 19:380-382

Macedo GA, Lozano MMS, Pastore GM (2003) Enzymatic synthesis of short chain citronellyl esters by a new lipase from *Rhizopus* sp. Electron J Biotechn 6:72-75

Magnusson AO, Takwa M, Harnberg A, Hult K (2005) An S-selective lipase was created by rational redesign and the enantioselectivity increased with temperature. Angewandte Chemie 44:4582-4585

Mancheño JM, Pernas MA, Martínez MJ, Ochoa B, Rúa ML, Hermoso.J.A. (2003) Structural insights into the lipase/esterase behavior in the *Candida rugosa* lipases family: crystal structure of the lipase 2 isoenzyme at 1.97 Å resolution. J Mol Biol 332:1059-1069

Martinez C, Geus P, Lauwereys M, Matthyssens G, Cambillau C (1992) Fusarium solani cutinase is a lipolytic enzyme with a catalytic serine accessible to solvent. Nature 356:615-618

Mate DM, Garcia-Ruiz E, Camarero S, Shubin VV, Falk M, Shleev S, Ballesteros AO, Alcalde M (2013) Switching from blue to yellow: altering the spectral properties of a high redox potential laccase by directed evolution. Biocatal Biotransform 31:8-21

Mattanovich D, Branduardi P, Dato L, Gasser B, Sauer M, Porro D (2012) Recombinant protein production in yeasts. In: Lorence A (ed) Recombinant gene expression: reviews and protocols. Humana Press-Springer, Totowa, pp 329-358

Miettinen TA, Puska P, Gylling H, Vanhanen H, Vartiainen E (1995) Reduction of serum cholesterol with sitostanol ester margarine in a mildly hypercholesterolemic population. N Engl J Med 333:1308-1312

Minning S, Serrano A, Ferrer P, Sola C, Schmid RD, Valero F (2001) Optimization of the high-level production of *Rhizopus oryzae* lipase in *Pichia pastoris*. J Biotechnol 86:59-70

Nettleship JE (2012) Structural biology of glycoproteins. In: Stefana Petrescu (ed) Biochemistry, Genetics and Molecular Biology "Glycosylation". InTech, pp 41-62

Noguchi S, Satow Y (2006) Purification of human beta (2)-adrenergic receptor expressed in methylotrophic yeast *Pichia pastoris*. J Biochem 140:799-804

Otero C, Fernández-Pérez M, Hermoso JA, Martínez Ripoll M (2005) Activation in the family of *Candida rugosa* isolipases by polyethylene glycol. J Mol Catal B-Enzym 32:225-229

Ottosson J, Fransson L, King JW, Hult K (2002) Size as a parameter for solvent effects on *Candida antarctica* lipase B enantioselectivity. Biochim Biophys Acta 1594:325-334

Park S, Viklund F, Hult K, Kazlauskas RJ (2003) Vacuum-driven lipase-catalysed direct condensation of L-ascorbic acid and fatty acids in ionic liquids: synthesis of a natural surface active antioxidant. Green Chem 5:715-719

Pernas MA, Lopez C, Pastrana L, Rua ML (2000) Purification and characterization of Lip2 and Lip3 isoenzymes from a *Candida rugosa* pilot-plant scale fed-batch fermentation. J Biotechenol 84:163-174

Pernas MA, López C, Rúa ML, Hermoso J (2001) Influence of the conformational flexibility on the kinetics and dimerisation process of two *Candida rugosa* lipase isoenzymes. FEBS Letters 501:87-91

Pleiss J, Fischer M, Peiker M, Thiele C, Schmid RD (2000) Lipase engineering database: understanding and exploiting sequence-structure-function relationships. J Mol Catal B-Enzym 10:491-508

Pletnev V, Addlagatta A, Wawrzak Z, Duax W (2003) Three-dimensional structure of homodimeric cholesterol esterase-ligand complex at 1.4 Å resolution. Acta Crystallogr D Biol Crystallogr 59:50-56

Qian Z, Horton JR, Cheng X, Lutz S (2009) Structural redesign of lipase B from *Candida antarctica* by circular permutation and incremental truncation. J Mol Biol 393:191-201

Rajarathnam S, Shashirekha MNJ, Bano Z (1998) Biodegradative and biosynthetic capacities of mushrooms: Present and future strategies. Crit Rev Biotechnol 18:91-236

Romanos MA, Makoff AJ, Fairwheather NF, Beesley KM, Slater DE, Rayment FB, Payne MM, Clare JJ (1991). Nucleic Acids Res 19:1461-1467

Rotticci D, Haeffner F, Orrenius C, Norin T, Hult K (1998) Molecular recognition of sec-alcohol enantiomers by *Candida antarctica* lipase B. J Mol Catal B-Enzym 5:267-272

Rotticci D, Rotticci-Mulder JC, Denman S, Norin T, Hult K (2001) Improved enantioselectivity of a lipase by rational protein engineering. Chembiochem 2:766-770

Rotticci-Mulder JC, Gustavsson M, Holmquist M, Hult K, Martinelle M (2001) Expression in *Pichia pastoris* of *Candida antarctica* lipase B and lipase B fused to a cellulose-binding domain. Protein Expr Purif 21:386-392

Ruiz-Dueñas FJ, Martínez AT (2009) Microbial degradation of lignin: How a bulky recalcitrant polymer is efficiently recycled in nature and how we can take advantage of this. Microbial Biotechnol 2:164-177

Schmitt J, Brocca S, Schmid RD, Pleiss J (2002) Blocking the tunnel: engineering of *Candida rugosa* lipase mutants with short chain length specificity. Protein Eng 15:595-601

Schrag JD, Cygler M (1993) 1.8 Å Refined structure of the lipase from *Geotrichum candidum*. J Mol Biol 230:575-591

Schrag JD, Li Y, Wu S, Cygler M (1991) Ser-His-Glu triad forms the catalytic site of the lipase from *Geotrichum candidum*. Nature 351:761-764

Shendure J, Ji H (2008) Next-generation DNA sequencing. Nat Biotechnol 26:1135-1145

Singh SM, Panda AK (2005) Solubilization and refolding of bacterial inclusion body proteins. J Biosci Bioeng 99:303-310

Storck R (1966) Nucleotide composition of nucleic acids of fungi II. Deoxyribonucleic acids. J Bacteriol 91:227-230

Tang SJ, Sun KH, Sun GH, Chang TY, Lee GC (2000) Recombinant expression of the Candida rugosa lip4 lipase in Escherichia coli. Protein Expr Purif 20:308-313

Tang SJ, Shaw JF, Sun KH, Sun GH, Chang TY, Lin CK, Lo YC, Lee GC (2001) Recombinant expression and characterization of the *Candida rugosa* LIP4 lipase in *Pichia pastoris*: comparison of glycosilation, activity, and stability. Arch Biochem Biophys 387:93-98

Terpe K (2003) Overview of tag protein fusions: from molecular and biochemical fundamentals to commercial systems. Appl Microbiol Biotechnol 60:523-533

Turner NA, Needs EC, Khan JA, Vulfson EN (2001) Analysis of conformational states of *Candida rugosa* lipase in solution: implications for mechanism of interfacial activation and separation of open and closed forms. Biotechnol Bioeng 72:108-118

Uppenberg J, Hansen MT, Patkar S, Jones TA (1994) The sequence, crystal structure determination and refinement of two crystal forms of lipase B from *Candida antarctica*. Structure 2:293-308

Uyama H, Kobayashi S (1993) Enzymatic ring-opening polymerization of lactones catalyzed by lipase. Chem Lett:1149-1150

Vaquero ME, Barriuso J, Medrano FJ, Prieto A, Martínez MJ (2015a) Heterologous expression of a fungal sterol esterase/lipase in different hosts: Effect on solubility, glycosylation and production. J Biosci Bioeng doi:10.1016/j.jbiosc.2015.04.005

Vaquero ME, Barriuso J, Prieto A, Martínez MJ (2015b) Expression and properties of three novel fungal lipases/sterol esterases predicted in silico: comparison with other enzymes of the *Candida rugosa*-like family. Appl Microbiol Biotechnol doi:10.1007/s00253-015-6890-9

Varma IK, Albertsson AC, Rajkhowa R, Srivastava RK (2005) Enzyme catalyzed synthesis of polyesters. Prog Polym Sci 30:949-981

Watanabe Y, Nagao T, Shimada Y (2009) Control of the regiospecificity of *Candida antarctica* lipase by polarity. New Biotechnol 26:23-28

Weber N, Weitkamp P, Mukherjee KD (2001a) Fatty acid steryl, stanyl, and steroid-esters by esterification and transesterification in vacuo using *Candida rugosa* lipase as catalyst. J Agric Food Chem 49:67-71

Weber N, Weitkamp P, Mukherjee KD (2001b) Steryl and stanyl esters of fatty acids by solvent-free esterification and transesterification in vacuo using lipases from *Rhizomucor miehei*, *Candida antarctica*, and *Carica papaya*. J Agric Food Chem 49:5210-5216

Wei W, Chen L, Zou G, Wang QF, Yan X, Zhang J, Wang CS, Zhou ZH (2013) N-glycosylation affects the proper folding, enzymatic characteristics and production of a fungal beta-glucosidase. Biotechnol Bioeng 110:3075-3084

Yan J, Li A, Xu Y, Ngo TPN, Phua S, Li Z (2012) Efficient production of biodiesel from waste grease: one-pot esterification and transesterification with tandem lipases. Biores Technol 123:332-337

Zorn H, Bouws H, Takenberg M, Nimtz M, Getzlaff R, Breithaupt DE, Berger RG (2005) An extracellular carboxylesterase from the basidiomycete *Pleurotus sapidus* hydrolyses xanthophyll esters. Biol Chem 386:435-440

Zsebo KM, Lu HS, Fieschko JC, Goldstein L, Davis J, Duker K, Suggs SV, Lai PH, Bitter GA (1986) Protein secretion from *Saccharomyces cerevisiae* directed by the prepro-alpha-factor leader region. J Biol Chem 261:5858-5865

5 Conclusiones/*Conclusions*

1. La esterol esterasa/lipasa de *O. piceae* (OPE) expresada en *E. coli* se encontró mayoritariamente en cuerpos de inclusión. Solo con la adición de 6-8 aminoácidos extra en el N- terminal de la proteína, o solubilizando los cuerpos de inclusión con el detergente Sarkosyl, se obtuvo enzima soluble pero no funcional. La falta de actividad se debe posiblemente a que este organismo no dispone de los mecanismos necesarios para realizar ciertas modificaciones post-traduccionales que parecen ser fundamentales para el correcto plegamiento de la proteína.

2. OPE se expresó con éxito en tres cepas de *S. cerevisiae*, consiguiendo los mejores resultados con la cepa BJ5465 deficiente en proteasas, y con el gen bajo el control de un promotor inducible por galactosa. Sin embargo, los niveles de actividad en *S. cerevisiae* fueron menores que los producidos por *P. pastoris*. En este hospedador se ha obtenido un clon que produce el doble de actividad.

3. El estado de agregación de la proteína difiere en los distintos hospedadores e influye en su eficacia catalítica: cuanta más agregación, menor eficacia. La mayor agregación tiene lugar en la enzima nativa de *O. piceae* mientras que la expresada en *P. pastoris* fue principalmente monomérica y dimérica, presentando la enzima producida en *S. cerevisiae* propiedades intermedias.

4. La resolución de la estructura cristalográfica de OPE, en su conformación abierta y cerrada, ha permitido dilucidar sus características estructurales más relevantes. La enzima funcional es un dímero, que se forma en presencia del sustrato, y presenta una gran apertura, no observada antes en enzimas diméricas de la familia *C. rugosa-like*. Esto, unido a factores como el número elevado de aminoácidos hidrofóbicos en la zona de la tapadera y la presencia de un túnel interno amplio y recto, podrían contribuir a explicar la mayor eficacia de OPE, al comparar con otras enzimas de la misma familia.

5. Se han expresado en *P. pastoris* tres lipasas/esterol esterasas hipotéticas de la familia la *C. rugosa-like,* identificadas mediante minería *in silico* de genomas fúngicos. La caracterización de las enzimas

pertenecientes a *N. haematococca*, *T reesei* y *A. niger* y su comparación con OPE, ha puesto de manifiesto que el contenido de aminoácidos hidrofóbicos en la región de la tapadera y la forma del túnel interno pueden ser parámetros útiles para la selección de este tipo de enzimas en bases de datos. No obstante, su expresión y caracterización es esencial para corroborar la versatilidad catalítica predicha para estas enzimas.

6. Se evaluó la actividad de estas nuevas enzimas en dos aplicaciones de interés, comparándola con la de OPE y la lipasa comercial de *C. rugosa.* En la síntesis de policaprolactona, estas dos últimas y la lipasa de *A. niger* fueron las más eficientes, aunque existen enzimas comerciales mucho más eficaces para llevar a cabo la síntesis de este compuesto. En cuanto a la síntesis enzimática de ésteres de sitoestanol, todas ellas, excepto la lipasa de *A. niger*, catalizaron esta reacción. Cabe destacar los altos rendimientos alcanzados por OPE a tiempos cortos, lo que sugiere que es la enzima más prometedora para esta aplicación.

7. Finalmente, se ha expresado y caracterizado la primera lipasa de un basidiomiceto amilocorticial, PlicB, relacionada filogenéticamente con la lipasa B de *C. anctartica* (CalB), una de las enzimas más utilizadas en distintas aplicaciones biotecnológicas. PlicB presenta semejanzas y diferencias con CalB destacando su mayor actividad sobre un análago de triglicérido. Estos resultados demuestran que la minería de genomas resulta eficaz para la búsqueda de nuevas enzimas, como alternativa a los métodos tradicionales.

1. The sterol esterase/lipase of *O. piceae* (OPE) expressed in *E. coli* was detected mainly inside inclusion bodies. Only the addition of 6-8 amino acids to the N-terminus and the use of the surfactant Sarkosyl to solubilize the inclusion bodies yielded partially soluble but inactive protein. In view of the results, it follows that post-translational modifications affected enzymes' folding, which seems to be crucial to obtain an active protein.

2. OPE was successfully expressed in three strains of *S. cerevisiae* achieving the best results in the protease-deficient strain, BJ5465, and under the control of the galactose-inducible promoter. However, the yields were lower than those obtained in *P. pastoris*. In this host, a novel clone with 2-fold activity was obtained.

3. The aggregation state of OPE varies in the different host and affects its kinetic parameters: the higher aggregation the lower efficiency. The native enzyme produced the biggest aggregates, while the protein expressed in *P. pastoris* appeared mainly as monomers and dimmers. OPE produced in *S. cerevisiae* showed intermediate properties.

4. The resolution of the three-dimensional structure of OPE in both, the open and closed conformations, contributes to deepen the molecular knowledge of this enzyme. The active form is a homodimer activated in the presence of the substrate creating a very large cavity between both monomers. This arrangement is not observed in other dimeric members of the *C. rugosa*-like family. This and other factors such as the high number of hydrophobic residues in the lid region and the presence of a long, straight inner tunnel could favor the higher efficiency of OPE when it is compared with other related enzymes.

5. Three putative lipases/sterol esterases from the *C. rugosa*-like family, selected from fungal genome mining, have been expressed in *P. pastoris*. The enzymes, from *Nectria haematococca, Trichoderma reesei* and *Aspergillus niger,* were characterized and compared with OPE, suggesting that the number of hydrophobic amino acids in the lid region and the shape of the internal tunnel could be useful parameters to select this

kind of enzymes from databases. However, proteins' expression and characterization seems to be essential to corroborate their catalytic properties.

6. The novel enzymes produced in this work were evaluated for two biotechnological applications and compared with OPE and the commercial lipase of *C. rugosa*. These two enzymes and the lipase of *A. niger* successfully synthesized polycaprolactone, albeit there are other commercial enzymes much more effective. Regarding the enzymatic synthesis of sitostanol esters, all the enzymes tested, except the *A. niger* lipase, were able to catalyze this reaction. OPE yielded the better acylation degree at short times, appearing as the most promising enzyme among the assayed catalysts.

7. Finally, the first lipase from an amylocorticial basidiomycete was expressed and characterized. PlicB is phylogenetically related to *C. antarctica* lipase B, one of the lipase most used at the industrial level. PlicB displays similarities and differences with CalB, and its higher activity against a triglyceride analogue should be emphasized. In view of the results, genome mining appears as an interesting alternative to traditional screening methods.